

AD-A041 208

ROCKWELL INTERNATIONAL. COLUMBUS OHIO COLUMBUS AIRCRA--ETC F/G 11/4  
EVALUATION OF COMPOSITE WING FOR XFV-12A AIRPLANE.(U)

DEC 76 D N ULRY, R W GEHRING, K I CLAYTON

N62269-74-C-0577

UNCLASSIFIED

NR76H-135

NADC-77183-30

NL

4 OF 4  
AD  
A041208



REPORT NADC-77183-30

*11*  
*NU*

ADA 041 208

# EVALUATION of COMPOSITE WING for XFV-12A AIRPLANE

DECEMBER 1976



FINAL REPORT 28 JUNE 1974 TO 31 AUGUST 1976

APPROVED FOR PUBLIC RELEASE; DISTRIBUTION UNLIMITED

Prepared Under Contract N62269-74-C-0577

For

NAVAL AIR DEVELOPMENT CENTER  
DEPARTMENT OF THE NAVY  
Warminster, Pennsylvania 18974



Rockwell International

Columbus Aircraft Division  
4300 East Fifth Avenue  
Columbus, Ohio 43216

DDC FILE COPY



Unclassified

SECURITY CLASSIFICATION OF THIS PAGE (When Data Entered)

REPORT DOCUMENTATION PAGE		READ INSTRUCTIONS BEFORE COMPLETING FORM
1. REPORT NUMBER 18 NADC-77183-30	2. GOVT ACCESSION NO.	3. RECIPIENT'S CATALOG NUMBER
4. TITLE (and Subtitle) 6 Evaluation of Composite Wing for XFV-12A Airplane	5. TYPE OF REPORT & PERIOD COVERED 9 Final rept 28 June 1974-31 August 1976	
7. AUTHOR(s) 10 D. N. Ulry, R. W. Gehring, K. I. Clayton	14. PERFORMING ORG. REPORT NUMBER NR76H-135	8. CONTRACT OR GRANT NUMBER(s) 15. N62269-74-C-0577 new
9. PERFORMING ORGANIZATION NAME AND ADDRESS Columbus Aircraft Division Rockwell International 4300 East Fifth Avenue Columbus, Ohio 43216	10. PROGRAM ELEMENT, PROJECT, TASK AREA & WORK UNIT NUMBERS	
11. CONTROLLING OFFICE NAME AND ADDRESS Code 30331 Naval Air Development Center Warminster, PA 18974	12. REPORT DATE 11 December 1976	13. NUMBER OF PAGES 245 (12 326p.)
14. MONITORING AGENCY NAME & ADDRESS (if different from Controlling Office)	15. SECURITY CLASS. (of this report) Unclassified 15a. DECLASSIFICATION/DOWNGRADING SCHEDULE N/A	
16. DISTRIBUTION STATEMENT (of this Report) Approved for public release; distribution unlimited		
17. DISTRIBUTION STATEMENT (of the abstract entered in Block 20, if different from Report) Unrestricted		
18. SUPPLEMENTARY NOTES		
19. KEY WORDS (Continue on reverse side if necessary and identify by block number) Composites V/STOL Structure Advanced Composites Wing Design Graphite/Epoxy		
20. ABSTRACT (Continue on reverse side if necessary and identify by block number) A prior study conducted for the Naval Air Systems Command for application of advanced composites in the XFV-12A aircraft indicated the wing torque box to be the component of airframe structure having the greatest potential for significant weight savings through composite material application. A Phase II design/development program was undertaken to develop detail design concepts for a XFV-12A composite wing box and fabricate a representative section of this wing box for development test and evaluation to provide a base for		

DD FORM 1 JAN 73 1473

EDITION OF 1 NOV 65 IS OBSOLETE

Unclassified

SECURITY CLASSIFICATION OF THIS PAGE (When Data Entered)

407390

next page

Unclassified

SECURITY CLASSIFICATION OF THIS PAGE(When Data Entered)

20. ABSTRACT (Continued)

→ subsequent Phase III full scale verification testing. ↗

A preliminary design/analysis investigation was conducted on several design concepts including conventional configurations and advanced configurations which capitalize on continuous bonded construction, automated manufacturing methods and reduced number of parts. From these studies a configuration was selected for detail design/analysis, fabrication and test. The selected configuration utilizes graphite/epoxy sandwich construction with glass/phenolic honeycomb core in the cover skins, front spar and intermediate spars; solid graphite/epoxy in the B.P. 33.93 rib and aluminum in the centerline rib, rear spar and wing to fuselage attachment fittings. The upper cover skin is mechanically fastened to the substructure to allow removal for inspection or repair. The lower skin is mechanically fastened to the centerline rib, B.P. 33.93 rib, rear spar and secondarily bonded to the remaining substructure.

Critical joint verification coupons were fabricated and tested, process specifications issued, and a composite wing center section test specimen manufactured and shipped to the Naval Air Development Center for subsequent structural test. The composite wing box design reflects a 19% weight saving over a baseline production metal FV-12A wing box design. This weight saving was achieved while conservatively limiting stress levels within the wing box test section to a maximum of approximately 35,000 psi.

Other significant accomplishments of the program include:

- o Demonstration of capability to fabricate complex double curved airfoil surfaces and wing spars with graphite/epoxy sandwich construction. Examples being the severely contoured wing lower cover skin inboard of B.P. 33.3 rib and the one-piece front spar with severe sweep angle change at B.P. 33.3.
- o Development of a tapered, interleaved centerline splice joint configuration that maintains .19 inch overlap per ply runout and transmits at least 94% of the full cover laminate load carrying capability. Cover skin material can therefore be efficiently utilized and is not limited by joint strength.
- o Development of a bolted cover design which allows removal of cover for inspection or repair, incorporates joint "softening" provisions for reduction of stress concentration, and includes integral fuel tank sealing provisions.
- o Investigated alternate design concepts which have potential for manufacturing cost saving and increased survivability capability in future aircraft. Examples being the filament wound spar concepts for configuration "C" and the full-depth sculptured Trussgrid core configuration with integral graphite/epoxy cover skins.

Unclassified

SECURITY CLASSIFICATION OF THIS PAGE(When Data Entered)

# FOREWORD

This final technical report was prepared by the Columbus Aircraft Division (CAD) of Rockwell International Corporation, Columbus, Ohio 43216, under Naval Air Development Center (NADC) Contract N62269-74-C-0577 entitled "Evaluation of Composite Wing for XFV-12A Aircraft." This work was administered by the Air Vehicle Technology Department, Naval Air Development Center, Department of the Navy, Warminster, Pennsylvania 18974. The NADC Project Engineer was Mr. M. S. Rosenfeld.

The Project Manager for the Columbus Aircraft Division was Mr. O. G. Acker. The program was conducted by the Advanced Structures Group of the Research and Engineering Department with Mr. K. I. Clayton as Principal Investigator. Major contributors were Messrs. G. Pollock - Design, R. E. Kester - Analysis, G. A. Clark - Material and Process Specifications, and R. E. Taylor - Manufacturing Engineering (tooling and non-metallic fabrication).

Valuable guidance was provided by Dr. E. J. McQuillen and Dr. S. L. Huang of the Naval Air Development Center.

ACCESSION FOR	
NTIS	White Section <input checked="" type="checkbox"/>
DNC	Buff Section <input type="checkbox"/>
UNANNOUNCED	
JUSTIFICATION	
BY	
DISTRIBUTION/AVAILABILITY CODES	
DTIC	AVAIL. AND/OR SPECIAL
A	

## TABLE OF CONTENTS

<u>Section</u>		<u>Page No.</u>
	FOREWORD	i
	TABLE OF CONTENTS	iii
	LIST OF ILLUSTRATIONS	vi
	LIST OF TABLES	xiii
1.0	INTRODUCTION, SUMMARY, AND ACCOMPLISHMENTS	1
2.0	DESIGN CRITERIA AND LOADS	8
	2.1 Baseline Description	8
	2.2 Design Load Conditions	11
	2.3 Stiffness Requirements	12
	2.4 Allowable Stresses	17
3.0	DESIGN CONCEPTS	23
	3.1 Selected Configuration	23
	3.1.1 Cover Skins	23
	3.1.2 Front Spar	26
	3.1.3 Intermediate Spars	29
	3.1.4 B.P. 33.93 Rib	31
	3.1.5 Centerline Splice	31
	3.1.6 Wing-to-Fuselage Attachment	33
	3.1.7 Weight Comparison	36
	3.2 Alternate Designs	38
	3.2.1 "Configuration "C"	38
	3.2.2 Trussgrid Concepts	40

PRECEDING PAGE, BLANK, NOT FILMED



TABLE OF CONTENTS (CONT'D)

<u>Section</u>		<u>Page No.</u>
4.0	MATERIAL SELECTION AND SPECIFICATIONS	43
4.1	Graphite/Epoxy Prepreg	43
4.2	Adhesives	44
4.3	Honeycomb Core	45
4.4	Potting Compound	48
4.5	Metal Components	48
5.0	STRUCTURAL ANALYSIS	50
5.1	Finite Element Analysis	50
5.2	Sandwich Panel Buckling	52
5.3	Bolted Joints	55
5.4	Flutter Evaluation	58
6.0	DESIGN DEVELOPMENT AND VERIFICATION	66
6.1	Laminate Strength Tests	66
6.2	Centerline Splice Joint	66
6.2.1	Static Tests	66
6.2.2	Fatigue Tests	74
6.3	Flatwise Tension	81
6.4	Edgewise Compression	81
6.5	Spar Joint Tests	81
6.6	Precure Vs. Cocure Tests	85
6.7	Hi-Lok Fasteners Installation	85

TABLE OF CONTENTS (CONT'D)

<u>Section</u>		<u>Page No.</u>
7.0	TOOLING AND FABRICATION	89
	7.1 Tool Design	89
	7.1.1 Cover Skin Panels	90
	7.1.2 Front Spar	95
	7.1.3 B.P. 33.93 Rib	98
	7.1.4 Intermediate Spars	98
	7.1.5 Metal Components	100
	7.2 Process Specifications	100
	7.3 Spar Cap Bonding	104
	7.4 Drilling and Final Assembly	106
8.0	QUALITY ASSURANCE	115
	8.1 Material Certification and Acceptance	115
	8.2 Process Control	116
	8.3 Inspection Techniques	117
	8.4 Material Review Dispositions	123
9.0	STRUCTURAL TEST	126
	9.1 Test Load Conditions	126
	9.2 Strain Gage Instrumentation	126
10.0	RECOMMENDATIONS	135
<u>APPENDIX</u>		
A	Structural Analysis	A-1
B	Composite Wing Drawings	B-1



## LIST OF ILLUSTRATIONS

<u>Figure</u>		<u>Page No.</u>
1	Composite Wing Box Assembly - Top View	4
2	Composite Wing Box Assembly - Bottom View	5
3	XFV-12A Structural Arrangement	9
4	XFV-12A Wing Box Geometry	10
5	Critical Condition Design Shear Curves	13
6	Critical Condition Design Bending Moment Curves	14
7	Critical Condition Design Torque Curves	15
8	Wing Bending and Torsional Stiffness Requirements and Composite Wing Stiffness	16
9	Code for Sandwich Skin Laminate Stacking Order	19
10	Skin Stacking Order and Thickness Transition, Panel M , Sections L-L and P-P	20
11	Skin Stacking Order and Thickness Transition, Panel P , Section P-P	20
12	Skin Stacking Order and Thickness Transition, Panel L , Sections G-G and O-O	21
13	Skin Stacking Order and Thickness Transition, Panel O , Sections O-O	21
14	Skin Stacking Order and Thickness Transition, Panels K , and N , Sections K-K and N-N	22
15	XFV-12A Composite Wing Box Structure	24
16	Upper Cover Skin Panel Inserts	27
17	Typical Front Spar Section	28

# LIST OF ILLUSTRATIONS (CONT'D)

<u>Figure</u>		<u>Page No.</u>
18	Typical Intermediate Spar Section	30
19	Typical B.P. 33.93 Rib Section	32
20	Center Line Splice Joint	34
21	Aft Wing to Fuselage Attach Fitting	35
22	Composite Wing Baseline Configuration Test Specimen	39
23	"Configuration C" Material Forms	41
24	Glass Layup on Trussgrid Core	42
25	Lap Shear Characteristics of the AF-147/EC-3917 Adhesive System	46
26	Composite Wing NASTRAN Model	51
27	Wing Upper Cover Stresses	53
28	Wing Lower Cover Stresses	54
29	Upper Rear Spar Centerline Splice	56
30	Lower Rear Spar Centerline Splice	57
31	Upper Rear Spar Centerline Splice; Design Ultimate Bolt Shear Load Distribution	59
32	Lower Rear Spar Centerline Splice; Design Ultimate Bolt Shear Load Distribution	60
33	Upper Rear Spar Centerline Splice; Design Ultimate Compression Stress Distribution	61
34	Lower Rear Spar Centerline Splice; Design Ultimate Tension Stress Distribution	62
35	XFV-12A Composite Wing Minimum Predicted Flutter Speed; Symmetric Condition Frequency and Damping Vs. Velocity	64

# LIST OF ILLUSTRATIONS (CONT'D)

<u>Figure</u>		<u>Page No.</u>
36	XFV-12A Composite Wing Minimum Predicted Flutter Speed; Anti-Symmetric Condition Frequency and Damping Vs. Velocity	65
37	Quality Conformance Tests - Fiberite Hy-E-1034C	67
38	Quality Conformance Tests - Fiberite Hy-E-1034C	68
39	<u>∅</u> Axial Load Specimen	69
40	<u>∅</u> Axial Load Specimen, Detail A	70
41	Failed <u>∅</u> Axial Load Specimens	71
42	Detail of <u>∅</u> Axial Load Specimen Test Failure	72
43	Revised Centerline Laminate Stacking Order	75
44	Failed Axial Load Specimens - Precured Facings with Revised Stacking Order	77
45	Failed Axial Load Specimens - Precured Facings with Revised Stacking Order	78
46	Centerline Joint Axial Fatigue Specimen SN-4 after 800,000 Cycles	79
47	Edgewise View of Axial Fatigue Specimen SN-4 after 800,000 Cycles	79
48	Specimen SN-5 in Anti-Buckling Guide	80
49	Centerline Joint Axial Fatigue Specimen SN-5 after 60000 Cycles	80
50	Edgewise View of Axial Fatigue Specimen SN-5 after 60000 Cycles	80
51	Joint Verification Specimens Fabricated for Flatwise Tension and Edgewise Compression Tests	82
52	Compression Test Specimen for Intermediate Spar Joint	83

# LIST OF ILLUSTRATIONS (CONT'D)

<u>Figure</u>		<u>Page No.</u>
53	Joint Verification Specimens Fabricated for Shear Tests	84
54	Failed Axial Load Specimens - Cocured Facings with Revised Stacking Order	87
55	Hi-Lok Fastener Installation	88
56	Layup of Upper Skin Panel Facing	91
57	Upper Skin Panel Facing After Cure	93
58	Layup of Lower Skin Panel Facing	94
59	Layup of $\pm 45$ Shear Web on Front Spar Tool	96
60	Graphite Front Spar	97
61	Graphite X <sub>w</sub> 33.93 Forward Rib	99
62	Aluminum Centerline Rib	101
63	Aluminum Rear Spar	102
64	Detail Parts - Composite Wing Center Section Specimen	103
65	Lower Intermediate Spar Caps Bonded to Lower Skin Panel	105
66	Front Spar Bonded to Lower Skin Panel	107
67	Detail Parts - Composite Wing Center Section Specimen	108
68	Composite Wing Detail Parts in Assembly/Drill Fixture	109
69	Composite Wing Detail Parts in Assembly/Drill Fixture	110
70	Composite Wing Box Substructure Assembly	111
71	Composite Wing Box Assembly - Rear View	113
72	Composite Wing Box Assembly - Front View	114

# LIST OF ILLUSTRATIONS (CONT'D)

<u>Figure</u>		<u>Page No.</u>
73	Ultrasonic Inspection Equipment	119
74	Ultrasonic Inspection Equipment Console	120
75	Ultrasonic Inspection of Lower Skin Sandwich Panel	122
76	Maximum Vertical Landing Condition Test Loads (Ultimate Loads)	127
77	Critical Flight Condition Test Loads (Ultimate Loads)	128
78	Maximum Vertical Landing Condition Applied Static Test Loads	130
79	Composite Wing Structural Test Setup	131
80	Strain Gage Locations	132
81	Proposed Deflection Transducer Locations	134
A-1	Wing Upper Cover Stresses - Max. Vertical Load Landing Condition	A-3
A-2	Wing Upper Cover Stresses - Max. Vertical Load Landing Condition	A-4
A-3	Wing Upper Cover Reduced Stresses - Max. Vert. Landing Condition	A-5
A-4	Wing Lower Cover Stresses - Max. Vertical Load Landing Condition	A-6
A-5	Wing Lower Cover Stresses - Max. Vertical Load Landing Condition	A-7
A-6	Wing Lower Cover Reduced Stresses - Max. Vert. Landing Condition	A-8



# LIST OF ILLUSTRATIONS (CONT'D)

<u>Figure</u>		<u>Page No.</u>
A-7	Wing Upper Cover Stresses - Symmetrical Flight Condition	A-9
A-8	Wing Upper Cover Stresses - Symmetrical Flight Condition	A-10
A-9	Wing Lower Cover Stresses - Symmetrical Flight Condition	A-11
A-10	Wing Lower Cover Stresses - Symmetrical Flight Condition	A-12
A-11	Final Rear Spar Cap Areas (Equiv. Al.)	A-13
A-12	Principal Stress Direction, Upper Cover Skin	A-14
A-13	Principal Stress Direction, Lower Cover Skin	A-15
A-14	Panel Identification for Stability Analysis	A-17
A-15	Wing Spar Shear Flows - Original Spar Cap Areas	A-31
A-16	Spar Shear Flows (Avg.) - Increased Spar Cap Areas	A-32
A-17	Free Body Diagram of Centerline Rib	A-34
A-18	Free Body Diagram of B.P. 33.93 Rib	A-35
A-19	Free Body Diagram of Rear Spar	A-36
A-20	Wing Vert. Deflections Relative to W.R.P.- Max. Vert. Landing Condition	A-72
A-21	Wing Vert. Deflections Relative to W.R.P.- Symm. Flight Condition	A-73



LIST OF ILLUSTRATIONS (CONT'D)

<u>Figure</u>		<u>Page No.</u>
B-1	Structure Assembly - Composite Wing Center Section	B-3
B-2	Panel - Upper Skin Composite Wing Center Section, Assy Of	B-11
B-3	Panel - Lower Skin Composite Wing Center Section, Assy Of	B-12
B-4	Production Flow Diagram - Selected Configuration	B-13
B-5	Composite Wing Concept, Configuration Baseline	B-15
B-6	Wing Structural Concept - "Configuration C"	B-19
B-7	Wing Structural Concept - "Configuration C" Section Looking Aft	B-20
B-8	Production Flow Diagram - "Configuration C"	B-21

LIST OF TABLES

<u>Table</u>		<u>Page No.</u>
1	Laminate Allowable Strengths	18
2	Weight Summary L.H. Composite Wing Center Section From $\varnothing$ to $X_{WRS}$ 79.54	37
3	Comparison of Honeycomb Shear Strength and Modulus	47
4	Theoretical Vibration Results XFV-12A Composite Wing	63
5	Original $\varnothing$ Skin Splice Specimens - Test Results	73
6	Revised $\varnothing$ Skin Splice Specimens - Test Results	76
7	Cocured $\varnothing$ Skin Splice Specimens - Test Results	86
8	Short Beam Test Data for Interlaminar Shear of Graphite/Epoxy Laminates	125
9	Flight Condition Node Point Loading for Applied Airloads (Ult.)	129

## SECTION 1.0

### INTRODUCTION, SUMMARY, AND ACCOMPLISHMENTS

#### INTRODUCTION

The objective of the program was to design, fabricate and test a major section of graphite/epoxy composite wing box structure in order to evaluate the feasibility and effectiveness of graphite/epoxy composite construction for application to the XFV-12A V/STOL technology prototype currently being designed by Columbus Aircraft Division under Contract N00019-73-C-0053. Goals of the program included demonstration of significant weight savings through the use of composites; development of sound structural configurations compatible with operational aircraft requirements; development of tooling and fabrication techniques for efficient production of primary composite components and assemblies; and demonstration of inspection techniques to insure quality conformance of bonded graphite/epoxy composite assemblies. The program is to culminate in static strength tests of a major section of the wing box to be conducted at the Naval Air Development Center structural test facility.

Basic design ground rules of the program included the requirement for physical compatibility with the XFV-12A prototype aircraft including the capability to mount the composite wing on the existing wing to fuselage attachment fittings, provide for wing tip attachment of the existing vertical tail and main landing gear pod, and provisions for interface with existing fuel system and control system components. The wing box was to be designed for the same critical loading conditions as the XFV-12A and was to have sufficient stiffness to meet flutter requirements for the existing XFV-12A flight envelope.

The program was organized in eight task areas:

- o Task 1 - Design Criteria and Loads. This task included definition of the physical interface requirements of the XFV-12A aircraft, definition of critical design load conditions and stiffness requirements, and establishment of design stress limits for the selected graphite/epoxy laminates.
- o Task 2 - Design Concepts. This task included design studies and layout of three different concepts of wing box construction; the selection of a low risk construction concept compatible with state of the art manufacturing technology and in-service inspection requirements; detail design of a composite wing center section test specimen; and evaluation of anticipated weight savings.

PRECEDING PAGE BLANK-NOT FILMED

- o Task 3 - Material Selection and Specifications. This task included selection of graphite/epoxy prepreg tapes, film adhesives, glass/epoxy prepreg fabric, honeycomb core, potting compounds and preparation of material specifications.
- o Task 4 - Structural Analysis. Tasks performed in this area included finite element computer analysis of the wing box structure; EI and GJ stiffness calculation, development of efficient  $\angle$  joint configuration, sandwich panel buckling analysis; detail joint and fitting analysis; and flutter speed evaluation.
- o Task 5 - Design Development and Verification. This task consisted of coupon and element tests conducted to verify design allowables, develop detail joint configurations and evaluate effects of process variations on laminate strength. These tests included basic laminate strength;  $\angle$  joint configuration development; sandwich flatwise tension and edgewise compression tests; spar joint tests; evaluation of precured and cocured laminate strengths; and fastener installation tests in sandwich spar assemblies.
- o Task 6 - Tooling and Fabrication. All work associated with fabrication and assembly of the wing box<sup>v</sup> test section and test fixtures was performed in this task and included development of tooling and assembly concepts; fabrication of master patterns, layup tools and assembly fixtures; layup and cure of graphite/epoxy laminates; fit up and secondary bonding of honeycomb sandwich assemblies; machining of metal components; indexing and drilling of cover skins and sub structure; and installation of fasteners.
- o Task 7 - Quality Conformance. Tasks in this area were performed to insure quality control of all aspects of the composite wing box assembly from raw material procurement through final assembly. These tasks included incoming material certification; process specification and verification; coupon tests; honeycomb core prefit verification; NDI standards fabrication and ultrasonic through transmission "C" scan inspection of laminates and sandwich assemblies; and material review disposition of any defects.

- o Task 8 - Structural Demonstration. This task is to demonstrate the static strength capability of the composite wing box test section and is to be performed by Navy personnel at the Naval Air Development Center structural test facility. Strain gage instrumentation is to be installed and test loads representative of the critical landing and flight load conditions are to be applied. Strain gage data is to be compared with stress distribution predicted by analysis and an assessment of the box strength capability will be made. This testing and evaluation will conclude the present program and further testing of the box will be the subject of future developments.

The completed wing box test section shown in Figures 1 and 2 was shipped to the NADC structural test facility on 27 August 1976. Testing of the wing box has been delayed due to higher priority work in the test laboratory and it is anticipated that testing will begin early in 1977. An addendum will be made to this interim final report to document results of these tests.

#### SUMMARY

A composite wing box test section was designed and fabricated to meet the structural and functional requirements of the XFV-12A V/STOL aircraft. The selected configuration utilizes graphite/epoxy face sheet laminates and glass/phenolic honeycomb core sandwich construction in the cover skins, front spar, and intermediate spars. Solid laminate graphite/epoxy construction is used in the B.P. 33.93 kick load rib at the side of the fuselage and aluminum was selected for use in the  $\angle$  splice rib, rear spar and for local back-up of the aft wing to fuselage attachment fitting.

A combination of bolted and bonded joints is used in the assembly of the cover skins to the sub structure, bonded joints being utilized on the lower cover skin to spar attachments and bolted joint being used on the upper cover skin to spar attachments,  $\angle$  splice joint, aluminum rear spar and cover skin to rib attachment. Conventional fuel seal groove provisions are included in the upper cover to sub structure interface and the bolted attachment allows removal of the upper cover for inspection or repair. The bonded attachment of lower cover skins to spars minimizes the number of fastener holes in the tension skin thereby minimizing stress concentration locations in the lower cover skins. Rear spar fastener holes are subjected to a combination of high skin stresses and high bearing stresses, resulting in high stress concentrations which would unduly limit skin stress levels. The area over the rear spar was therefore "softened" by replacing all spanwise ( $0^\circ$ ) plies with  $\pm 45^\circ$  plies and sandwiching a glass/epoxy strip between the facing laminates. Glass strips were used in all bolted skin to spar joints and solid graphite/epoxy tapered laminates replaced the honeycomb core in all bolted skin to rib and  $\angle$  splice joints. Bonding of lower cover



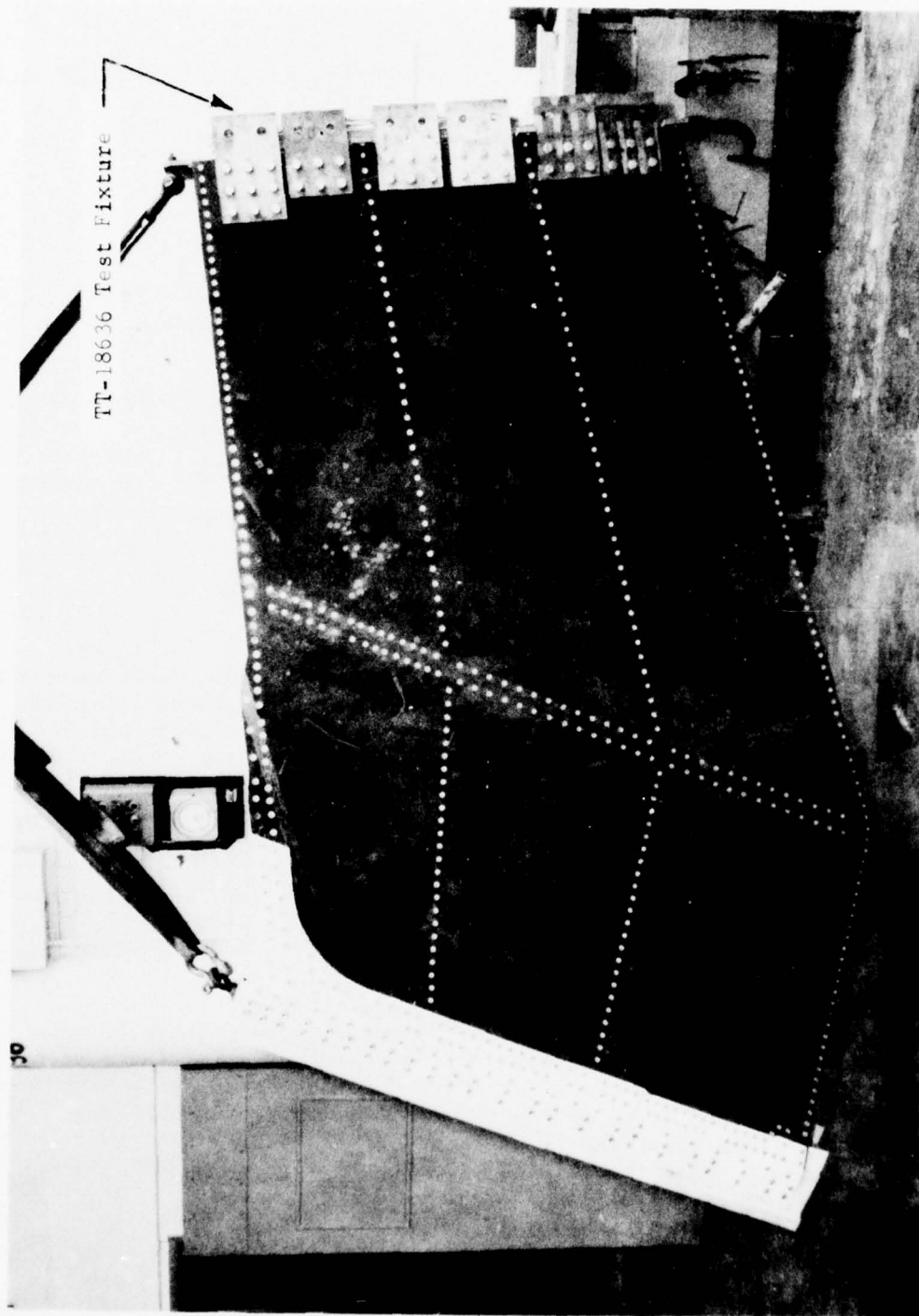


FIGURE 1 COMPOSITE WING BOX ASSEMBLY - TOP VIEW



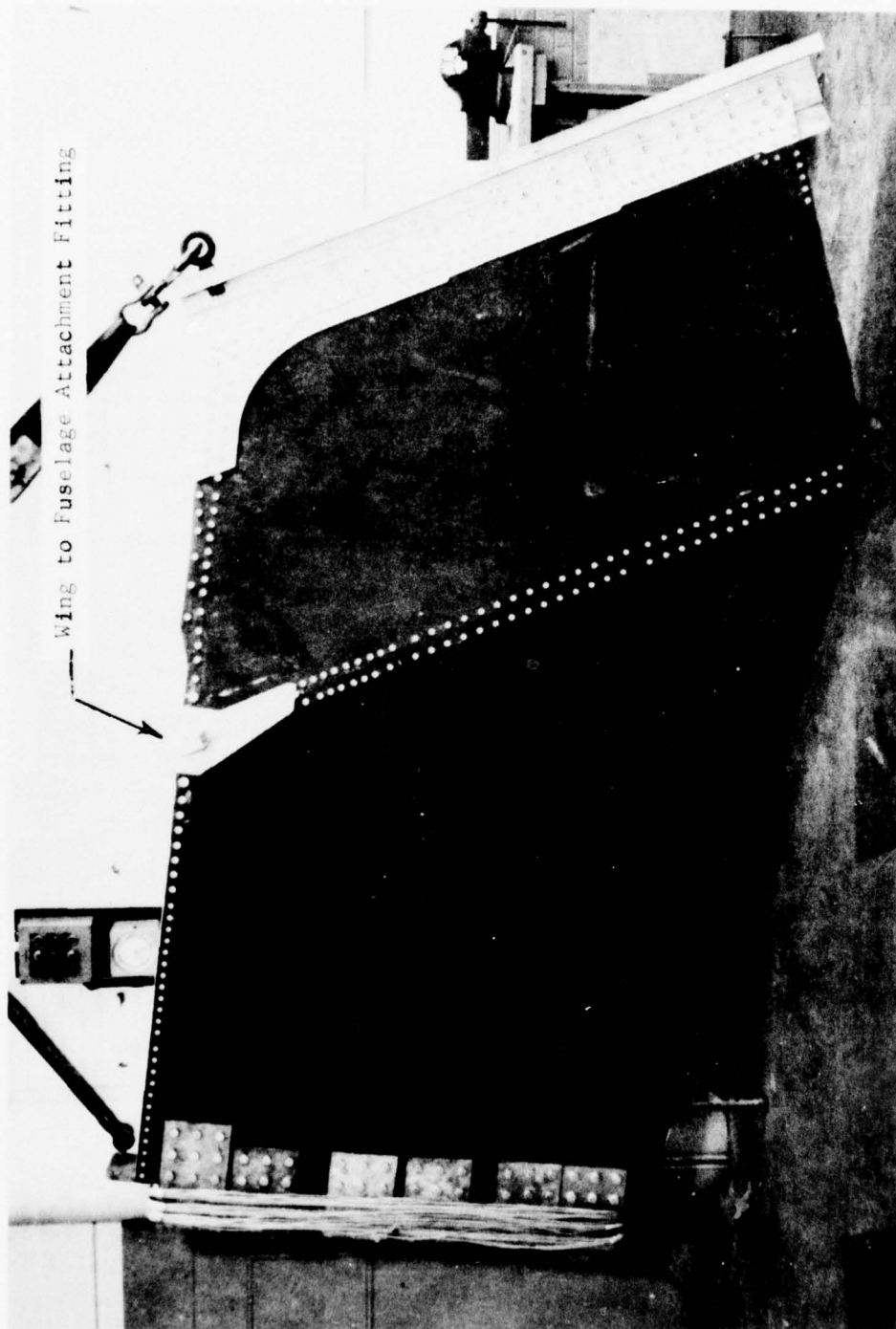


FIGURE 2 COMPOSITE WING BOX ASSEMBLY - BOTTOM VIEW

skins to the front spar and intermediate spars utilized the "captured fillet" principal for high flatwise tensile strength and element tests confirmed the load carrying capability of the selected joint configuration.

The sharp sweepback angle change of the rear spar at the centerline, necessitates a concentration of axial load material at the aft edge of the skin to control skin stresses at the edge. The large concentrated load that results is difficult to splice and a graphite splice would have entailed considerable risk. Aluminum was therefore selected. Similarly, aluminum was selected for the wing centerline rib to accommodate tapped inserts for the outer splice plate "kick-load" fasteners and to more efficiently incorporate an integral fwd wing-fuselage attach fitting. Back-up of the aft wing-fuselage attach fitting also was accomplished more efficiently and with less risk using aluminum alloy. Aluminum shear clips were used at the ends of spar webs and caps, with aluminum thickness selected to make fasteners bearing critical in aluminum, thus controlling fastener loads. Aluminum spar cap end clips with 5 to 6 fasteners attachments were used to provide cap continuity at rib intersections. Glass/phenolic "Fibertrus" core was utilized to give high shear strength and stiffness in the honeycomb sandwich panels. Glass core was selected in preference to aluminum to eliminate the concern over corrosion potential between aluminum and graphite.

Fabrication, assembly, and inspection of the composite wing box test section was accomplished at the Columbus Aircraft Division facility utilizing personnel and equipment normally engaged in the production of conventional reinforced plastic components and bonded structural assemblies. Layout and trim of all graphite/epoxy laminates was performed by hand utilizing a single master mylar template for ply trim. Successive plies were laid "black on black" to the specified orientation and ply pattern. Complex thirty-seven ply cover skin laminates were successfully assembled and autoclave cured in this manner without intermediate debulking steps. Rolled steel plate with back up framework was utilized as the layup and cure tool for the upper cover skins. Glass reinforced plastic tooling was utilized for the double contoured lower cover skin and curved one-piece front spar. Flat aluminum plate was utilized for the intermediate spar laminate layup, cure, and secondary honeycomb face sheet bonding. Machined Kirksite plates were utilized for the layup, cure, and secondary bonding of the B.P. 33.93 rib assembly. Secondary bonding of the front spar and intermediate spar caps to the lower cover skin was accomplished in the lower cover skin layup tool. A large drill cage fixture was constructed for indexing and drilling fastener holes for final assembly of the cover skins to substructure. Carbide drill bits and reamers were used with automatic feed drill motors to machine close tolerance fastener holes in the cover skins and substructure.

Principal quality conformance techniques utilized throughout the program consisted of incoming material certification, process monitoring, visual inspection, honeycomb prefit mark off records, and 100% inspection of all bonded assemblies by C-scan ultrasonic through transmission.

#### ACCOMPLISHMENTS

The most significant accomplishment of the program is the demonstration of a substantial weight saving in a primary aircraft structural assembly through the use of graphite/epoxy composite material. A weight reduction of 194 pounds or approximately 19% is projected for a complete Xfv-12A composite wing box when compared with an all metal design weighing 1037 pounds. This weight reduction estimate is based upon actual weight of the composite wing box test section extrapolated to the full span of the Xfv-12A wing box. It should be noted that principal stress levels in the composite wing box cover skin have been conservatively limited to a maximum of approximately 35,000 psi ultimate in this design and could probably be safely extended to 50,000 psi. The degree of conservatism in the design will be assessed after completion of static testing.

Other significant accomplishments of the program include:

- o Demonstration of capability to fabricate complex double curved airfoil surfaces and wing spars with graphite/epoxy sandwich construction. Examples being the severely contoured wing lower cover skin inboard of B.P.33.93 rib and the one-piece front spar with severe sweep angle change at B.P.33.93.
- o Development of a centerline splice joint configuration that transmits at least 94% of the full cover laminate load carrying capability. Cover skin material can therefore be efficiently utilized and is not limited by joint strength.
- o Development of a bolted cover design which allows removal of cover for inspection or repair, incorporates joint "softening" provisions for reduction of stress concentration, and includes integral fuel tank sealing provisions.
- o Investigated alternate design concepts which have potential for manufacturing cost saving and increased survivability capability in future aircraft. Examples being the filament wound spar concepts of configuration "C" and the full-depth sculptured Trussgrid core configuration with integral graphite/epoxy cover skins.

## SECTION 2.0

### DESIGN CRITERIA AND LOADS

#### 2.1 BASELINE DESCRIPTION

The baseline vehicle specified for evaluation of composite materials application on this program is the prototype version of the XTV-12A V/STOL aircraft currently being developed by the Columbus Aircraft Division of Rockwell International under Navy Contract N00019-73-C-0053.

Figure 3 illustrates the basic structural arrangement of the airplane and indicates the portion of primary wing box structure selected for restructuring in graphite/epoxy composite materials as described in this report. The prototype airplane is a research vehicle designed to demonstrate the thrust augmented wing concept for vertical take-off and landing capability with forward flight speed capability in excess of Mach 2.0. The current prototype vehicle utilizes aluminum alloy construction in the primary airframe components and titanium alloy in the hot gas ducts and augmentor surfaces of the wing and canard. Main landing gears and vertical tail surfaces are mounted to wing tip structure which attaches to the wing box at the existing fold rib.

The wing structure selected for evaluation of composite materials application is the primary torque box which includes that portion of the wing located between the front and rear spar and extending from the centerline of the airplane to the wing tip pod attachment. This portion of the wing forms a full span integral fuel cell and contains the wing to fuselage attachments. A three-point attachment is used for mounting the wing box to the fuselage, with a single front spar attachment located at the centerline of the airplane and a rear spar attachment at each side of the fuselage. The wing is positioned on the top of the fuselage with a constant  $10^\circ$  anhedral angle extending from the centerline outboard. A sharp break in the lower wing surface contour exists inboard of the side of the fuselage at B.P.33.93 due to wing clearance requirements above the engine. The rear spar plane extends outboard from the centerline at a constant sweep angle of  $28.35^\circ$  while the front spar extends from the centerline to B.P.33.93 at an angle of  $10.26^\circ$  and from B.P.33.93 outboard at a sweep angle of  $38.89^\circ$ . Maximum chord height of the wing mold line is 7.28 inches at the centerline rib, 12.40 inches at the B.P.33.93 rib and 4.80 inches at wing tip attachment rib. This basic wing box configuration is illustrated in Figures 4 and B-5.

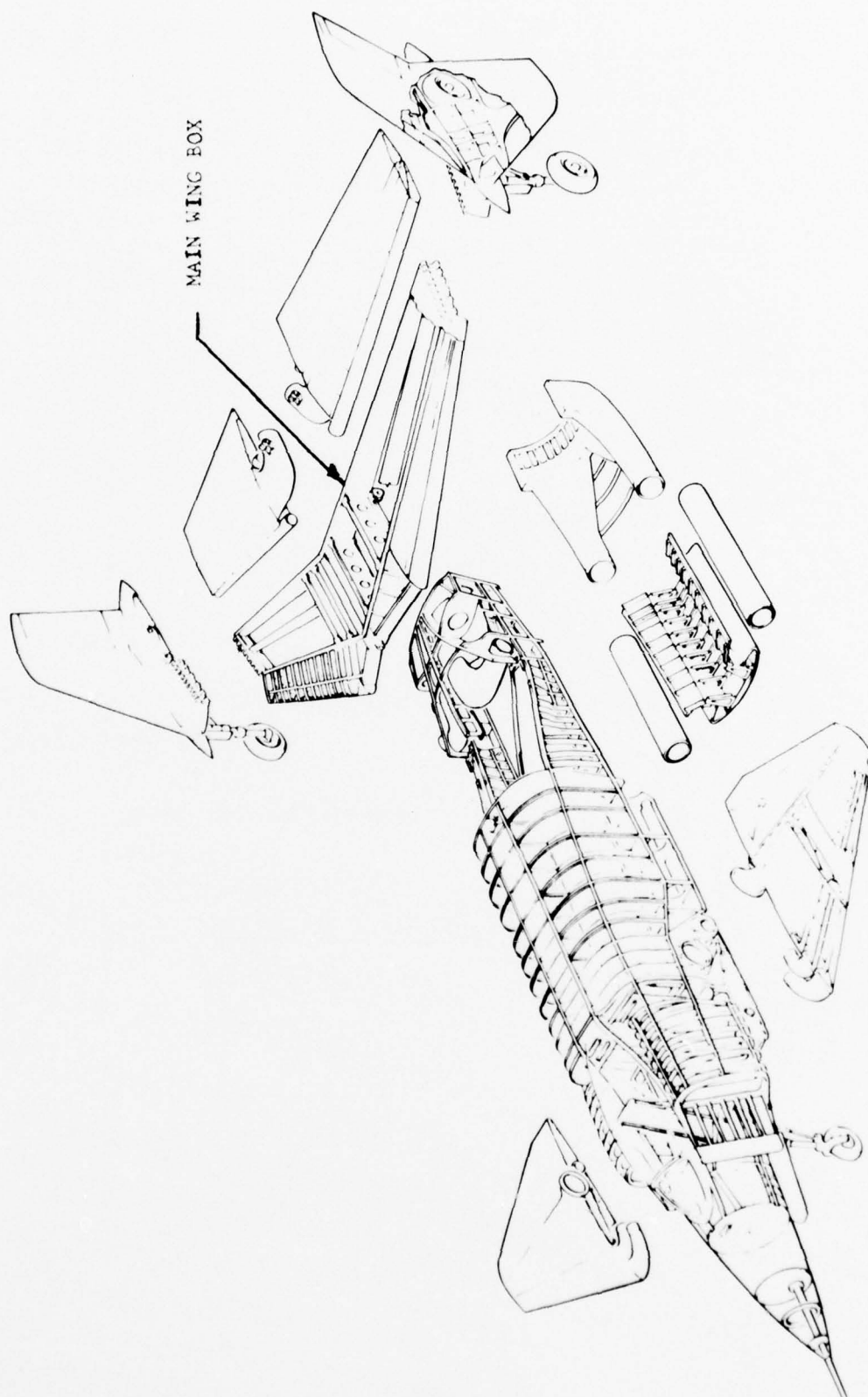


FIGURE 3 XFV-12A STRUCTURAL ARRANGEMENT



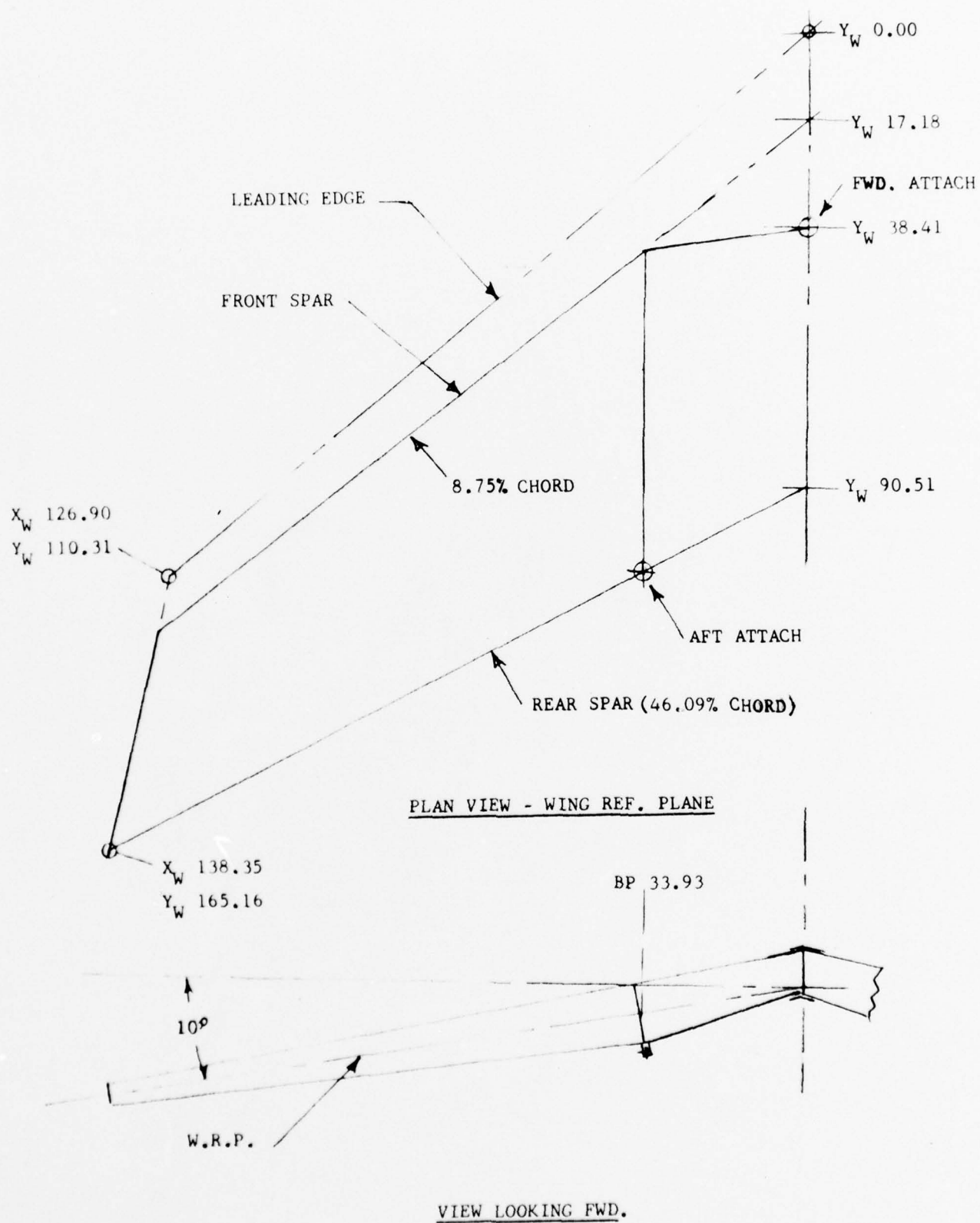


FIGURE 4 XFV-12A WING BOX GEOMETRY



Baseline physical interface ground rules specified that the existing Xfv-12A external mold lines be preserved in the composite wing box design and that the wing supports be capable of attachment to the existing Xfv-12A fuselage wing mount fittings. Provisions were also to be included for interfacing with the Xfv-12A wing tip pod and the Xfv-12A fuel system and control system installations.

Elevated temperature effects were not considered to be a significant design influence in the Xfv-12A wing torque box. The hot augmentor surfaces located aft of the rear spar are separated from the wing box structure by a cove fairing and wing box structural temperatures in this area are expected to be less than 200°F during "V" landing and take-off operational periods. The front spar is located sufficiently aft of the leading edge to limit wing box temperatures to less than 200°F for aerodynamic heating effects at flight velocities up to Mach 2.0. The engine bay area beneath the wing lower surface is ventilated and wing structural temperatures in this area are also expected to be less than 200°F. A 350°F curing prepreg and adhesive system was selected for fabrication of the composite wing box and it is considered that these materials will provide adequate strength and stiffness throughout the range of temperatures to be experienced in the wing box structure. Laminate stress levels have been conservatively limited in the design of the wing box test section as noted in Para. 2.4 to provide a margin of safety against potential strength degradation effects of moisture and thermal cycling.

## 2.2 DESIGN LOAD CONDITIONS

Two design load conditions were determined to be critical for the composite wing and are defined as follows:

### (1) MAX VERTICAL LANDING CONDITION

Landing Design Weight = 16,500 Lb.

Sink Speed,  $V_v$  = 14.4 fps

Vertical Load Factor,  $N_z$  = 2.95 g

$\theta = 4.0$  Deg,  $\dot{\theta} = 1.8$  Deg.

$\ddot{\theta} = -1.318$  rad/sec<sup>2</sup>

$N = -0.18$  g

$\ddot{\phi} = 14.179$  rad/sec<sup>2</sup>

$\dot{\phi} = .324$  rad/sec

$\dot{\phi} = -.337$  rad/sec

② CONDITION NO. 470303

SYMMETRICAL PULL-UP FLIGHT CONDITION

Flight Design Weight = 17,500 Lb.

$M = 0.96$ ,  $\alpha = 3.5^\circ$  (angle of attack)

$N_z = 6.5$  g,  $h = \text{Sea Level}$

The landing load condition produces the maximum operational landing gear loads on the aircraft which are considered as "ultimate" loads in the structural analysis. The flight load condition listed above is a maximum "limit" load condition. Ultimate shear, bending and torque loads in the wing box for these two load conditions are shown in Figures 5, 6, and 7. From these curves it may be seen that the wing tip mounting of the landing gear results in generally higher loads throughout the wing box due to max sink speed landings than the maximum symmetrical pull-up flight condition. A NASTRAN structural model was developed for the composite wing box as defined in Para. 5.1 and distributed grid node point loads were defined for these two critical loading conditions. The NASTRAN analysis shows that the landing condition produces the critical stresses and joint loads throughout the wing box structure.

The applied shear, moment, and torque curves presented in this section are for the total wing for comparison only. For actual applied test loads to the wing box test section refer to Section 9.0.

2.3 STIFFNESS REQUIREMENTS

Stiffness requirements for the composite wing were based on the requirements for the production FV-12A wing although physical compatibility was maintained with the prototype XFV-12A. The FV-12A requirements are shown in Figure 8 in addition to the existing bending and torsional stiffness inherent in the prototype XFV-12A wing. The higher values shown in Figure 8 for the prototype wing are not significant and do not represent a design criterion. This is due to the use of an F-4 wing box on the metal prototype airplane where this wing box had inherent stiffness and strength above that required for the XFV-12A prototype. The design requirements are represented by the lower curves of Figure 8 for the FV-12A. However, the primary effect of wing bending and torsional stiffness is on the flutter speed where this is discussed in Section 5.5.

A comparison of bending and torsional stiffness distributions for the prototype XFV-12A wing and the composite wing is shown in Figure 8 in addition to the bending and torsional stiffness requirements for the FV-12A production wing. The composite wing bending and torsional stiffness exceeds these requirements except for EI in the outboard region. However, torsional stiffness (GJ) is critical in this area and exceeds the required torsional stiffness.

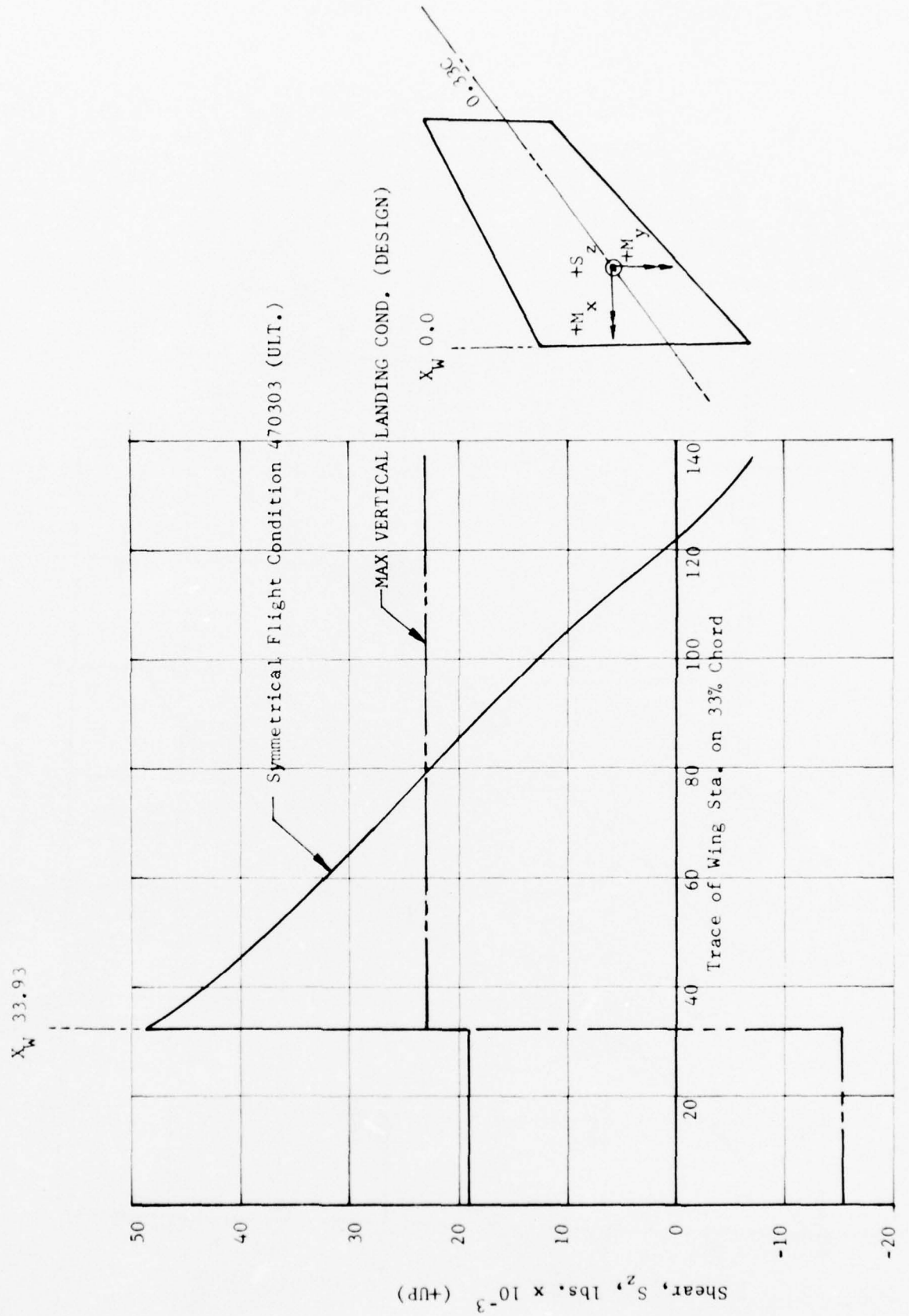


FIGURE 5 CRITICAL CONDITION DESIGN SHEAR CURVES

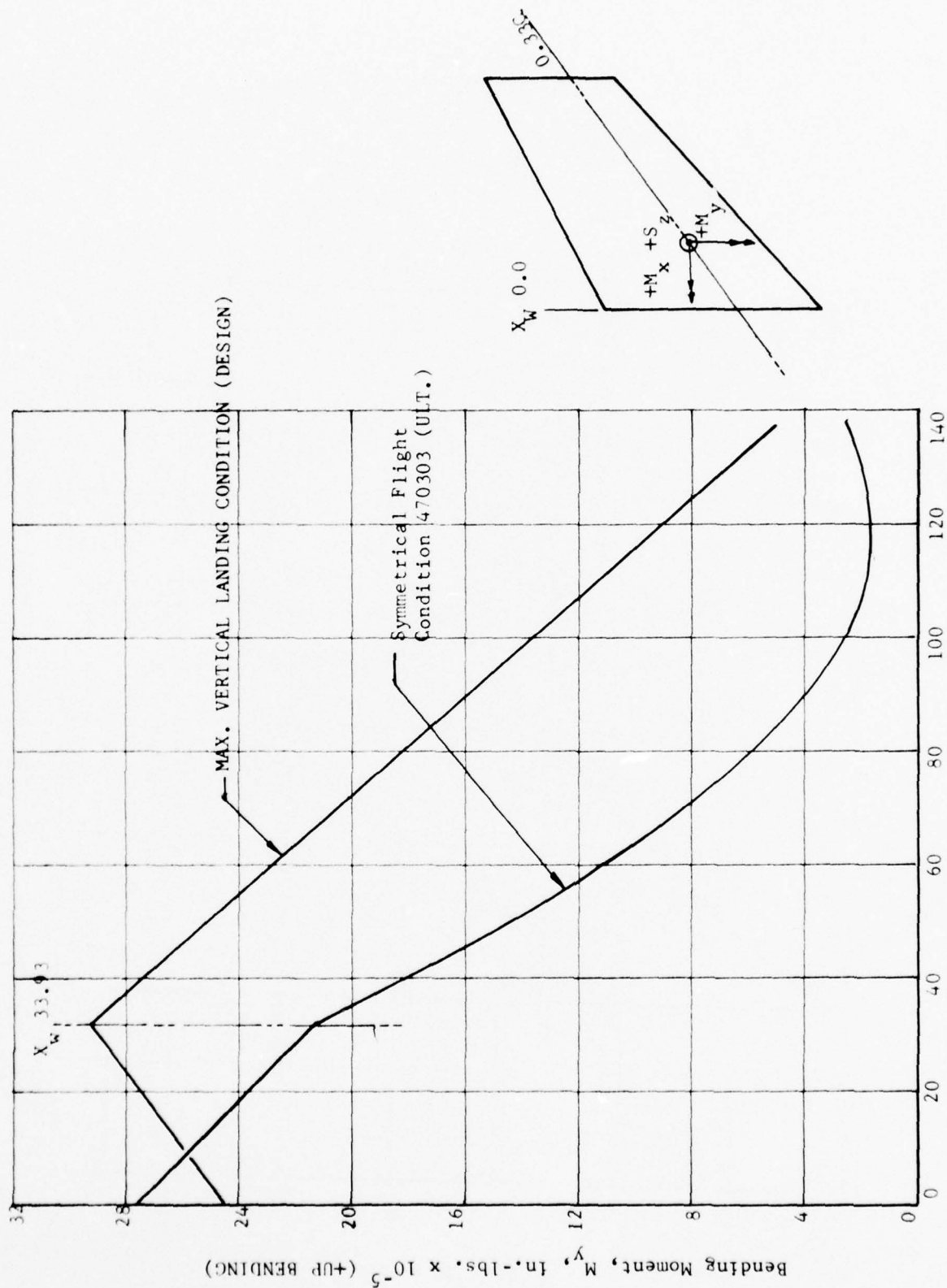


FIGURE 6 CRITICAL CONDITION DESIGN BENDING MOMENT CURVES

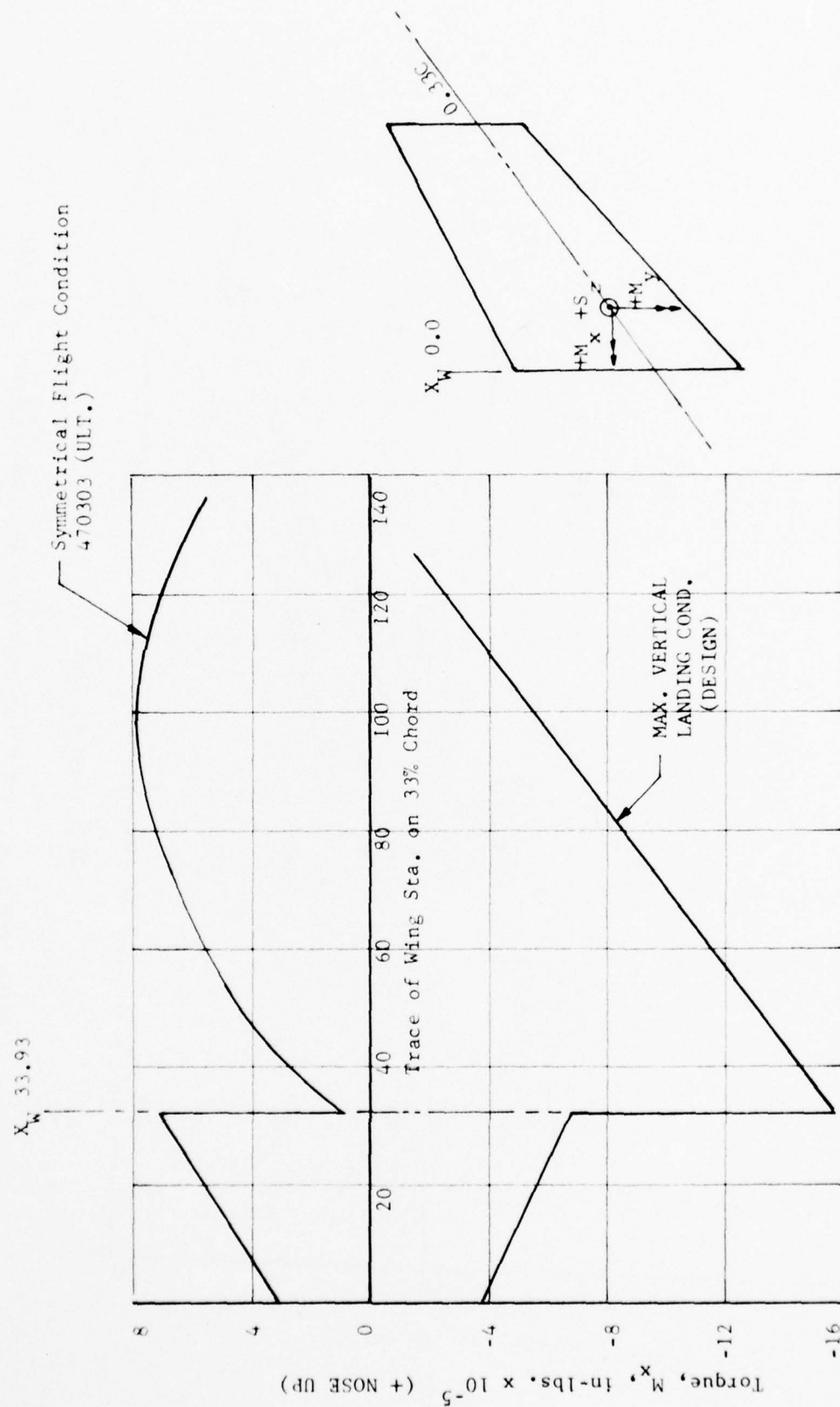


FIGURE 7 CRITICAL CONDITION DESIGN TORQUE CURVES



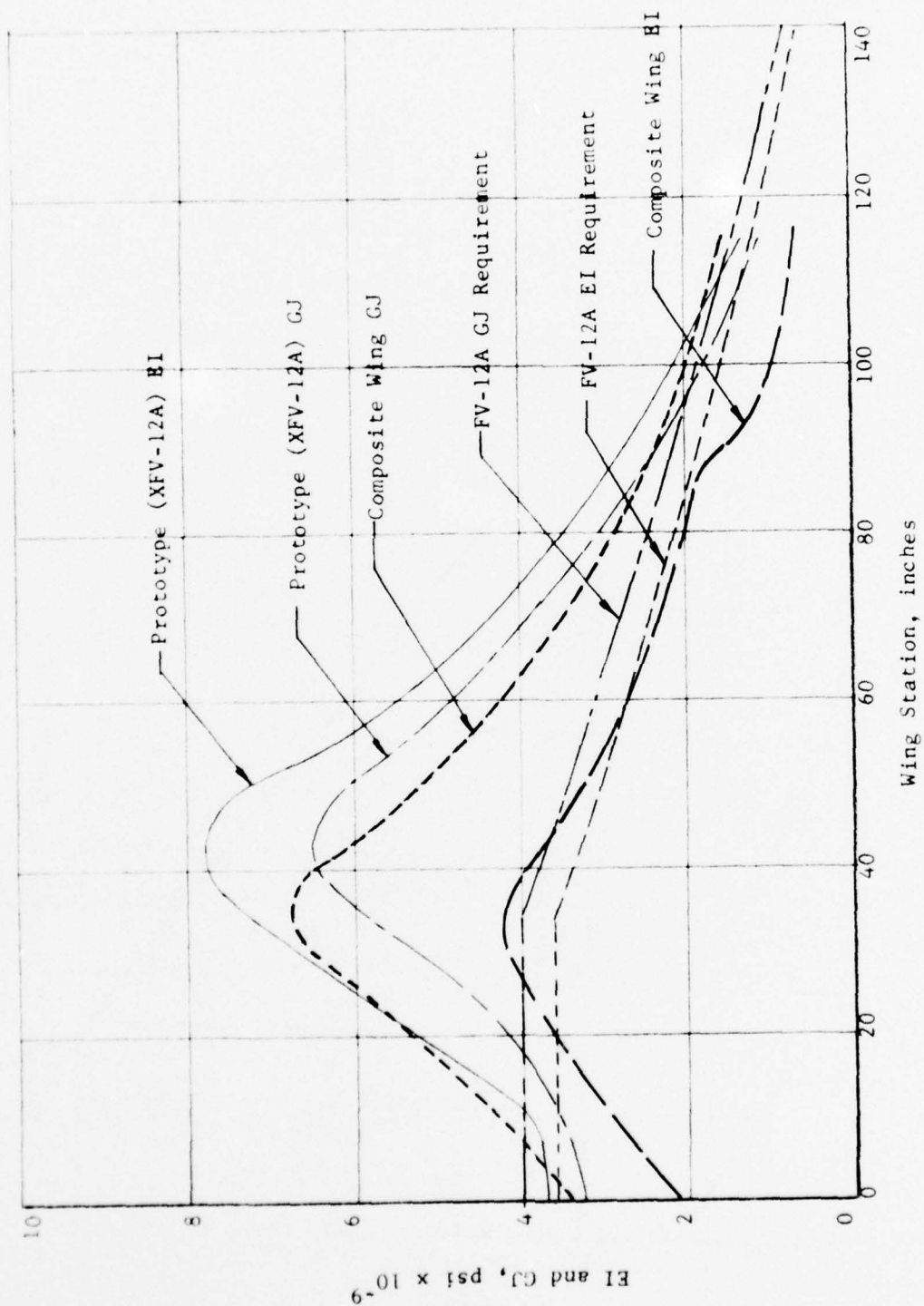


FIGURE 8 WING BENDING AND TORSIONAL STIFFNESS REQUIREMENTS AND COMPOSITE WING STIFFNESS

## 2.4 ALLOWABLE STRESSES

Allowable stresses for the graphite/epoxy laminate were based on properties obtained from the "Advanced Composite Design Guide," Volume I except in specific cases where test data from the design development tests of Section 6.0 were used to verify design stresses or loads. The primary areas which used test data to verify design values included the centerline splice joint which was mechanically fastened, flatwise tension data obtained to simulate pressure loading on the sandwich panel, and the shear strength of bonded and mechanically fastened joints between the upper and lower intermediate spar caps and the cover panels. Sandwich panel buckling allowables were determined by the methods described in Volume II of the "Advanced Composites Design Guide" for bi-axially loaded panels utilizing the basic panel buckling equation:

$$(N_x)_{cr} = \frac{K_x \pi^2 \sqrt{D_{11} D_{22}}}{b^2}$$

where

$$D_{11} = \frac{E_x t_f c^2}{2 (1 - \nu_{xy} \nu_{yx})} \left( 1 + \frac{t_f}{c} \right)$$

$$D_{12} = D_{11} \frac{E_y}{E_x}$$

The buckling constant  $K_x$  was determined and detailed sizing calculations were performed by means of the AC-5 computer program for crossplied filamentary laminates sandwich buckling.

In general the laminate design stress levels were maintained comfortably below the allowable stresses throughout the wing box to insure success in demonstrating the static strength capability of the wing box test specimen and to provide a margin of safety against potential environmental degradation effects of moisture absorption and thermal cycling. Stress levels in the cover skin laminates were reduced from an initial maximum principal stress value of approximately 50,600 psi to approximately 35,000 psi in the final configuration sizing. This stress reduction was achieved primarily by beef-up of the aluminum rear spar caps and thus a convenient method is provided for future evaluation of higher stress levels in the cover skins by installation of a redesigned lightweight rear spar. Strain gage monitoring of critical stress areas of the wing box during static load test will determine the degree of conservatism in the design.

For design and analysis purposes of the basic cover panel areas defined in Figure 9 the basic laminate strength values of each area were defined by cross-ply laminate curves in the Advanced Composites Design Guide. Stacking sequences for the critical areas are shown in Figures 10 through 14. Essentially, six sets of  $[\pm 45]$  plies were used to obtain the required torsional stiffness (GJ) and augmented by  $[0]$  plies to obtain the required spanwise axial load capability for the skins. The addition of  $[0]$  plies varies in the critical areas according to the stacking sequences shown in Figures 10 through 14 where higher concentrations of  $[0]$  plies are included in the aft inboard areas of the skins in the area of high spanwise axial loads. The outboard portion of the wing includes higher concentrations of  $[\pm 45]$  plies for increased torsional stiffness. Basic material allowables for the critical inboard laminate areas are shown in Table 1 as determined from the Advanced Composites Design Guide.

TABLE 1 LAMINATE ALLOWABLE STRENGTHS

Panel (Ref. Fig. 9)	Laminate Orientation	Laminate Properties				
		$F_x^{tu}$ $\text{psix}10^{-3}$	$F_x^{cu}$ $\text{psix}10^{-3}$	$F_{xy}^{su}$ $\text{psix}10^{-3}$	$E_x$ $\text{psix}10^{-6}$	$G_{xy}$ $\text{psix}10^{-6}$
K	80% $[\pm 45]$ , 20% $[0]$	54	54	54	6	4.5
L	71% $[\pm 45]$ , 29% $[0]$	69	69	48	8	4
M	67% $[\pm 45]$ , 33% $[0]$	75	75	47	8.5	3.8
O	75% $[\pm 45]$ , 25% $[0]$	61	61	51.5	7	4.25
P	71% $[\pm 45]$ , 29% $[0]$	69	69	48	8	4

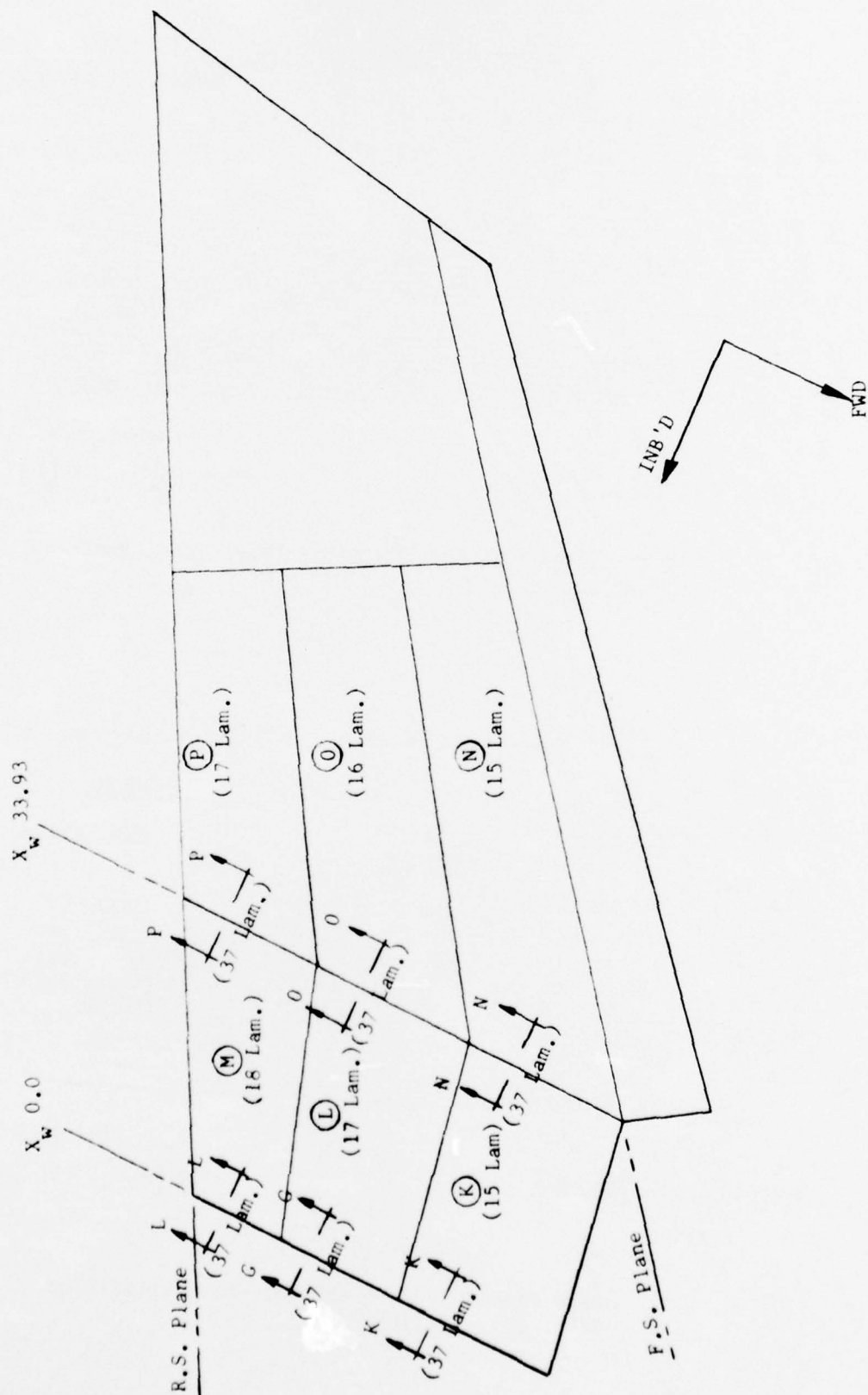
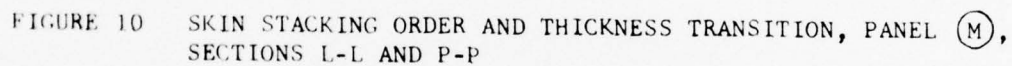
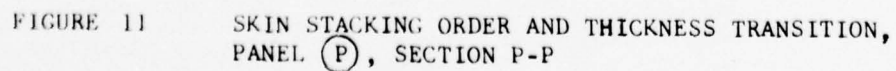


FIGURE 9 CODE FOR SANDWICH SKIN LAMINATE STACKING ORDER

X<sub>w</sub> 33.93 (SECT. P-P)

 $X_w = 33.93$ 



$X_W$  0.0 (SECT. G-G)  
 $X_W$  33.93 (SECT. O-O)

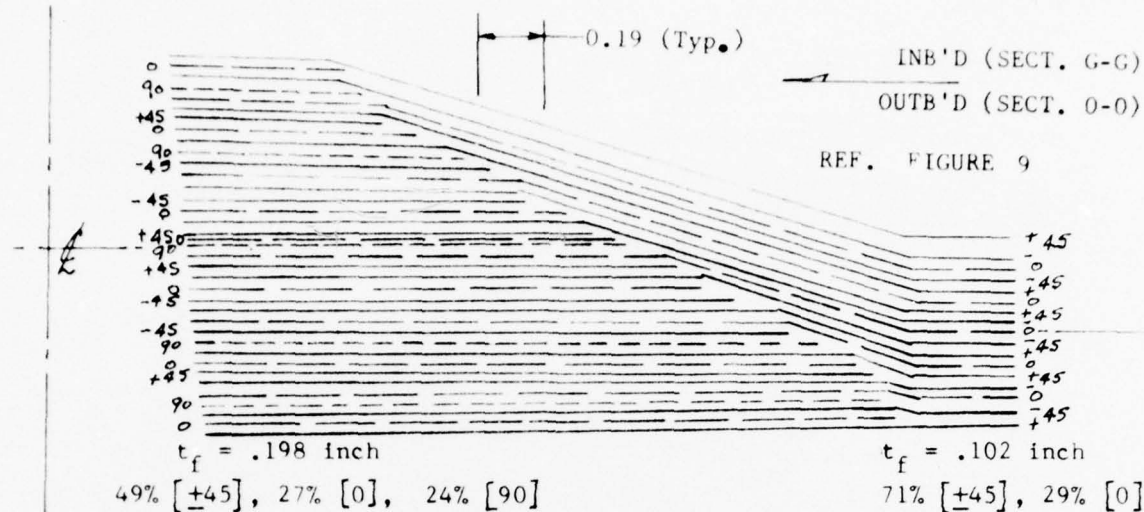


FIGURE 12 SKIN STACKING ORDER AND THICKNESS TRANSITION, PANEL (L), SECTIONS G-G AND O-O

$X_W$  33.93

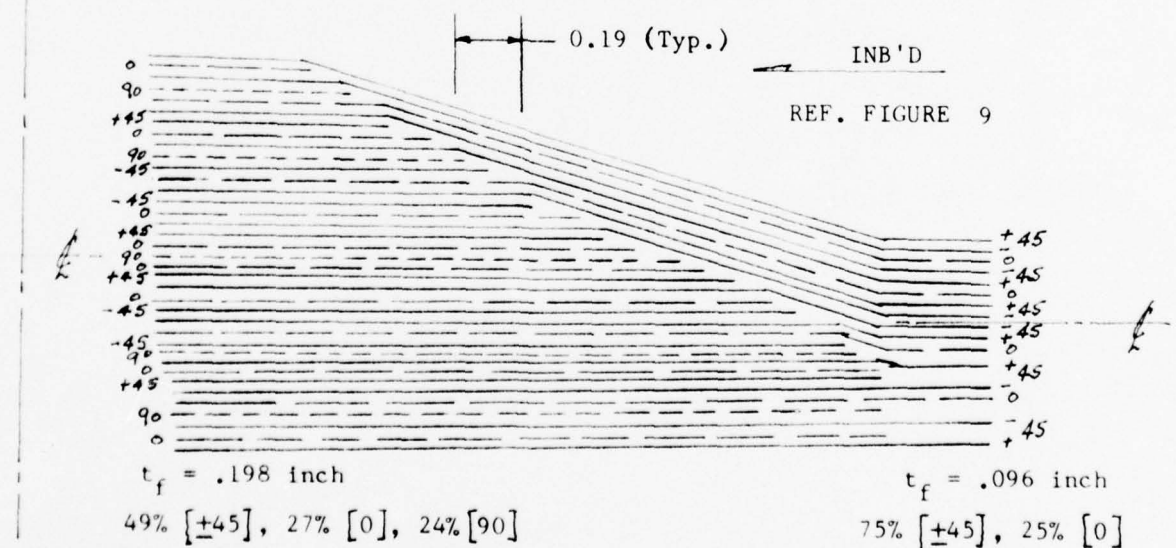


FIGURE 13 SKIN STACKING ORDER AND THICKNESS TRANSITION, PANEL (O), SECT. O-O

$X_w$  0.0 (SECT. K-K)

$X_w$  33.93 (SECT. N-N)

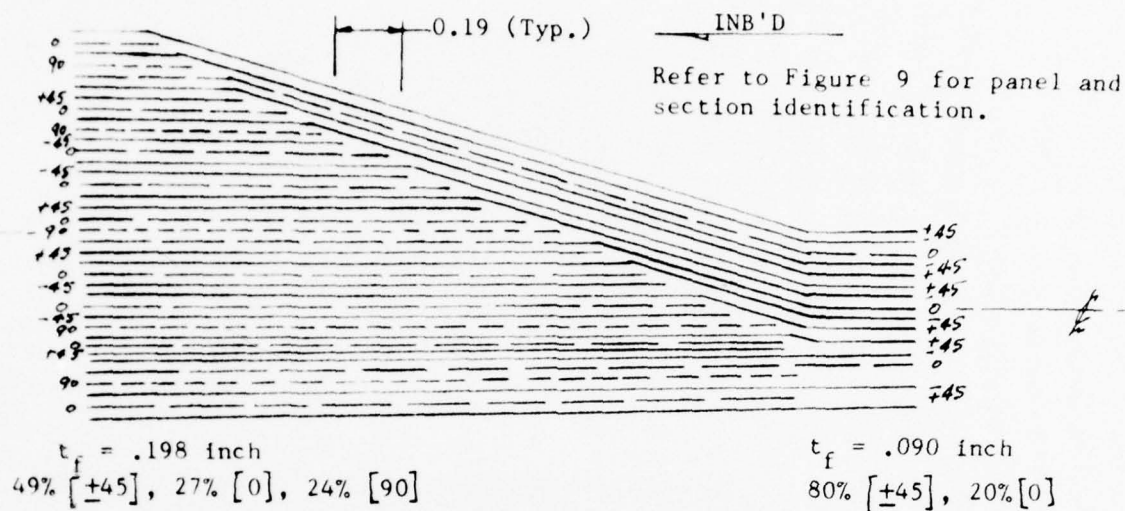


FIGURE 14 SKIN STACKING ORDER AND THICKNESS TRANSITION, PANELS (K) AND (N), SECTIONS K-K AND N-N

## SECTION 3.0

### DESIGN CONCEPTS

Three basic design concepts for construction of the composite wing box were considered during this program. The first of these was a fully bonded 3-cell sandwich construction in which three spar "boxes" were laid up and cured on wash out mandrel tooling, secondarily bonded together and covered with outer graphite/epoxy face skin laminates. The second concept was a fully bonded construction utilizing full-depth Trussgrid honeycomb core covered with a wrap-around graphite/epoxy skin. The third concept shown in Figure 15 is a 3-cell sandwich construction which utilizes individual cover skin panels, spars and ribs assembled with a combination of bonded joints and mechanical fasteners. The third concept was selected for design of the wing box test section because the mechanically fastened upper cover skin offered the capability for inspection of all bonded joints and surfaces at all stages of the fabrication and assembly and can be disassembled for field inspection and/or repair. Concept 1 and 2 offer the potential for increased weight saving and/or cost saving over concept 3, however, concept 3 offered a lower risk approach and would be more readily accepted in near term aircraft programs. Section 3.1 presents a description of the selected design configuration and Section 3.2 lists the salient features of the alternate design concepts. Detail drawings of the wing box test section are presented in Appendix B.

#### 3.1 SELECTED CONFIGURATION

##### 3.1.1 Cover Skins

The upper and lower cover skins are similar in construction and consist of 1/8 cell, 5.5 lb/Ft.<sup>3</sup> glass/phenolic "Fibertruss" honeycomb core faced with graphite/epoxy laminates. Glass/phenolic core was selected in preference to aluminum honeycomb core to eliminate the concern over a corrosion potential between the aluminum core and the graphite/epoxy face sheet laminates. "Fibertruss" core material was selected in preference to conventional glass/phenolic core because of its superior shear modulus which provides increased sandwich panel buckling stability. Constant core height was used in each cover skin assembly for manufacturing simplicity with the lower cover core height being 0.226 inches and the upper cover core height being 0.418 inches. Core height for these panels was determined by sizing for panel compression buckling stability and internal fuel pressure loads. It should be noted that the honeycomb core is replaced at all bolted ribs and spar interfaces with either graphite/epoxy or glass/epoxy solid laminate material. Chordwise rib interfaces use tapered graphite laminate build up with mating tapered core interface and spanwise spar interfaces use rectangular glass/epoxy inserts for joint "softening".

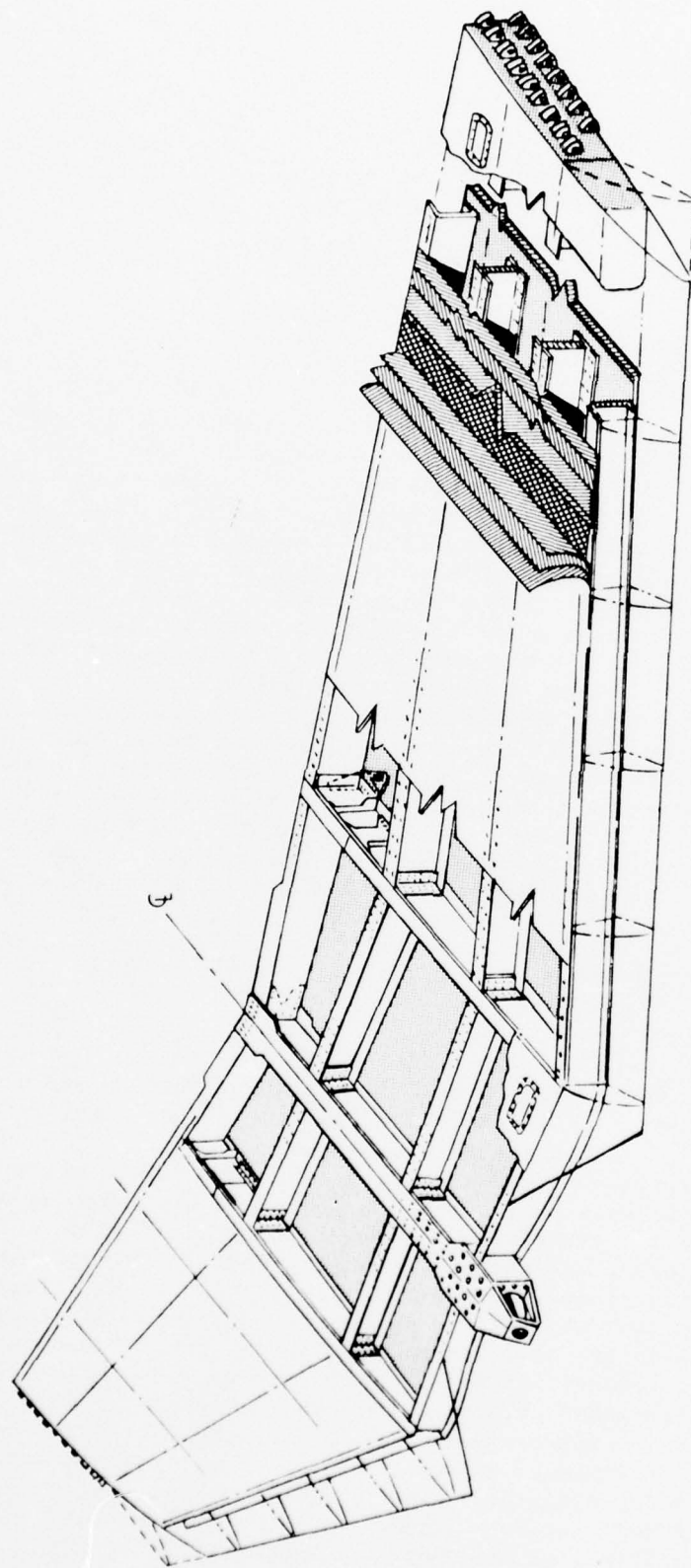


FIGURE 15 XFV-12A COMPOSITE WING BOX STRUCTURE



Face sheet laminates are essentially identical for the upper and lower cover skins, with the exception of mold line contour, with each inner and outer face sheet containing a maximum of thirty-seven plies of 0.0055 inch thick graphite/epoxy tape. Each of the inner and outer face sheet laminates is built up from a basic arrangement of six sets of  $\pm 45^\circ$  plies which satisfy the basic GJ torsional stiffness requirements and are augmented for axial load carrying capability by three  $0^\circ$  plies in areas K, N; four  $0^\circ$  plies in area O; five  $0^\circ$  plies in areas P, L; and six  $0^\circ$  in area M of the wing test box as shown in Figure 9. Additional  $\pm 45^\circ$  plies were added in the wing box analysis outboard of rear spar station 79.54 to provide increased GJ stiffness in the outer portions of the wing cover skins.

The ply stacking order for these cover skin laminates is shown in Figures 10 through 14 and is arranged to produce a completely balanced laminate with  $\pm 45^\circ$  outer plies and  $0^\circ$  plies between each set of  $\pm 45^\circ$  plies adding up to a total thickness of 18 plies (0.099 inch) in area M. The  $0^\circ$  plies were omitted in the area of the rear spar attachment screws and replaced with  $\pm 45^\circ$  plies to reduce stress concentrations at the bolt interface. At the centerline splice joint, additional plies of  $0^\circ$ ,  $\pm 45^\circ$  and  $90^\circ$  are interleaved to produce a tapered laminate build up to 37 plies at the bolted rib interface as shown in Figure 9. This tapered ply build up is designed to reduce the net laminate stress at the bolt holes, reduce the stress concentration factor at the bolt hole and provide a smooth load transition through 0.19 inch ply steps between the bolted joint area and the basic skin laminate. Test development of this joint is discussed in Section 6.0. This same 37 ply bolted joint laminate build up is utilized at the B.P. 33.93 rib attachment and the rear spar station 79.54 test load joint.

Twelve inch wide graphite/epoxy prepreg tape was used for the construction of these sandwich cover skin laminates and each face skin was cured separately and secondarily bonded to the core to form a honeycomb sandwich panel assembly as described in Section 7.0. The total sandwich thickness of the lower skin is 0.408 inch (74 plies) at the rib joints and varies between 0.391 inch and 0.424 inch in areas depending on laminate thickness 15 ply, (0.825) inch to 18 ply (.0990 inch) with constant core height of 0.226 inch. The sandwich thickness of the upper skin is 0.601 inch (74 plies + 0.193 inch glass/epoxy insert) at the rib joint and varies between 0.583 and 0.616 in various areas of the panel. In the design of the tooling for these panels the mold line surface is maintained and the inner sandwich surface location is dependent on the build up of laminate and core thickness.



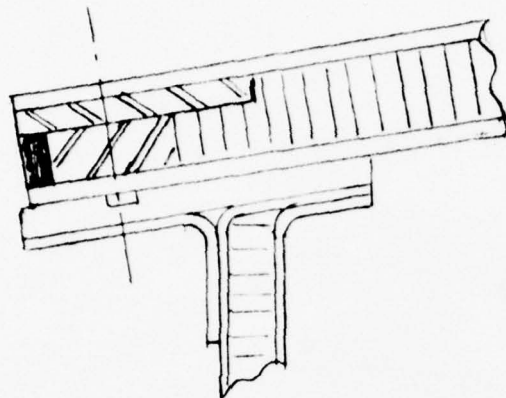
Glass/epoxy inserts are included in the upper cover skin sandwich panel assembly at all bolted spar joints as shown in Figure 16. At the front and rear spars the honeycomb core is completely replaced with the glass inserts to provide additional bolt bearing area, clamp-up bearing strength, "softening" of the graphite/epoxy bolt interface and sufficient material for countersinking of the screws. At the intermediate upper cover spar joints the core is removed to a depth of 0.10 inch and replaced with a glass/epoxy insert which provides sufficient material for countersinking and installation of O-ring fuel seals. The remaining core material in this area is filled with a lightweight epoxy potting compound to provide sufficient stability for fastener clamp up.

Glass/epoxy inserts also replace the core in the upper cover skins at all bolted rib joints between the 37 ply graphite/epoxy skin laminate buildups as shown in Figure 16 to provide a solid bolt clamp up with good interlaminar shear transfer capability. Glass/epoxy inserts replace the core in the lower cover skin sandwich assembly only at the bolted rear spar attachment. Bolts are used in the lower cover skin attachment to the center line splice rib and B.P. 33.93 rib with the 37 ply graphite/epoxy buildup of the inner and outer facings providing the total sandwich thickness (74 plies = .408 inch). Detail drawings of the upper and lower cover skin panels are presented in Figures B-2 and B-3.

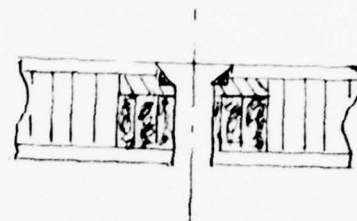
### 3.1.2 Front Spar

As noted in Section 2.0 the front spar contains a sharp change in sweep angle outboard of B.P. 33.93 rib and several concepts were investigated for splicing the spar at this joint with a separate inboard and outboard spar section. All of these concepts proved to be heavy and require many separate pieces due to the requirement for providing fuel sealing provisions at all joints. A one-piece spar extending from root to tip was finally selected for this component and is considered to be a significant improvement over a two-piece spar design from the standpoint of weight, cost, and fuel sealing reliability. A 9.00 inch radius transition section was used to change the spar sweep angle at B.P. 33.93 and it proved feasible to lay up the basic spar channel section to this relative severe contour change utilizing three inch wide graphite/epoxy tape hand worked to the mold shape.

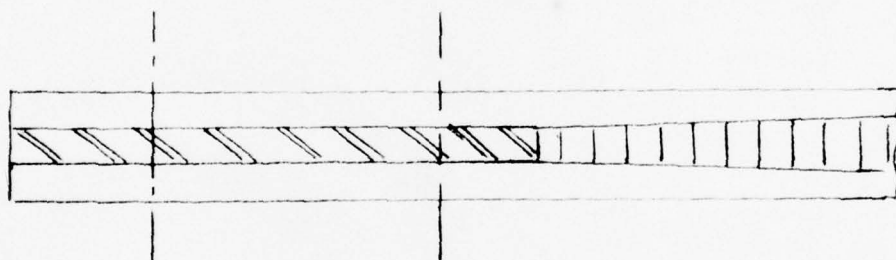
The spar design consists of a glass/phenolic honeycomb core faced with  $\pm 45^\circ$  graphite/epoxy skin laminates and  $\pm 45^\circ$  spar caps as shown in Figure 17. A constant core height of 0.25 inch is used with ten ply  $\pm 45^\circ$  skin laminates to satisfy the GJ stiffness requirements of the wing box while providing sufficient shear buckling strength along the full span of the spar. The lower caps of the spar are formed as an aft facing angle extension of the spar skins combined with a forward facing secondarily bonded ten ply  $\pm 45^\circ$  laminate angle section. This double flanged cap



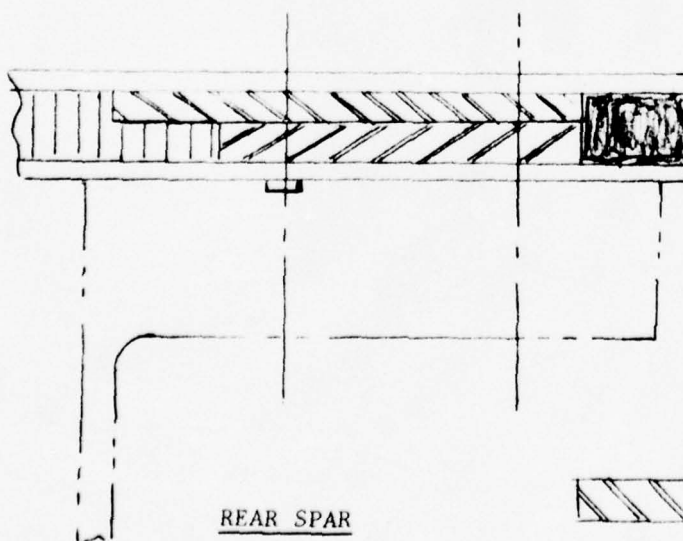
FRONT SPAR



INTERMEDIATE SPAR



RIB ATTACHMENT



REAR SPAR



GLASS/EPOXY FABRIC



EPOXY POTTING COMPOUND

FIGURE 16 UPPER COVER SKIN PANEL INSERTS

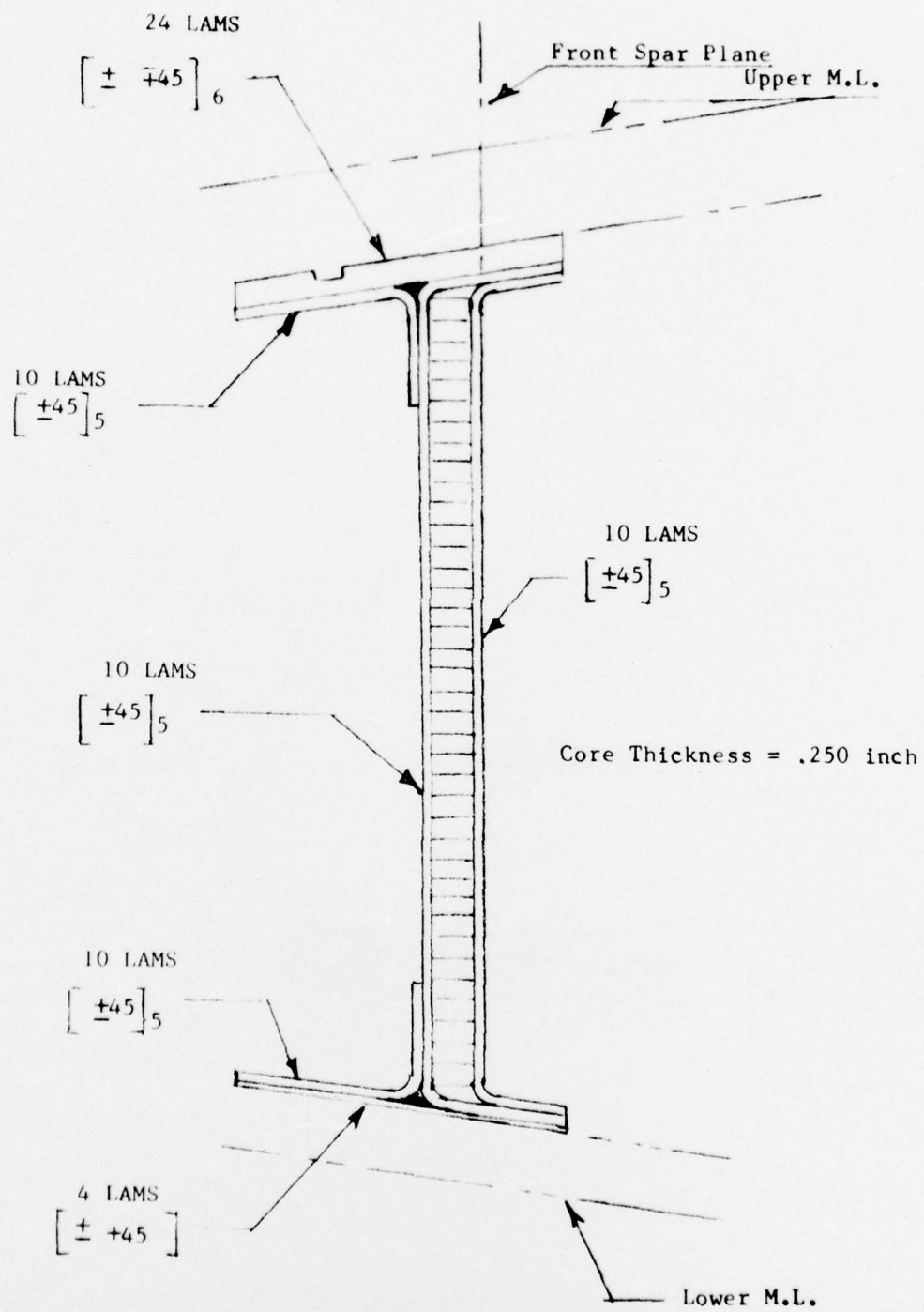


FIGURE 17 TYPICAL FRONT SPAR SECTION

provides a peel resistant joint for the secondarily bonded attachment of the spar to the lower cover skin. The upper spar cap is similar to the lower cap but includes an additional 24 ply  $\pm 45^\circ$  graphite/epoxy strap for clamp-up of the upper cover attachment screws. The additional thickness in the upper cap is required for machining of an .050 inch x .188 inch fuel seal groove and to provide sufficient rigidity to maintain clamp-up pressure between fasteners. The honeycomb core is replaced with glass/epoxy laminates at each end of the spar and at B.P. 33.93 rib to allow installation of fuel tight rib attachment bolts and O-rings.

### 3.1.3 Intermediate Spars

Two intermediate spars are located between the front and rear spars. The function of these spars is to carry wing box shears, react internal fuel pressure loads and stabilize the compression cover skins. These intermediate spars are spliced at the B.P. 33.93 rib and attached to the ribs at each end with aluminum clips. Construction of the intermediate spars is similar to the front spar with the exception of the spar caps which are fabricated as separate pieces and mechanically fastened to the spar web as shown in Figure 18. The concept of mechanically attaching the spar caps to the web was selected to simplify the wing box final assembly and allow for tolerance build up between the inner surfaces of the sandwich cover skins.

The lower spar caps consist of a  $0/\pm 45/90$  laminate U-shaped center section with  $0/\pm 45/90$  laminate angle sections on each side to provide a peel resistant double flanged joint with captured fillet when secondarily bonded to the lower cover skin. The upper spar caps consist of a single U-shaped laminate built up of  $0^\circ$ ,  $\pm 45^\circ$ ,  $90^\circ$  plies. Floating nutplates are installed within this cap to mate with the upper cover skin attachment screws. Mechanical attachment of the upper cap to the spar web allows pilot hole indexing of the nutplate locations with the upper cover fastener holes prior to subsequent installation of the spar web and cover skin fasteners. Graphite/epoxy caps are utilized in the spars inboard of B.P. 33.93 and glass/epoxy caps are used in the less highly loaded caps outboard of B.P. 33.93. A graphite/epoxy laminate doubler is secondarily bonded to the upper cover skins at the inboard intermediate spar cap interface and additional plies are added to these spar caps as shown in Figure 18 to provide sufficient bolt bearing strength required for shear transfer in these highly loaded areas.

Spar web construction consists of glass/phenolic honeycomb core with  $\pm 45^\circ$  graphite/epoxy laminate facings. Inboard spar web core thickness is 0.580 inch with eight-ply facings and outboard spar web core thickness is 0.625 inch with four-ply facings sized for shear buckling strength. Six ply  $\pm 45^\circ$  graphite/epoxy doubler strips are located at the upper and lower edges of the spar web for reinforcement of the spar cap fastener holes and the core is filled with lightweight epoxy potting compound for Hi-Lok fastener clamp up as described in Section 6.0 Tapered graphite/epoxy doublers are located at each end of the spar web with core potted



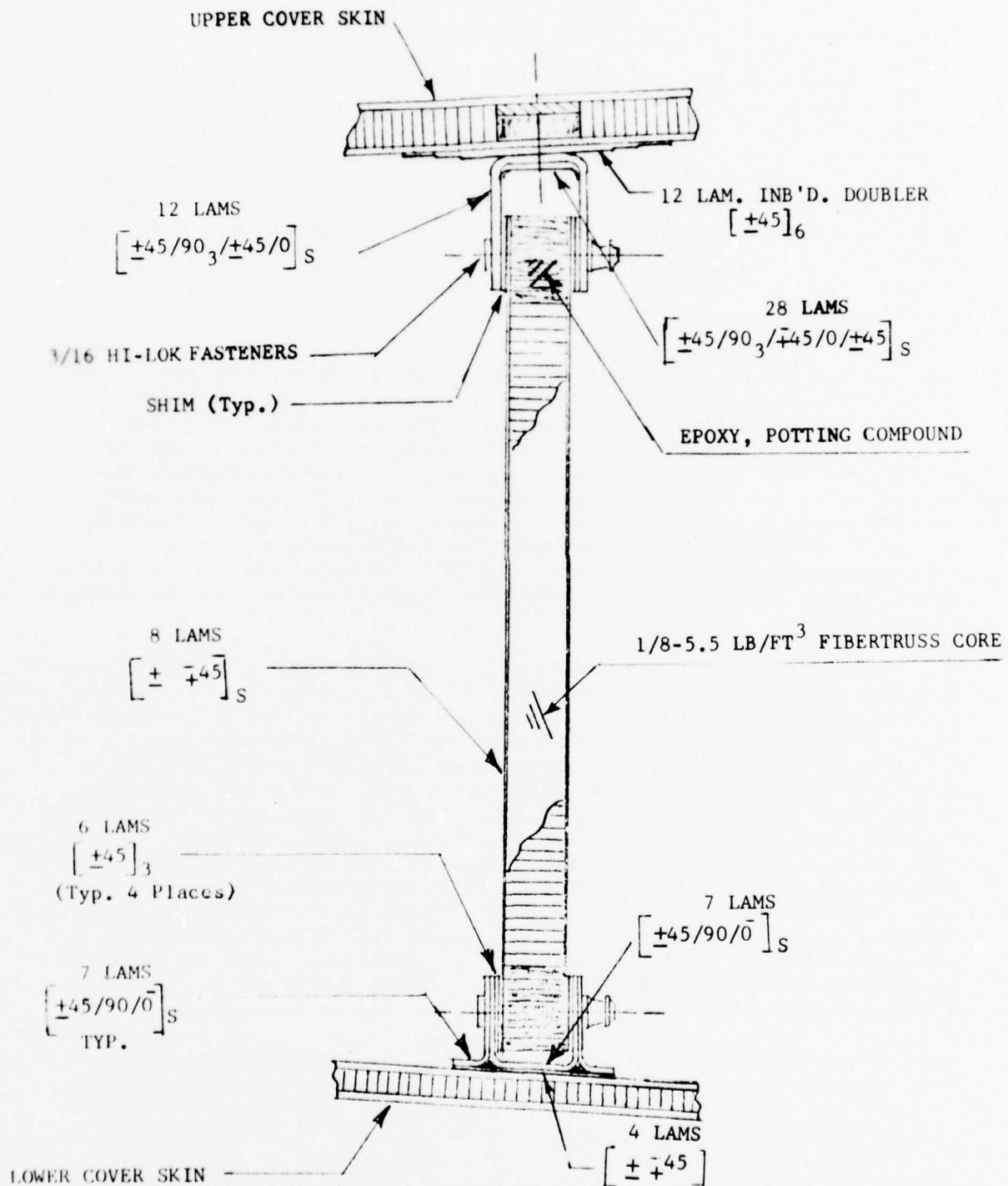


FIGURE 18 TYPICAL INTERMEDIATE SPAR SECTION



for rib attachment fasteners. Aluminum clips are used to attach the spar webs to the adjacent ribs with the thickness of the clips sized to yield at the maximum design shear allowable of the spar webs, thus preventing over loading of the intermediate spars. Intermediate spar caps are also spliced with aluminum clips at each rib to provide cap axial load transfer across the rib joint.

#### 3.1.4 B.P. 33.93 Rib

The rib at B.P. 33.93 is a primary load transfer rib with the following functions: (1) Reaction of kick loads resulting from a sharp change in lower cover skin contour at B.P. 33.93, (2) Redistribution of front spar, intermediate spar, rear spar, and wing to fuselage attachment loads, and (3) Stabilization of compression cover skins. Solid graphite/epoxy laminate construction was selected for the forward portion of this rib in combination with an aluminum machined fitting at the aft end of the rib which picks up the aft wing to fuselage attachment fitting. Aluminum was selected for local backup and attachment of the wing/fuselage fitting because of its greater ductility at concentrated load points and for the convenience of machining a one piece part to interface with the rear spar, upper cover skin and lower cover skin at this highly loaded joint.

The composite portion of this rib is an I-section formed from two back-to-back channel sections with upper and lower cap strips as shown in Figure 19. The upper and lower cover skins are both bolted to this rib because of the high peeling forces produced by the lower cover skin kick loads. The rib web is stabilized by four sets of vertical graphite/epoxy angles which are secondarily bonded to each side of the web. Solid graphite laminates were selected in preference to honeycomb sandwich construction for this rib because of the heavy laminate thickness required to transfer the flange bolt kick loads to the rib web.

The basic channel is laid up and cured with eleven plies of 0.0055 inch thick tape in a  $[90/0/90/0/90(+45)_3]$  stacking order. The channels are then secondarily bonded together and fifteen ply cap strips of  $[+45(+45)_4/90/0/90/0/90]$  laminate are added to complete the I section.

#### 3.1.5 Center Line Splice

The wing centerline joint presents a complex area of load transfer and redirection due to the sharp break in cover skin anhedral angle at the centerline rib and abrupt change in cover skin sweep angle as shown in Figure 4. Several different approaches were considered for transferring covering skin loads in this area including reshaping the mold line surfaces to eliminate concentrated kick loads at the center line rib. In the alternate design concepts discussed in Section 3.2 the cover skins were to be continued unbroken across the  $\angle$  with the mold lines reshaped to provide

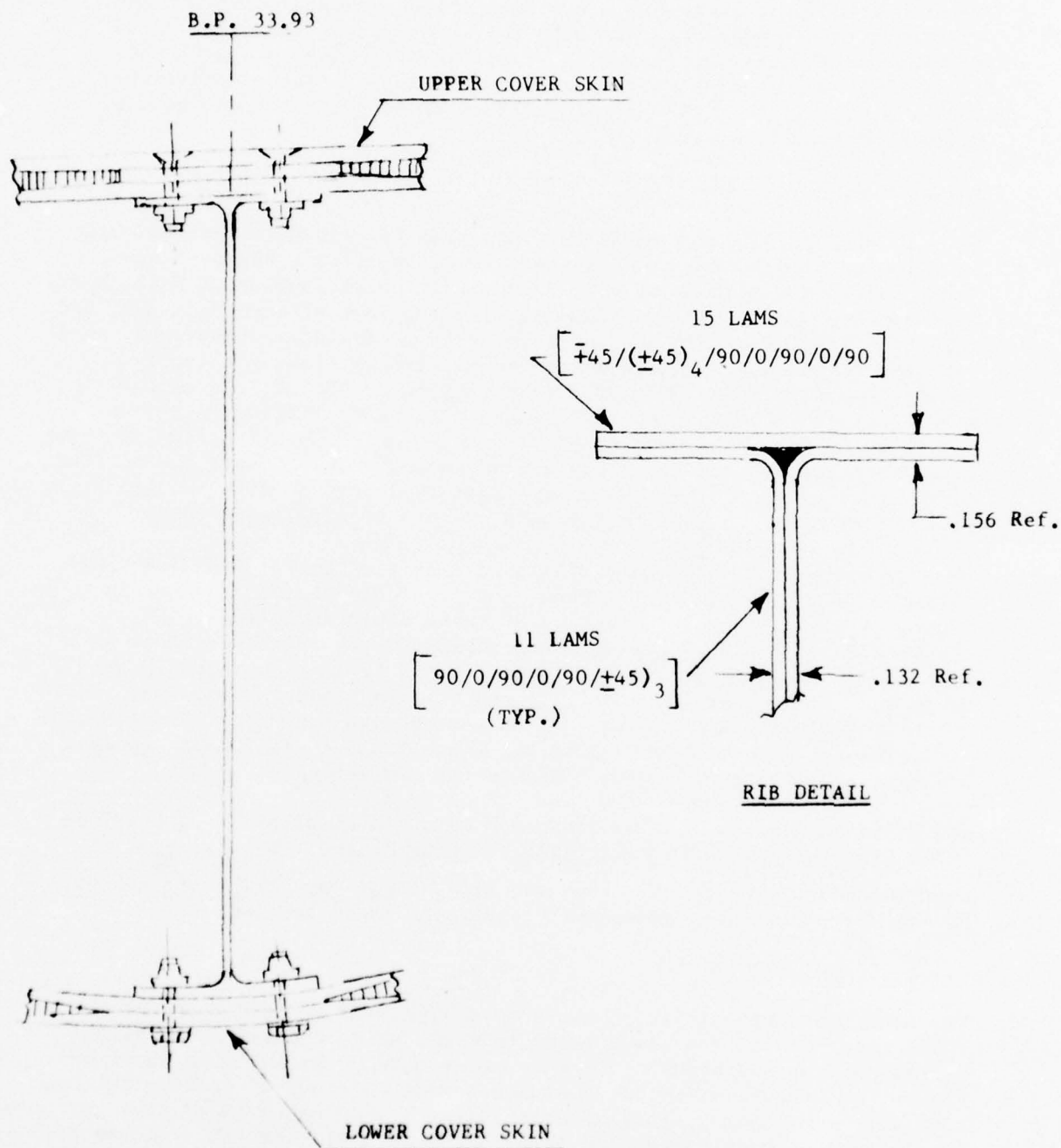


FIGURE 19

TYPICAL B.P. 33.93 RIB SECTION

a radius curvature of both the anhedral angle and rear spar sweep angle. In this design full depth Trussgrid honeycomb core was used to react the distributed tension and compression "kick" loads acting normal to the cover skin and spar radii surfaces. This design provided a lightweight configuration because the composite cover skin remained unbroken in this highly loaded portion of the structure and no beef up was required to compensate for fastener holes in a splice joint, however, the all bonded construction was considered a high risk design with the present state-of-the-art and was discarded for a more conventional bolted splice joint which provides capability for removal and inspection.

The selected  $\nabla$  splice joint design is shown in Figure 20 and consists of a one-piece machined aluminum rib with aluminum cap strips which provide a double shear bolted attachment to the upper and lower cover skin laminates. This double shear joint eliminates bending eccentricities in the cover skin laminates and kick load components are transferred to the rib web through a row of bolts in the aluminum cap strips. Design and analysis of this joint is identical to conventional metallic construction with the exception of the graphite/epoxy cover skin laminates where special consideration was given to prevention of local failure of the laminate at the bolt holes or interlaminar failure in the transition between the bolts and the basic cover skin laminates. As noted in Paragraph 3.1.1 the maximum sandwich cover skin laminate thickness is 18 plies of  $0^\circ+45^\circ$  tape built up to 37 plies (74 plies for inner and outer faces) of  $0^\circ$ ,  $\pm 45^\circ$ ,  $90^\circ$  at the bolted rib joints. Subelement development tests conducted on this  $\nabla$  splice joint, as described in Section 6.0, demonstrated the ability to transfer at least 94% of the full cover skin laminate load carrying capability across this bolted connection.

Detail drawings of the centerline splice joint and test fixture are presented in Figure B-1, and structural analysis of this joint is included in Appendix A. A description of the rear spar centerline splice and joint analysis are presented in Section 5.0.

### 3.1.6 Wing to Fuselage Attachment

As noted in Section 2.0 the XFV-12A airplane utilizes a three-point wing to fuselage attachment with a single front spar attachment at the centerline of the airplane and a rear spar attachment at each side of the fuselage. The front spar attachment consists of a large hollow pin or stud cantilevered fwd from the  $\nabla$  wing rib which mates with a self aligning bearing mounted in a fuselage frame. This forward attach fitting transmits vertical and side loads only. The aft wing attachment consists of a fitting bolted to the rear spar and lower cover skin at B.P. 33.93, as shown in Figure 21 and transmits vertical, drag, and a limited amount of side load.

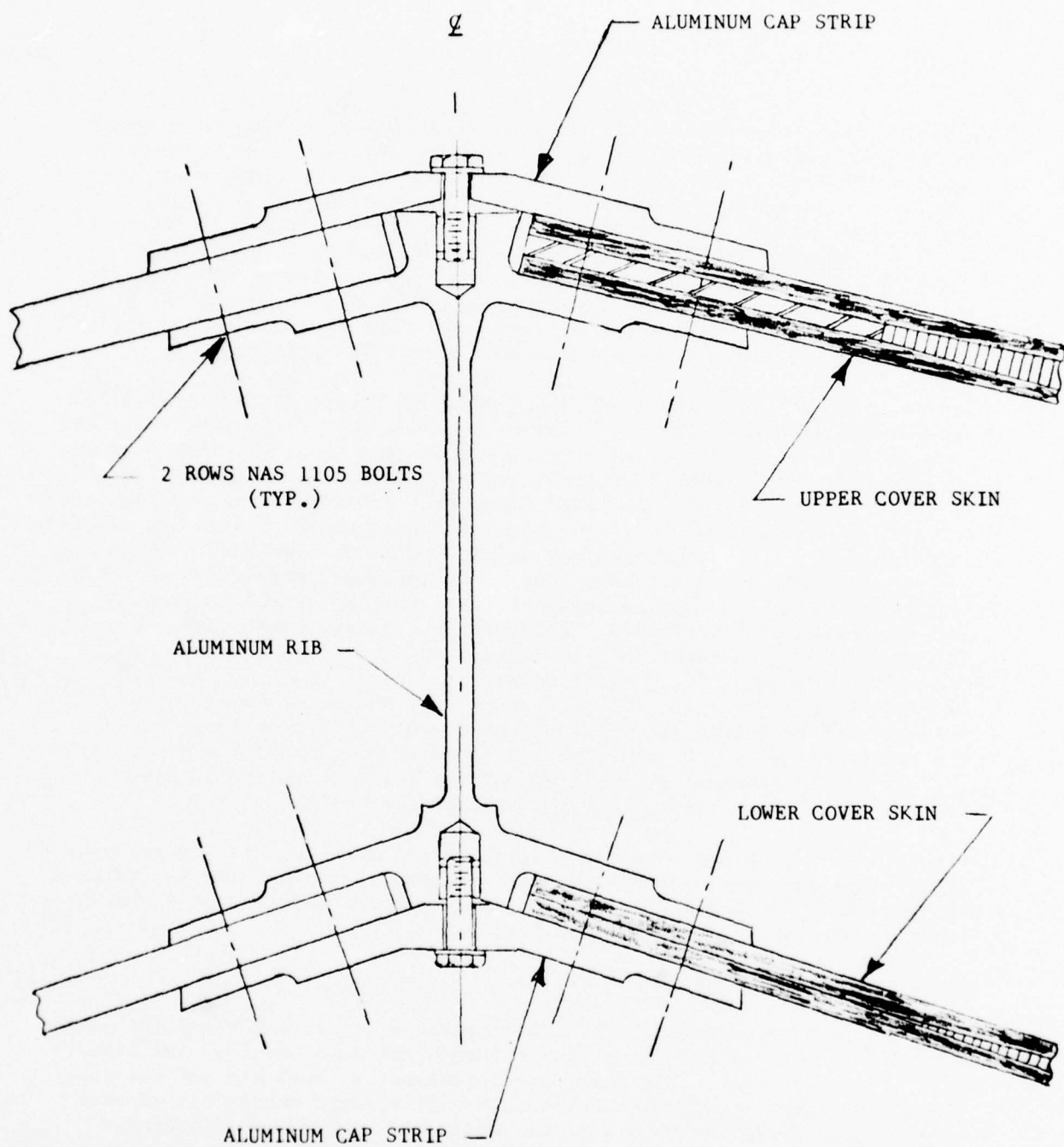


FIGURE 20 CENTER LINE SPLICE JOINT

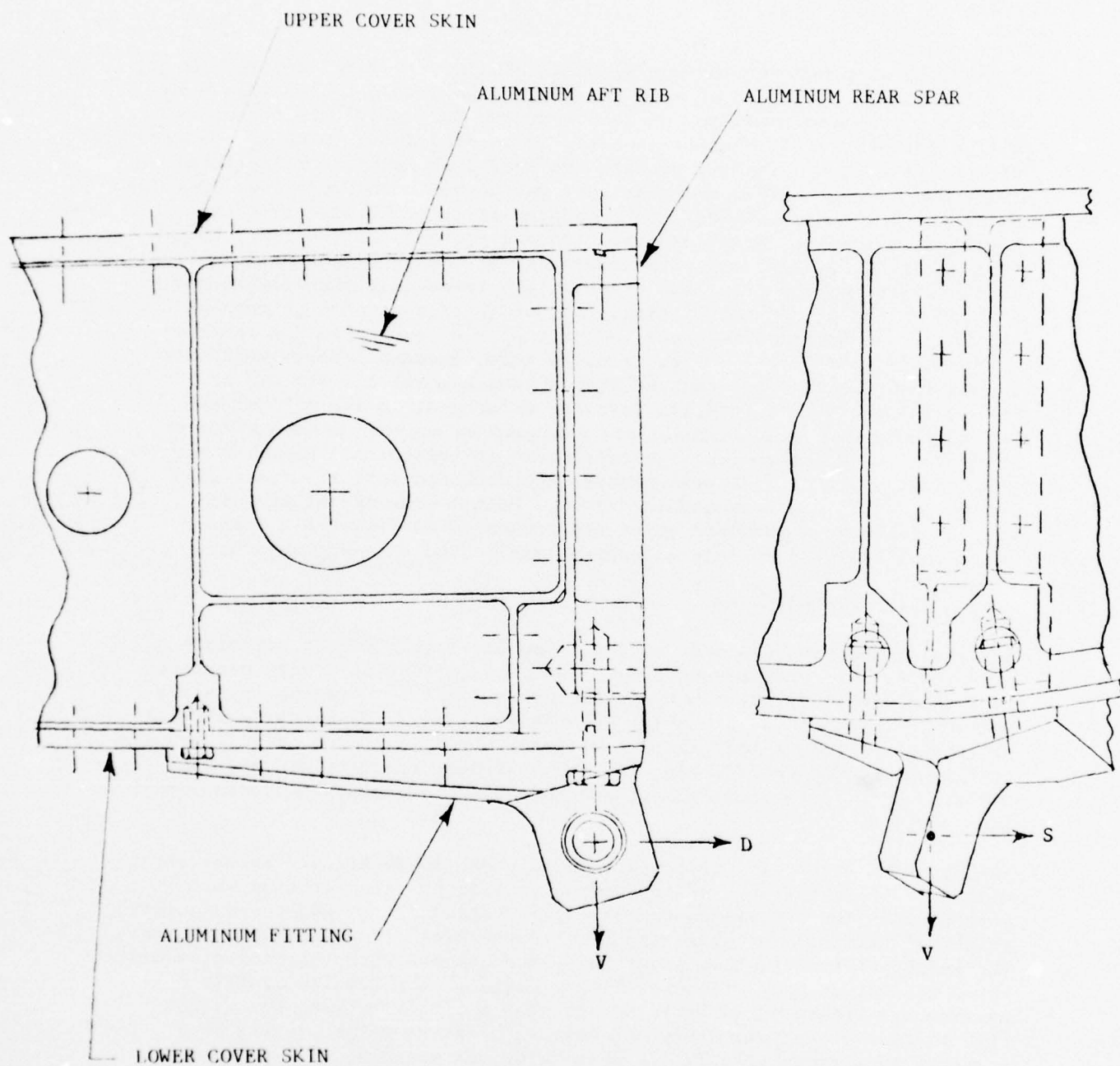


FIGURE 21 AFT WING TO FUSELAGE ATTACH FITTING



A machined aluminum fitting and aluminum back-up rib were selected for use in this aft joint to pick up the concentrated wing to fuselage loads and transmit these loads to the rear spar and B.P. 33.93 rib through bolted fasteners. A spherical bearing is mounted in the wing to fuselage attachment fitting directly beneath the rear spar and primary vertical loads are transmitted to the rear spar web through two 0.625 inch diameter bolts which screw into barrel nuts mounted in machined pockets of the aluminum rear spar. Drag loads are transmitted through the lower cover skin to the B.P. 33.93 rib with mechanical attachments and vertical couple loads resulting from drag load transfer are reacted at the forward and aft end of the attachment fitting. All of these fasteners go through the 74 ply solid graphite/epoxy laminate of the lower skin and the forward couple load attachment bolts screw into threaded inserts which are tapped into the aluminum back-up fitting which forms the aft end of B.P. 33.93 rib. This integral fastener attachment to the rib web and build up of cover skin laminate are designed to prevent delamination of the cover skins due to local joint flexure at this highly loaded attachment point. O-ring fuel seal grooves are machined into the cover skin laminate at all rib fastener locations. Detail drawings of the aft wing to fuselage attachment joint are presented in Figure B-1 and structural analysis of this attachment are included in Appendix A.

### 3.1.7 Weight Comparison

A weight comparison was made of the composite main wing box structure produced in this program and a metal wing box structure design developed in a separate study program by the Columbus Aircraft Division for a production version of the prototype XfV-12A airplane. The existing XfV-12A prototype utilizes a modified F-4 wing box which is conservatively heavier than required for the XfV-12A load and stiffness requirements and thus would not provide a realistic weight comparison of composite versus metal construction.

The approach used here for comparison purposes is to use the actual part weight of the components of the composite wing box test section which extends from the centerline to rear spar station 79.54, add the calculated weight of extension of this structure to the wing tip attachment, subtract the weight of test fixture provisions, and compare with the estimated weight of an equivalent production metal wing design. The results of this comparison are presented in Table 2 and show a composite wing box weight (tip to tip) of approximately 843 pounds, or a 19% weight saving when compared to a production FV-12A metal wing box weighing 1037 pounds.

TABLE 2  
WEIGHT SUMMARY  
L.H. COMPOSITE WING CENTER SECTION  
FROM  $\varnothing$  TO  $X_{WRS}$  79.54

Component	Weight, Pounds		
	Actual Part	Test Provisions	Flight Wing
Wing-to-Fus. Attach Fitting	6.00	-	6.00
Rear Spar	37.65	-	37.65
Fwd. & Aft Intermediate Spar Webs & Upper Caps	22.95	-	22.95
Rear Spar Splice Fitting	14.60	5.62	8.98
$X_w$ 33.93 Fwd. Rib	6.10	-	6.10
$X_w$ 33.93 Aft Rib	5.00	-	5.00
$X_w$ 33.93 Rib Splice	-	-	1.76
Centerline Rib	144.20	129.74	14.46
Centerline Splice Plates	39.95	25.16	14.79
Lower Skin Panel with Front Spar & Lower Intmd. Spar Caps Installed	100.15	-	100.15
Upper Skin Panel (Estimated weight only)	-	-	84.10
Clips & Hardware (Estimated weight only)	-	-	13.70
			315.64
Outboard Wing Estimate to Tip Excluding Tip Rib			106.00
			<u>421.64</u>

Structural Wing Box =  $421.64 \times 2 = 843.28$  pounds

Proposed FV-12A Metal Structural Wing Box = 1037 pounds

Weight Saving = 194 lbs/ship (19%)

It should be noted that the stress levels in this design have been conservatively limited to approximately 35,000 psi ultimate and additional weight reduction could be achieved by reducing the aluminum rear spar cap material to produce higher stress levels in the graphite/epoxy cover skins. It should also be noted that no provisions for lightning strike protection of the composite wing box test section were included in this program and an additional small weight increment would be required depending on the type of protection system used in a production aircraft design.

### 3.2 ALTERNATE DESIGNS

In addition to the configuration selected for fabrication of the wing box test section other concepts were considered to a limited degree in the preliminary design stages.

#### 3.2.1 "Configuration C"

Initially, preliminary design layout and analysis of the overall composite wing structural concept, identified as "Configuration C", was undertaken under NAVAIR Contract N00019-73-C-0432, "Feasibility Study of Fibrous Composites (XFV-12A)," and was based on XFV-12A design criteria. Accomplishments under the present contract included design layout of a structural configuration which incorporated full depth aluminum Trussgrid core in the center wing section (inboard of  $X_w$  33.93) and three-cell graphite/epoxy sandwich construction outboard of  $X_w$  33.93.

The three spar "boxes" were to be laid up and cured on wash out mandrel tooling, secondarily bonded together and covered with graphite/epoxy outer face skin laminates.

To assure physical compatibility between the graphite/epoxy wing and the XFV-12A technology prototype wing, mold line cuts were developed at existing front and rear spars including the three point wing-to-fuselage attachment locations, B.P. 0.0, Wing Sta. 33.93, and at the tip rib attachment area. To accommodate existing routing of systems with minimum rework to the prototype vehicle the front spar and routing "tunnel" were located at the leading edge based on a layout of fuels, controls, hydraulic, and electrical lines. A plan view of this configuration is shown in Figure B-6. Figure 22 presents a perspective sketch of the test specimen configuration. A perspective view looking aft through the center of the "Configuration C" wing configuration is shown in Figure B-7. For this configuration conic mold lines were developed locally in the wing center section to eliminate concentrated kick loads resulting from the straight line geometry of the prototype metal structure. Master dimension modifications were made at the front and rear spar planes to accomplish smooth flow of continuous fibers and distributed load paths.

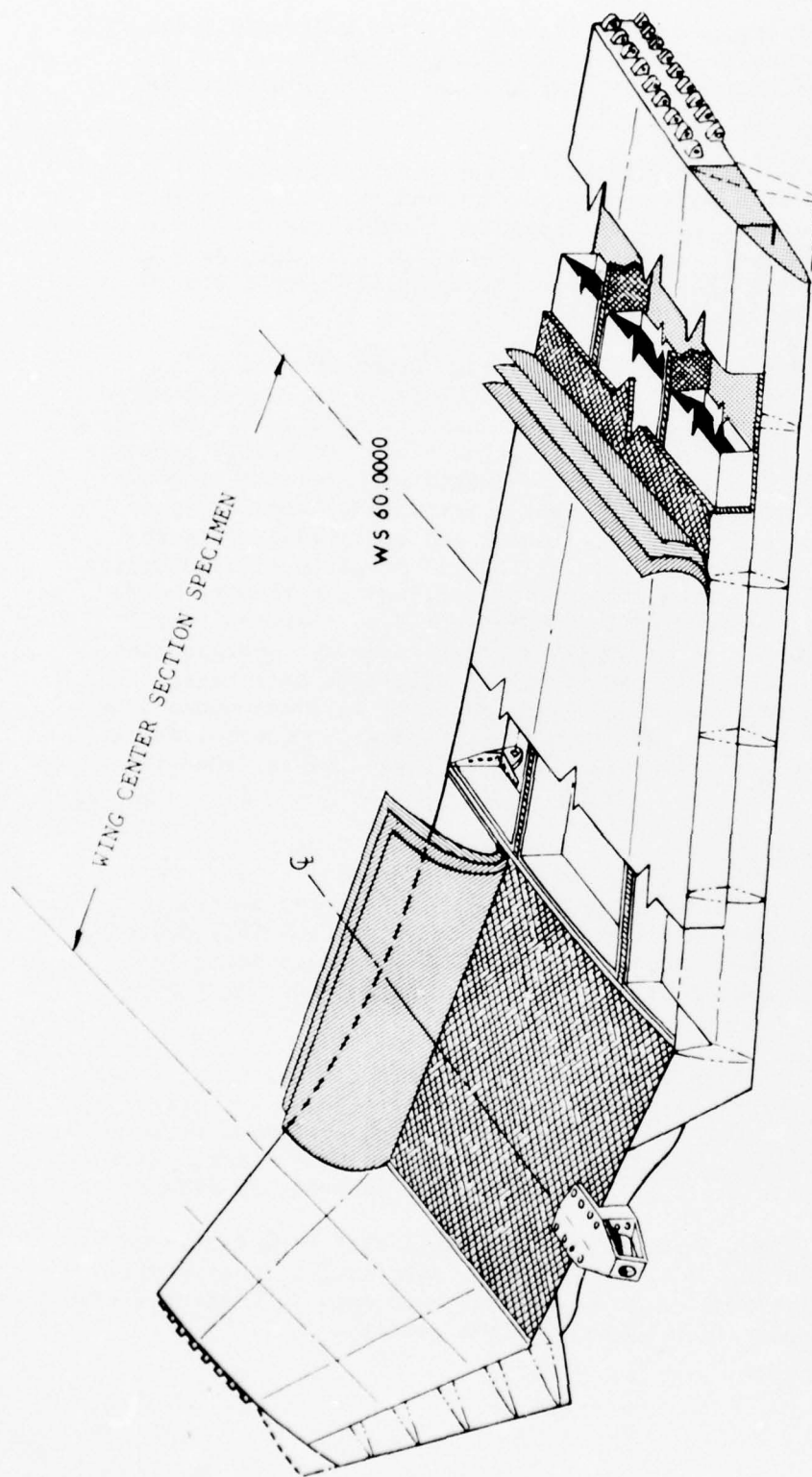


FIGURE 22 COMPOSITE WING BASELINE CONFIGURATION TEST SPECIMEN



As shown in the perspective sketch of Figure 23 three different forms of reinforcement are included in the "Configuration C" concept, i.e., unidirectional tape, woven bidirectional fabric, and woven unidirectional fabric.

A production flow diagram was developed for the manufacture of the "Configuration C" composite wing center section and this is shown in Figure B-8. A weight estimate for the graphite "Configuration C" wing, based on preliminary NASTRAN analysis and sizing for strength and stiffness required by the critical landing condition, is 628 pounds for the composite wing forward of the augmentor.

However, it was concluded that extension of the "Configuration C" composite wing design was beyond the present state-of-the-art and presented problems of inspection of bond lines in the internal structure. Excluding wing bending fatigue and environmental effects, flatwise tensile stresses of 439 psi were calculated to exist in the center wing section (inboard of  $X_w$  33.93). Four (2 x 2) flatwise tension specimens, graphite/epoxy bonded to 6.0 pcf Trussgrid core, were tested and resulted in failure stresses of 512, 496, 505, and 477 psi ultimate. Based on limited static test data, substantiation of the center wing section face to core bond strength must be considered marginal when subjected to flatwise tensile loads. Therefore, in order to establish a graphite/epoxy configuration which could be more fully substantiated by the available data base, the incorporation of Trussgrid core and consideration of filament-wound substructure with bonded skins was deferred in preference to consideration of conventional precured substructure with a mechanically fastened removable skin panel.

### 3.2.2 Trussgrid Concepts

In addition to the use of Trussgrid core in the wing center section of "Configuration C", concepts were investigated to extend the full depth Trussgrid core construction outboard of  $X_w$  33.93. These concepts included three cell and one cell structures, with and without lightening holes.

To investigate the feasibility of a wrap-around skin concept using Trussgrid core with staggered ply splices along the leading edge and utilizing one final cocure, two 4 1/2 x 16 x 16 inch full depth specimens were successfully processed without evidence of wrinkles. Glass fabric facings were used on a full depth 8 1/2 pcf Trussgrid core as shown in Figure 24.

Assuming that Trussgrid may become interchangeable with reticulated polyurethane foam as baffle material for explosion suppression in aircraft fuel tanks, its potential use as integral structure appears cost-effective throughout wet wing application without weight penalty.



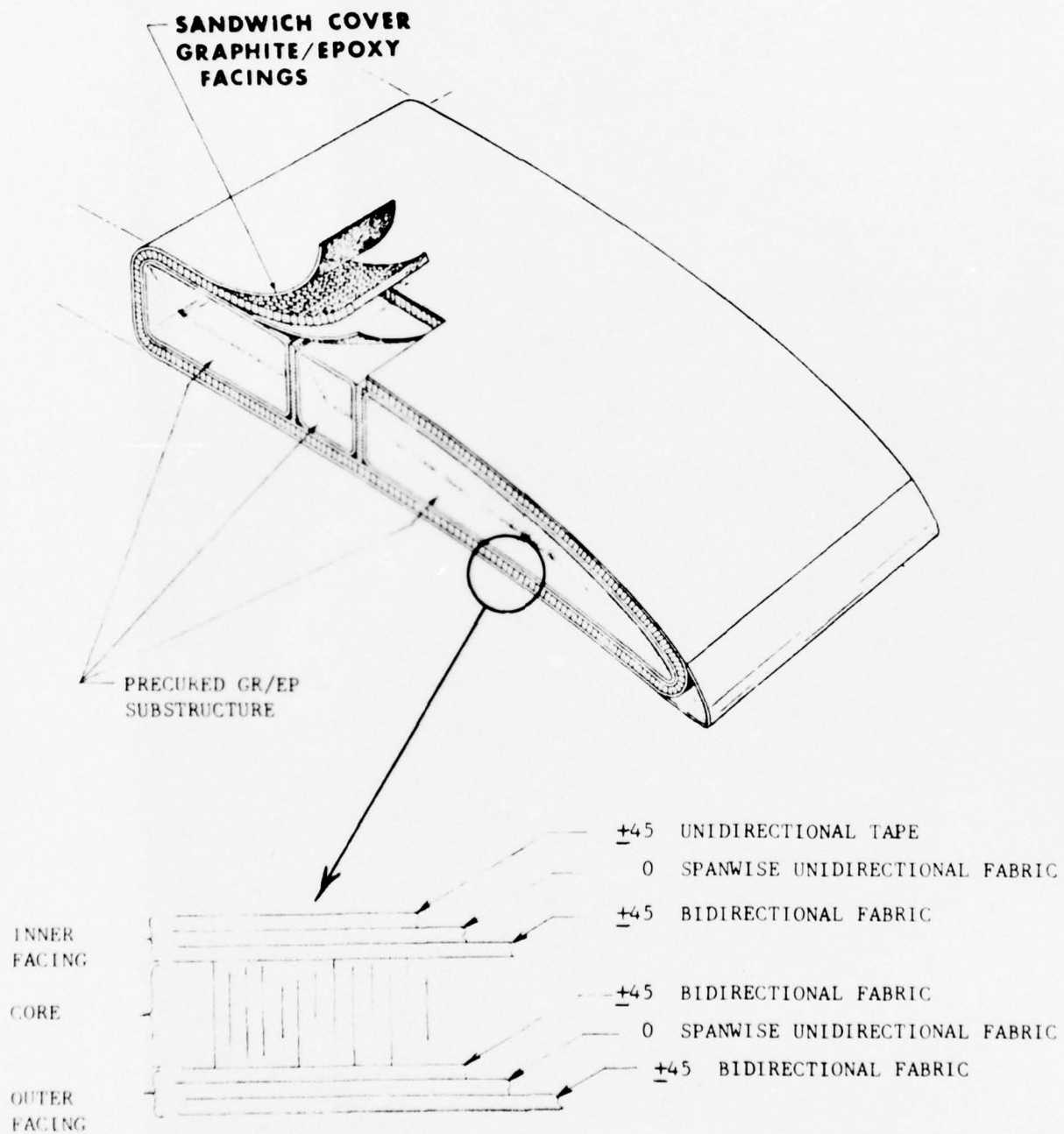


FIGURE 23 "CONFIGURATION C" MATERIAL FORMS

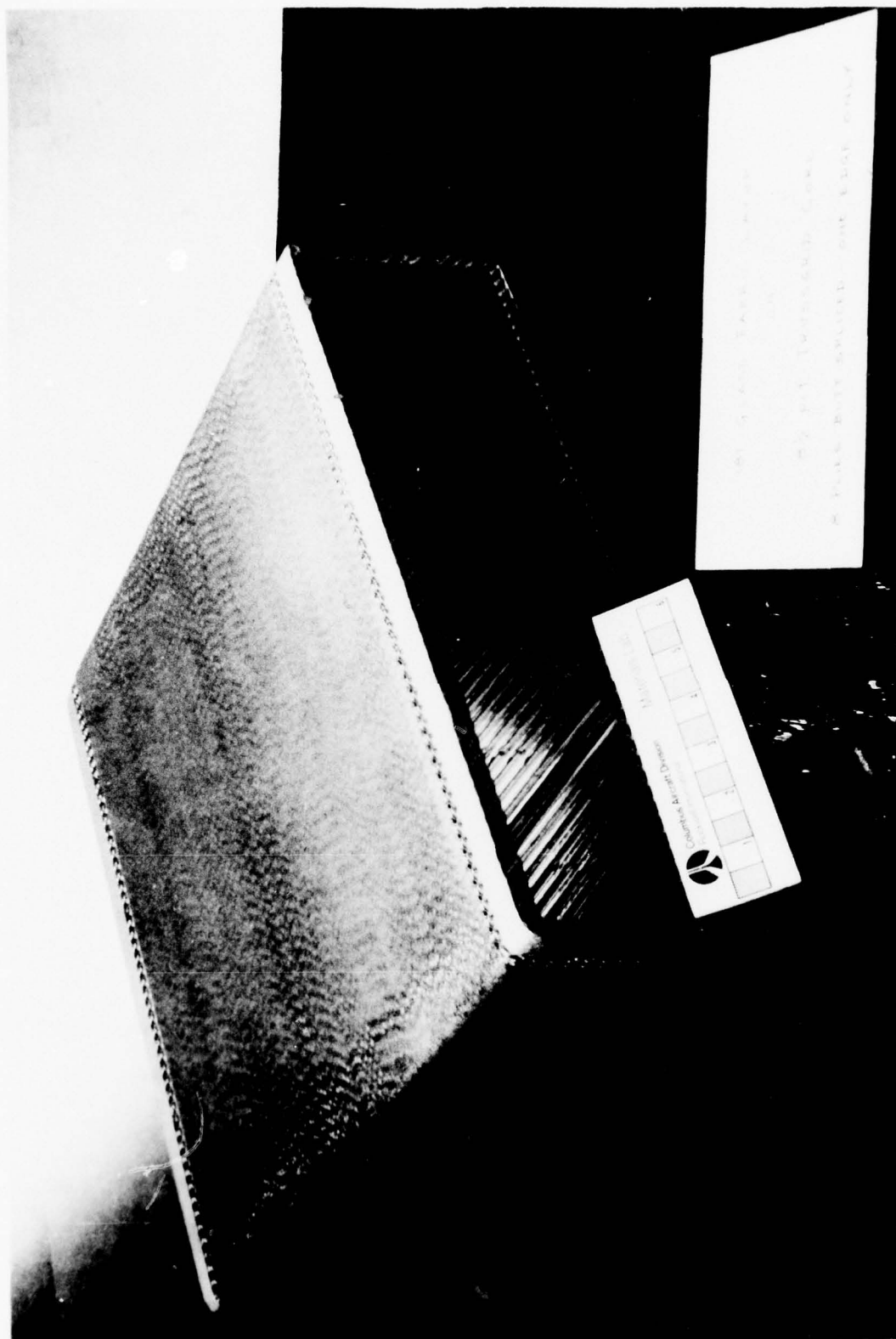


FIGURE 24 GLASS LAYUP ON TRUSSGRID CORE

## SECTION 4.0

### MATERIAL SELECTION & SPECIFICATIONS

Graphite/epoxy prepreg was specified as the primary structural composite material to be considered for use in this program. Graphite/epoxy was selected in preference to boron/epoxy primarily due to the current lower cost of the graphite materials with projected further cost reduction of carbon fibers in the future and escalation in the price of boron fibers. Other considerations favoring the use of graphite fibers included better machinability and capability to form graphite around the sharp bend radii encountered in spar and rib caps and severe contours of the lower cover skins. Temperature extremes in the wing box structure are expected to range between  $-20^{\circ}\text{F}$  and  $+200^{\circ}\text{F}$  with possible future extension to  $+250^{\circ}\text{F}$ , therefore a  $350^{\circ}\text{F}$  curing epoxy resin system was specified for the prepreg and adhesive materials. Other requirements of the prepreg and adhesive materials included compatibility with conventional autoclave curing and secondary bonding tools and processes. The following paragraphs define the specific materials selected for use in the fabrication of the wing box test section and the specifications used for procurement and certification of these materials.

#### 4.1 GRAPHITE/EPOXY PREPREG

A balanced high-strength, high-modulus  $350^{\circ}\text{F}$  curing graphite/epoxy prepreg material was desired to satisfy the strength and stiffness requirements of the wing box. Various candidate material systems were evaluated and several were found which would meet the general requirements of this application. Fiberite Corporation's Hy-E-1034C unidirectional graphite/epoxy tape which combines Union Carbide's T-300 fiber with Fiberite's X934 resin system was selected from the list of potential candidate materials. Primary reasons for this selection included previous experience with this material system at the Columbus Aircraft Division (CAD), concurrent use of this material by Tulsa Division of Rockwell International for space shuttle door fabrication, and use of the material on the Lockheed Trident missile program from which a relatively large material data base was available. Other factors influencing the selection of this material included its availability in woven fabric and mat forms, however, only unidirectional tape was used in the final wing box test section.

Physical properties of this material are specified in CAD specification HB0130-102 which covers a full range of prepreg requirements such as resin content, tack, fiber alignment, allowable defects and cured laminate strength and modulus. Material for this program was purchased under Type II, Class 2, Grade 1, category T-A of this specification which requires 0.045 inch thick cured unidirectional tensile and compression coupons to exhibit the following minimum strength and modulus values:

Minimum Value Requirements: The following strength and modulus values shall be equalled or exceeded 90 percent of the time based on tests of at least ten coupons per lot for each requirement.

Tested at 75  $\pm$  5°F

$F_{tu} = 190,000 \text{ psi}$	$E_t = 18 \times 10^6 \text{ psi}$
$F_{cu} = 180,000 \text{ psi}$	$E_c = 18 \times 10^6 \text{ psi}$

Tested at 350  $\pm$  10°F after 1/2 hour at test temperature

$F_{tu} = 175,000 \text{ psi}$	$E_t = 18.0 \times 10^6 \text{ psi}$
$F_{cu} = 140,000 \text{ psi}$	$E_c = 18.0 \times 10^6 \text{ psi}$

Scatter Factors: The mean value divided by minimum value shall not exceed 1.25.

Approximately 300 pounds of twelve inch wide and three inch wide prepreg tape were procured to this specification for use in this program, the twelve inch wide tape being used for large gently contoured areas and three inch tape used for the more severely contoured areas of the front spar and lower cover skins.

#### 4.2 ADHESIVES

A reliable 350°F curing film adhesive system was required for secondary bonding of all cured graphite/epoxy laminate face skins to the glass/phenolic honeycomb core and for faying surface bonding of spar caps and glass/epoxy inserts.

The 3M Company AF-143 film adhesive has been certified by Rockwell International and is used extensively in bonding of production components of the B-1 aircraft and space shuttle. A modification of this adhesive, designated AF-147 was selected for use in fabrication of the composite wing box test section. The modification consists of the addition of a flexibilizer to provide increased toughness and resiliency with increased peel strength. Metal-to-metal peel is three times greater

and honeycomb peel is 1 1/2 to 2 times better. The shear strength of the two materials is comparable with a 2000 psi lap shear strength retention at 300°F.

Figure 25 illustrates the lap shear strength characteristics of this material as a function of temperature. Supported 0.08 lb/ft.<sup>2</sup> film AF-147 adhesive was selected for all bonded surfaces of the composite wing box. In flatwise tension tests of a typical intermediate spar cap to sandwich cover skin, bonded joint failures were produced in the cover skin laminates but no adhesive failures occurred in the spar cap to skin faying surface joint or in the core to face sheet bonded joint.

#### 4.3 HONEYCOMB CORE

Honeycomb sandwich construction was selected for most of the primary structural components of the composite wing box including the cover skins, front spar and intermediate spars. Principal characteristics required in the honeycomb core were (1) high shear strength for transmitting fuel pressure and aerodynamic loadings, (2) high shear modulus for stabilizing facing skins against compression-buckling and shear-buckling, (3) high flatwise tension and compression strength, (4) corrosion resistance, (5) fuel and moisture resistance, (6) impact resistance, and (7) formability and machinability.

The following three basic types of material were considered for this application:

1. Aluminum
2. Glass Fabric Reinforced Phenolic
3. Nylon-fiber Reinforced Phenolic

All of these materials would satisfy the basic design requirements with varying degrees of efficiency. Table 3 presents a comparison of shear strength and shear modulus values for honeycomb core fabricated from these materials and it may be seen that aluminum honeycomb has a clear cut advantage based on the important shear modulus value and also has a better strength/density characteristic than the other materials. However, a serious concern has arisen over the corrosion potential between aluminum and graphite/epoxy laminates and therefore it was decided to select a nonmetallic core for use in the severe Navy aircraft operating environment.

A new type of glass/phenolic honeycomb core designated as "Fibertruss" was introduced by the Hexcel Company at the time of this material selection. This material, made of phenolic impregnated fiberglass, has the fibers oriented at 45 degrees to the cell axis. This bias weave construction markedly improves the shear modulus properties compared to straight weave fiberglass reinforced core. Orienting the fibers in the direction of shear stress not only improves the shear characteristics,



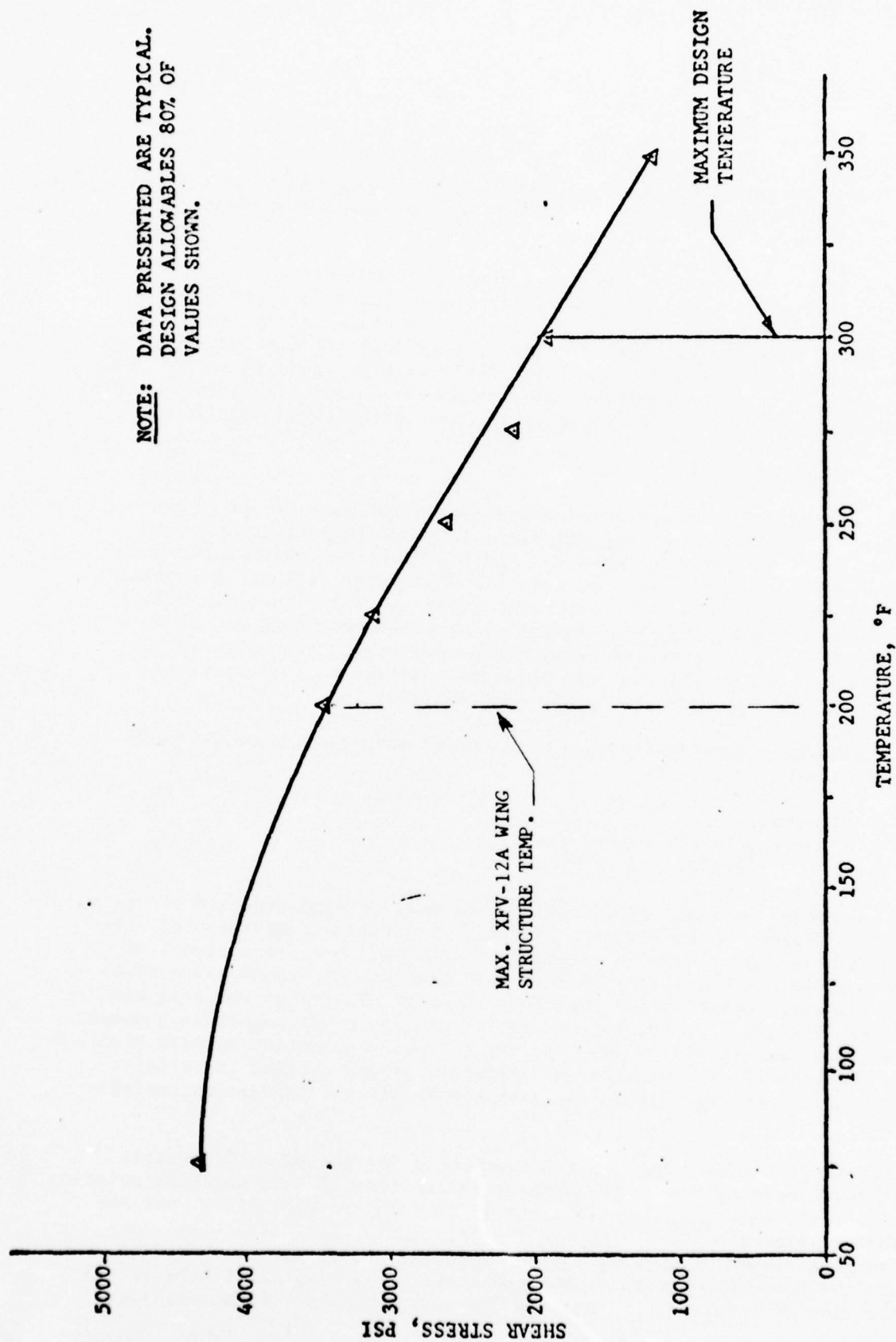


FIGURE 25 LAP SHEAR CHARACTERISTICS OF THE AF-147/EC-3917 ADHESIVE SYSTEM

TABLE 3  
COMPARISON OF HONEYCOMB SHEAR STRENGTH AND MODULUS

Designation	Density, lbs./ft. <sup>3</sup>	"L" Direction*		"W" Direction*	
		Shear Strength, psi	Shear Modulus, psi	Shear Strength, psi	Shear Modulus, psi
Hexcel Hexagonal Aluminum 3/16-.0015-4.5	4.5	410 (Typ.) 340 (Min.)	68000	245 (Typ.) 198 (Min.)	27500
Hexcel Hexagonal Glass Reinforced Phenolic HRP-3/16-5.5	5.5	425	19500	220	8500
Hexcel Fibertruss Hexagonal Glass Reinforced Phe- nolic HFT-1/8-5.5	5.5	460	33000	215	15000
Hexcel Hexagonal Nylon Reinforced HRH-10-3/16-6.0	6.0	390	14500	185	6000

\* "L" and "W" are the longitudinal and transverse ribbon directions, respectively.

but also helps impact resistance of the core. The material is designed for continuous service temperature to 350°F.

Based on these considerations the Fibertruss core material was selected for use in this program. A 1/8 inch cell size 5.5 lb/ft.<sup>3</sup> density was used in all sandwich panel assemblies, the 1/8 cell size being selected to provide maximum bond area to the face sheet and to give good compression stability in the autoclave cure cycle. It was found that this core material could be readily machined or sanded to match the tapered laminate interfaces of the sandwich assemblies and could be fine sanded to obtain perfect mark off in the core prefit inspection.

#### 4.4 POTTING COMPOUND

Potting compound was used to stabilize the Fibertruss honeycomb core at all mechanical fastener locations. This consisted of a two part 180°F curing epoxy paste adhesive manufactured by the Hysol-Dexter Corporation designated ADX-3111.1 filled with 3M Company B-25-B glass bubbles mixed in the following proportions.

100 parts by weight ADX-3111.1 Part A  
18 parts by weight ADX-3111.1 Part B  
25 parts by weight B-25-B glass bubbles

This lightweight potting compound was effective in stabilizing the core as discussed in Section 6.0, however, filling the core in specific locations with this compound proved time consuming and difficult to inspect. It is recommended that consideration be given to the use of heavier density core in lieu of potting compound on future designs.

#### 4.5 METAL COMPONENTS

As noted in Section 1.0 several components of the wing box test section were fabricated from aluminum alloy. These include the following:

<u>Item</u>	<u>Material</u>
Center Line Rib	7075-T73 Hand Forged Billet
Center Line Splice Plates	7075-T73 Hand Forged Billet
Rear Spar	7075-T73 Hand Forged Billet
Rear Spar Splice Fitting	7075-T73 Hand Forged Billet
Wing to Fuselage Attach Fitting	7075-T73 Hand Forged Billet
B.P.33.93 Rib Aft Section	7075-T73 Hand Forged Billet
Miscellaneous Clips	2024-T62 Sheet

Aluminum alloy was selected for these components primarily due to concentrated load applications requiring sharp directional changes and splices at the center line joint and wing to fuselage attachment fitting. Machined fittings allow tri-directional load transfer in these areas and capability for using threaded fasteners and tapped threads in the centerline kick load rib with less risk than a composite build up.

## SECTION 5.0

### STRUCTURAL ANALYSIS

The structural analyses of major significance included the determination of stress distributions in the full wing (semi-span) and the test wing section fabricated (cut off at R.S. Sta. 79.54) using the NASTRAN finite element program, sandwich panel buckling analysis for critical cover and intermediate spar sandwich panels, analysis of major splice joints, and a flutter evaluation.

The analytical methods and limited results are discussed in the following paragraphs with more detailed analysis of critical areas presented in Appendix A.

#### 5.1 FINITE ELEMENT ANALYSIS

For overall stress analysis of the composite wing the NASTRAN finite element computer program was utilized using the model shown in Figure 26. Analyses were performed for two critical conditions, i.e., Max. Vertical Landing and a symmetrical flight condition. The analytical model utilized several types of elements from the NASTRAN library as follows:

- (a) Main wing box sandwich covers - CQUAD1 and CTRIA1
- (b) Vertical webs - CSHEAR in conjunction with CONROD elements
- (c) Spar caps - CONROD
- (d) L.E. skins - CQDMEM 1

Analyses were performed on both the total wing panel as shown in Figure 26 and on the actual wing box test section which extends outboard to R.S. Sta. 79.54. In addition, analyses were performed for the original configuration and for the final version with increased rear spar cap areas to reduce the skin stresses to approximately 35000 psi.

Test loads for application at R.S. Sta. 79.54 for the Max. Vertical Landing Condition were obtained in the following manner:

- (a) Initial analysis applied the outboard loads and determined reactions at the inboard end.
- (b) Stress levels in the inboard critical areas were noted as target values for test load application



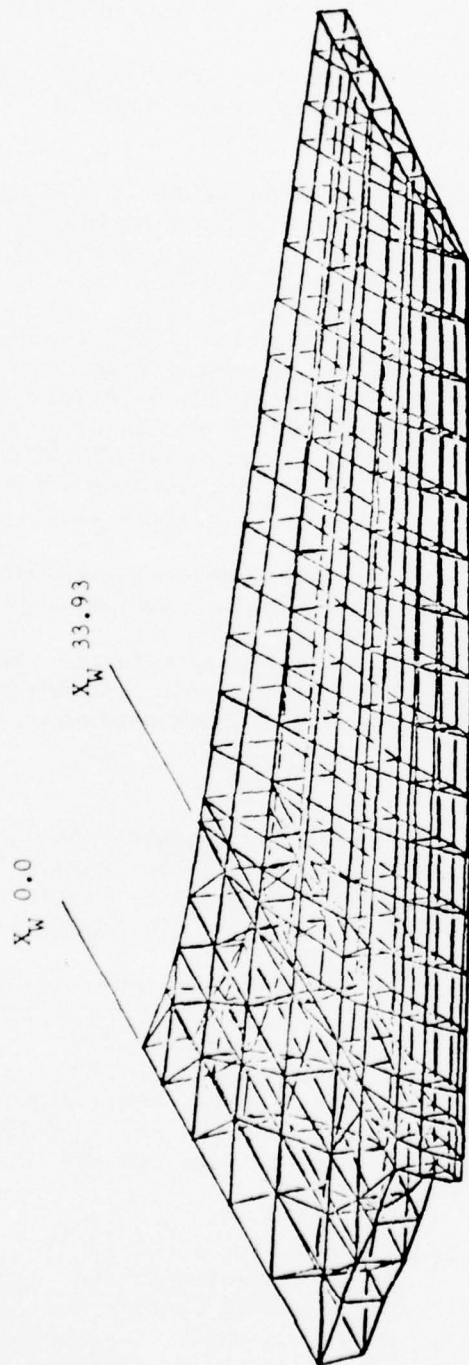


FIGURE 26 COMPOSITE WING NASTRAN MODEL

- (c) analysis of the test wing configuration was performed by applying the original reaction loads at the inboard end and obtaining reactions at R.S. Sta. 79.54
- (d) critical area stress levels were compared and the loads at R.S. Sta. 79.54 verified as the applied static test loads.

The desired skin stress level of approximately 35000 psi was controlled purely by an increase in the aluminum rear spar cap areas. The reduced skin stress levels resulting from increased spar cap areas are shown in Figures 27 and 28 for the upper cover and lower cover, respectively. This analysis reflects a maximum compression stress of 38400 psi in the upper cover and a maximum tension stress of 36400 psi in the lower cover. These stresses compare favorably with the desired target value of 35000 psi. The NASTRAN analysis also reflects the tapered, interleaved thickness buildup provided in the skins at  $X_w$  33.93 and skin splice areas.

Additional results of the NASTRAN finite element analysis are presented in Appendix A for preliminary cover stress distribution and outer panel stresses.

Applied loads as defined by analysis for static and/or fatigue testing of the wing test section are described in Section 9.0 for both the Max. Vertical Landing Condition and the critical symmetrical flight condition.

## 5.2 SANDWICH PANEL BUCKLING

The buckling analysis of critical graphite/epoxy sandwich panels included the determination of compression buckling allowables for biaxially-loaded main box cover panels and defining shear buckling allowables for intermediate spar webs.

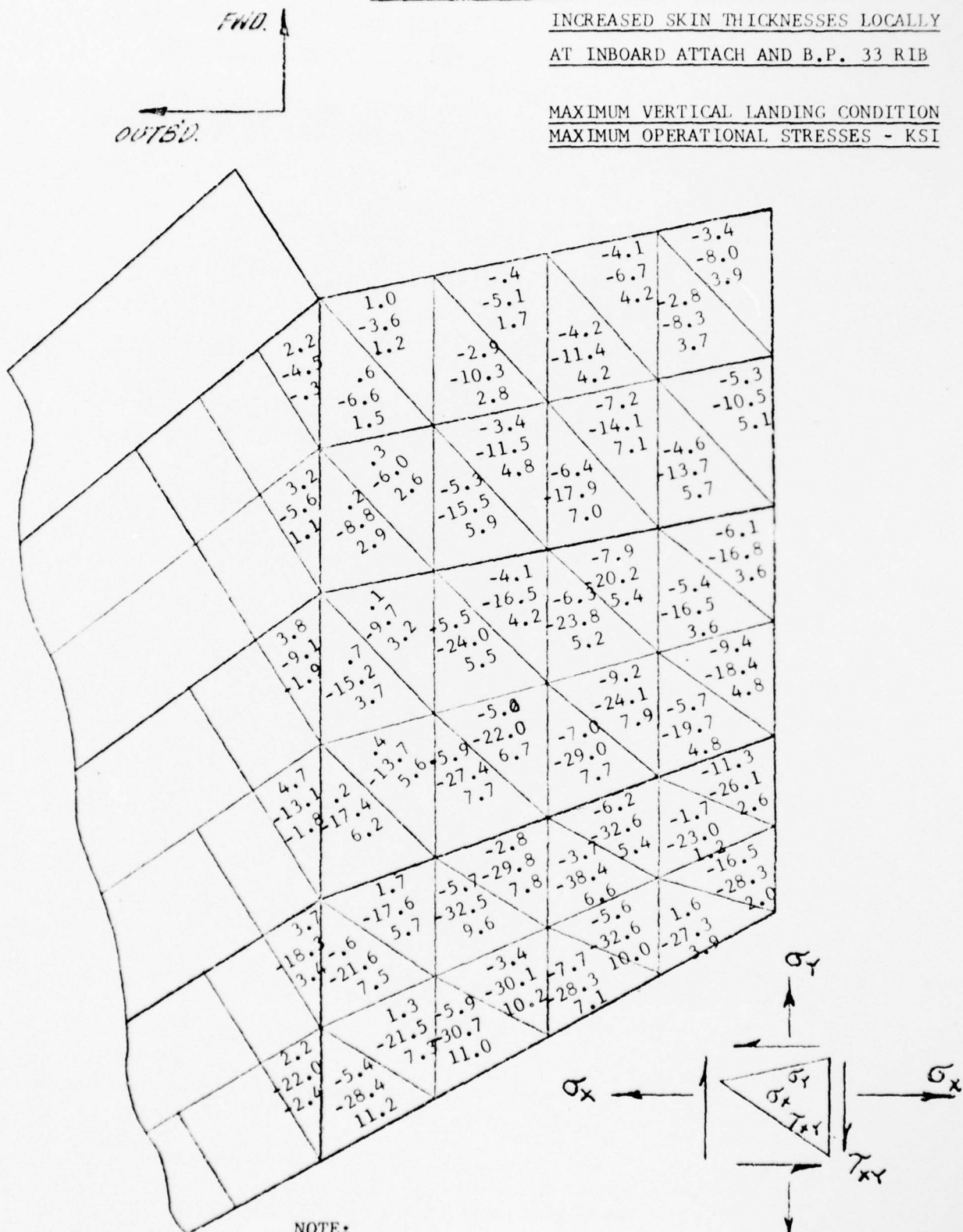
Room temperature, elastic buckling allowables for the biaxially-loaded cover panels were defined by the methods presented in the "Advanced Composites Design Guide," Volume II and the use of Program AC-5, Honeycomb Sandwich Panel Stability Under Inplane Biaxial Loading. Buckling coefficients,  $K$ , were defined as a function of load ratio, panel aspect ratio, no. of half-waves in the  $x$  and  $y$  directions, and the panel stiffness parameters. Shear stresses in the cover panels were low and were considered negligible in the panel buckling analysis.

Room temperature, elastic shear buckling allowables for the intermediate spar sandwich webs were defined by methods presented in the "Advanced Composite Design Guide," Volume II and the use of Program AC-11, Honeycomb Sandwich Panel Stability for Inplane Shear Loading. Shear loading only was considered on these panels since they were modeled as CSHEAR elements in the finite element analysis.

FIGURE 27 - WING UPPER COVER STRESSES

INCREASED SKIN THICKNESSES LOCALLY  
AT INBOARD ATTACH AND B.P. 33 RIB

MAXIMUM VERTICAL LANDING CONDITION  
MAXIMUM OPERATIONAL STRESSES - KSI



NOTE:

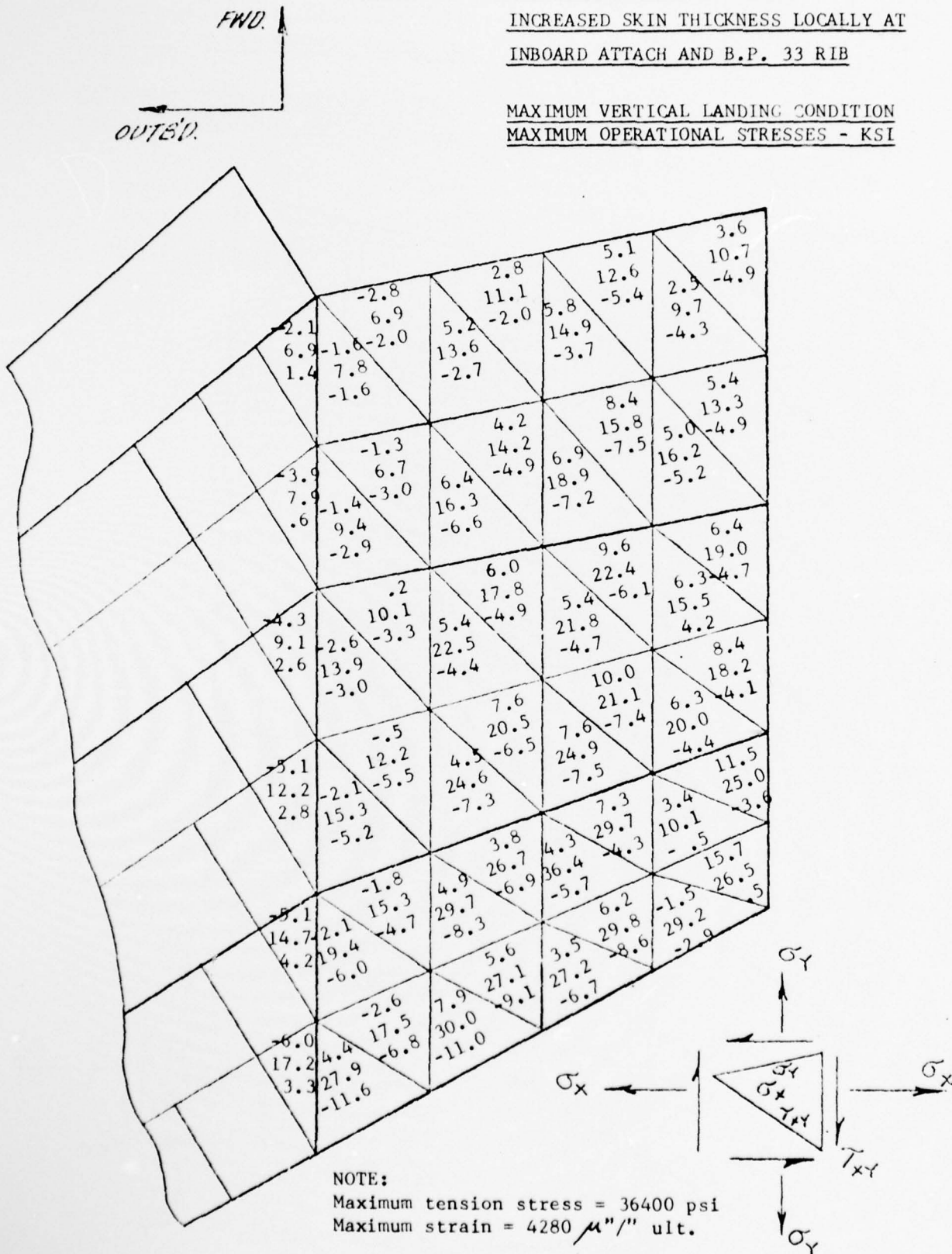
Maximum compression stress = 38400 psi

Maximum strain = 4520  $\mu$ "/" ult.

FIGURE 28 - WING LOWER COVER STRESSES

INCREASED SKIN THICKNESS LOCALLY AT  
INBOARD ATTACH AND B.P. 33 RIB

MAXIMUM VERTICAL LANDING CONDITION  
MAXIMUM OPERATIONAL STRESSES - KSI





Material properties for the laminates and orientations of interest were obtained for the high strength graphite/epoxy from the "Advanced Composites Design Guide," Volume I as described in Section 2.4.

Analyses of typical critical main box cover panels under biaxial loading are shown in Appendix A.

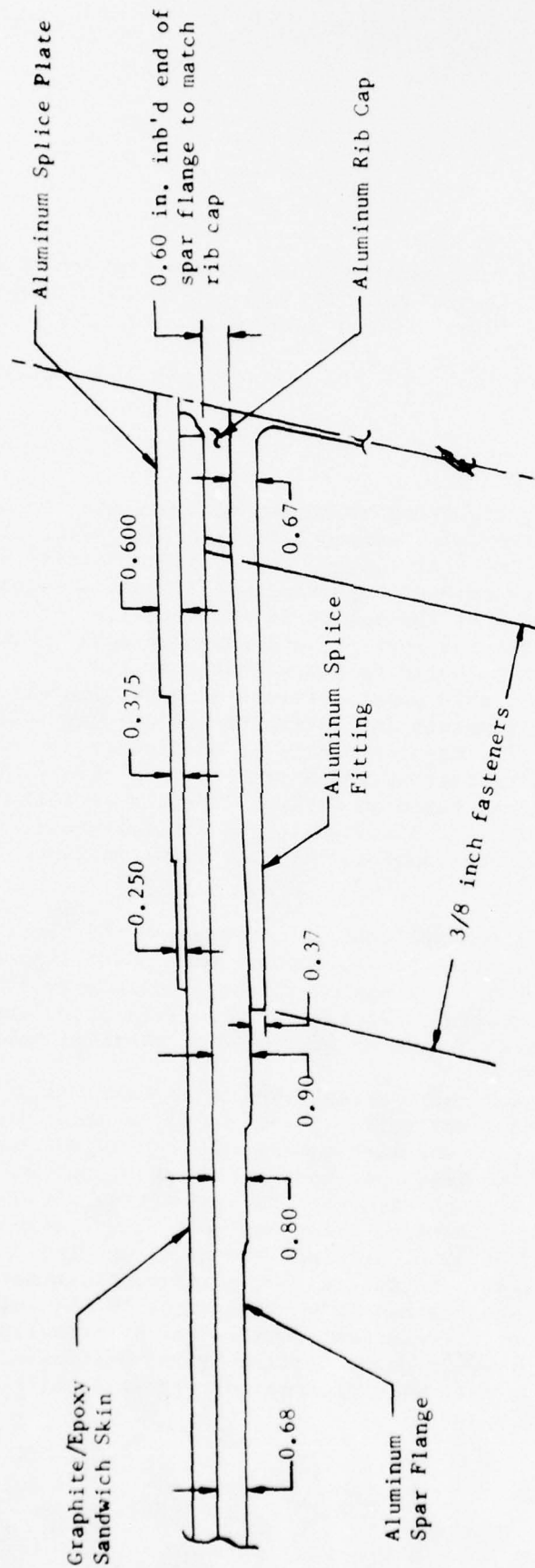
### 5.3 BOLTED JOINTS

The major bolted joint requiring extensive analysis was the rear spar splice at the centerline which includes an external splice plate, graphite/epoxy sandwich skin, rear spar flange, and a splice fitting nested in the rear spar. This splice extends approximately 15 inches outboard on each wing panel. The purpose of the splice is twofold; i.e., to transfer axial loads from the discontinuous spar cap and graphite/epoxy skin to the splice plate and fitting, and to build up equivalent spar cap area in order to maintain graphite/epoxy skin panel stresses of approximately 35000 psi. Therefore, the splice elements and fasteners are not particularly critical for static strength. The major elements in the splice are the spar cap, splice plate, and splice fitting which are aluminum alloy. These are either tapered or stepped based on fatigue life considerations and to obtain a nearly uniform load distribution in the fasteners. Sketches of the upper and lower rear spar splices are shown in Figure 29 and 30 respectively.

Preliminary sizing was accomplished by considering the required equivalent aluminum spar cap area, and the preliminary bolt shear load distribution was obtained using a shear lag approximation procedure to determine required bolt size and spacing. Because of the large grip lengths required, a fastener diameter of 3/8-inch was selected to minimize bolt bending.

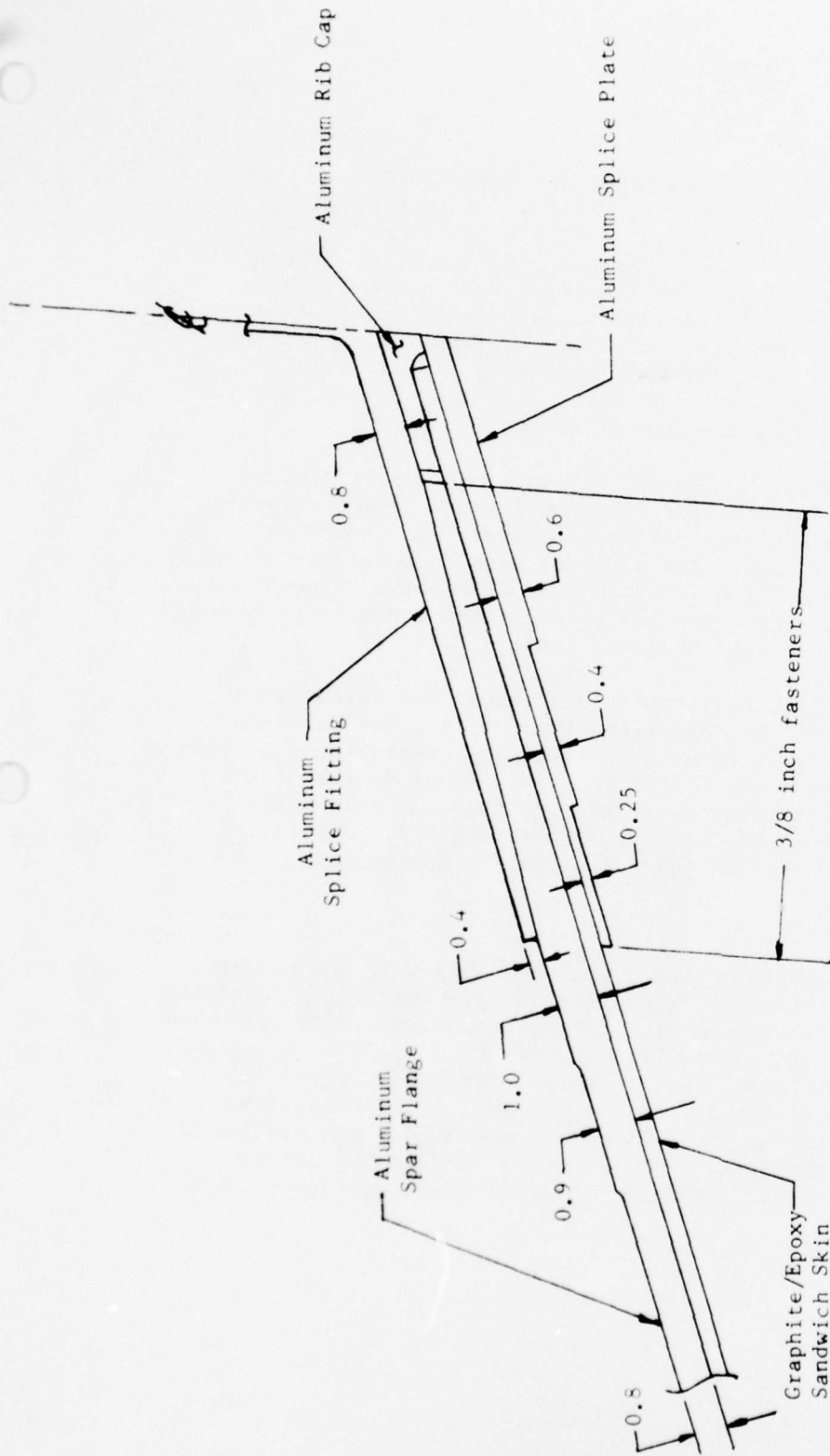
Once the final dimensions were established a computer analysis was performed for both the upper and lower splice joints using an axial load applied at the outboard end of the joint with a magnitude of 120,000 pounds which was slightly higher than the rear spar load indicated by the NASTRAN finite element analysis. The computer method for joint analysis was based on the methods of "Inelastic Mechanical Joint Analysis Method with Temperature and Mixed Materials," by B. E. Gatewood and R. W. Gehring. Stiffness factors for the joint were estimated from available test data and an investigation revealed that rather large variations in the joint stiffness factors had relatively little effect on the load distribution. For example, an analysis was performed assuming that the joint stiffness factors were twice those originally used which indicated very small differences in the joint load distribution.





VIEW LOOKING FORWARD IN REAR SPAR PLANE

FIGURE 29 UPPER REAR SPAR CENTERLINE SPLICE



VIEW LOOKING FORWARD IN REAR SPAR PLANE

FIGURE 30 LOWER REAR SPAR CENTERLINE SPLICE

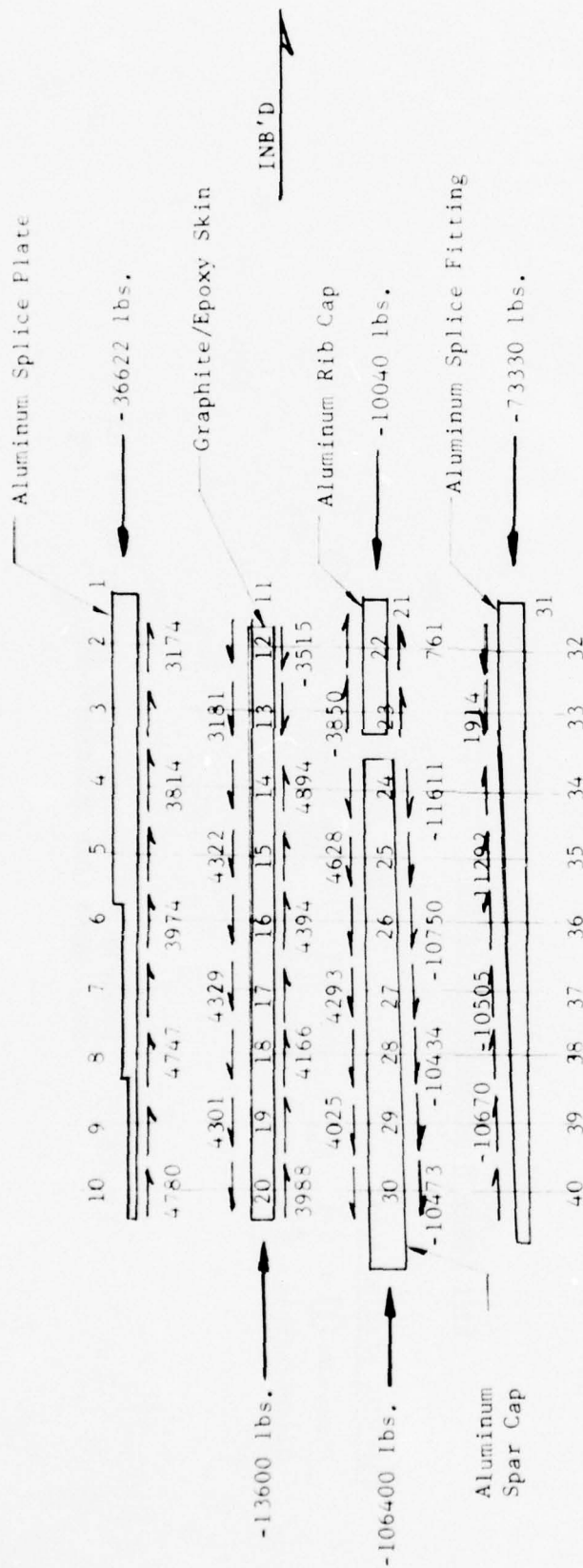
The results of this analysis for both upper and lower flange splices indicated no critical static bolt shear, bearing, or tension in the plates at the maximum design load. Bolt load distributions for the upper and lower splices are shown in Figures 31 and 32, respectively. Critical bearing areas and critical bolt elements are noted in these figures. Plate stress distributions for the upper and lower splice are shown in Figures 33 and 34, respectively. Critical axial loads in the plates are noted on these figures. However, for all critical areas noted in the figures it should be noted that the stresses are low and reflect relatively high margins of safety.

Four bolts at the junction of the splice fitting, rib cap, graphite/epoxy skin, and splice plate transfer very small loads from the spanwise component and are essentially designed to carry the chordwise load component into the rib cap. The vertical load component is transferred into the web of the splice fitting by tension bolts through the splice plate and rib cap. These tension bolts attach directly into the splice fitting through the use of helicoil inserts.

The other significant mechanically fastened joint is the splice joint between the cover skins and the centerline rib. This joint was especially critical with the cover skins transferring a considerable portion of the bending moment across the centerline rib. Final design of the joint, to reduce stress concentrations, was accomplished only after performing development tests as described in Section 6.2. A detailed analysis of the centerline splice joint is shown in Appendix A.

#### 5.4 FLUTTER EVALUATION

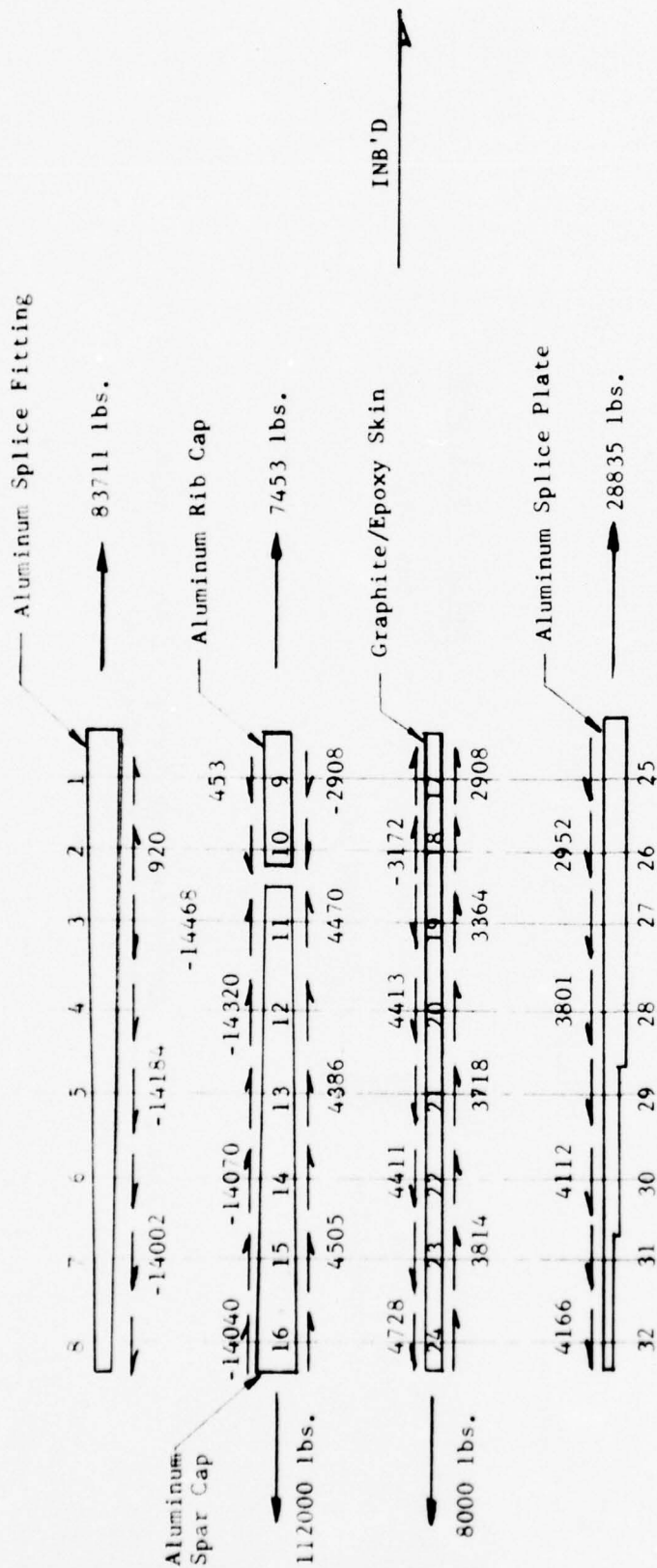
A flutter evaluation was performed with the composite wing box modeled as a single beam-rod with rigid vertical stabilizers and control system. Pin-pinned symmetric and anti-symmetric vibration analyses were performed using a three-point wing restraint. Results of these analyses are presented in Table 4. Theoretical flutter analyses were then performed using three-dimensional incompressible aerodynamics. The analytical solutions for the symmetric and anti-symmetric conditions are plotted in Figures 35 and 36, respectively, as frequency and damping versus velocity. The minimum predicted flutter speed is shown in Figure 36 to be 697 knots.



Bolt Shear Loads Shown in lbs.

CRITICAL BEARING NODES		CRITICAL BOLT SHEAR	
Aluminum (24) & (40)	$\sigma_{br} = 35810 \text{ psi}$	Bolt Segment (24) - (34)	(2 bolts)
Graphite/Epoxy (13)	$\sigma_{br} = 15624 \text{ psi}$		

FIGURE 31 UPPER REAR SPAR CENTERLINE SPLICE; DESIGN ULTIMATE BOLT SHEAR LOAD DISTRIBUTION



Bolt Loads Shown Above are in lbs.

#### CRITICAL BEARING NODES

Aluminum (8) & (11)  
Graphite/Epoxy (13)

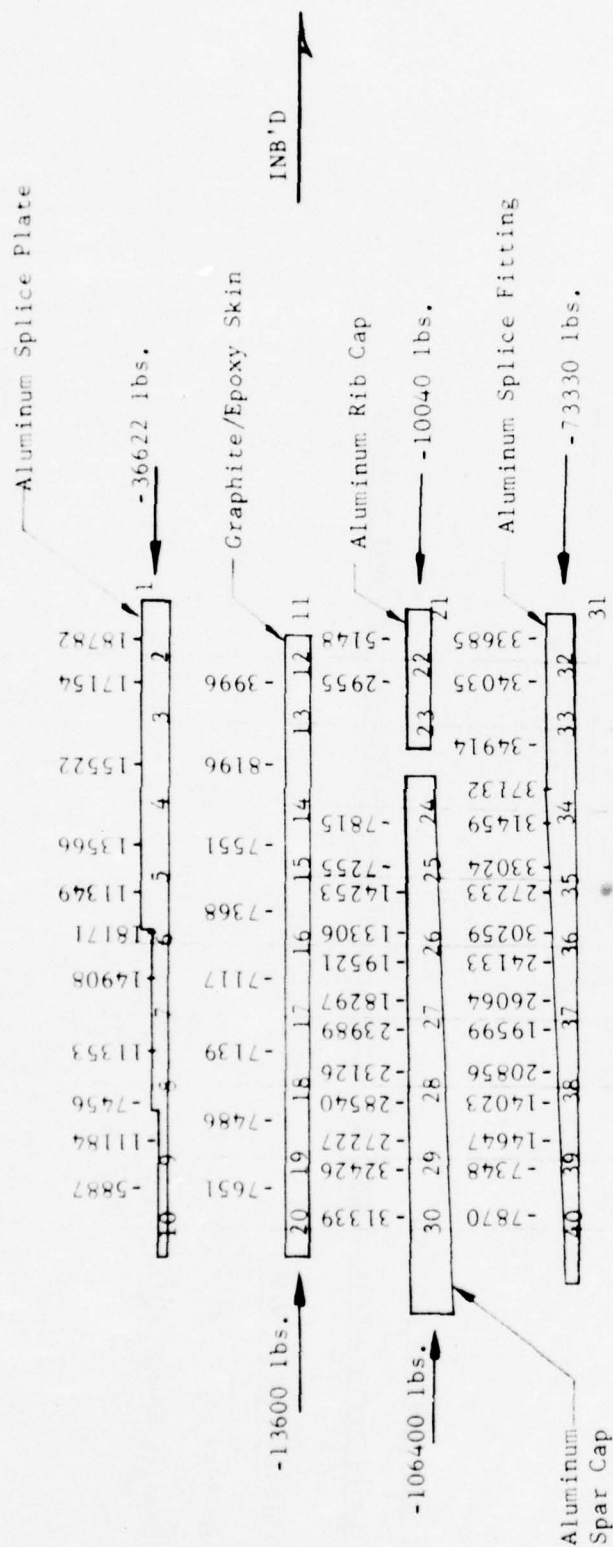
$\sigma_{br} = 41600$  psi  
 $\sigma_{br} = 17497$  psi

#### CRITICAL BOLT SHEAR

Bolt Segment (3) - (11) (2 bolts)

FIGURE 32 LOWER REAR SPAR CENTERLINE SPLICE; DESIGN ULTIMATE BOLT SHEAR LOAD DISTRIBUTION





(-) Stresses are compression

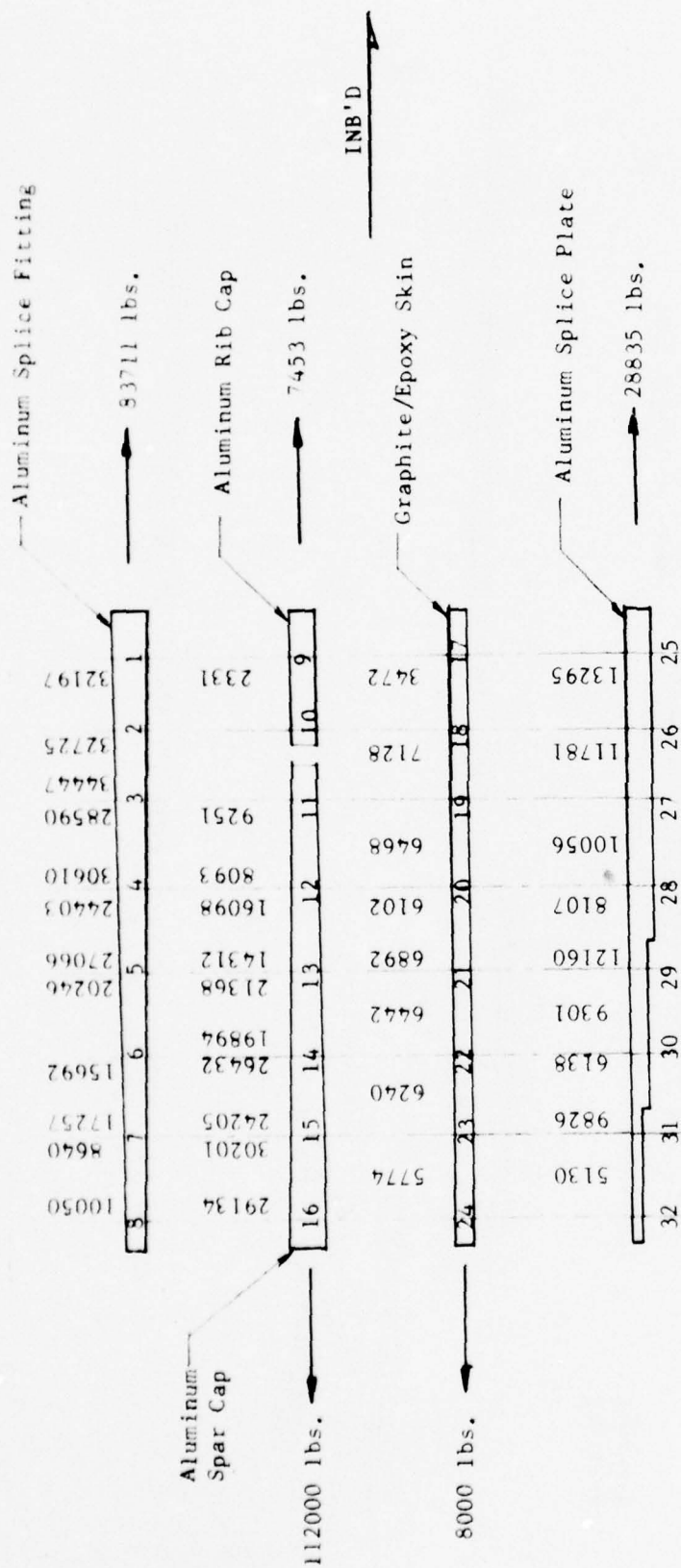
Stresses shown are gross stresses (not corrected for net section including bolt holes).

#### CRITICAL COMPRESSION NODES

Aluminum (34),  $\sigma_c = -37132$  psi

Graphite/Epoxy (13) - (14),  $\sigma_c = -8196$  psi

FIGURE 33 UPPER REAR SPAR CENTERLINE SPLICE; DESIGN ULTIMATE COMPRESSION STRESS DISTRIBUTION



(+) stresses are tension

Stresses are gross stresses (not corrected for net section through bolt holes).

#### CRITICAL TENSION NODES

Aluminum (3)  $\sigma_t = 34447$  psi

Graphite/Epoxy (18) - (19)  $\sigma_t = 7128$  psi

FIGURE 34 LOWER REAR SPAR CENTERLINE SPLICE, DESIGN ULTIMATE TENSION STRESS DISTRIBUTION

TABLE 4  
THEORETICAL VIBRATION RESULTS  
XFV-12A COMPOSITE WING

Mode	Frequency (Hz)		Symbols (Reference Figures 18 and 19)
	Symm.	A/S	
$W_1$	4.2	4.7	⊙
$W_2$	15.3	14.0	△
$W_3$	19.4	20.8	□
$W_4$	39.2	36.4	◇

See Table 2 for symbols.

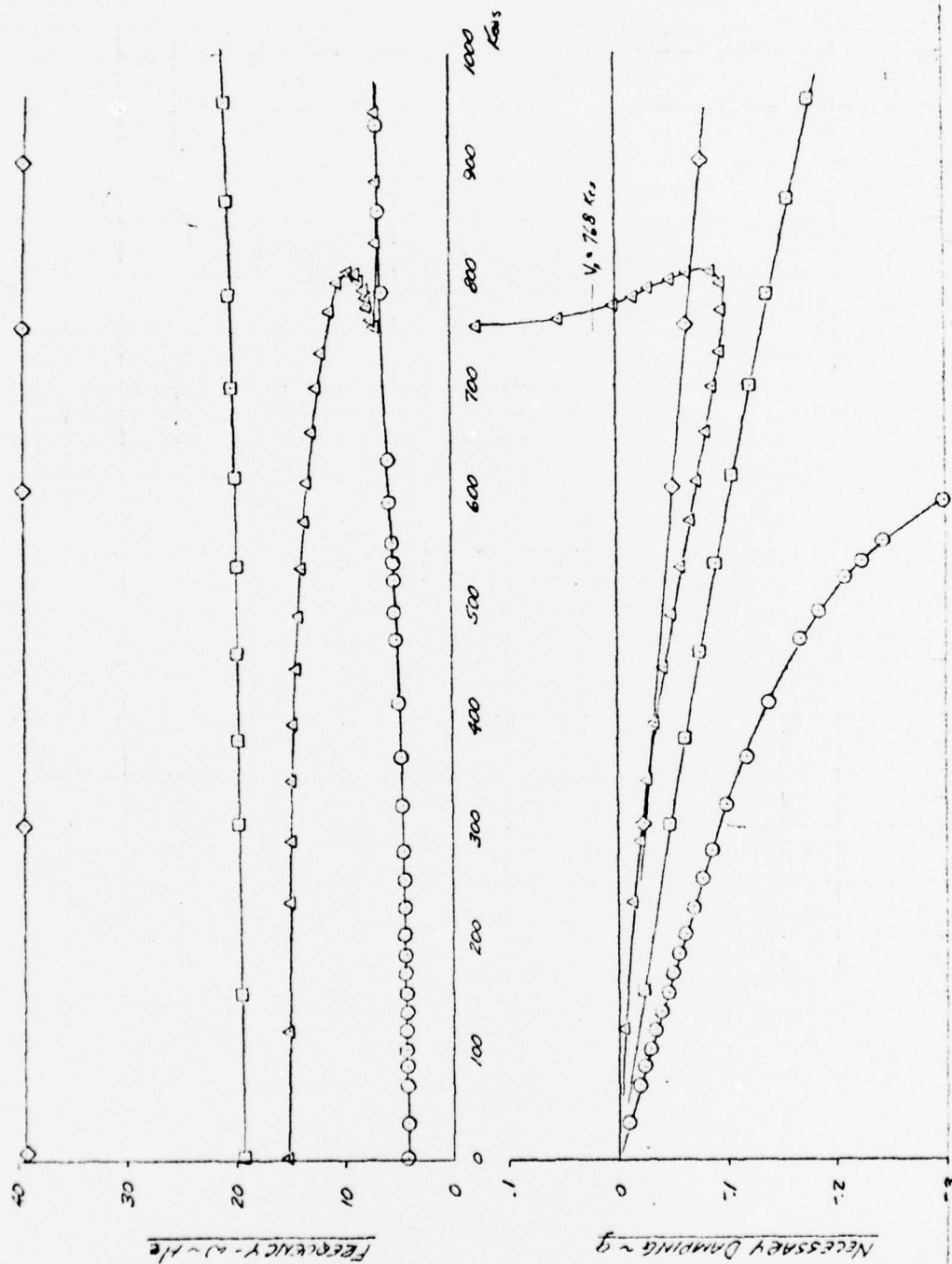


FIGURE 35 MINIMUM PREDICTED FLUTTER SPEED; SYMMETRIC CONDITION  
FREQUENCY AND DAMPING VS. VELOCITY

See Table 2 for symbols.

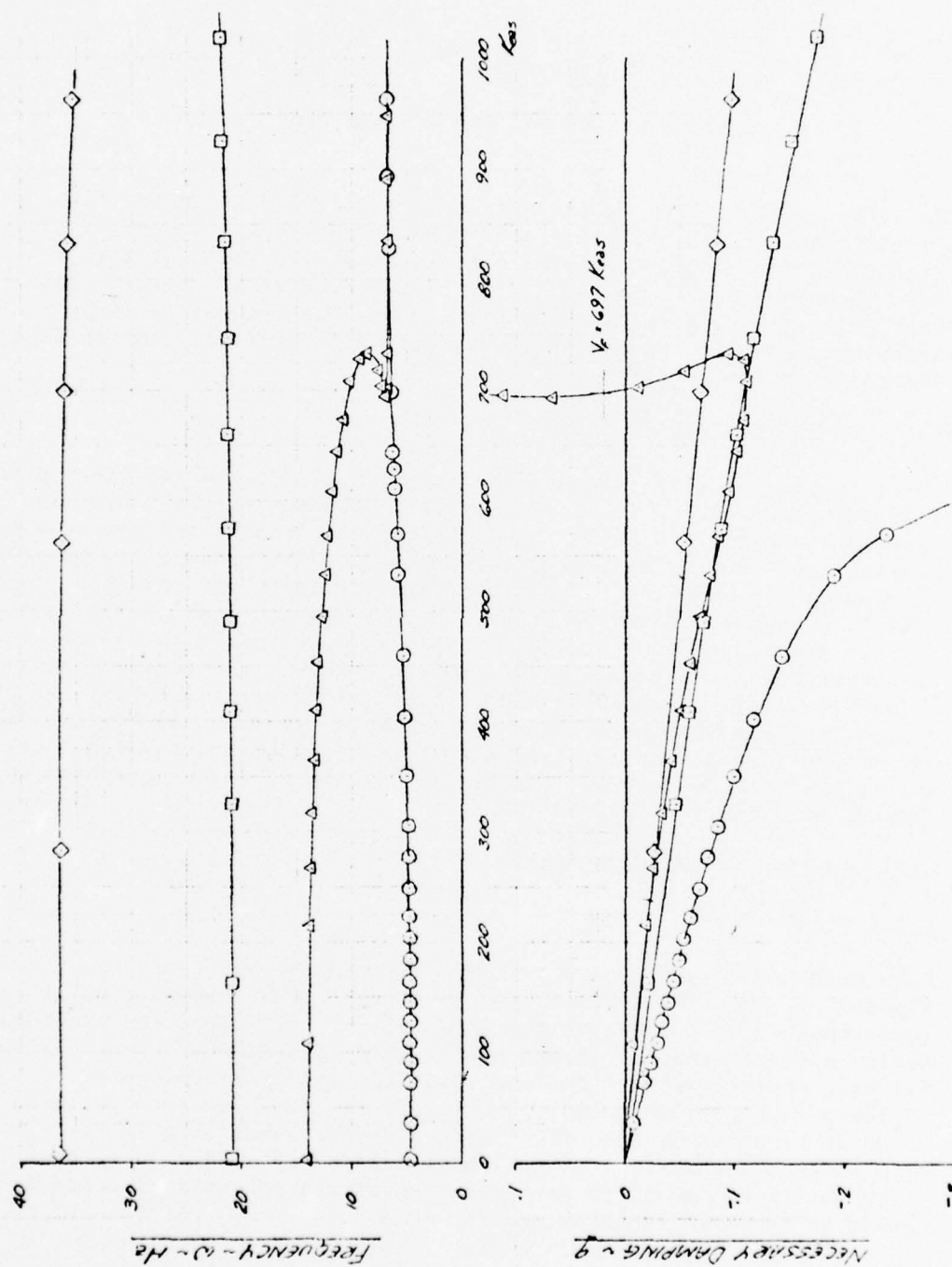


FIGURE 36 MINIMUM PREDICTED FLUTTER SPEED; ANTI-SYMMETRIC CONDITION  
FREQUENCY AND DAMPING VS. VELOCITY



## SECTION 6.0

### DESIGN DEVELOPMENT AND VERIFICATION

Verification tests for design development included laminate tests for certification of the Fiberite Hy-E-1034C graphite/epoxy prepreg tape, static and fatigue tests of the centerline splice joint, flatwise tension and edgewise compression of sandwich material, intermediate spar joint tests, comparison of precured versus cocured laminate-sandwich construction, and an investigation for installation of Hi-Lok fasteners in the sandwich material.

#### 6.1 LAMINATE STRENGTH TESTS

Certification of 12-inch-wide Fiberite Hy-E-1034C graphite/epoxy prepreg tape was accomplished in accordance with Columbus Aircraft Division Specification No. HB0130-102. Unidirectional tension and compression strength and modulus data were obtained where the results are presented in Figures 37 and 38 for unidirectional strength and modulus, respectively. Data were obtained at both room temperature and 350°F. except for the tension modulus at 350°F. This was due to the unavailability of an extensometer calibrated above 180°F. However, the tension modulus is primarily filament dependent and certification of the material was not delayed. Minimum specification requirements are shown in Figures 37 and 38 and the data met or exceeded these requirements for the material tested where these data are typical for a 250-lb. lot of graphite/epoxy prepreg material.

#### 6.2 CENTERLINE SPLICE JOINT

##### 6.2.1 Static Tests

Four axial load specimens were fabricated to the configuration shown in Figures 39 and 40 and static tested at room temperature to verify axial load transfer at the centerline skin splice. All specimens exceeded the design ultimate load of 16,085 pounds with interlaminar shear and shearout failures predominating. Failing loads for the specimens were 17,680 pounds, 18,100 pounds, 19,500 pounds, and 19,000 pounds. Specimen failures are shown in Figures 41 and 42. These data are summarized in Table 5 which also indicates a maximum stress concentration of 1.28. Therefore, the joint design was modified to reduce the stress concentration and incorporate an improved stacking order.

FIGURE 37

QUALITY CONFORMANCE TESTS  
 FIBERITE Hy-E-1034C UNIDIRECTIONAL TAPE LAMINATE  
 LOT NO. 4D-82  
 PURCHASE ORDER H-562-K-006083  
 TESTED PER SPECIFICATION HB0130-102

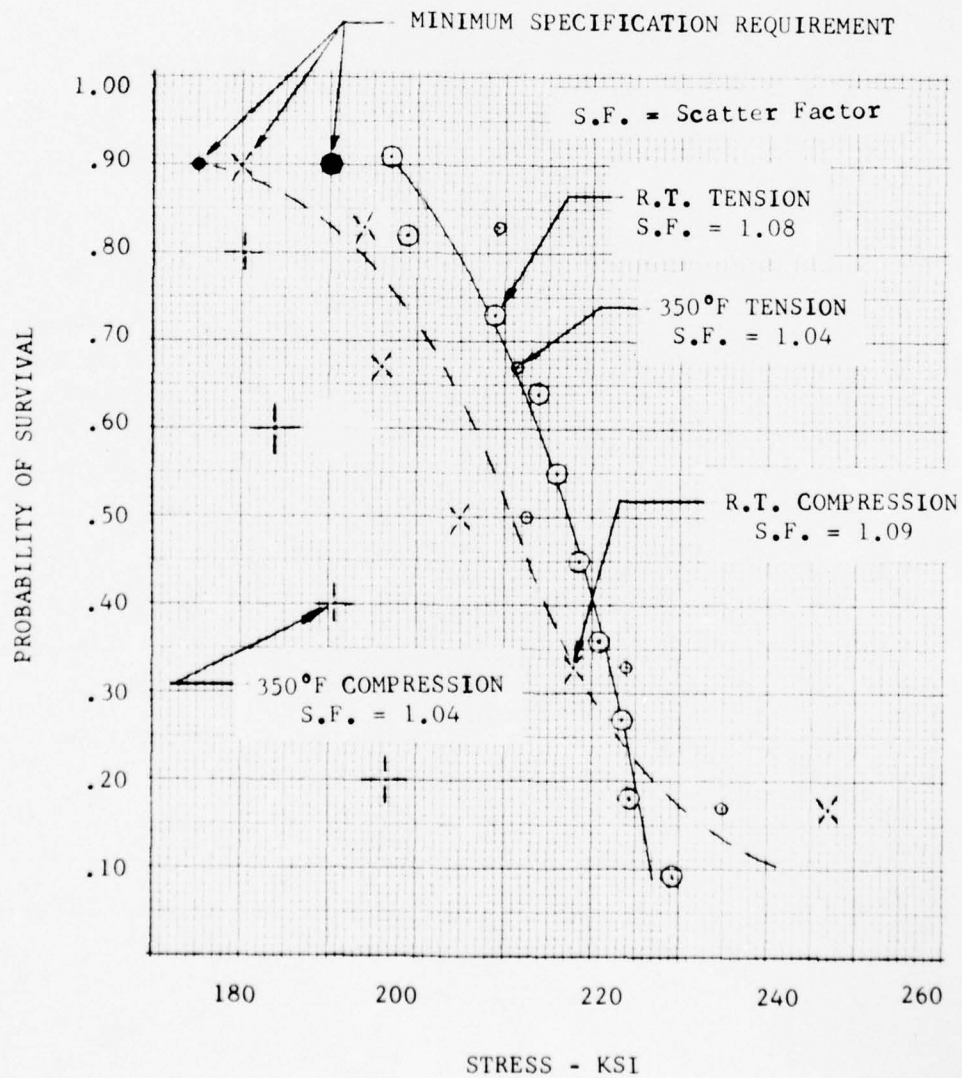
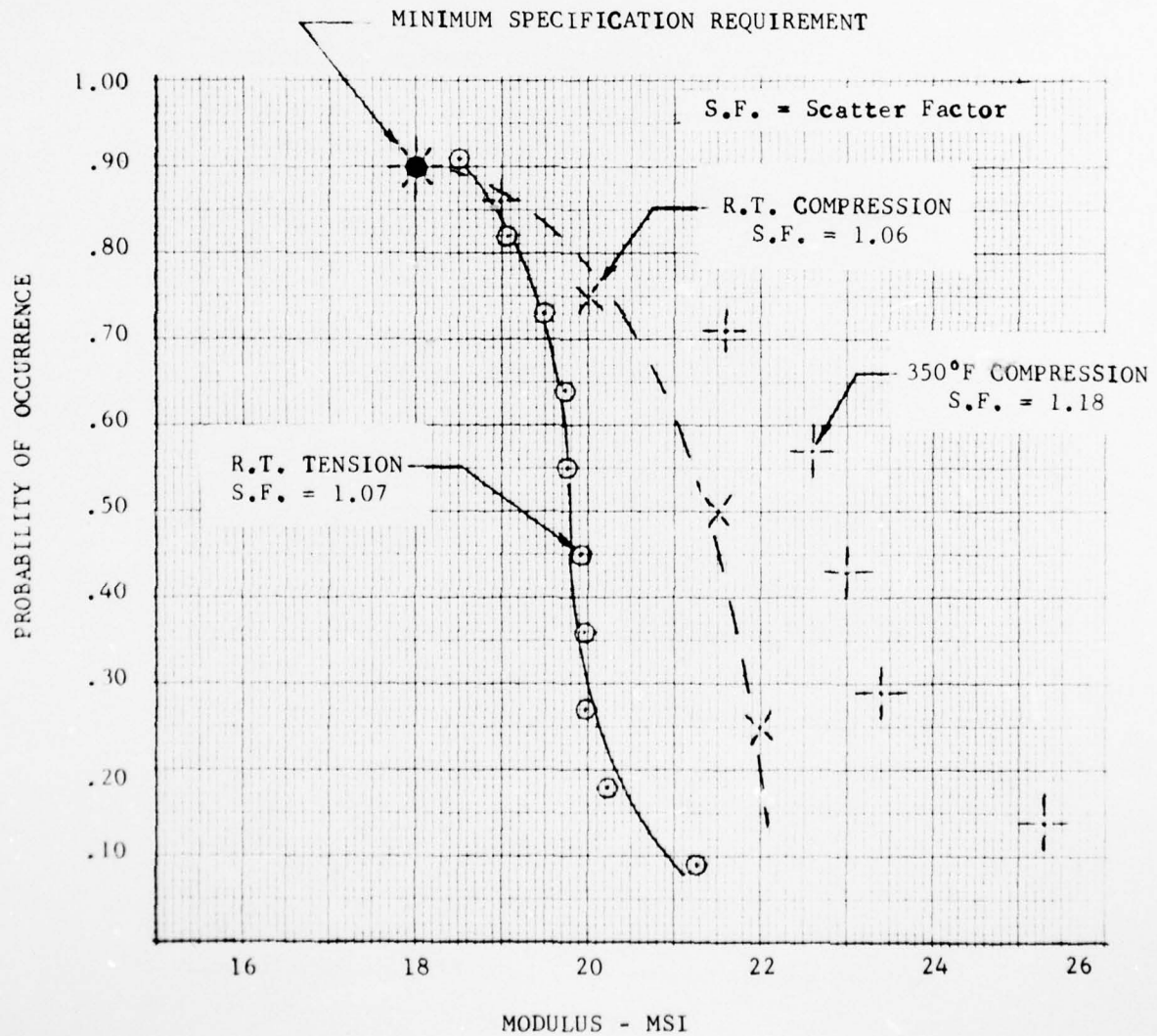


FIGURE 38

QUALITY CONFORMANCE TESTS  
 FIBERITE Hy-E-1034C UNIDIRECTIONAL TAPE LAMINATE  
 LOT NO. 4D-82  
 PURCHASE ORDER H-562-K-006083  
 TESTED PER SPECIFICATION HB0130-102



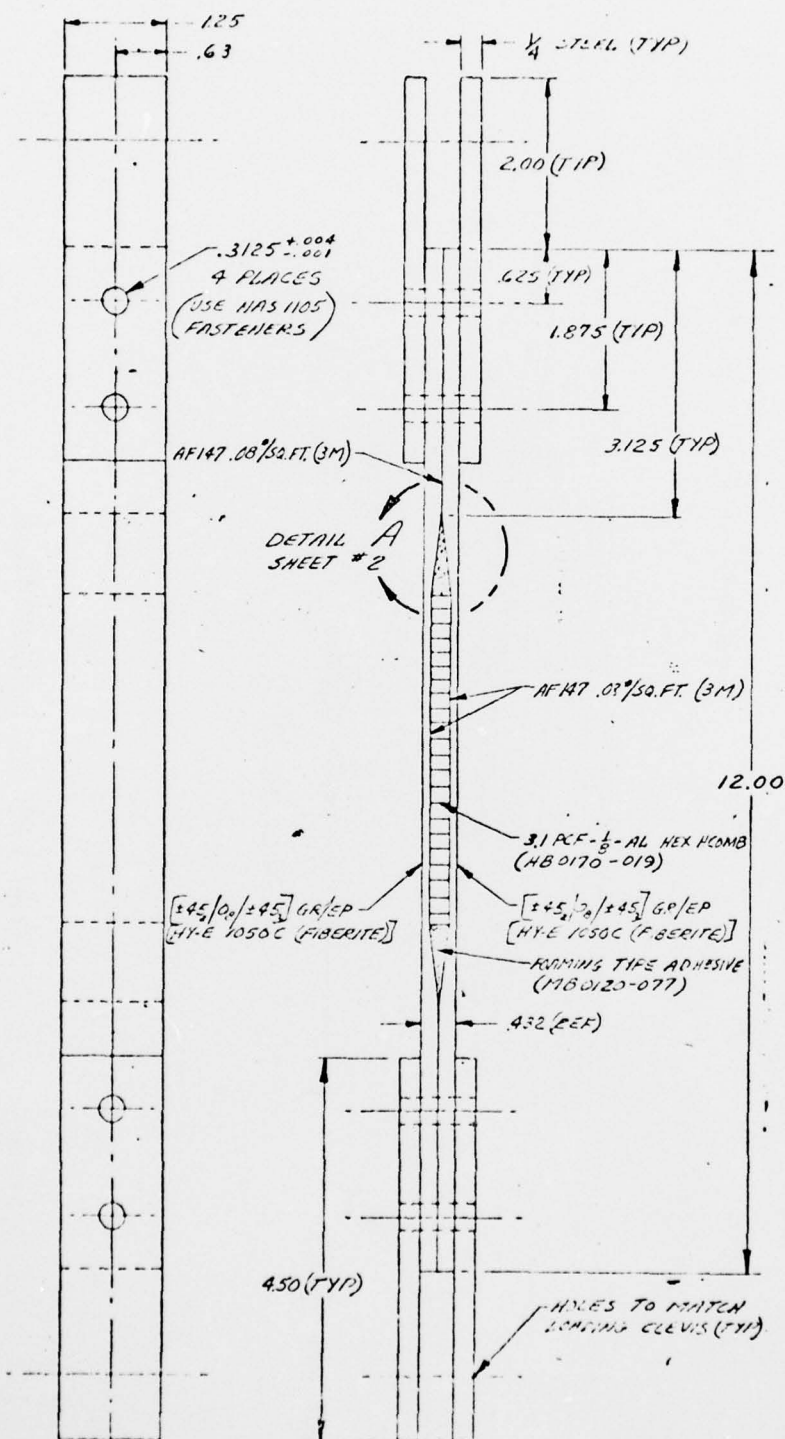


FIGURE 39  $\bar{Q}$  AXIAL LOAD SPECIMEN

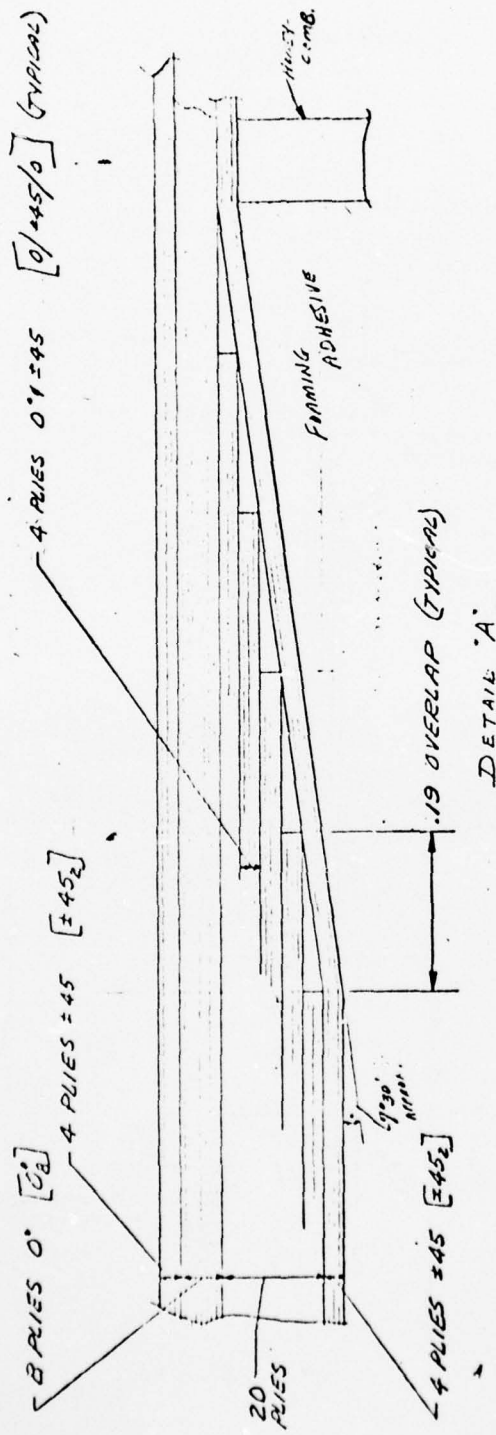


FIGURE 40 Z AXIAL LOAD SPECIMEN, DETAIL A



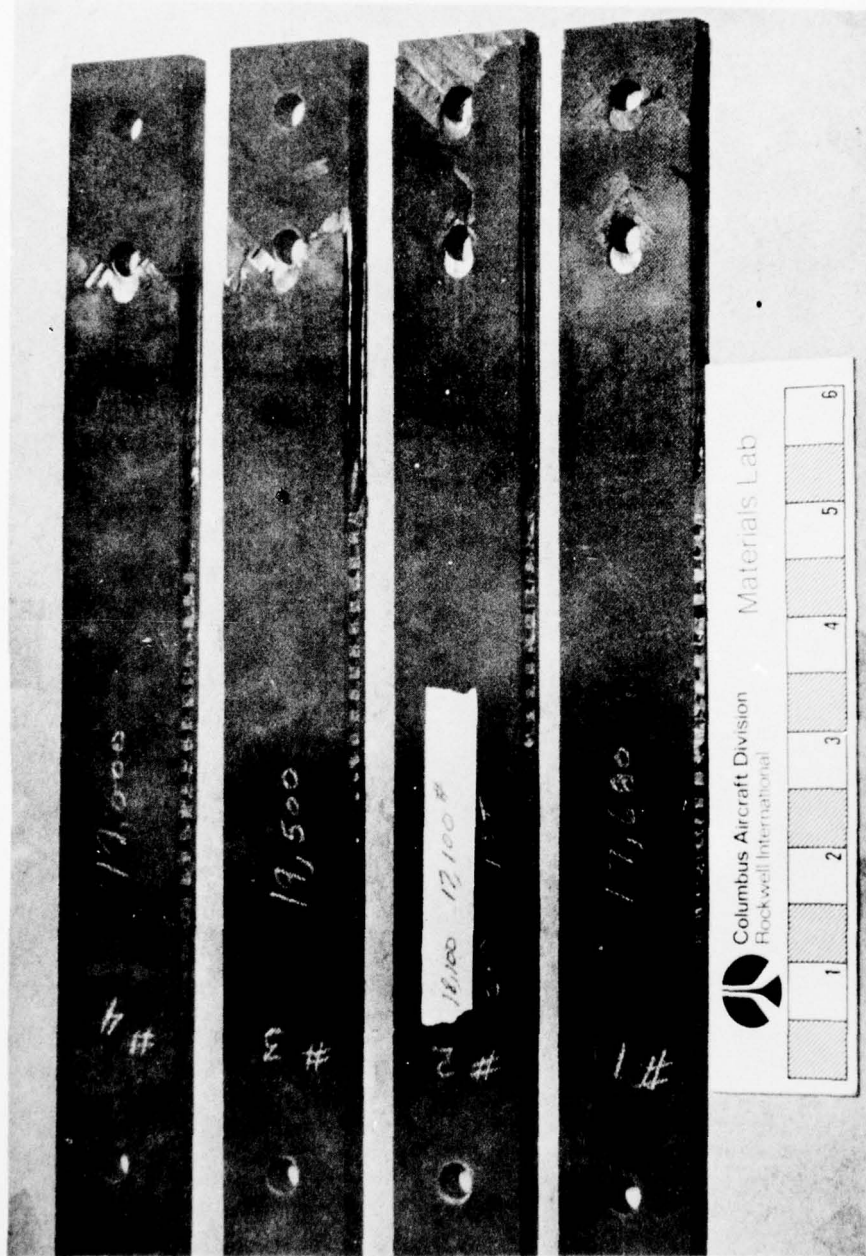


FIGURE 41 FAILED  $\bar{Q}$  AXIAL LOAD SPECIMENS



FIGURE 42 DETAIL OF  $\bar{Q}$  AXIAL LOAD SPECIMEN TEST FAILURE

TABLE 5  
ORIGINAL Q SKIN SPLICE SPECIMENS - TEST RESULTS

$[0_8/\pm 45_4]$  Basic Laminate Allowable Gross Stress\* = 103,000 #/In.<sup>2</sup>

Reference Figure 40;  $K_{tc} = 2.4 @ \text{joint}$

Predicted Net Tension Stress Allowable\* = 42,900 #/In.<sup>2</sup>

Specimen	Failing Load (lbs.)	Test Gross Stress (#/In. <sup>2</sup> )	Test Gross Stress/Laminate Stress	Test Net Stress (#/In. <sup>2</sup> )	Test Net Predicted Net
1	17,680	80,400	.78	47,700	1.11
2	18,100	82,300	.80	48,800	1.14
3	19,500	88,600	.86	52,600	1.23
4	19,000	86,400	.84	51,200	1.19

$$\text{Max Stress Concentration} = \frac{1}{.78} = 1.28$$

\* Ref. Pg. 1.2.2-14 & Pg. 1.3.2-26 of Composite Des. Guide

Five specimens were fabricated for static testing using the improved stacking order shown in Figure 43 which includes 32% [0], 14% [90], and 54% [ $\pm 45$ ] plies. These data also exceeded the design ultimate load and the test results are summarized in Table 6 which indicates a lower stress concentration of 1.06. The failed specimens are shown in Figures 44 and 45 where three specimens failed in the basic laminate with no failure in the net section at the joint. It is noted that the revised laminate using 32% [0] fibers achieved the same net stress level as the original laminate which used 50% [0] fibers.

### 6.2.2 Fatigue Tests

Three centerline joint specimens were fabricated using precured laminates of the revised stacking order of Figure 43 and provided to the Naval Air Development Center for fatigue testing. Specimen SN-3 was cycled in tension-tension with  $R = 0$  and an initial loading of 0 to 6500 pounds. The net calculated stress was 16807 psi through the bolt hole at the specimen ends and the gross stress was 25890 psi at the center of the specimen. Testing was stopped after  $1.3 \times 10^6$  cycles with no failure. The load level was increased to 9750 pounds for continued cycling but the specimen was inadvertently overloaded to 18800 pounds and failed through the net section ( $\sigma_{net, ult} = 48610$  psi,  $\sigma_{gross, ult} = 74882$  psi),

indicating that no degradation of static strength had occurred due to prior cycling.

Specimen SN-4 was cycled in tension-compression without an anti-buckling guide with  $R = -5$  and an initial loading of +1300 to -6500 pounds. The net calculated stress was -17135 psi through the bolt hole and the gross stress was -26363 psi at the center of the specimen. Testing was stopped after  $1.0 \times 10^6$  cycles with a surface ply delamination which occurred after approximately 800,000 cycles as shown in Figures 46 and 47. Specimen SN-4 was then static tested in compression to failure at -15900 pounds ( $\sigma_{gross, ult} = -64487$  psi) using an anti-buckling guide.

Specimen SN-5 was cycled in tension-compression with  $R = -5$  and a 25% increase in loading over that for specimen SN-4 which gave limits of +1625 pounds to -8125 pounds. For the maximum compression load the net calculated stress was -29476 psi and the gross stress was -32947 psi. This specimen was tested using an anti-buckling guide as shown in Figure 48 which allowed approximately 1/16-inch deflection laterally. Surface delamination began after approximately 60000 cycles as shown in Figures 49 and 50. Testing was stopped after 100,000 cycles and the specimen was static compression tested to failure at -13950 pounds ( $\sigma_{gross, ult} = -56567$  psi).



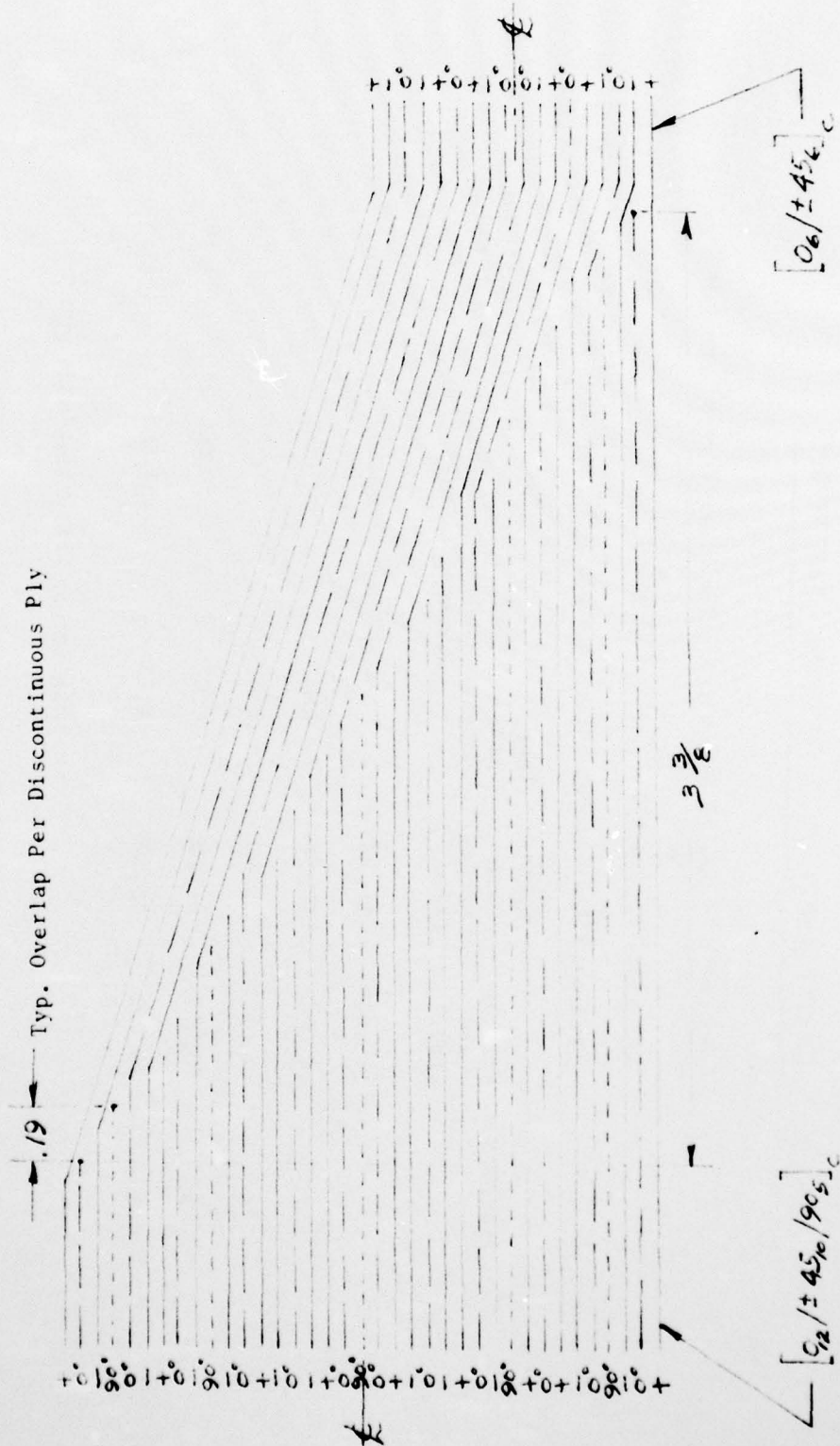


FIGURE 43 REVISED CENTERLINE LAMINATE STACKING ORDER



TABLE 6

REVISED  $\bar{Q}$  SKIN SPLICE SPECIMENS - TEST RESULTS

$[0_6^{\circ}/\pm 45_6^{\circ}]_c$  Basic Laminate Allowable Gross Stress  $\Delta = 76,000 \text{ \#/In.}^2$

Reference Figure 43;  $K_{tc} = 1.7$  @ joint  $\Delta$

Predicted Net Tension Stress Allowable  $\Delta = 44,700 \text{ \#/In.}^2$

Specimen	Failing Load (Lbs.)	Test Gross Stress ( $\text{\#/In.}^2$ )	Test Gross Stress/Laminate Stress	Test Net Stress ( $\text{\#/In.}^2$ )	Test Net Predicted Net Stress
1	17,650*	71,300	.94	46,200	1.03 *
2	19,075*	77,100	1.01	49,900	1.12 *
3	19,050*	77,000	1.01	49,900	1.12 *
4	20,075	81,100	1.07	52,600	1.18
5	21,170	85,500	1.13	55,400	1.24

$$\text{Max Stress Concentration} = \frac{1}{.94} = 1.06$$

\* No Net Section Failure

$\Delta$  Ref. Pg. 1.2.2-14 & Pg. 1.3.2-26 of Composite Des. Guide

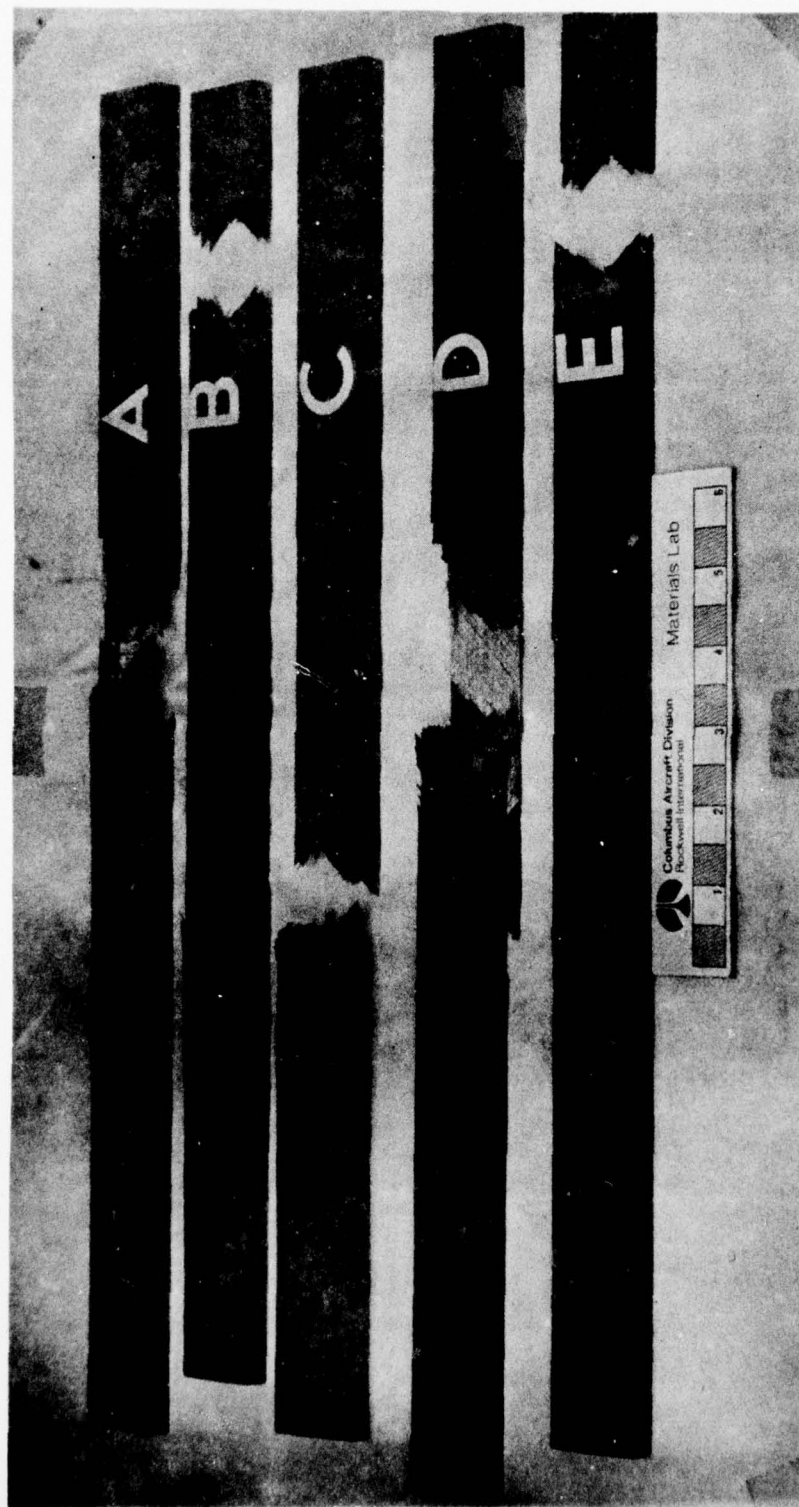


FIGURE 44 FAILED AXIAL LOAD SPECIMENS - PRECURED FACINGS WITH REVISED STACKING ORDER

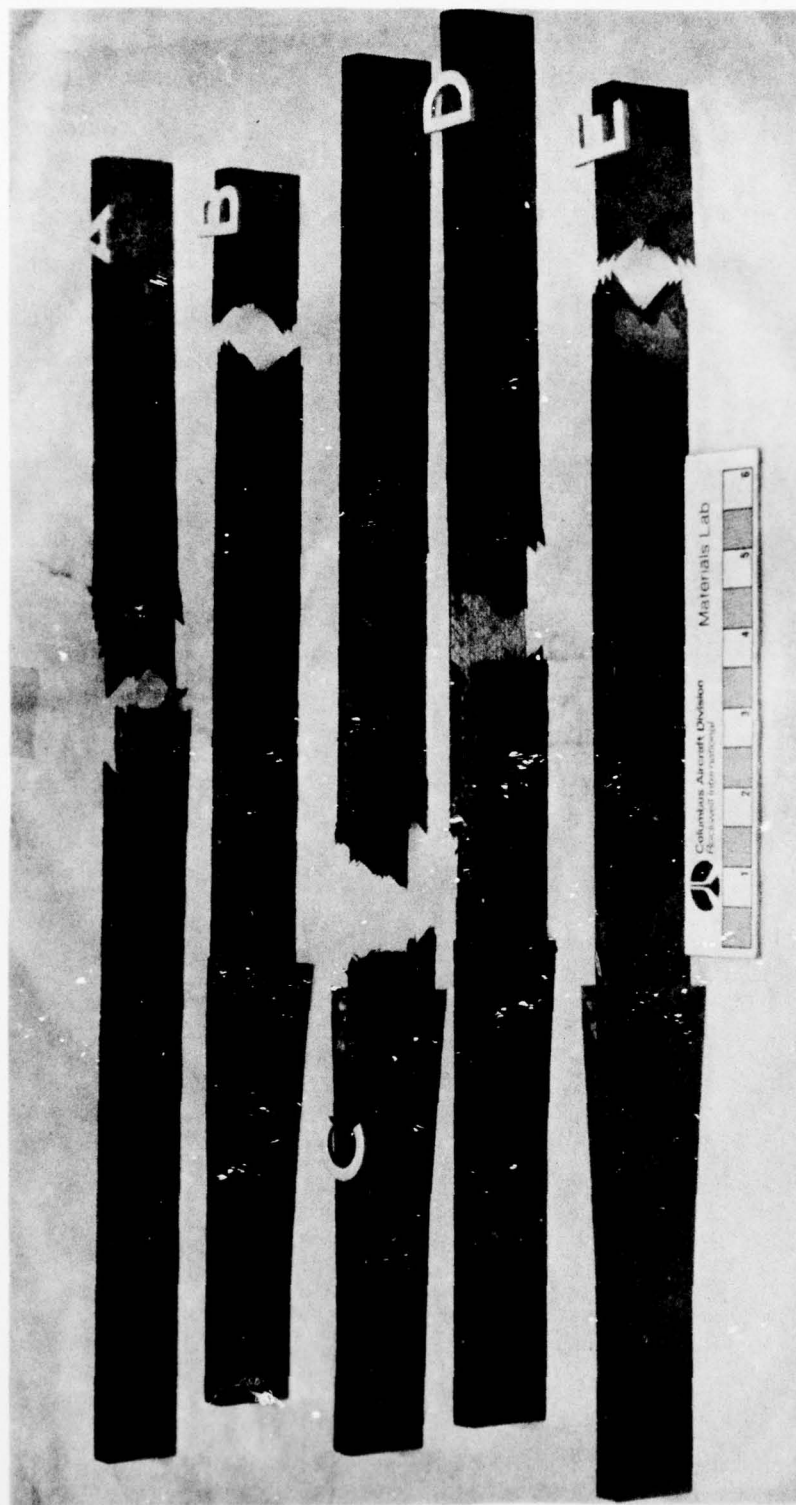


FIGURE 45 FAILED AXIAL LOAD SPECIMENS - PRECURED FACINGS WITH REVISED STACKING ORDER

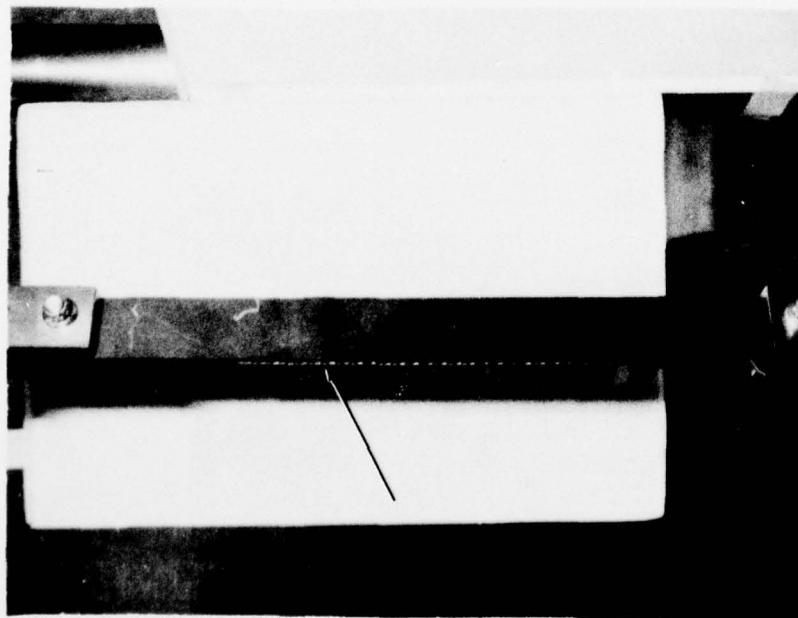


FIGURE 46 CENTERLINE JOINT AXIAL FATIGUE  
SPECIMEN SN-4 AFTER 800,000 CYCLES

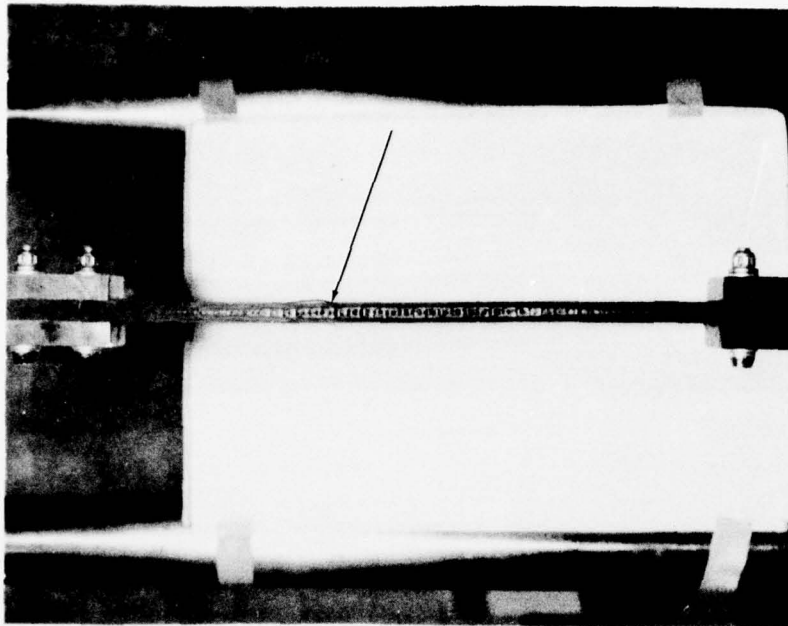


FIGURE 47 EDGEWISE VIEW OF AXIAL FATIGUE  
SPECIMEN SN-4 AFTER 800,000 CYCLES

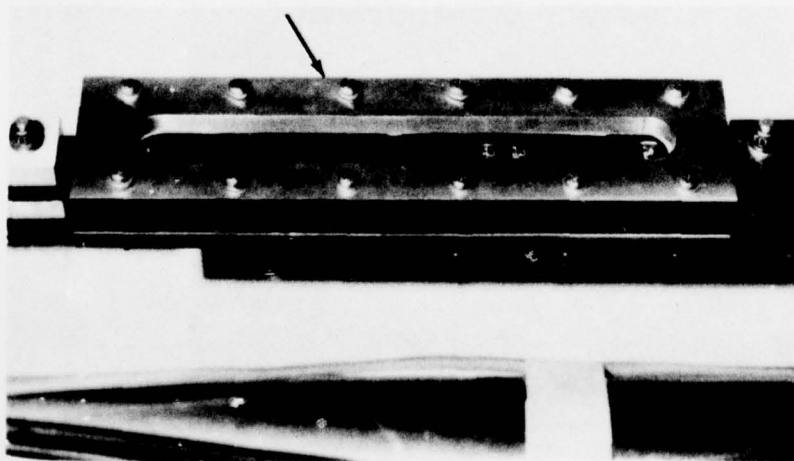


FIGURE 48 SPECIMEN SN-5 IN  
ANTI-BUCKLING GUIDE

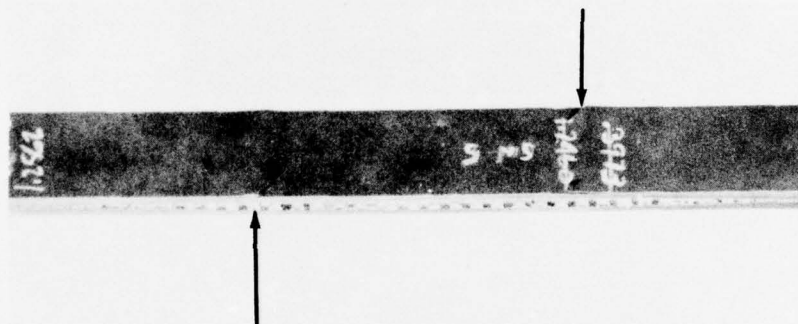


FIGURE 49 CENTERLINE JOINT  
AXIAL FATIGUE  
SPECIMEN SN-5 AFTER  
60000 CYCLES

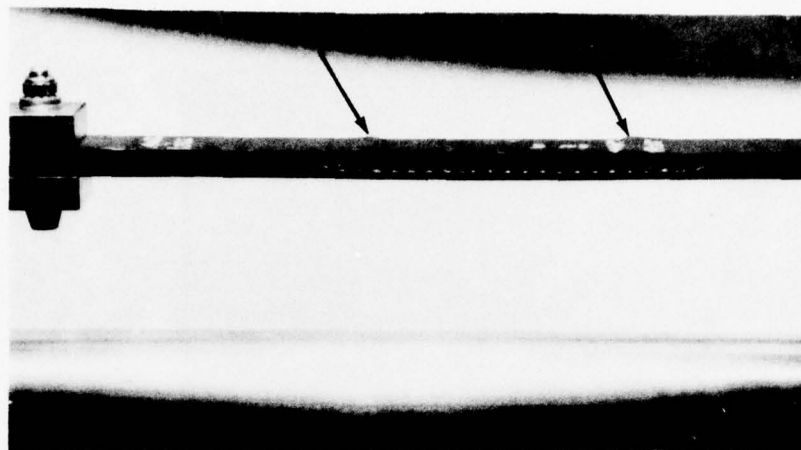


FIGURE 50 EDGEWISE VIEW OF  
AXIAL FATIGUE  
SPECIMEN SN-5 AFTER  
60000 CYCLES



### 6.3 FLATWISE TENSION

To simulate pressure loading at the intermediate spar to lower skin panel bonded joint, five 2-inch by 2-inch flatwise tension specimens were fabricated by bonding a precured graphite intermediate lower spar cap to a precured graphite lower skin using .08 psf AF 147 supported film adhesive. The sandwich skin panel incorporated Fibertruss core (HFT-1/8-5.5) and the final test configurations are shown in Figure 51. Test failure loads of 1575, 1815, 1750, 2040, and 1850 pounds were attained with failure occurring within the laminate. This resulted in a minimum flatwise tensile strength of 394 psi versus a predicted ultimate design value of 300 psi.

### 6.4 EDGEWISE COMPRESSION

To simulate edgewise compression of the upper skin panel at an intermediate spar attachment, two 3-inch by 4-inch specimens were fabricated from a precured graphite sandwich panel as shown in Figures 51 and 52. As shown in Figure 52 the specimen incorporates a 7S34 1/4-inch flush head fastener with an O-ring installed through a glass insert, backed up with HFT-1/8-5.5 core filled with potting compound. Test failure loads of 26,625 and 27,625 pounds were attained resulting in a minimum edgewise compression stress of 53787 psi. For comparison, the maximum calculated compression stress at such a hole in the upper cover panel is approximately 29000 psi.

### 6.5 SPAR JOINT TESTS

Room temperature static testing of joint shear verification specimens was performed on configurations simulating both the intermediate spar to lower skin bond and the intermediate spar to upper skin attachment.

To simulate the spar to lower skin bond six 1-inch wide lap shear specimens with a 2-inch overlap were fabricated from precured graphite laminates of 15-ply thickness using .08 psf AF 147 supported film adhesive. These specimens are shown in Figure 53. Test failure loads of 3340, 3580, 3425, 3530, 3620, and 3500 pounds were attained resulting in a minimum single lap shear stress of 1670 psi. This compares favorably with the value of 1500 psi used for design of the spar to lower skin bond joint.

For simulation of the shear transfer joint at the upper spar cap to upper skin mechanically fastened joint five 2-inch wide specimens were fabricated from a precured graphite sandwich panel with each specimen incorporating two 1/4-inch flush head fasteners with O-rings. Specimen panels are shown in Figure 53. The sandwich panel was joined to a 15-ply laminate on two specimens and to a 30-ply graphite laminate on three specimens.

AD-A041 208

ROCKWELL INTERNATIONAL. COLUMBUS OHIO COLUMBUS AIRCRA--ETC F/G 11/4  
EVALUATION OF COMPOSITE WING FOR XFV-12A AIRPLANE.(U)

DEC 76 D N ULRY, R W GEHRING, K I CLAYTON

N62269-74-C-0577

UNCLASSIFIED

NR76H-135

NADC-77183-30

NL

2 OF 4.  
AD  
A041208



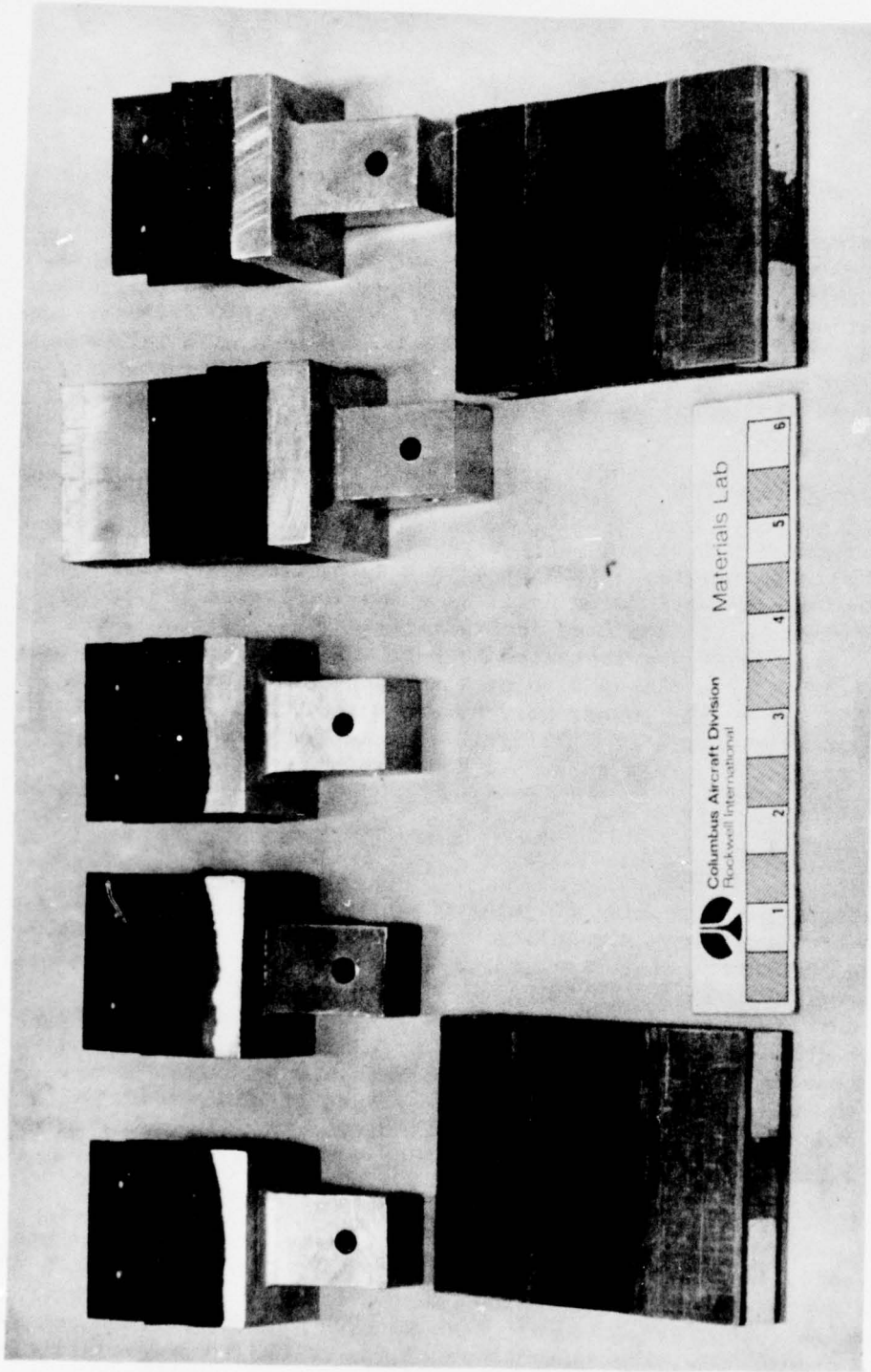


FIGURE 51 JOINT VERIFICATION SPECIMENS FABRICATED FOR FLATWISE TENSION  
AND EDGEWISE COMPRESSION TESTS

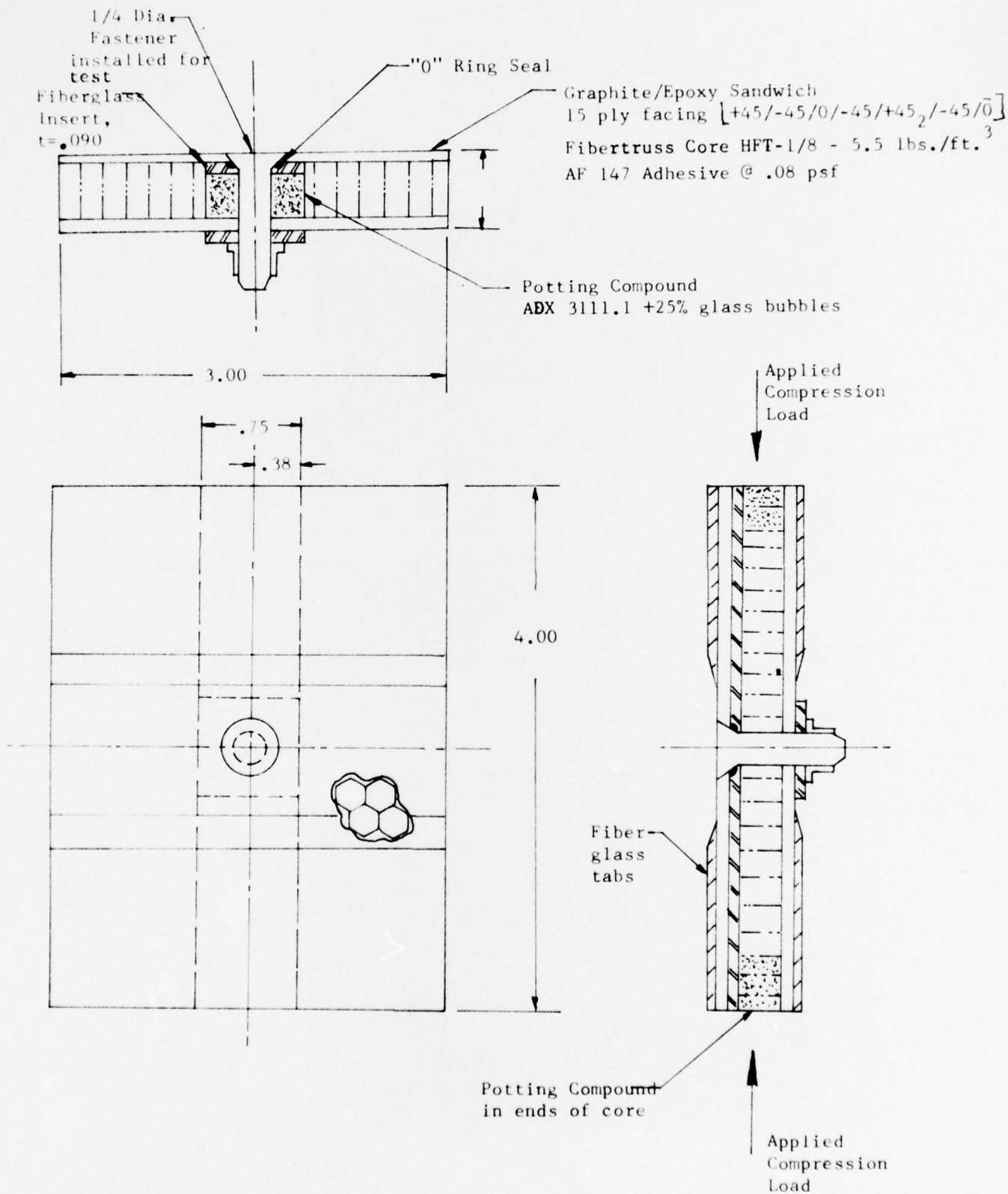


FIGURE 52 COMPRESSION TEST SPECIMEN FOR INTERMEDIATE SPAR JOINT

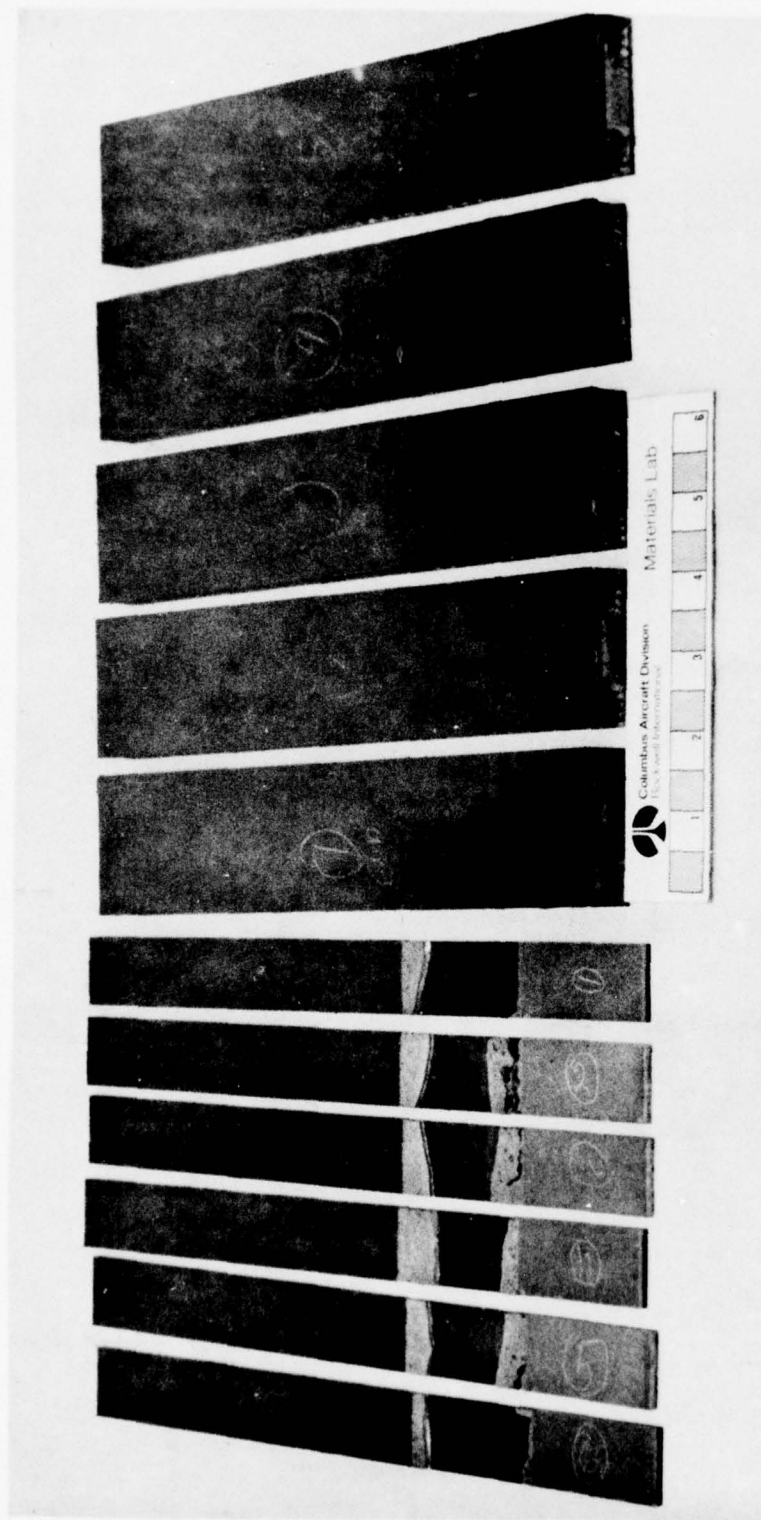


FIGURE 53 JOINT VERIFICATION SPECIMENS FABRICATED FOR SHEAR TESTS



Test failure loads of 3535 and 3600 pounds were attained for the 15-ply laminate specimens. Failure loads for the 30-ply laminate specimens were 6480, 6100, and 6480 pounds, or a minimum of 3050 pounds per fastener. The maximum design ultimate shear flow at the inboard intermediate spar is 2458 lbs./inch for a 28 lamination spar cap or 3073 pounds per fastener based on a 1 1/4-inch fastener spacing. Two specimens were retested with the spar cap fixed and load applied to the skin panel resulting in similar failures at 5920 and 5530 pound loads. The test data are considered conservative due to local bending moments present in the joint area causing pull-through failure of the flush head fasteners. Protruding head fasteners were incorporated into the design of the wing inboard of X 15.00 with the spar shear flows being considerably lower outboard of this station. In addition, a 12-ply doubler was incorporated into the upper cover panel design at the inboard intermediate spar locations.

#### 6.6 PRECURE VS. COCURE TESTS

An in-house investigation evaluated precured versus cocured processing using three specimens identical to the revised joint specimens defined by Figures 39 and 43. In these specimens one facing was precured and one facing was cocured. Static tests to failure gave maximum loads of 14,760, 15,525, and 15,500 pounds with a maximum stress concentration of 1.28. Test data are summarized in Table 7. These results indicate a 20% increase in stress concentration at the splice joint based on cocured versus precured laminates. Failures are shown in Figure 54.

#### 6.7 HI-LOK FASTENERS INSTALLATION

Installation techniques for Hi-Lok fasteners into the graphite/epoxy honeycomb sandwich panels were investigated. Standard 3/16-inch diameter Hi-Lok fasteners were successfully installed in graphite sandwich panels using glass-reinforced core filled with potting compound to simulate intermediate spar fabrication. The potting compound used consists of a two-part epoxy adhesive system (ADX-3111.1) obtained from the Hysol Corporation. To this adhesive system was added 25% of 3M glass bubbles. Figure 55 illustrates the results of using filled versus unfilled core during Hi-Lok installation. It is recommended that densified core plugs having a density of approximately 42 lbs/cu.ft. be investigated as an alternate to the potting compound on a production design due to the time-consuming process of injecting the compound and subsequent uncertainties associated with homogeneity of the compound after installation.

TABLE 7

COCURED  $Q$  SKIN SPLICE SPECIMENS - TEST RESULTS

$[0_6/\pm 45_6]_c$  Basic Laminate Allowable Gross Stress\* = 76,000 #/In.<sup>2</sup>

Reference Figure 43;  $K_{tc} = 1.7$  @ joint

Predicted Net Tension Stress Allowable\* = 44,700 #/In.<sup>2</sup>

Specimen	Failing Load (lbs.)	Test Gross Stress (#/In. <sup>2</sup> )	Test Gross Stress/Laminate Stress	Test Net Stress (#/In. <sup>2</sup> )	Test Net Predicted Net
1	14,760	59,600	.78	38,700	.87
2	15,525	62,800	.83	40,700	.91
3	15,500	62,700	.83	40,600	.91

$$\text{Max. Stress Concentration} = \frac{1}{.78} = 1.28$$

\* Ref. Pg. 1.2.2-14 & Pg. 1.3.2-26 of Composite Design Guide

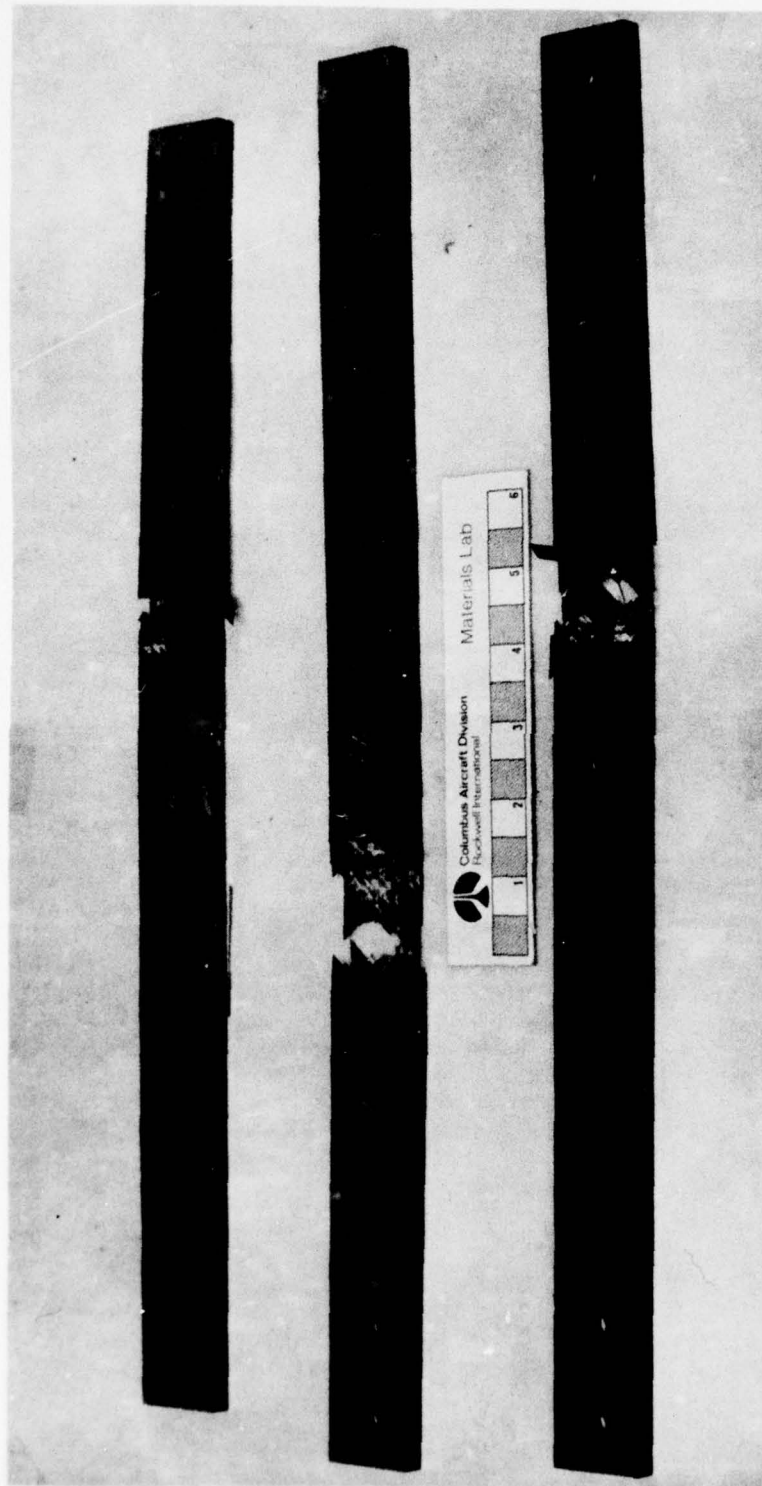


FIGURE 54 FAILED AXIAL LOAD SPECIMENS - COCURED FACINGS WITH REVISED STACKING ORDER

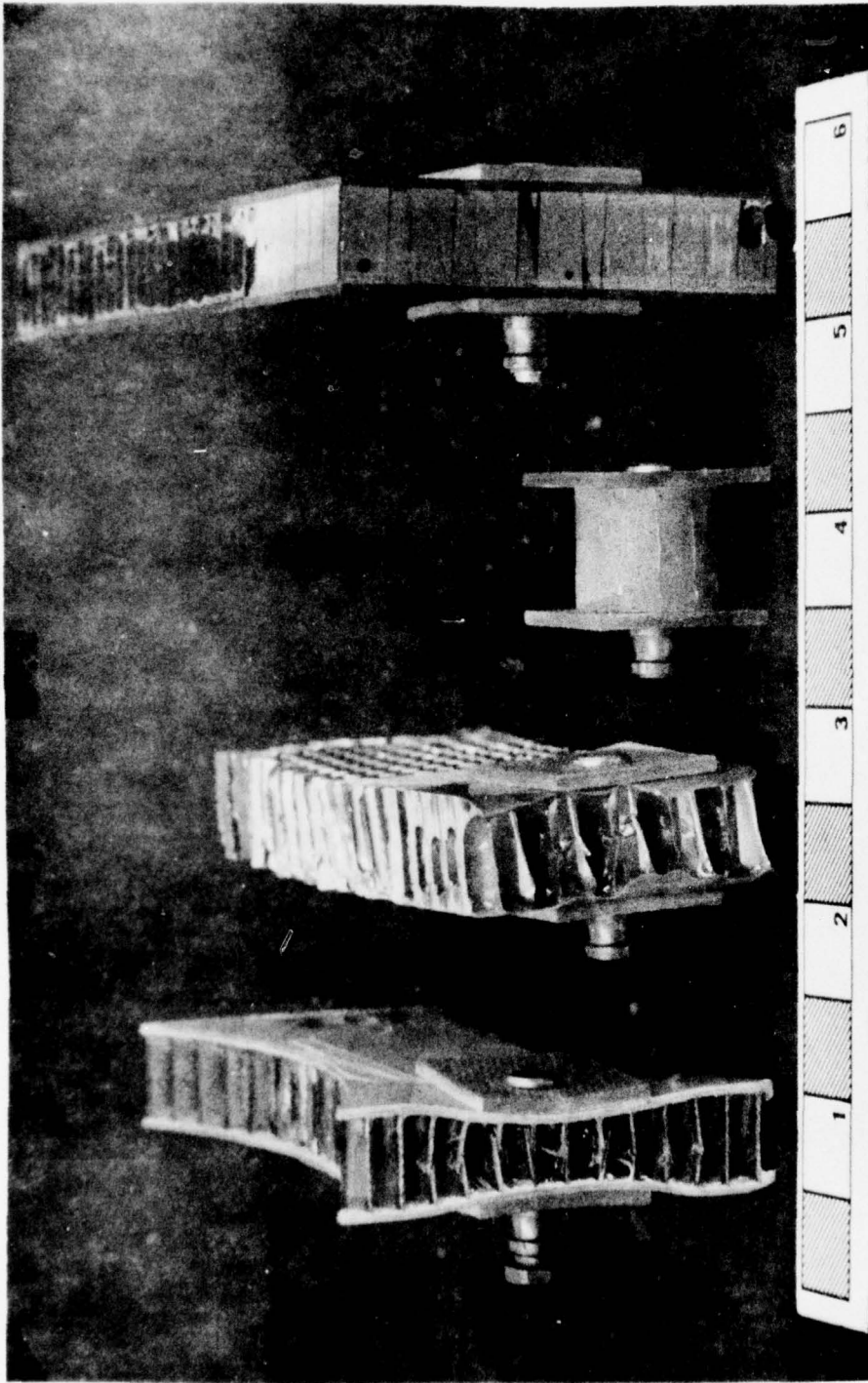


FIGURE 55 HI-LOK FASTENER INSTALLATION



## SECTION 7.0

### TOOLING & FABRICATION

The following paragraphs describe the tooling and fabrication techniques used in the construction of the composite wing box test section. The wing box test section consists of a left hand XFV-12A main wing box extending from the  $\mathcal{Q}$  of airplane to rear spar station 79.54 and includes provisions for mounting of the wing to a structural test stand at the center line rib with load application points at the aft wing to fuselage attachment fitting and R.S. station 79.54 as defined on drawing 8679-110100 (Figure B-1 ). Included in this composite test section assembly are the following detail parts:

8679-110101	Upper Skin Panel
8679-110102	Lower Skin Panel
8679-110103	Front Spar
8679-110105	Forward Intermediate Spar
8679-110106	Forward Inboard Intermediate Spar
8679-110107	Aft Intermediate Spar
8679-110108	Aft Inboard Intermediate Spar
8679-110109	Rear Spar
8679-110110	Centerline Rib
8679-110111	Wing Station 33.93 Forward Rib
8679-110112	Wing Station 33.93 Aft Rib
8679-110113	Wing-to-Fuselage Attach Fitting
8679-110114	Rear Spar Splice Fitting
8679-110115	Centerline Splice Plate
8679-110116	Wing Station 33.93 Rib Splice
8679-110117	Clips
8679-110118	Nutplate Retainers
TT-18636	Test Fixture

A production flow diagram for the fabrication and assembly of these parts is presented in Figure B-4. An alternate design concept, designated Concept "C" and described in Section 3.2, was also evaluated for manufacturing feasibility in the preliminary design phase of this program. A production flow diagram for this design concept is presented in Figure B-8.

#### 7.1 TOOL DESIGN

An overall tool design approach was established in conjunction with the basic engineering design and manufacturing process specifications which allowed fabrication and inspection of detail parts and subassemblies with subsequent final assembly into a geometrically correct wing box section.



The basic requirements included maintaining the external mold line contours, spar plane locations, rib plane locations and wing to fuselage attachment points. In addition to the overall dimensional tolerance control and mating requirements it was necessary to provide sufficient rigidity and durability in the layup tools to withstand autoclave pressure and cure cycles.

Early in the design cycle a decision was made to tool to the outer mold line surface of the honeycomb sandwich skin panels and let the inner sandwich surface float with the laminate and core tolerance buildup. All edges of the sandwich panel and sandwich height at B.P. 33.93 rib were maintained at a nominal constant thickness of 0.600 inch on the upper cover skin and 0.408 inch on the lower cover skin. Tooling dimensions were then set to machine the aluminum centerline rib caps and rear spar caps with these nominal offsets from the theoretical mold lines. Layup tools for the front spar and B.P. 33.93 rib were also set up with these nominal cap height offsets from the theoretical mold lines. Control of these rib, spar cap, and sandwich edge heights thereby established the wing box mold line heights at these locations. The intermediate spar cap mold line heights were established in the final wing box assembly and any tolerance build up between the cover skin sandwich assembly and spar web assembly was adjusted for in the mechanical attachment of the spar caps to the spar webs. Aluminum clips and mechanical fasteners provided positioning flexibility for attachment of the ends of the intermediate spar webs to the mating rib web.

#### 7.1.1 Cover Skin Panels

Prior to the start of fabrication of detail parts, a master plaster female model of the upper and lower mold line surfaces was constructed. This master model was used throughout the program for establishing and checking tool surface contours and for checking the accuracy of fabricated parts. The upper wing surface consists of straight line conic elements with modest curvature and a 0.090 inch steel plate was rolled to match this contour and used as a female tool for layup and cure of the outer skin laminate. This curved plate was mounted to a steel framework with adjustable studs and checked with contour templates for final positioning of the tool surface. A master mylar template was draped over the master plaster model surface and all ply laminate boundaries and fastener locations were laid out on the mylar and indexed with the skin layup tool. Individual ply laminations of twelve inch wide graphite/epoxy tape were laid out and trimmed to contour on this mylar master template then transferred to the steel tool for layup "black on black" as shown in Figure 56.

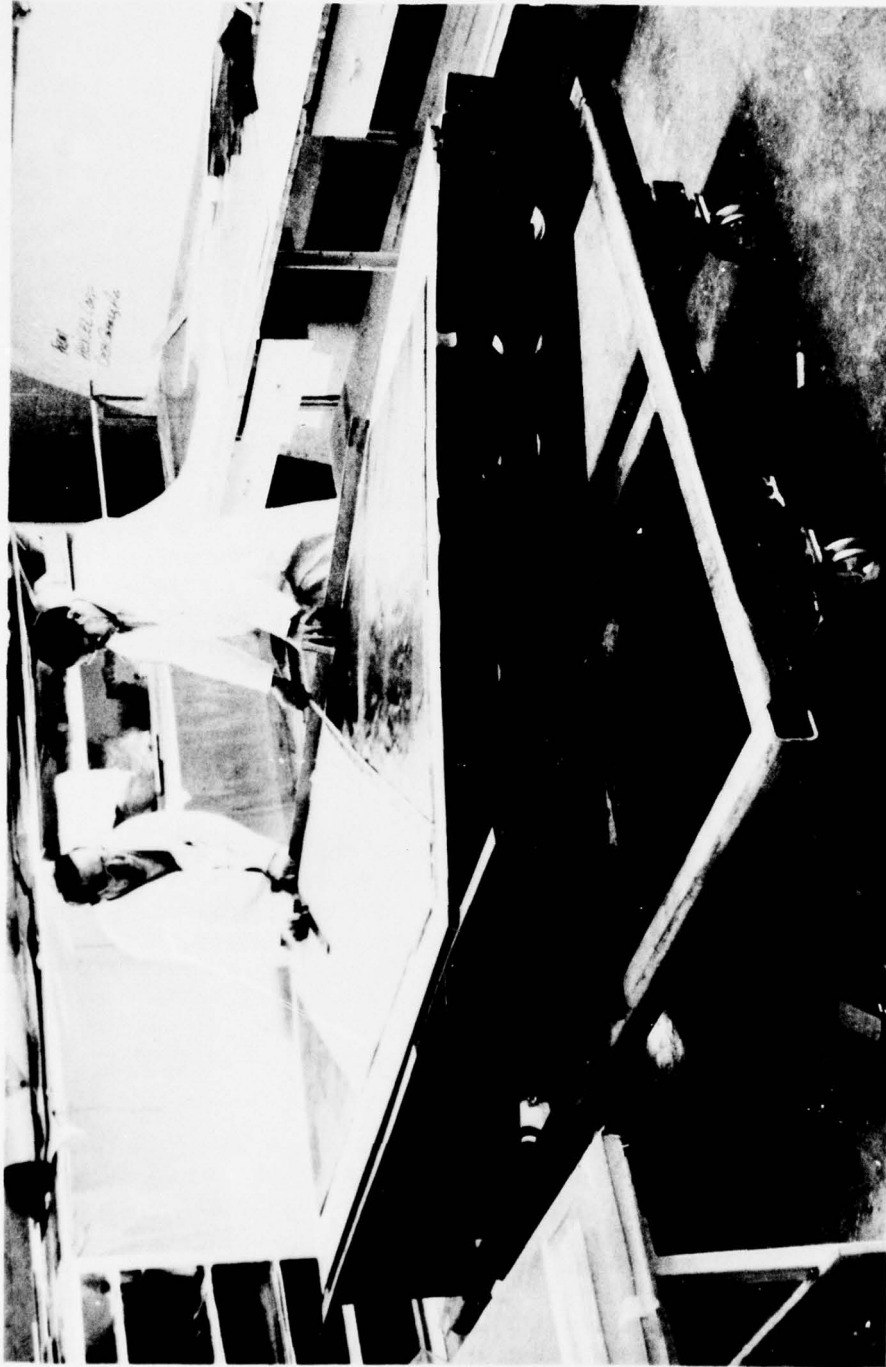


FIGURE 56 LAYUP OF UPPER SKIN PANEL FACING

A similar steel plate was rolled to contour to form a male layup tool for the inner skin of the upper cover skin sandwich panel. Graphite/epoxy laminations were stacked to the specified 37 ply pattern described in Section 3.0, covered with release mylar, bleeder material, vacuum bagged, and cured in the autoclave according to the cure cycle described in the process specifications of Paragraph 7.2. This layup and cure was accomplished in a one pass operation with no intermediate debulking steps required during the 37 ply skin laminate layup. The cured upper skin laminates were checked against the master plaster model and found to match the contour. A cured upper cover skin laminate is shown in Figure 57.

Glass/phenolic honeycomb core was then trimmed to match the edge contours defined on the master mylar template, tapered to match the laminate steps at rib locations, routed for precured glass/epoxy inserts, filled with potting compound at specified locations, cleaned and bonded to the outer skin with 0.08 Lb/Ft.<sup>2</sup> AF 147 film adhesive on the outer skin tool in an autoclave cure cycle. Tapering of the Fibertruss core to match the tapered skin laminates was readily accomplished by hand sanding. A layer of Vinylite verification film was then placed between the core and the inner skin laminate, bagged and pressurized in the autoclave at 180°F. to check fit up. High spots in the core were sanded lightly and a second prefit check was made to verify core contact over the entire skin surface prior to adhesive bonding of the inner skin to the core. The completed upper cover skin sandwich panel assembly was checked against the master plaster model and found to match the contour.

A similar procedure was used for fabrication of the lower cover skin panel, however, the severe contour changes at B.P. 33.93 required a different tooling approach to produce the layup tool. For the outer mold line surface a male plaster splash was made from the master plaster model. A 3/8 inch thick fiberglass/epoxy female tool surface was laid up and cured from this splash and stud mounted to an egg crate backup frame constructed of fiberglass sandwich frames. A similar male fiberglass/epoxy tool was constructed for the inner cover skin. Layup of a skin laminate on this tool is shown in Figure 58.

Prefit and bonding of the honeycomb core was performed in the outer skin tool with bonding of the inner and outer skins being performed in the same cure cycle on this panel. During this cure cycle distortion of the graphite sandwich panel occurred, deviating approximately 0.9 inches from moldline at X<sub>w</sub> 33.93 along the rear spar plane. Two options to re-form the skin were considered: 1) hot post forming, and 2) forcing the skin to moldline and then installing the front, intermediate and rear spars. Based on short beam test data, hot post forming appears to reduce interlaminar shear strength. "Forcing" the skin to moldline would produce beneficial compression stresses in the outer face sheet. It was therefore decided by NADC and CAD personnel to proceed with the assembly of the lower panel and "force" it to moldline. Ultrasonic through transmission inspection confirmed overall good quality of the secondary bonding operation; small voids were documented and repaired.

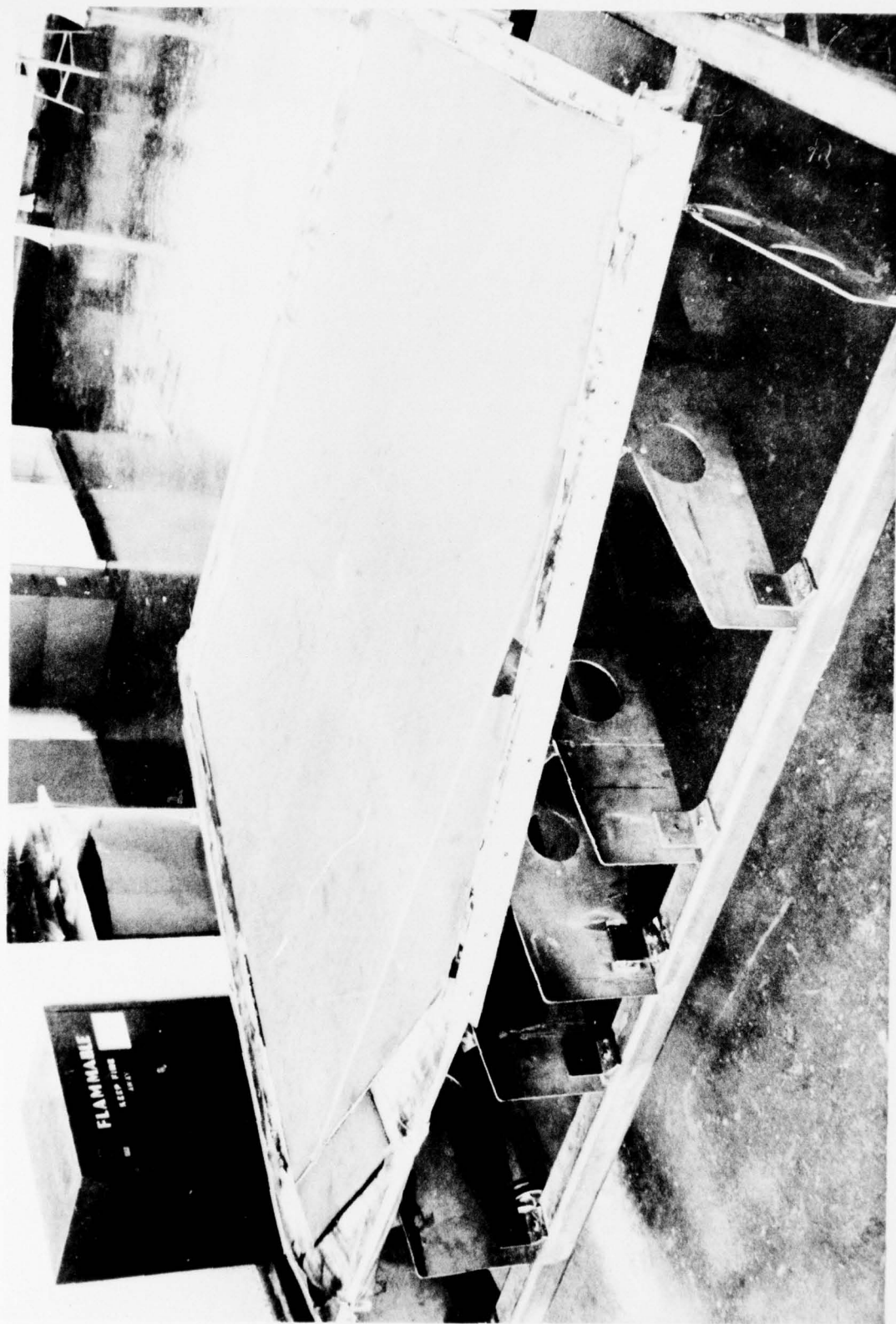


FIGURE 57 UPPER SKIN PANEL FACING AFTER CURE



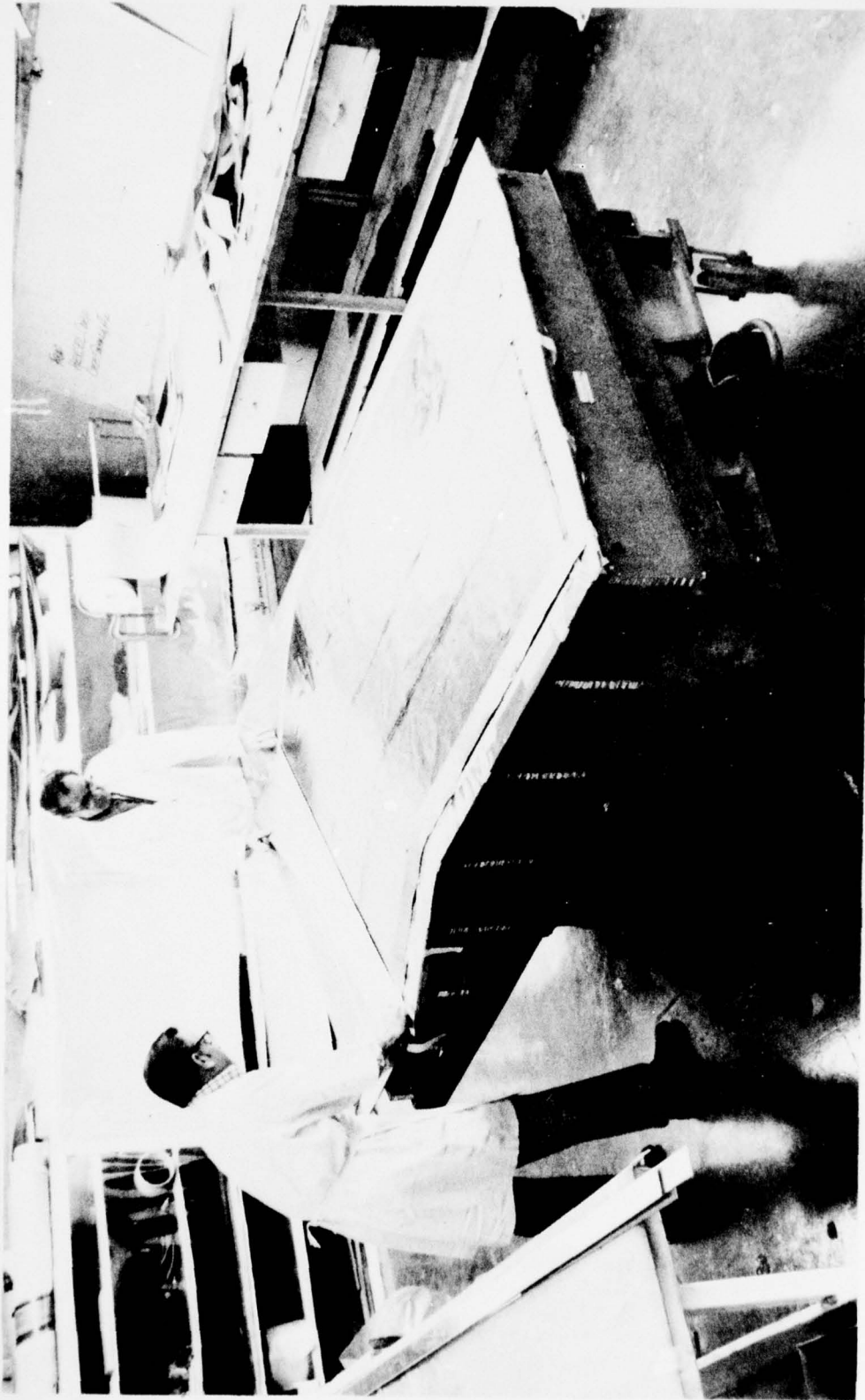


FIGURE 58 LAYUP OF LOWER SKIN PANEL FACING



### 7.1.2 Front Spar

The one-piece curved sandwich front spar presented a unique tooling problem for graphite/epoxy layup and secondary bonding of the honeycomb core and spar cap angles shown in Figure 17 of Section 3.0. It was originally planned to fabricate this spar in two straight sections, inboard and outboard, and mechanically splice these pieces at the B.P. 33.93 rib. However, engineering design considerations of weight and fuel sealing requirements dictated the design of a one-piece spar.

A female plaster master model of the inner spar surface was constructed and a male fiberglass/epoxy layup tool for the inner  $\pm 45^\circ$  face sheet laminates was produced. This surface was stud mounted on fiberglass/epoxy sandwich backup boards as shown in Figure 59 and aligned to contour. Ten ply  $\pm 45^\circ$  inner face sheet laminates were laid up on this tool using three inch wide graphite/epoxy prepreg tape and hand working the material to form the upper and lower cap flanges around the 9.0 inch radius of the spar bend at B.P. 33.93. This operation proved easier to perform than anticipated and no cutting, slitting, or bunching of the graphite tape was required.

The inner laminate was covered with mylar release, bleeder plies, vacuum bag and cured in the autoclave. A tooling shim of the thickness of the honeycomb core was added to the layup tool and the ten ply outer skin laminate was laid up and cured in the same manner. A curved fiberglass/epoxy insert for the B.P. 33.93 rib attachment was also produced on this front spar tool. The honeycomb core and fiberglass inserts were fitted to the cured face sheets on the layup tool, film adhesive was applied to each surface and the sandwich assembly was secondarily bonded in the autoclave. A separate set of tools was fabricated for layup of the upper and lower forward facing flange angles. These consisted of curved bars which were molded to the contour of the plaster master tools. The material used to form these bars was an epoxy tooling resin filled with aluminum needles to a putty like consistency and was hand worked to the model contour. Ten ply  $\pm 45^\circ$  flange angles were laid up on these bars and cured in the autoclave. The cured flanges were then mated to the honeycomb sandwich spar panel in the layup tool and the entire assembly was vacuum bagged and autoclave cured for secondary bonding of the flanges to outer spar skin.

The final bonding operation consisted of layup and cure of the upper and lower  $\pm 45^\circ$  cap strips on the spar flanges, bagging and cure in the autoclave. The completed front spar assembly, shown in Figure 60, exhibited good dimensional stability with exact matching of the spar sweep angles. Some shimming was required to mate the contoured lower spar cap with the lower cover skin surface.

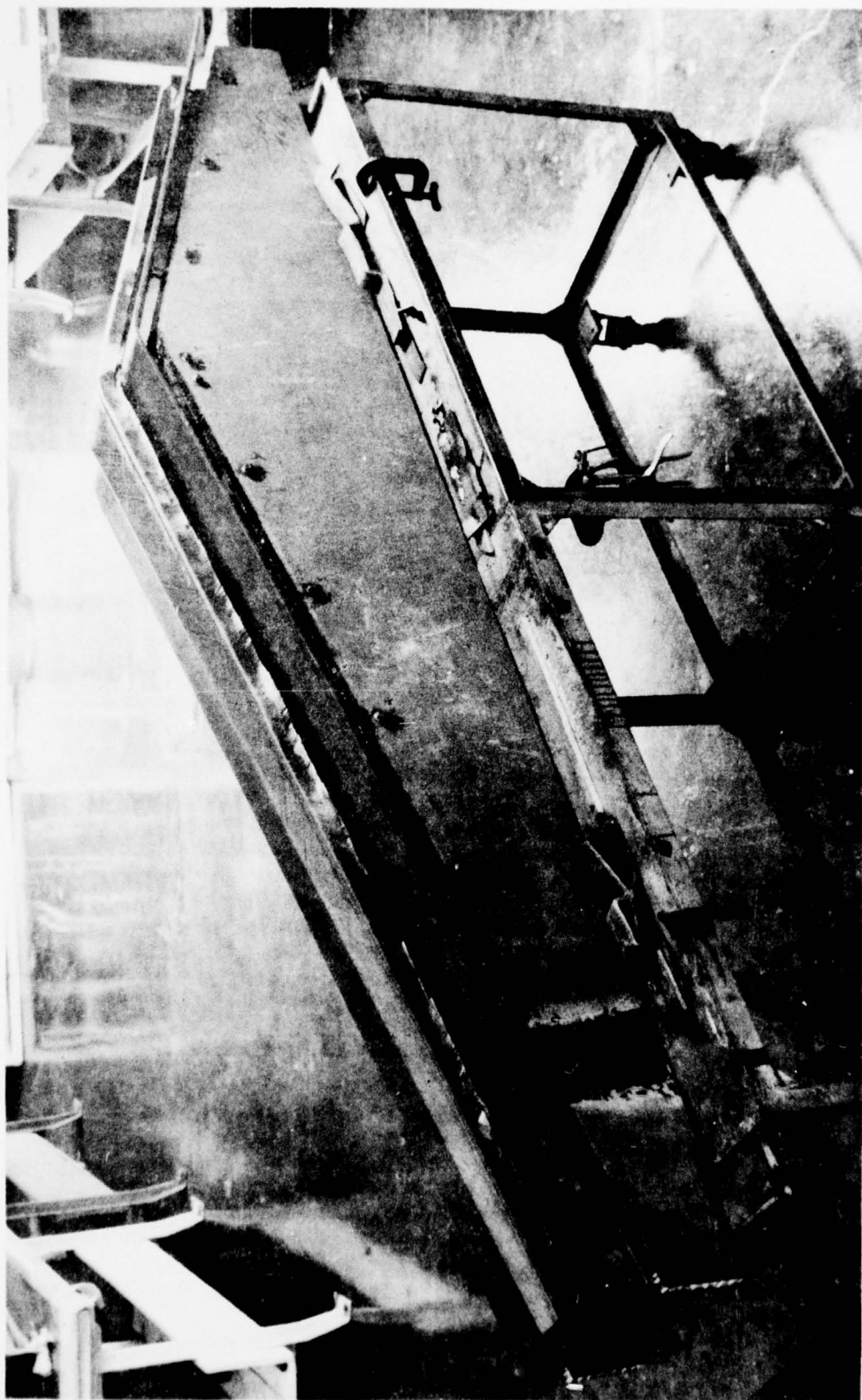


FIGURE 59 LAYUP OF  $\pm 45^\circ$  SHEAR WEB ON FRONT SPAR TOOL



FIGURE 60 GRAPHITE FRONT SPAR

#### 7.1.3 B.P. 33.93 Rib

Machined kirksite dies were used for the layup and cure of the solid laminate graphite/epoxy B.P. 33.93 rib. The basic I-section of this rib, shown in Figure 19 of Section 3.0, was fabricated of four separate pieces; (1) Inner channel, (2) Outer channel, (3) Upper cap strip, (4) Lower cap strip. The eleven ply channel sections were laid up by hand on the kirksite dies, vacuum bagged and cured in the autoclave. The flange angle on the layup dies was opened  $1^\circ$  beyond nominal to compensate for thermal expansion and spring back effects.

The fifteen ply cap strips for this rib were cured on flat plates and the four parts of the rib were secondarily bonded together with the channels back to back on the kirksite dies and the cap strips vacuum bagged to conform to the flange contour. Rib stiffener angles were fabricated separately and secondarily bonded to the rib web. The completed B.P. 33.93 graphite rib is shown in Figure 61.

#### 7.1.4 Intermediate Spars

The intermediate spars consist of a honeycomb sandwich web with separate mechanically attached caps as shown in Figure 18 of Section 3.0. The graphite epoxy web face sheets are  $\pm 45^\circ$  laminates and were laid up and cured on flat aluminum plates. The faces for all four intermediate spar webs were laid up and cured in one piece and indexed to match the honeycomb core blanket. The core blanket was indexed, filled with potting compound in specified areas and run through an oven cycle to cure the potting compound. Faces and core blanket were then mated and secondarily bonded with AF 147 film adhesive in an autoclave cycle. Individual spar webs were subsequently cut and trimmed from this honeycomb sandwich panel and inspected to verify proper location of the potting compound in the edges of the spar web. Precured edge doublers were then secondarily bonded to the sandwich spar webs.

The upper spar caps consist of a U-shaped laminate which follows the contour of the upper cover skin. The intermediate spar caps follow a compound curvature in the inboard section and straight line elements in the outboard section. Machined steel bars were used for layup and cure of these spar cap laminates. The lower spar caps consist of four separate pieces; (1) Center U section, (2) Forward angle flange, (3) Aft angle flange, (4) Cap strip. The center U sections were laid up and cured on steel bars in the same manner as the upper caps. The fwd and aft angles were laid up on this same U section tool in one piece and split down the middle to form the angle sections. The cap strip was cured separately on a flat plate. The four pieces were then secondarily bonded together by vacuum bagging around the steel layup tool.



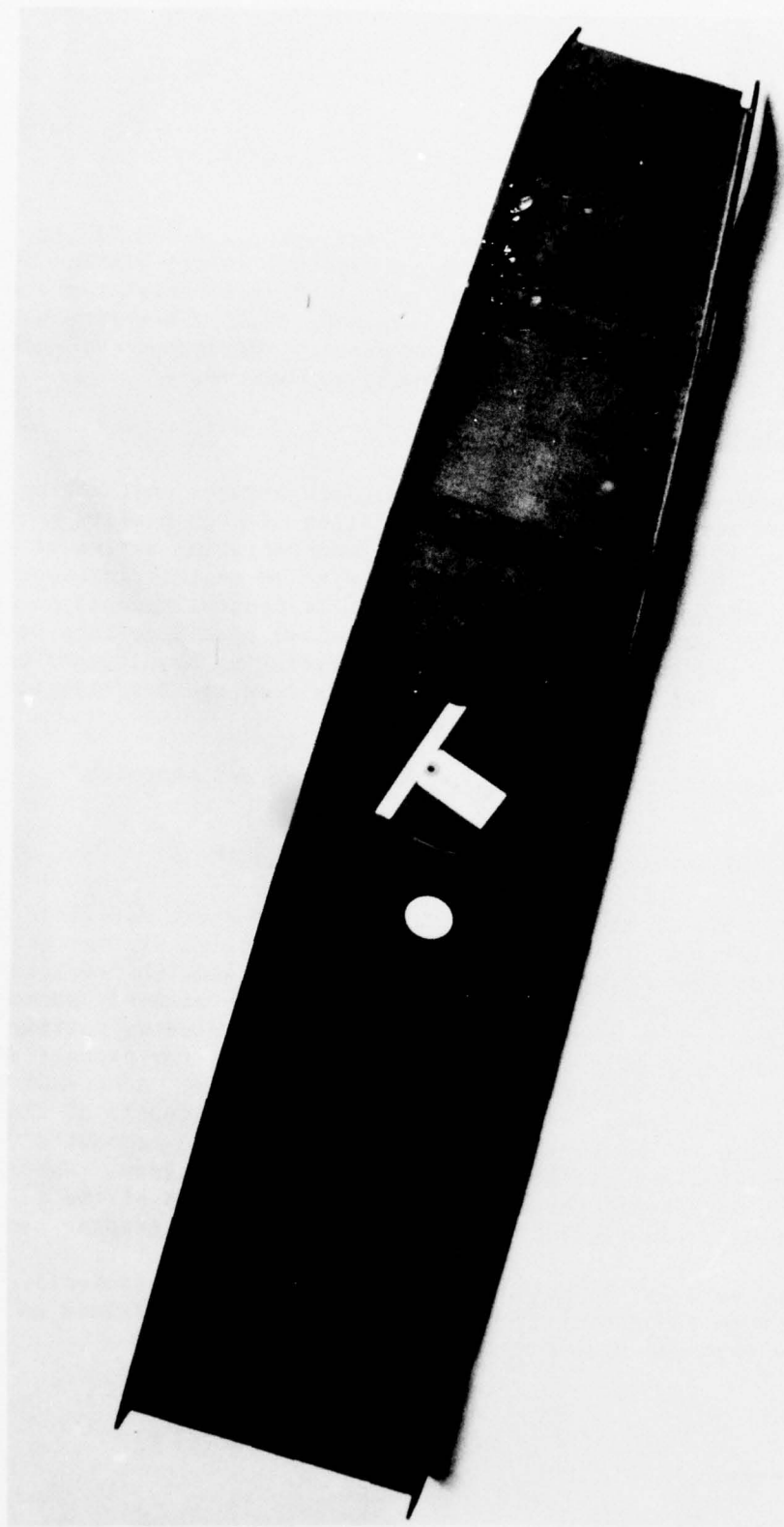


FIGURE 61 GRAPHITE  $X_w$  33.93 FORWARD RIB



#### 7.1.5 Metal Components

The centerline rib, centerline splice plates, rear spar, B.P. 33.93 aft rib, rear spar splice fitting, and aft wing to fuselage attach fitting were machined from aluminum billets. Dimensions and contours of these parts were controlled from tooling transfer patterns. The B.P. 33.93 rib splice and miscellaneous clips were formed from aluminum sheet. Photographs of machined aluminum components are presented in Figures 62, 63, and 64.

#### 7.2 PROCESS SPECIFICATIONS

Throughout the program a cooperative effort was made between engineering, tooling, and manufacturing to insure the fabrication of high quality parts in an efficient manner, starting with a tooling/manufacturing review of all parts while in the design stage and culminating with an engineering approval of all layups and bonding prefits prior to cure. To control operations necessary to produce high quality graphite parts, process specifications were written by M&P personnel in conjunction with Manufacturing Development personnel. The following two specifications were developed specifically for this program:

HA0605-102 "Fabrication of Graphite/Epoxy Laminate and Sandwich (GO 8679)"

HA0605-103 "Assembly of Graphite/Epoxy Wing (GO 8679)"

HA0605-102 specifies all of the productive and non-productive materials to be used in the fabrication of composite components, material storage requirements, laminate layup procedures, laminate cure cycle, sandwich fabrication procedure, and adhesive cure cycle. HA0605-103 specifies assembly procedures for individual components of the wing box test section including potting of honeycomb core, sandwich prefit and assembly, requirements for process control specimens, and non-destructive inspection requirements. Adherence to these detail process specifications was one of the major elements of the quality assurance plan to insure structural integrity of the composite laminates and sandwich panel assemblies produced on this program. The following autoclave cure cycle was specified and used for all of the graphite/epoxy laminates fabricated from Fiberite Hy-E 1034C prepreg tape:

Place vacuum bagged part in the autoclave at ambient pressure (autoclave unpressurized) at room temperature. Full vacuum shall be maintained on the part until the part has been completely cured.

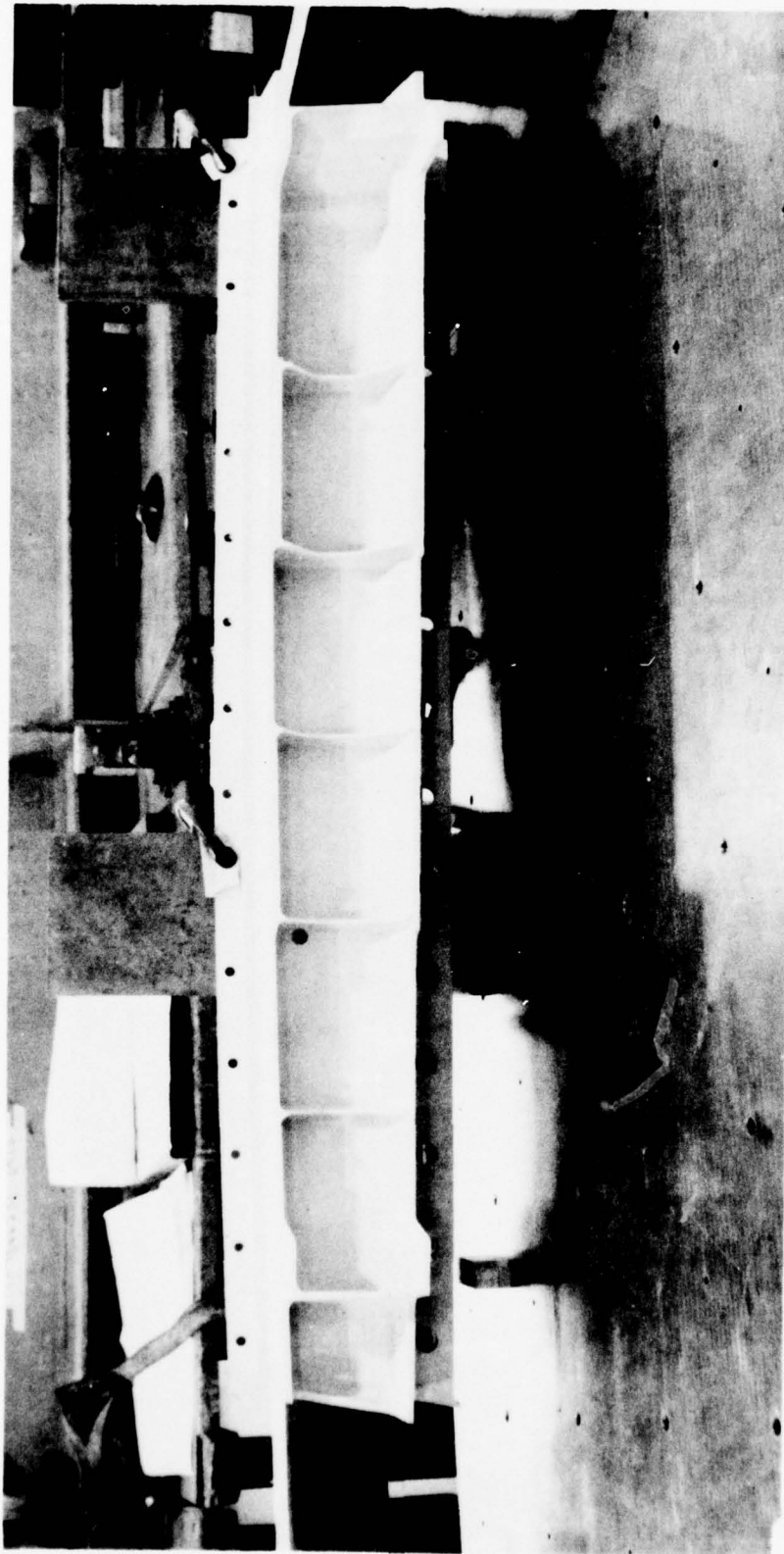


FIGURE 62 ALUMINUM CENTERLINE RIB

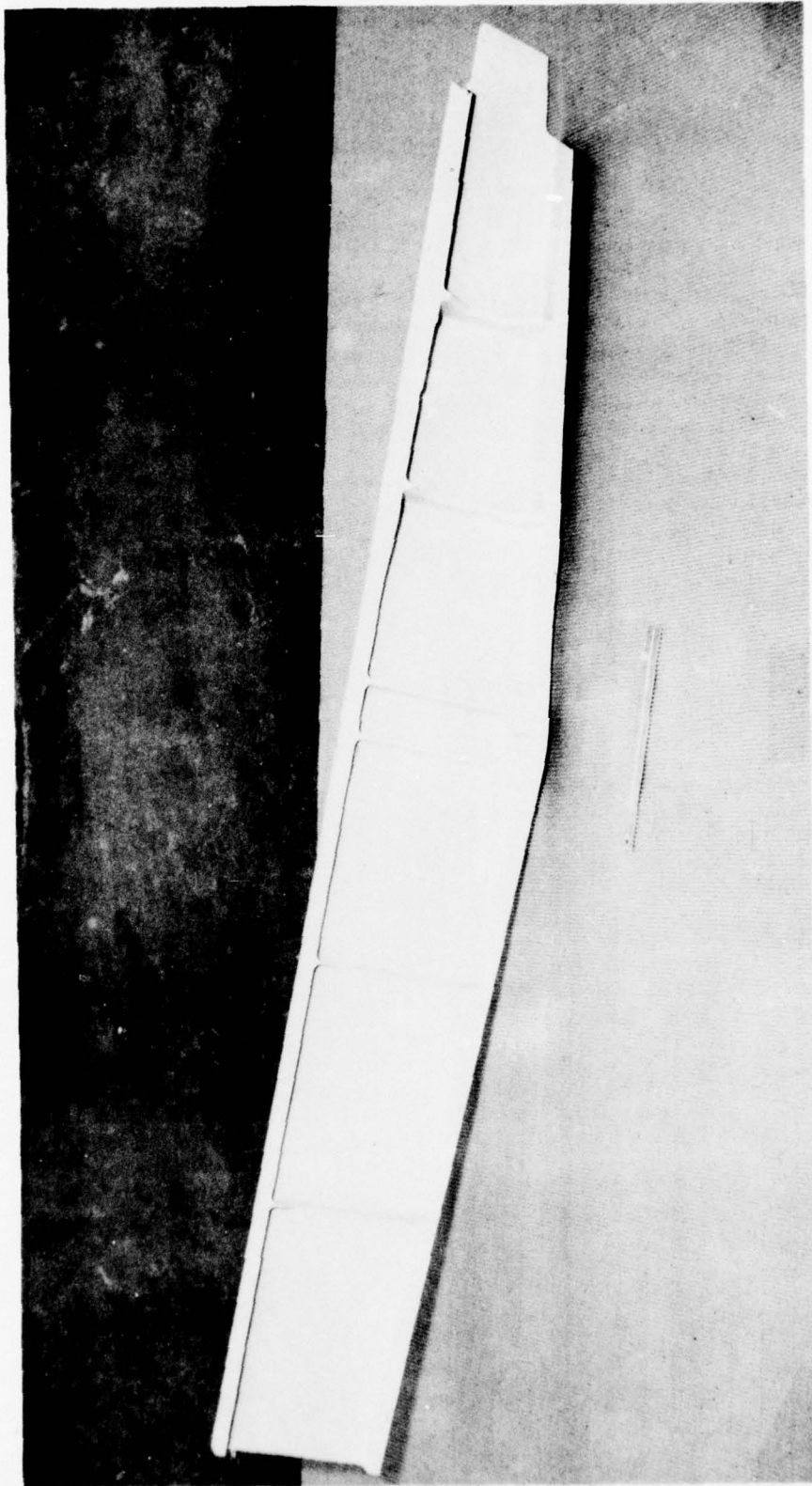


FIGURE 63 ALUMINUM REAR SPAR

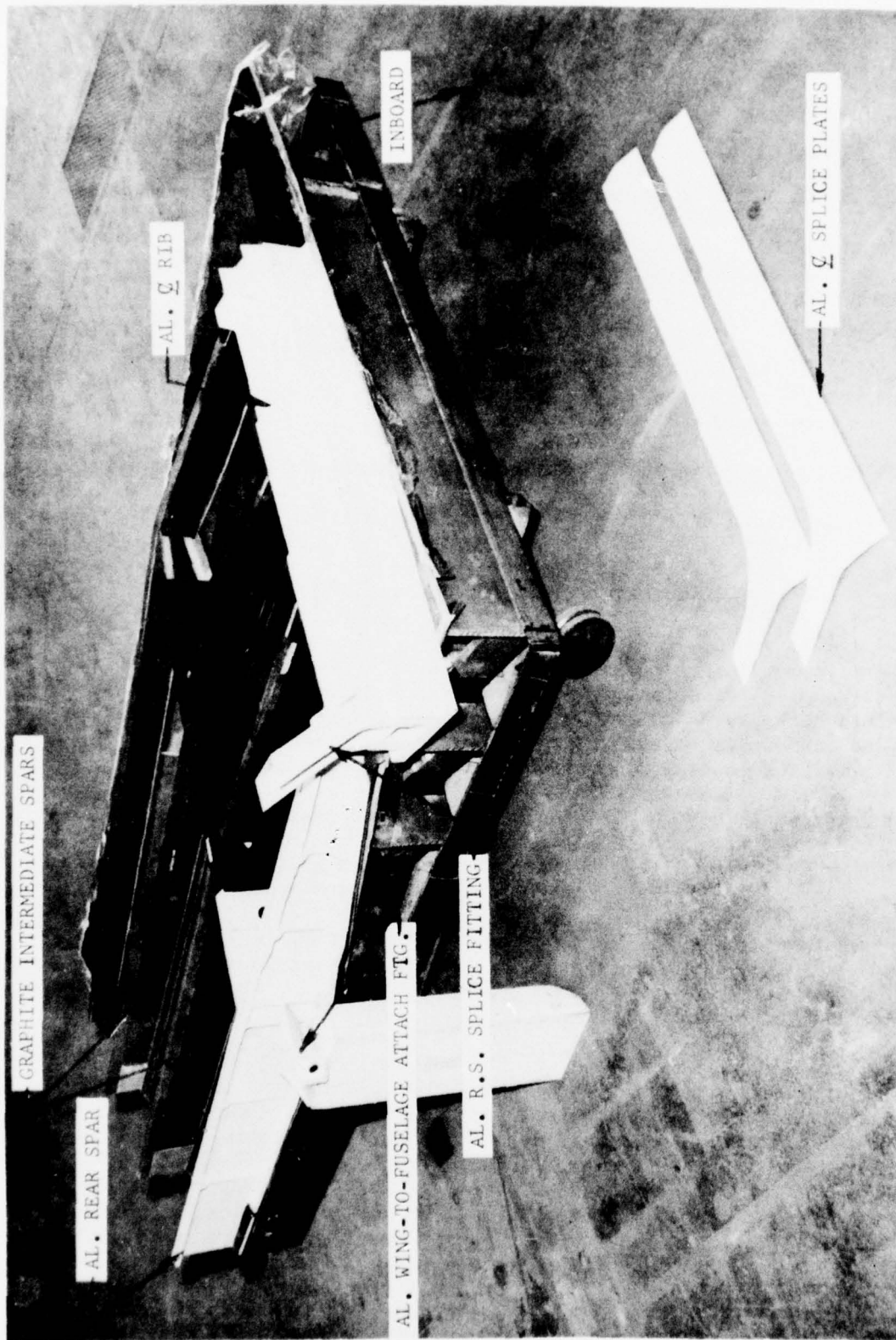


FIGURE 64 DETAIL PARTS - COMPOSITE WING CENTER SECTION SPECIMEN



Raise temperature of the part from ambient to 122°C (250°F)  $\pm 5.5^\circ\text{C}$  (10°F) at a rate of 3°C (5°F) per minute. If this rate of increase cannot be achieved, MAP shall be contacted for revised cure and pressure cycle. The revised cure cycle authorized shall be recorded on the appropriate Quality Control document and subsequently signature approved by the responsible engineer.

Allow the laminate to dwell for 15  $\pm 1$  minutes at 122°C (250°F) under full vacuum only.

Pressurize autoclave to 85  $\pm 5$  psi.

Maintain 122°C (250°F)  $\pm 5.5^\circ\text{C}$  (10°F) and 85  $\pm 5$  psi for 45  $\pm 1$  minutes.

Increase temperature to 177°C (350°F)  $\pm 5.5^\circ\text{C}$  (10°F) at a rate of 3°C (5°F) per minute.

Cure for 3 hours  $\pm 5$  minutes at 177°C (350°F)  $\pm 5.5^\circ\text{C}$  (10°F) and 85  $\pm 5$  psi.

After cure is complete, cool autoclave to below 60°C (140°F), release autoclave pressure. If the contraction of the tool on cool down will cause over forming in areas such as radii of angles, the vacuum pressure may be dumped and the positive pressure reduced to the minimum controllable in the autoclave and cooling accomplished under these conditions.

Similar detail instructions are included in the process specifications for assembly and secondary bonding of cured laminates and honeycomb core for each of the major composite subassemblies of the composite wing box test section. Sign off of process control cards accompanying each component throughout the fabrication sequence was required to confirm material handling procedures and the performance of each curing and bonding operation according to the schedule set forth in the process specifications.

### 7.3 SPAR CAP BONDING

After fabrication and inspection of the individual wing box test section components was completed, the lower cover skin was mounted in the outer cover skin layup tool and secondary bonding of the intermediate spar caps to the lower cover was initiated. Spar caps were located by indexing with the master mylar template and held in position with the steel bar tools used for layup of the spar cap U-sections. AF-147 film adhesive was placed between the spar cap and skin and taped along the edges to contain squeeze out overflow. Clamp pressure was applied by steel cross bars extending across the spar cap bars to C-clamps at the edges of the support frame. The part was then oven cured at 350°F with additional C-clamp pressure applied after heat up. Figure 65 shows the lower cover skin after bonding of the intermediate spar caps.



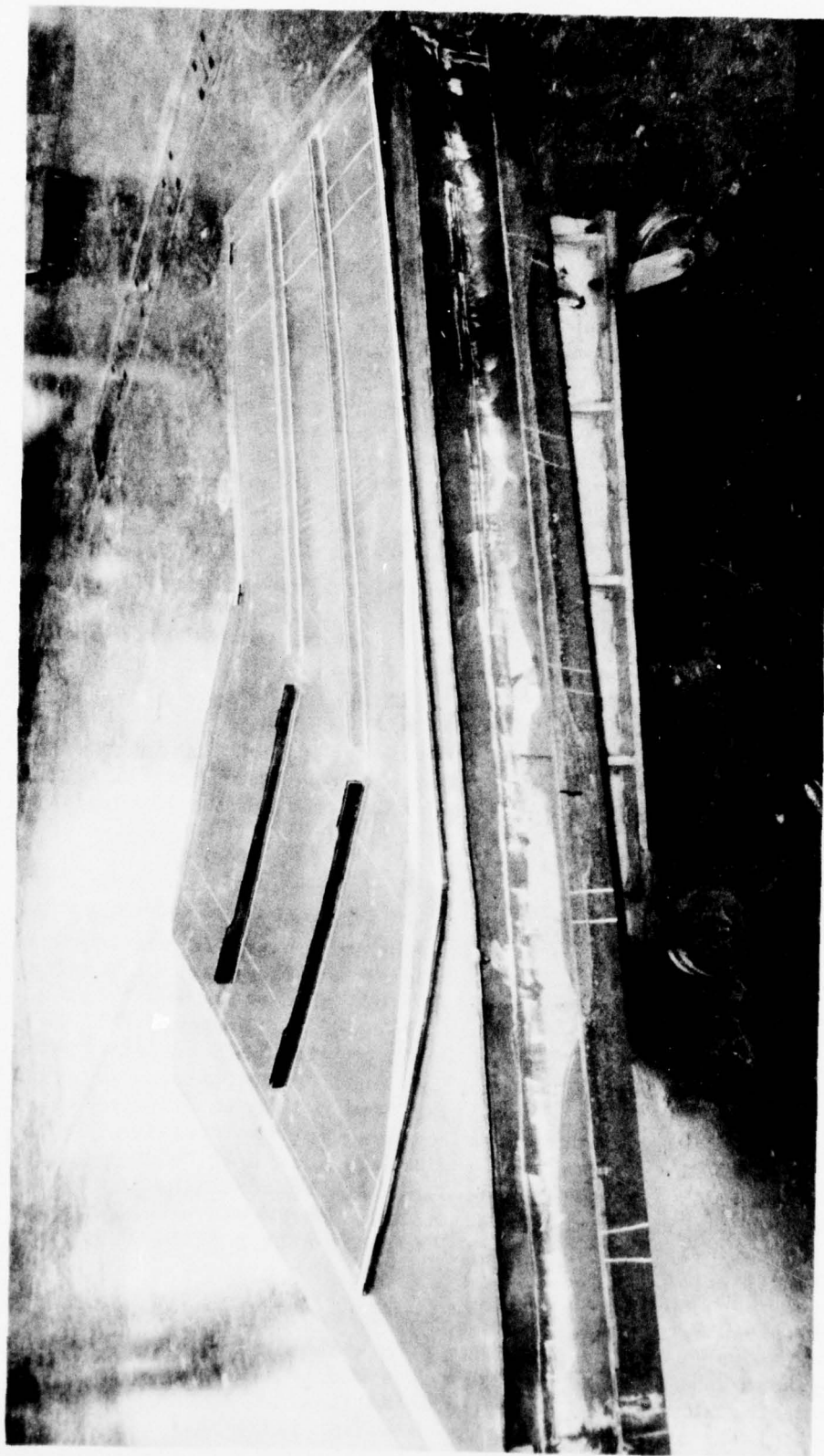


FIGURE 65 LOWER INTERMEDIATE SPAR CAPS BONDED TO LOWER SKIN PANEL

The front spar was secondarily bonded to the lower cover skin in a similar oven cure cycle, however, for this component a prefit check was made with the spar vacuum bagged to the skin. Fiberglass shims were added as required, AF-147 film adhesive was placed between the faying surfaces and the vacuum bag reinstalled over the complete spar and lower cover skin panel. Additional clamp pressure was applied on the spar flanges with bearing blocks and clamp plates spaced along the forward and aft edges of the spar and the part was oven cured at 350°F with vacuum applied. Figure 66 shows the assembly after bonding the front spar to the lower skin panel.

#### 7.4 DRILLING AND FINAL ASSEMBLY

A final assembly/drill fixture was constructed to position and hold the various components of the wing box test section during the final assembly operation. All of the upper and lower cover skin fastener locations were laid out on a master mylar template draped on the mold line master plaster model as described in Paragraph 7.1.1 and indexed to the final assembly/drill fixture. The assembled detail parts, consisting of graphite lower skin panel, front spar, intermediate spars,  $X_w$  33.93 fwd. rib, and aluminum rear spar, rear spar splice fitting, centerline rib,  $X_w$  33.93 aft rib, centerline splice plates, and wing-to-fuselage attach fitting are shown in Figures 64 and 67 prior to positioning in the assembly/drill fixture. Figures 68 and 69 show the detail parts located in the fixture ready for drilling and installation of fasteners.

Drilling of the graphite lower skin started along the rear spar and  $X_w$  33.93 locations, followed by the centerline rib, and subsequently the intermediate spar attachment. Full back-up pressure was required on the graphite to prevent the exit side of drilled holes from splintering. Those exit holes that showed signs of splintering were brush coated with epoxy to stop further splintering. Both manual hand drilling or controlled feed and speed were used to provide good quality fastener holes. The combination of graphite skin panel and aluminum centerline rib was drilled using a Keller positive feed drill; it being necessary to back off the drill several times to clean out the abrasive graphite powder and/or aluminum chips. Approximately four 1/4" holes can be drilled through .400" thick graphite laminate before resharpening of the carbide drill bit is required. Liquid epoxy shims were incorporated into the installation of the wing-to-fuselage attach fitting and the rear spar splice fitting.

The intermediate spar webs were attached to the lower spar caps with Hi-Lok fasteners and to the adjacent ribs with aluminum clip angles. The upper spar caps were temporarily attached to the spar webs prior to drilling the upper cover fastener holes to allow subsequent installation of nutplates in the spar cap as shown in Figure 70. Hi-Lok fasteners were installed through the upper spar cap and spar webs after all drilling and nutplate installation operations were completed.

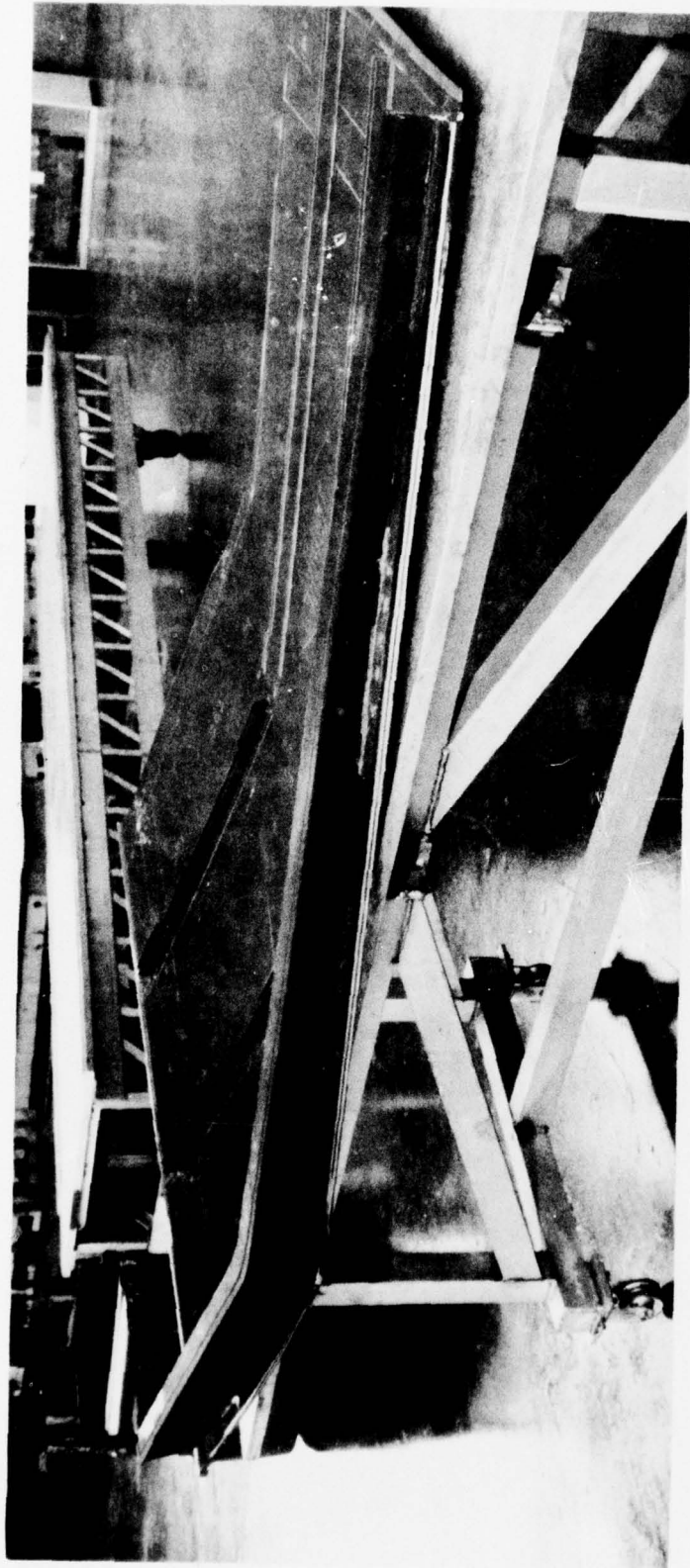


FIGURE 66 FRONT SPAR BONDED TO LOWER SKIN PANEL



FIGURE 67    DETAIL PARTS - COMPOSITE WING CENTER SECTION SPECIMEN



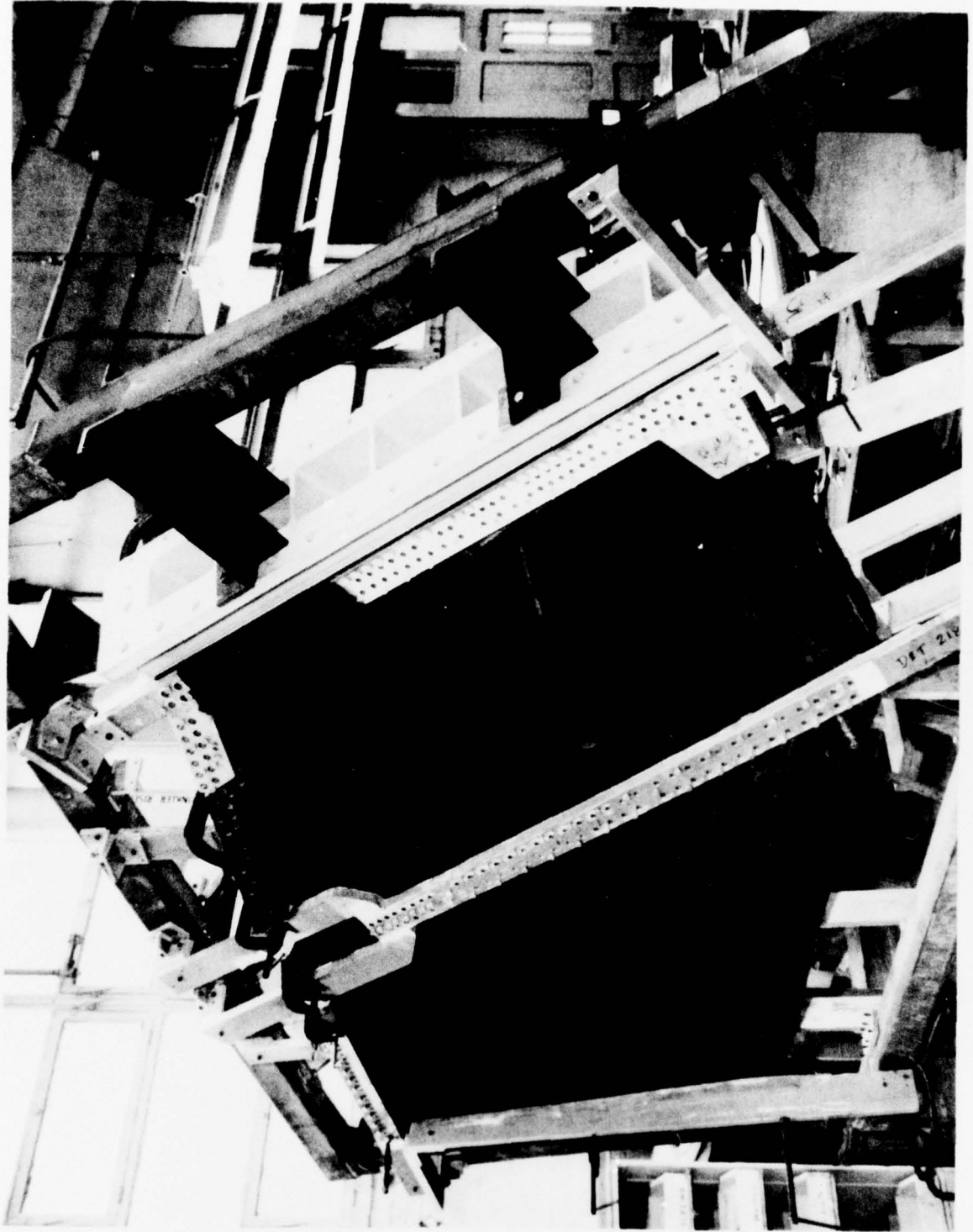


FIGURE 68 COMPOSITE WING DETAIL PARTS IN ASSEMBLY/DRILL FIXTURE



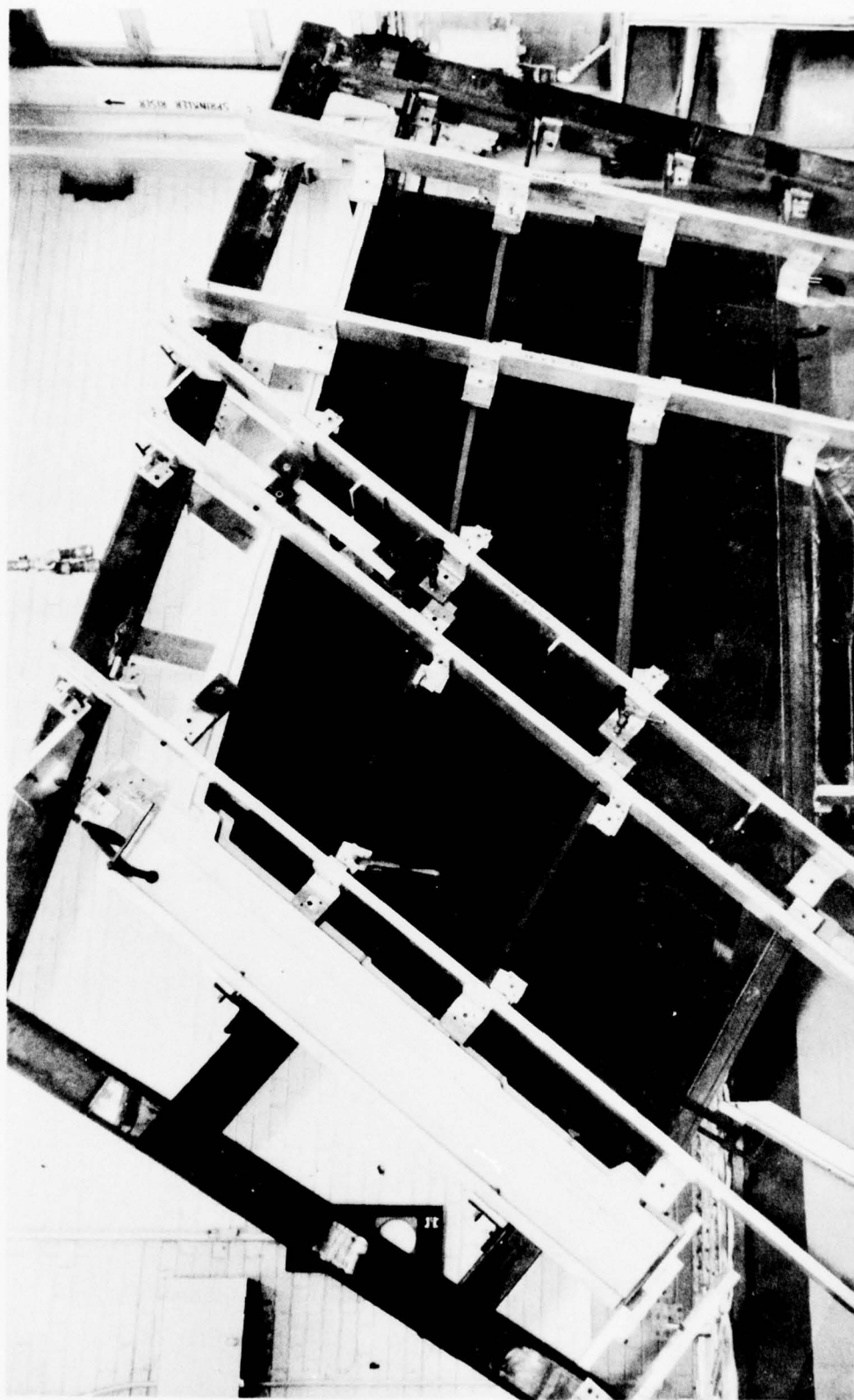


FIGURE 69 COMPOSITE WING DETAIL PARTS IN ASSEMBLY/DRILL FIXTURE

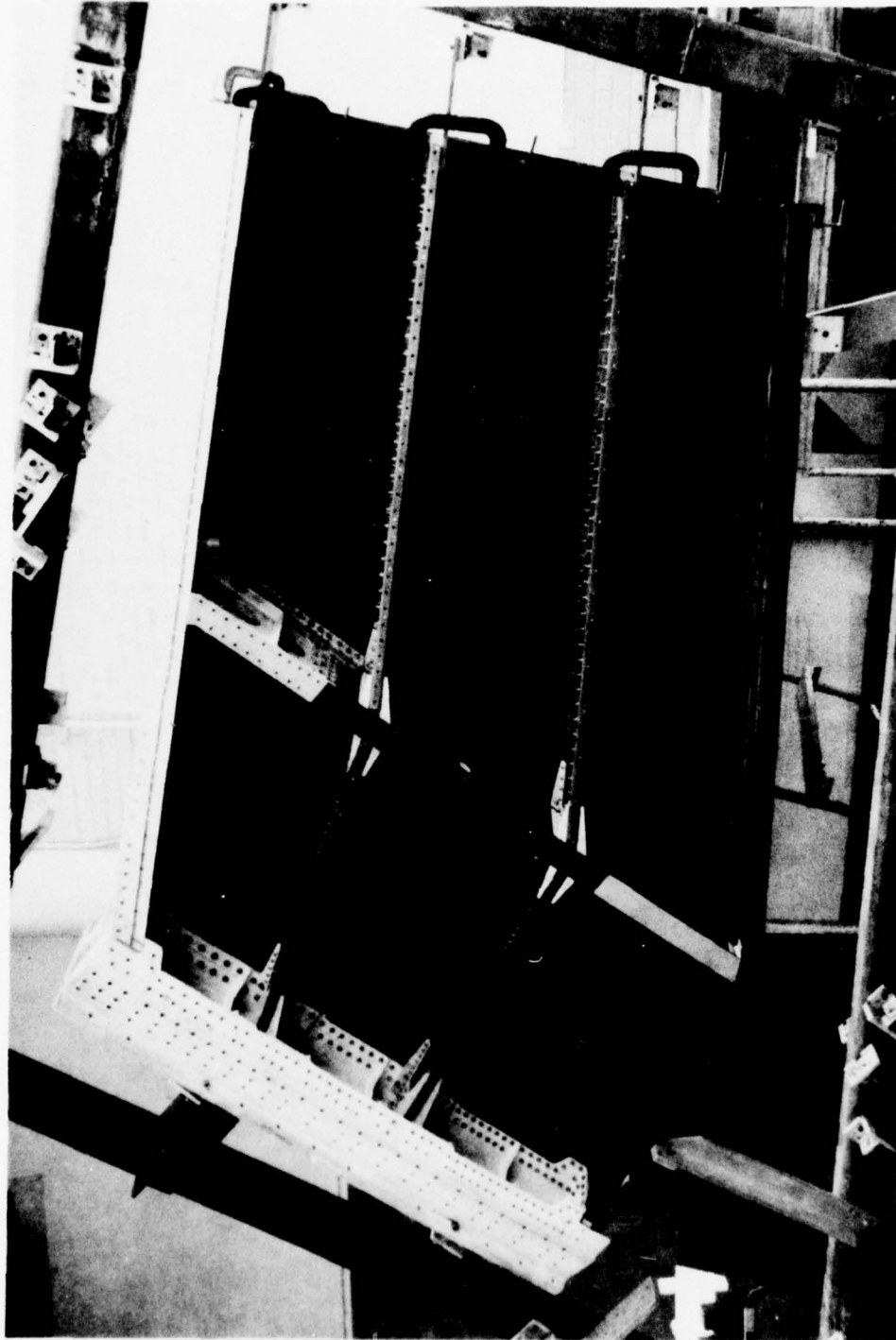


FIGURE 70 COMPOSITE WING BOX SUBSTRUCTURE ASSEMBLY

Fit up of the upper cover skin to the sub structure was checked with clay mark off prior to installation of fasteners and showed good contact at all faying surfaces with minimum pull-up pressure. One tapered aluminum shim was added to the fwd portion of B.P. 33.93 rib to eliminate an 0.050 inch step condition at the rib to spar intersection. A small amount of splintering was encountered during drilling and countersinking of the upper cover skin fastener holes and these areas were brushed with epoxy to prevent further splintering. Drilling of the upper cover skin panel was accomplished with no hole mislocations and no hole rework required. Only two holes in the graphite/epoxy sub structure required bushing to eliminate an out of round condition.

Six rosette strain gages were bonded to the inner surface of the wing skins and the inboard aft intermediate spar prior to installation of the upper cover skin. The gages and individual wire leads were installed at locations ① upper, ① lower ⑤ upper, ⑤ lower, ⑬ spar and 14 spar as shown in Figure 80. The upper skin panel fasteners were installed and the centerline splice plate and outboard loading plates were added to complete the assembly. Figures 1, 2, 71 & 72 show the completed composite wing center section specimen prior to shipment to the Naval Air Development Center for subsequent structural test and evaluation.

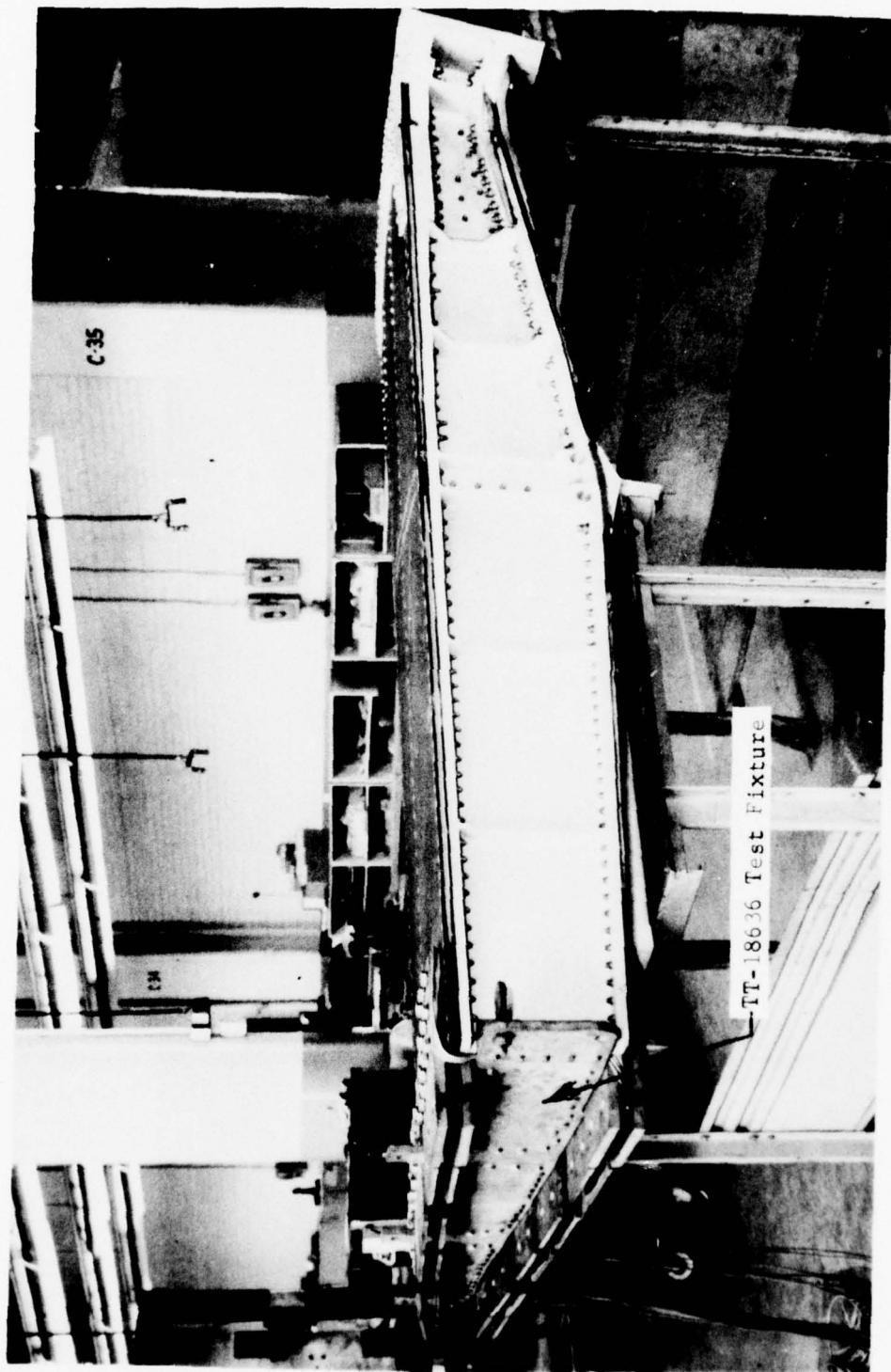


FIGURE 71 COMPOSITE WING BOX ASSEMBLY - REAR VIEW

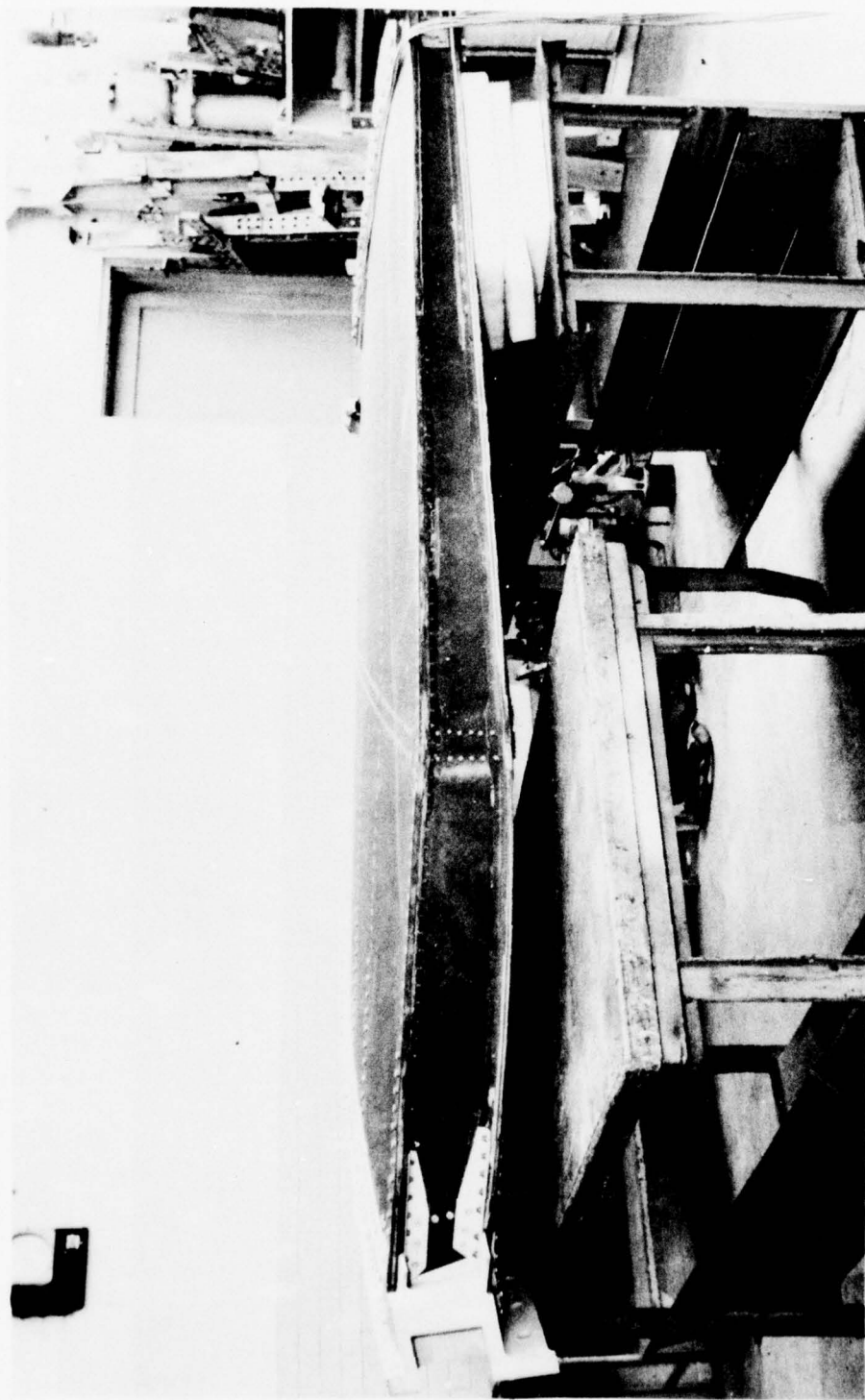


FIGURE 72 COMPOSITE WING BOX ASSEMBLY - FRONT VIEW



## SECTION 8.0

### QUALITY ASSURANCE

A general plan was established at the outset of the program to provide quality assurance checking of all components of the wing box test section. This plan covered all aspects of fabrication and assembly of the test section including certification of incoming materials; storage of composite materials; handling, layup and cure of composite materials; prefit check of honeycomb panel assemblies; dimensional, strength and bond line interrogation checking of cured laminates and bonded assemblies; and procedures for repair and disposition of discrepancies. The following paragraphs describe the methods used to implement this plan and also summarize the type and extent of discrepancies encountered and repair procedures employed.

#### 8.1 MATERIAL CERTIFICATION AND ACCEPTANCE

All materials procured for fabrication of the wing box test section were certified to meet the requirements of a military specification, industry specification, vendor specification, or Rockwell specification. The specifications listed below were invoked for procurement of the primary constituent materials of the wing box test section:

<u>Material</u>	<u>Specification</u>
1. Graphite/Epoxy Prepreg Tape	Rockwell International Corp., Columbus Aircraft Division Specification HB0130-102
2. Fibertruss Honeycomb Core	Hexcel Specification
3. AF 147 Film Adhesives	3M Co. Specification
4. Hysol Adhesive ADX 3111.1 Potting Compound, Parts A & B	Dexter Corp., Hysol Division Specification
5. 7075-F Aluminum Billet	Mil Spec. QQA367-H

Conformance of the graphite/epoxy prepreg tape to the strength and stiffness requirements of HB0130-102 at room temperature and 350°F was confirmed by in-house material acceptance tests. Results of these material acceptance tests are presented in Figures 37 and 38 of Paragraph 6.1. Incoming material acceptance tests were also performed to confirm the conformance of the 7075-F aluminum billets to the strength and stiffness requirements of QQA367-H. All other materials were accepted on the basis of the vendor's certification.

## 8.2 PROCESS CONTROL

Process control specifications HA0605-102 and HA0605-103, described in Paragraph 7.2, were developed to define in detail all aspects of material handling and storage, laminate layup and cure, sandwich panel assembly, adhesive bonding, and non-destructive inspection requirements for the wing box test section components. Process control cards were prepared for each component and traveled with the component through layup, cure, sandwich assembly, secondary bonding and inspection. Temperature and pressure were monitored and recorded throughout all autoclave cure cycles and these records were verified and signed off by shop supervision. Strict adherence to the specified cure cycle temperature and pressure schedule was the prime method of insuring consistent high quality graphite/epoxy laminates on the program.

Another critical area of process control was in the prefit check of secondarily bonded honeycomb sandwich assemblies. Face to core disbands are a common type of defect in honeycomb sandwich construction and are often the result of improper fit between the core and face sheet. This condition is aggravated in sandwich assemblies containing areas of tapered honeycomb core. Special attention was therefore directed to inspection of the Vinylite prefit verification film records. These films were placed between the graphite/epoxy face sheets and Fibertruss core, vacuum bagged and placed in the autoclave for prefit check. Any areas showing lack of complete imprint of the honeycomb core were reworked by sanding the Fibertruss core blanket to remove high spots and resubmitted for prefit check to verify an acceptable mark off condition. An additional layer of AF-147 film adhesive was included in areas showing light imprint in the final prefit check. These prefit mark off film records were documented and stored for future reference along with the cure cycle records. As a result of this prefit check procedure no face to core disbands were detected in any honeycomb sandwich panel assemblies with the exception of one intermediate spar panel which disbonded during the secondary bonding of edge doublers with the center of the panel inadvertently exposed to the 350°F cure temperature without a constraining vacuum bag.

Graphite/epoxy process control specimens were laid up and cured with each face sheet laminate using materials from the same lot and roll. These specimens were of the same ply orientation and thickness as the basic face sheet laminate and cured on a portion of the same layup tool, and were available for fabrication into tensile, compression or short beam shear test coupons for laminate strength evaluation in the event that a cure cycle deviation should occur. Test results of process control specimens produced with the lower cover skin face sheets are discussed in Paragraph 8.4.

### 8.3 INSPECTION TECHNIQUES

The basic requirements for inspection of the composite wing box test section were means for checking the dimensional accuracy of the various components and assemblies, and means for detection of defects and discrepancies within these components and assemblies. Dimensional checking of wing surface contours was accomplished by reference to the master plaster models described in Section 7.0 and to various plaster splashes and contour templates made from these master models. Location of spars, ribs, and fasteners was checked by reference to a mylar master template indexed to the master plaster models and by optical alignment in the assembly/drill fixture described in Section 7.0. Detail part dimensions were checked by shop inspection personnel for conformance to tolerances specified on engineering drawings prior to being stamped for approval.

The type of defects required to be detected by non-destructive inspection methods were set forth in process control specification HA0605-103 and are as follows:

#### Honeycomb Core-to-Face Voids

Voids in the core-to-face area detectable when standardized on a 3/8-inch void.

#### Faying Surface Voids

Visual examination shall reveal no voids at the edge of the bond line and in addition there shall be no detectable voids when standardized on a 3/16 inch void.

#### Interply Delaminations

Detectable voids revealed by visual examination or by ultrasonic through-transmission when standardized on a 1/4-inch void.

#### Crushed or Split Core

Crushed or split (glass-reinforced honeycomb) core revealed by visual and/or X-ray inspection.

#### Fiber Fracture and Cracks

Surface fractures or cracks detectable by visual examination.

#### Scratches

Scratches extending into the graphite filament.

### Holes

Drilled holes in either the graphite or glass epoxy shall be visually examined to establish any delamination as the result of push-out, lift of the external ply at drill entry, and peeling of fibers on the exit side.

The following equipment, test standards, and procedures were utilized in this program to interrogate the laminates and bonded honeycomb sandwich assemblies for evidence of the defects listed above:

Ultrasonic through transmission inspection was performed for the detection of nonbonds or delaminations of .187 inch in diameter or larger. The ultrasonic system that was utilized is designed specifically for through transmission inspection and utilizes two transducers.

Ultrasonic Inspection System - Automation Industries, Inc. squirter type system for performing through-transmission ultrasonic inspection techniques. (Reference: Figures 73 and 74). The system includes:

- Model US 640 Series 8 ft. scanning bridge with automated X-Y positioning assemblies. The scanning bridge is mounted 8 1/2 ft. above the floor.
- Model UM 771B Reflectroscope
- Model US 950 Remote X-Y Recorder, 22 inch usable scan width, designed to produce permanent high quality "C" scan recordings on a dry type recording paper. The recorder has 1/2:1, 1:1, 2:1, 4:1, and 8:1 recording ratios.

One transducer transmits the sound into the test material and the second transducer receives the sound transmitted to the opposite surface of the material. If the material is sound, ultrasonic energy will be transmitted and an indication shown on the cathode ray tube. If, however, a flaw exists in the material, all or a portion of the sound energy will be reflected and the presence of the flaw shown on the CRT by a complete or partial loss of the indication. Flaws that have a cross-sectional area less than the sound beam diameter will cause only a partial loss of the indication. The loss will normally be in proportion to the difference between the flaw cross-sectional area and the sound beam diameter as shown below. Flaws with cross-sectional areas equal or greater than the sound beam diameter will cause complete loss of the indication.





FIGURE 73      ULTRASONIC INSPECTION EQUIPMENT



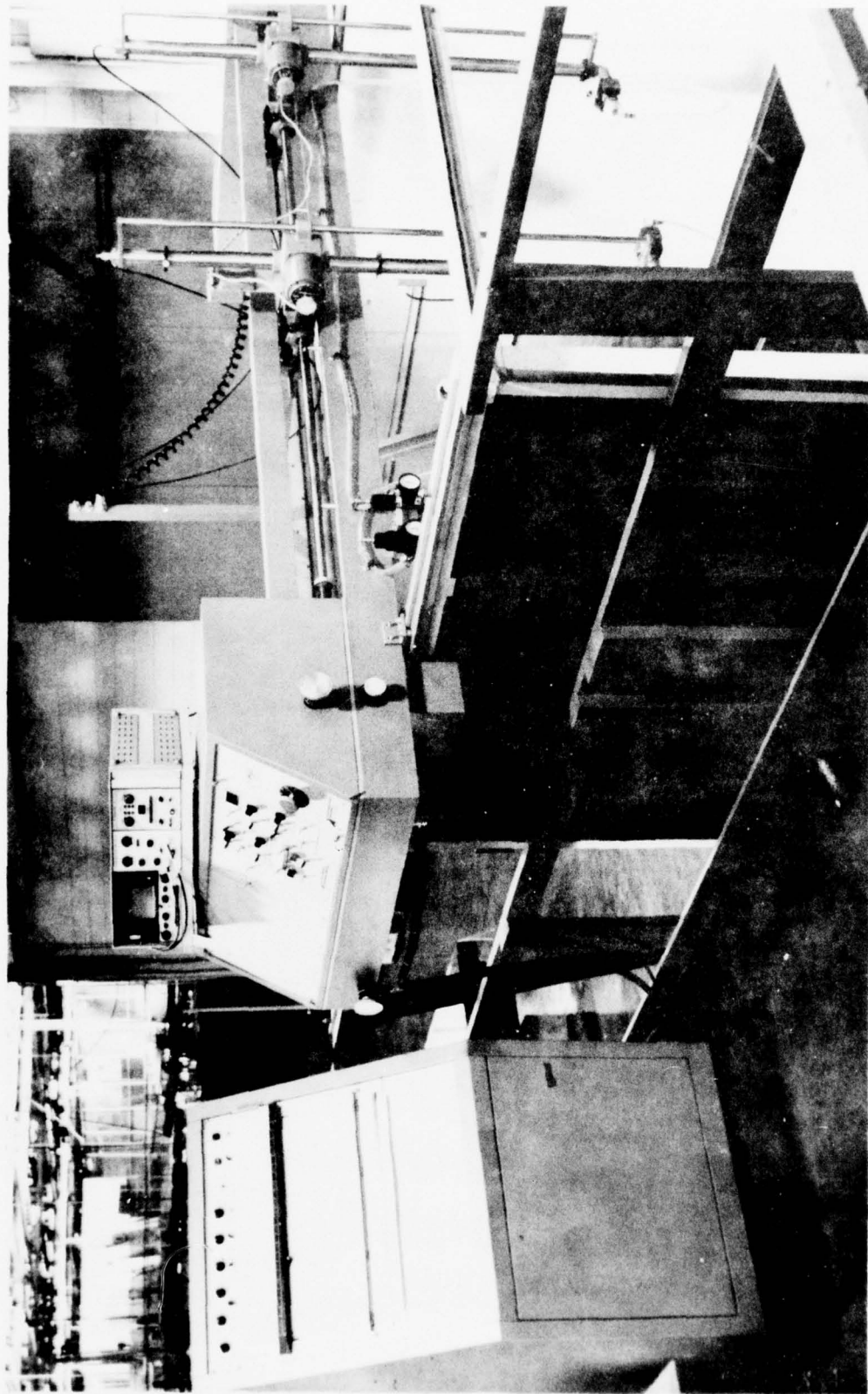
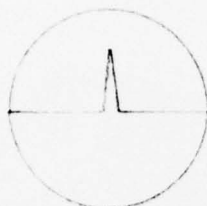
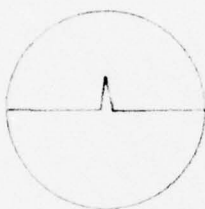


FIGURE 74 ULTRASONIC INSPECTION EQUIPMENT CONSOLE



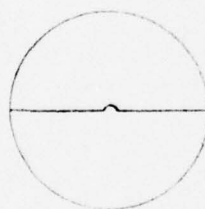
CRT

Sound Material



CRT

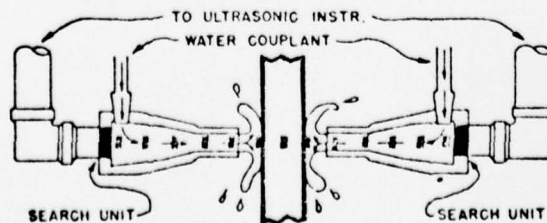
Small Flaw (cross-sectional area less than sound beam diameter)



CRT

Flaw cross-sectional area equal to or greater than sound beam diameter

Transducers must be tightly coupled to the test material since air has a very high absorption of ultrasound. Coupling between the transducers and graphite test panels was accomplished by water squirters attached to the transducers as shown below. Water forced through the nozzles carries the sound beam between the transducers and test part as shown below. This coupling method provides all the advantages offered by the immersion test and in addition does not require submersion of the test material in water. Ultrasonic inspection of the lower skin sandwich panel is shown in Figure 75.



Squirter through-transmission technique

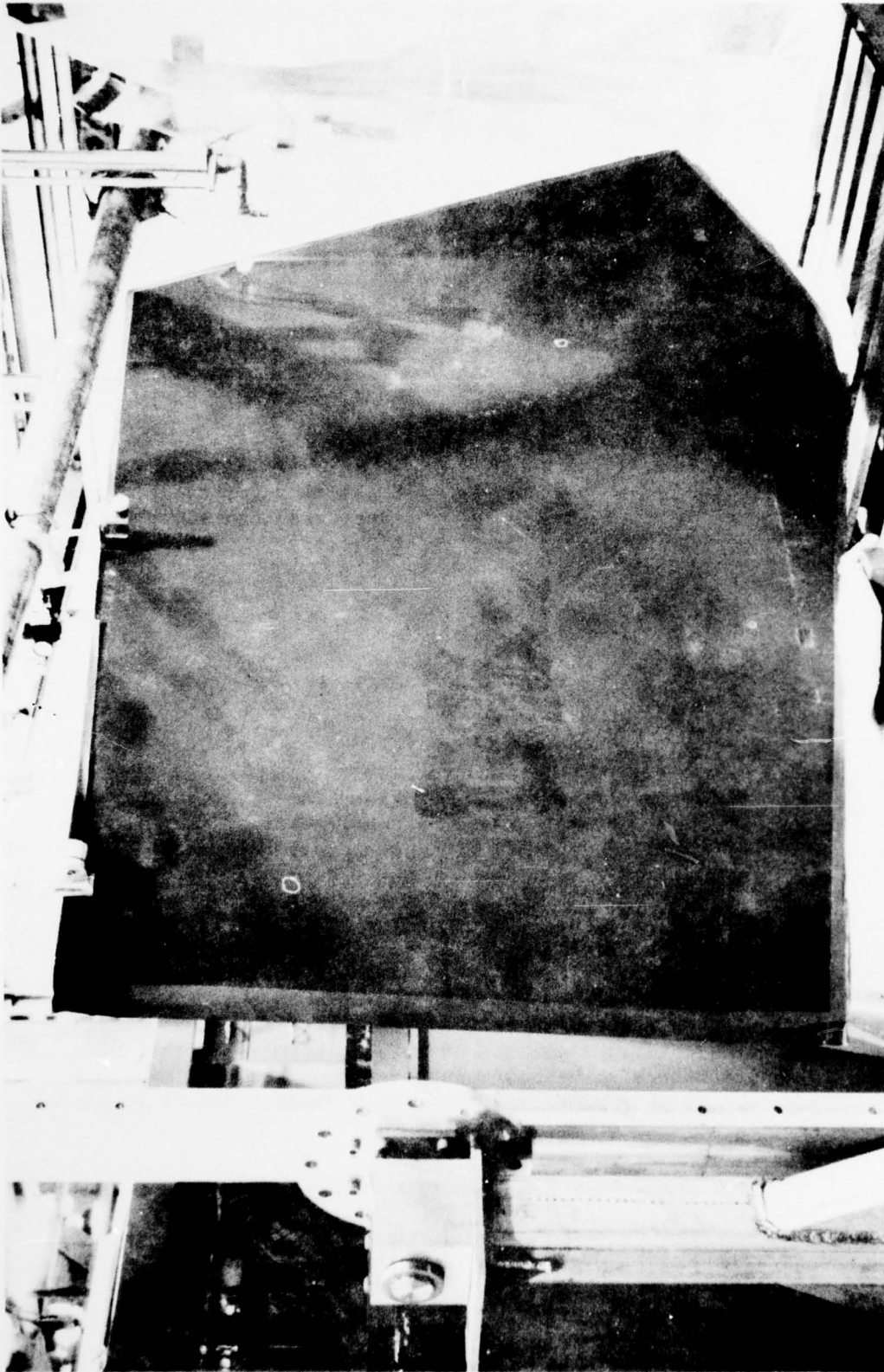


FIGURE 75 ULTRASONIC INSPECTION OF LOWER SKIN SANDWICH PANEL

Reference standard panels simulating the X<sub>w</sub> 33.93 rib, skins, and spars in regard to material, cross section, and processing and containing intentional known voids were provided for equipment calibration. Voids were installed in the standards by using folded strips of 0.004 inch thick glass-filled teflon to result in a width of 3/16 inch. Intentional voids were well identified; porous foaming adhesive was revealed as unintentional voids.

#### 8.4 MATERIAL REVIEW DISPOSITIONS

The philosophy for material review dispositions implemented procedures to meet quality assurance goals while avoiding constraints which cause delay or undue cost. When a discrepancy was detected, the Responsible Engineer was immediately contacted by Manufacturing for disposition. The squawk/defect and disposition were recorded on a manufacturing planning ticket and the ticket signed off by the Responsible Engineer after rework was satisfactorily accomplished. Semi-major rework was authorized by internal letter while major rework was discussed with the NADC Project Engineer.

In general, the fabrication of the wing box test section progressed with only minor discrepancies. No evidence of face to core disbands were detected with the exception of the case where the vacuum bag was inadvertently omitted from the web of the intermediate spar during secondary bonding of edge doublers. The most common types of defects detected were porosity in the core potting compound, small voids at the edge of secondarily bonded spar caps, laminate outer ply delamination, and splintering of the exit ply of cover skins and rib caps during fastener hole drilling. EC-2214 "Hi-Temp" adhesive was used to fill non-bond areas in the front spar flange edge; EC-2216 room temperature adhesive being used in the lower intermediate spar caps after assembly on the lower skin panel. Epox 828 epoxy resin was injected and cured to repair a small delamination of the center ply of the inner facing of the front spar; mold line facing of the lower skin panel; and B.P. 33.93 rib cap; no graphite filaments being fractured. Splintering at drilled holes was brush coated with room temperature cure epoxy resin.



After distortion of the lower skin sandwich panel occurred as described in 7.1.1, short beam test coupons were cut from the inner and outer facings of the upper and lower skin panel process control panels. Resultant test data presented in Table 8 showed some scatter in interlaminar shear properties which was evaluated along with the stresses used in the analysis of the composite wing and the effect of the lower material properties evident in the outer facing of the lower skin panel. It was concluded that forcing the panel to mold line on assembly would pre-stress the panel, producing beneficial compression stresses in the outer face sheet, thereby off-setting the low properties for applied tension stresses and continued fabrication was authorized.

Material review action taken to correct discrepancies that occurred during the installation of the upper skin panel consisted of substituting seven NAS1669-4L23 Jo-Bolts in place of NAS-1104 fasteners in the centerline rib where nutplates were inadvertently omitted and substituting one NAS1670-4L13 Jo-Bolt for a NAS1580A4T13 fastener in the 33.93 rib where a nutplate stripped. A Heli-Coil was also added to the aluminum centerline rib where a nutplate could not be installed.



TABLE 8  
 SHORT BEAM TEST DATA FOR INTERLAMINAR SHEAR  
 OF GRAPHITE/EPOXY LAMINATE  
 (Coupons cut from process control panels)

Upper Skin Panel		
	$f_{isu}$ (psi)	
	Outer Facing	Inner Facing
Longitudinal	10733	10875
	7979	8244
	8703	8533
Transverse	6480	6501
	5882	6057
	6139	6067
Lower Skin Panel		
	$f_{isu}$ (psi)	
	Outer Facing	Inner Facing
Longitudinal	7351	10042
	7304	10260
	7131	8958
Transverse	5174	7353
	5488	6683
	4974	6249

## SECTION 9.0

### STRUCTURAL TEST

#### 9.1 TEST LOAD CONDITIONS

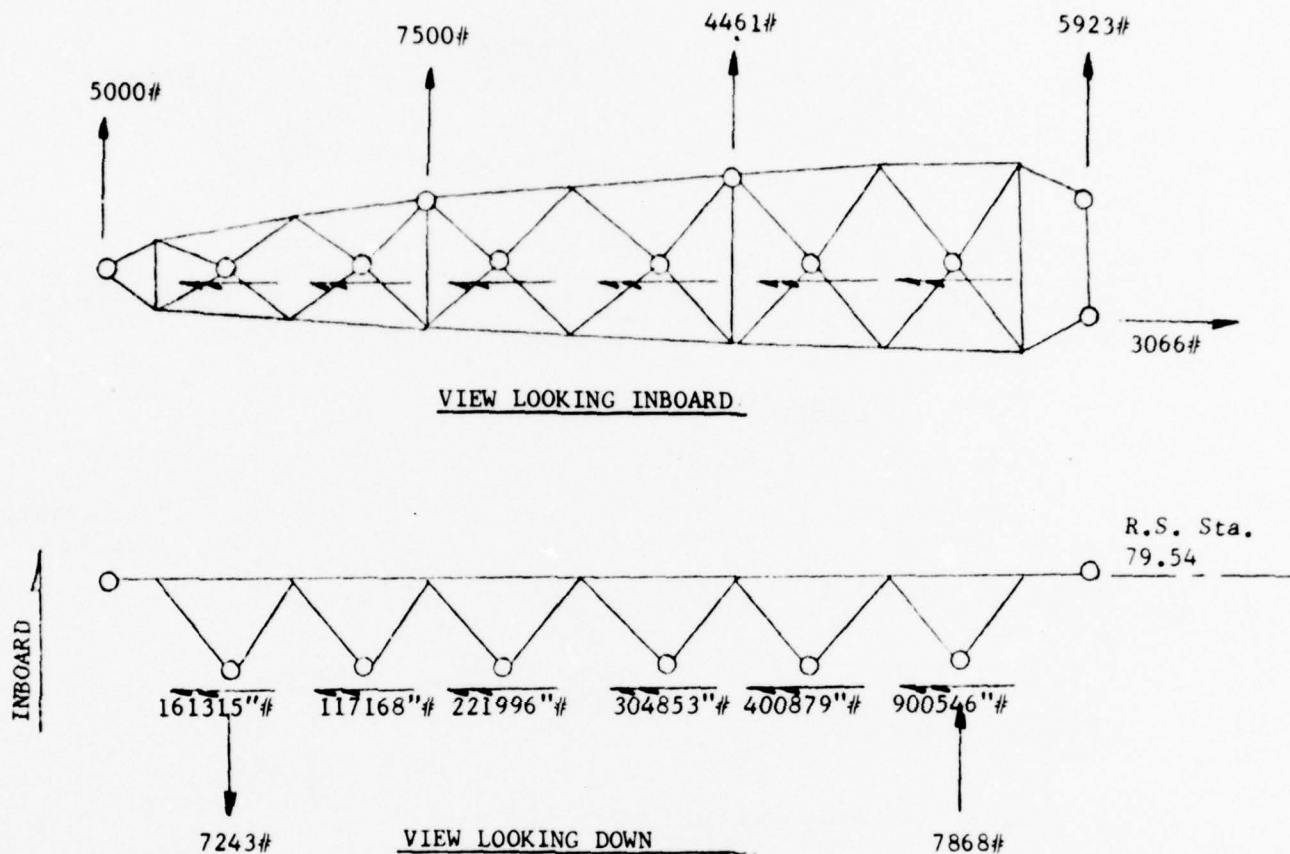
Two loading conditions were determined to be critical for the wing; i.e., maximum vertical landing and a symmetrical 6.5g pull-up at 0.96 Mach number,  $q = 1249$  PSF limit load. The maximum vertical landing condition was critical for static strength and this condition is proposed for static testing. Applied loads at R.S. Sta. 79.54 for the maximum vertical landing condition are shown in Figure 76. For further static and/or fatigue testing of the composite wing specimen applied loads are shown in Figure 77 and Table 9. The loads shown in Figure 77 represent the net outboard loads which are applied at R.S. Sta. 79.54 with the distributed air load inboard of R.S. Sta. 79.54 presented in Table 9 as applied to NASTRAN node points for convenience in defining pad loads. Figure 77 and Table 9 constitute the net applied loads for the symmetrical pull-up condition to obtain the correct inboard stress distributions in the composite wing test specimen.

Steel loading straps were added to the wing test specimen at R.S. Sta. 79.54 to facilitate attachment of the necessary loading beams and hydraulic jacks to apply the net loads shown in Figure 78. A general arrangement of the structural test set up is shown in Figure 79.

Testing will be performed by the Naval Air Development Center and the test procedures and test results will be published as Appendix C to this report later date.

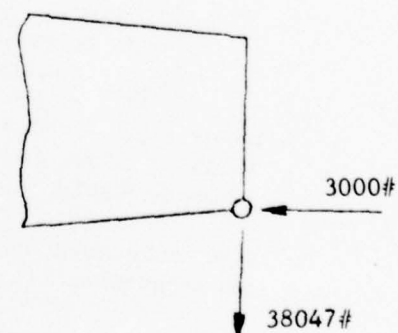
#### 9.2 STRAIN GAGE INSTRUMENTATION

Proposed instrumentation for the static test is shown in Figures 80 and 81 for strain gages and deflection transducers, respectively. Since several rosette strain gages were either back-to-back or installed on intermediate spar webs the internal gages were mounted on the wing test specimen during final assembly, numbered, and wire bundles brought to the outboard end (R.S. Sta. 79.54) for convenient pick-up. Six rosette strain gages were bonded to the inner surface of the wing skins and the inboard aft intermediate spar prior to installation of the upper cover skin. The gages and individual wire leads were installed at locations (1) upper, (1) lower, (5) upper, (5) lower, (13) spar and (14) spar as shown in Figure 80. Figure 80 also shows the remaining external gages proposed for installation by the Naval Air Development Center prior to testing.



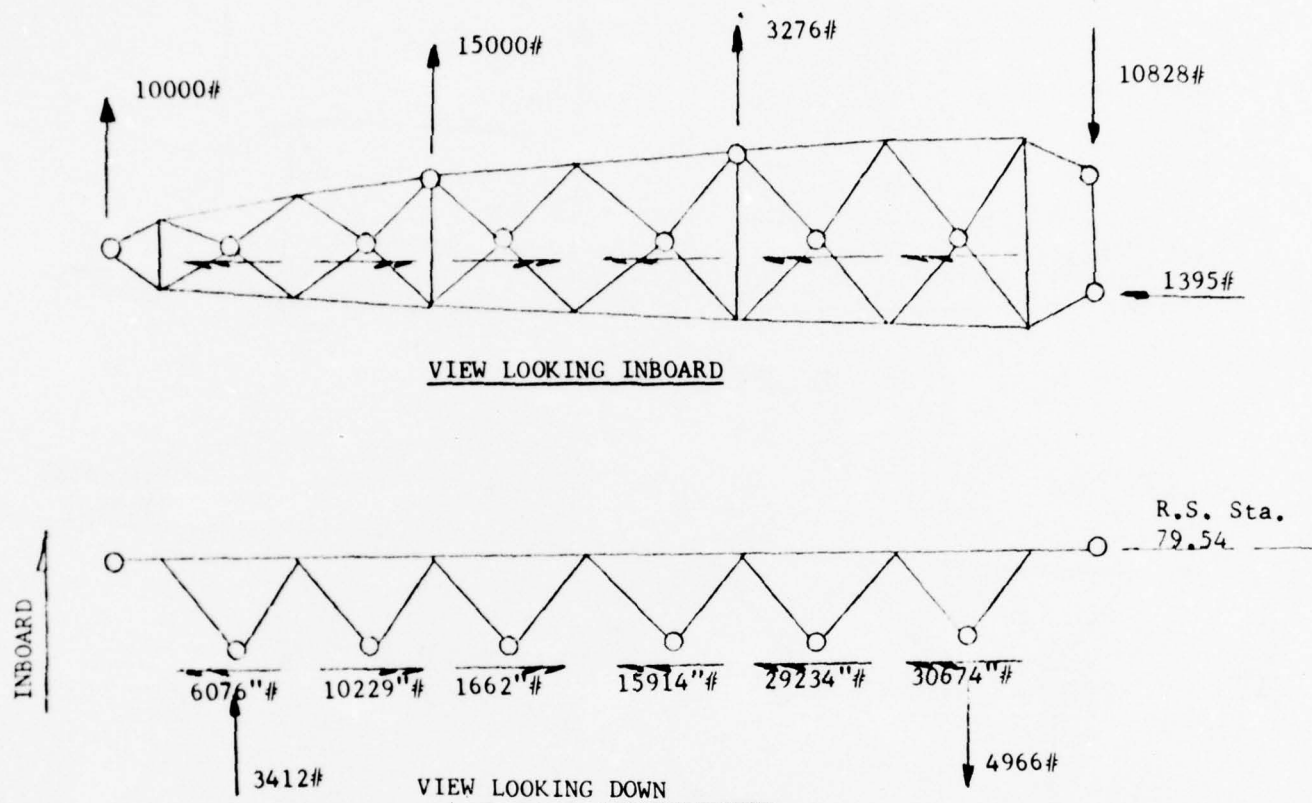
Loads applied to wing at R.S. Station 79.54 as shown. R.H. rule applies for moments acting on structure.

Note: R.S. Sta. 79.54 loads to be applied to TT-18636 test fixture lugs shown in Figures 1 & 71. Sta. 33.93 rib loads to be applied at wing to fuselage attach fitting shown in Figure 2.



STATION 33.93 RIB AT REAR SPAR

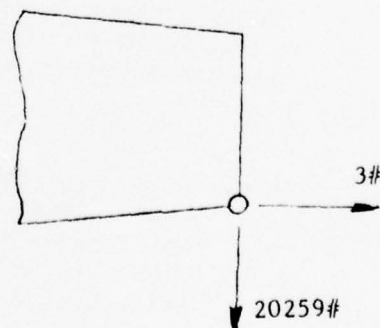
FIGURE 76 MAXIMUM VERTICAL LANDING CONDITION TEST LOADS  
(ULTIMATE LOADS)



Note: R.S. Sta. 79.54 loads to be applied to TT-18636 test fixture lugs shown in Figures 1 & 71. Sta. 33.93 rib loads to be applied at wing to fuselage attach fitting shown in Figure 2.

Loads applied to wing at R.S. Station 79.54 as shown in addition to airloads shown in Table 9.

R.H. rule applies for moments acting on structure.



STATION 33.93 RIB AT REAR SPAR

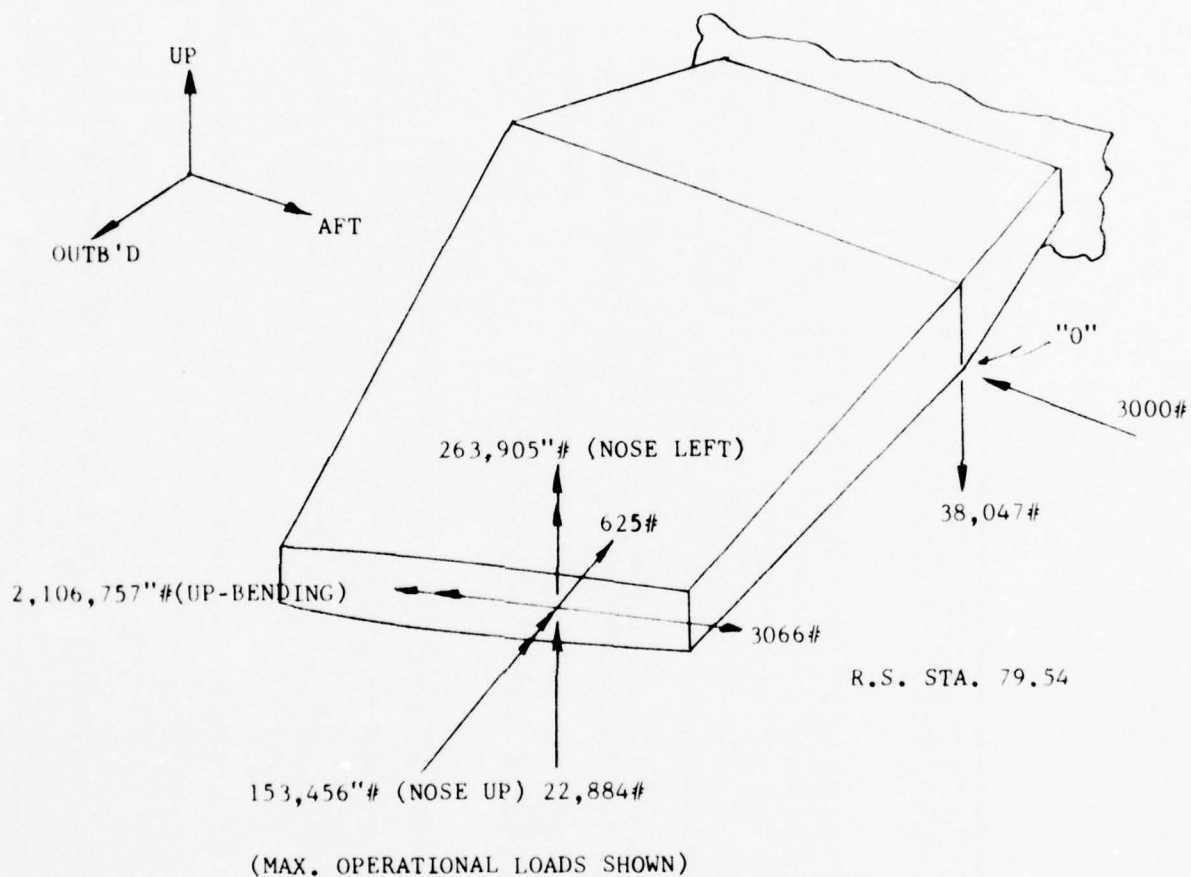
**FIGURE 77 CRITICAL FLIGHT CONDITION TEST LOADS  
(ULTIMATE LOADS)**

TABLE 9 FLIGHT CONDITION NODE POINT LOADING FOR APPLIED AIRLOADS (ULT.)

NOTE: Sign Convention: +Px Outb'd, +Py Aft +Pz Up  
See Figure 67 for  $X_w$ ,  $Y_w$  locations

NODE POINTS		$X_w$	$Y_w$	$P_x$		$P_y$		$P_z$ (Net)
Lower	Upper			Upper	Lower	Upper	Lower	
50513	50533	33.93	44.55	6	-26	-11	9	247
50514	50534	33.93	55.52	25	-18	-15	12	323
50515	50535	33.93	66.49	43	-8	-17	15	400
50516	50536	33.93	77.93	60	3	-19	17	479
50517	50537	33.93	89.36	76	15	-21	18	558
50518	50538	33.93	99.09	90	25	-21	19	626
50519	50539	33.93	108.82	102	36	-22	19	694
50613	50633	38.46	48.21	10	-21	-17	3	239
50713	50733	43.00	51.87	-15	15	-3	1	57
50714	50734	38.55	59.04	29	-13	-20	6	313
50813	50833	47.73	55.68	-14	15	-3	0	106
50814	50834	43.37	62.71	-18	20	-4	1	71
50815	50835	38.84	70.01	46	-3	-23	8	387
50913	50933	52.46	59.50	-13	15	-4	-1	156
50914	50934	48.19	66.38	-18	20	-4	1	121
50915	50935	43.75	73.52	-21	26	-4	1	86
50916	50936	38.94	81.28	63	7	-25	10	465
51013	51033	56.48	62.74	-7	7	-3	0	99
51014	51034	52.29	69.49	-17	20	-4	0	164
51015	51035	47.93	76.51	-20	25	-4	1	129
51016	51036	43.21	84.13	-23	30	-4	2	91
51017	51037	38.28	92.07	79	18	-26	12	545
51113	51133	60.50	65.98	-6	8	-3	-1	121
51114	51134	56.39	72.61	-9	10	-3	0	107
51115	51135	52.11	79.50	-19	25	-5	0	172
51116	51136	47.47	86.98	-22	30	-5	1	135
51117	51137	42.64	94.77	81	22	-31	6	531
51118	51138	38.38	101.66	92	29	-26	13	611
51213	51233	66.00	70.42	-5	8	-3	-1	150
51214	51234	61.99	76.88	-8	10	-4	0	137
51215	51235	57.82	83.59	-10	13	-4	0	124
51216	51236	53.31	90.87	-20	29	-5	1	195
51217	51237	48.60	98.47	-22	33	-5	1	157
51218	51238	44.43	105.18	-23	36	-5	2	124
51219	51239	40.11	112.15	105	41	-30	11	671
51313	51333	71.49	74.85	16	-9	-2	-2	200
51314	51334	67.59	81.14	-7	10	-4	-1	167
51315	51335	63.54	87.68	-7	13	-4	0	154
51316	51336	59.14	94.77	-10	15	-4	0	140
51317	51337	54.55	102.16	-21	32	-6	1	218
51318	51338	50.50	108.70	-22	35	-5	1	186
51319	51339	46.29	115.49	-22	37	-5	2	152
51413	51433	76.99	79.29	15	-9	-2	-3	138
51414	51434	73.20	85.41	21	-11	-2	-3	179
51415	51435	69.25	91.77	25	-16	-2	-2	222
51416	51436	64.97	98.67	-9	15	-4	0	170
51417	51437	60.51	105.86	-10	17	-4	1	156
51418	51438	56.56	112.22	-10	19	-4	1	143
51419	51439	52.47	118.82	-21	37	-6	1	214
51513	51533	82.49	83.73	25	-14	-2	-4	326
51514	51534	78.80	89.67	20	-11	-2	-3	116
51515	51535	74.97	95.85	24	-15	-2	-3	158
51516	51536	70.80	102.56	26	-18	-2	-3	203
51517	51537	66.47	109.55	-9	17	-5	0	187
51518	51538	62.63	115.74	-9	19	-4	0	174
51519	51539	58.65	122.16	-9	20	-4	1	161
51613	51633	87.99	88.16	22	-14	-2	-4	221
51614	51634	84.40	93.94	33	-18	-1	-4	282
51615	51635	80.68	99.94	38	-25	-1	-5	345
51616	51636	76.64	106.46	25	-18	-2	-3	137
51617	51637	72.42	113.25	27	-21	-2	-3	183
51618	51638	68.70	119.26	29	-23	-1	-3	223
51819	51639	64.83	125.49	-8	20	-5	0	193





NOTE: Loads @ R.S. Sta. 79.54 are in R.S. Sta. 79.54 plane and are located @ intersection of W.R.P. and aft inter. spar plane. Aft wing-to-fuselage attach loads @ Pt. "O" are in Fuse. Ref. System.

FIGURE 78 MAXIMUM VERTICAL LANDING CONDITION APPLIED STATIC TEST LOADS

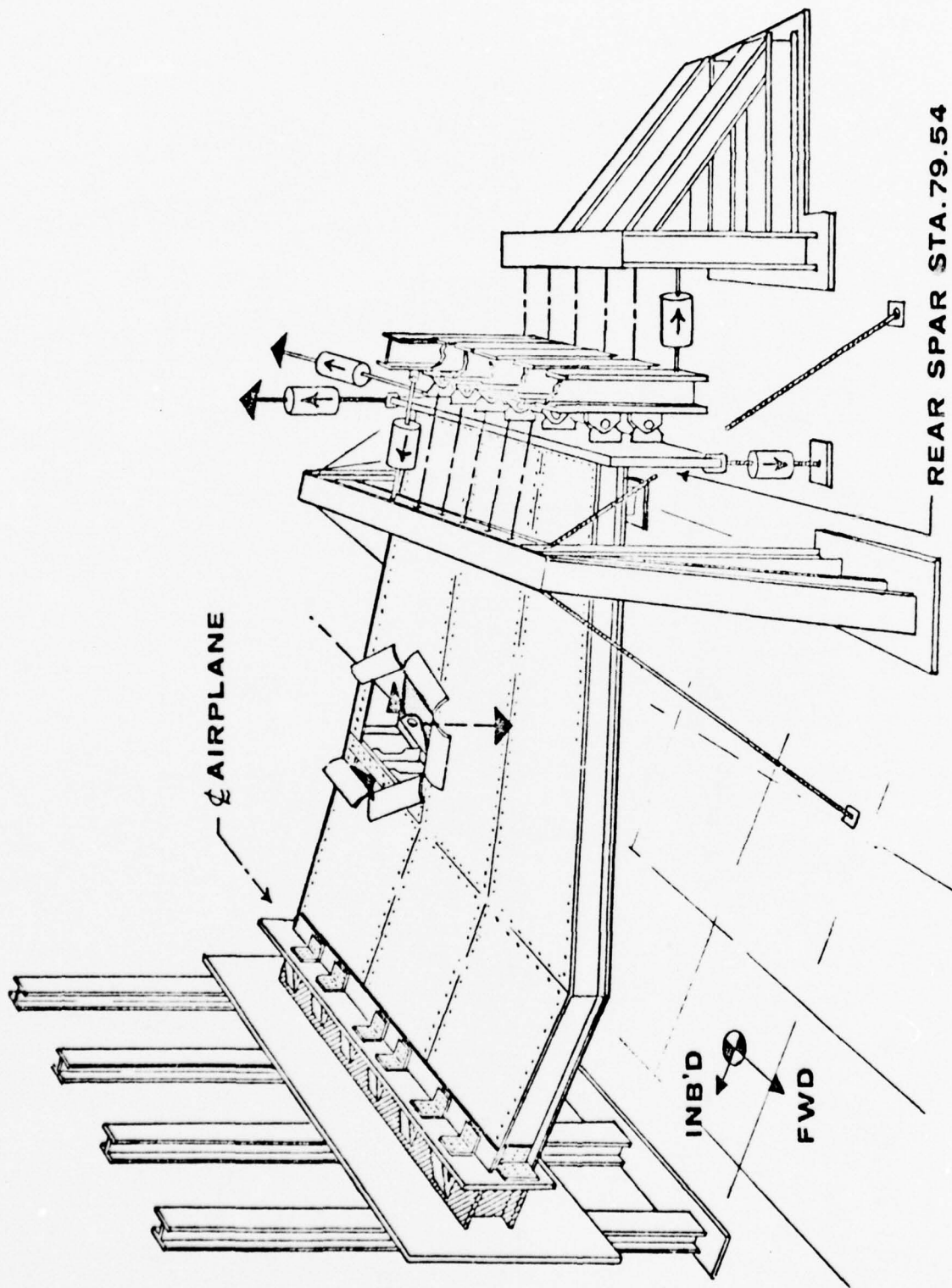
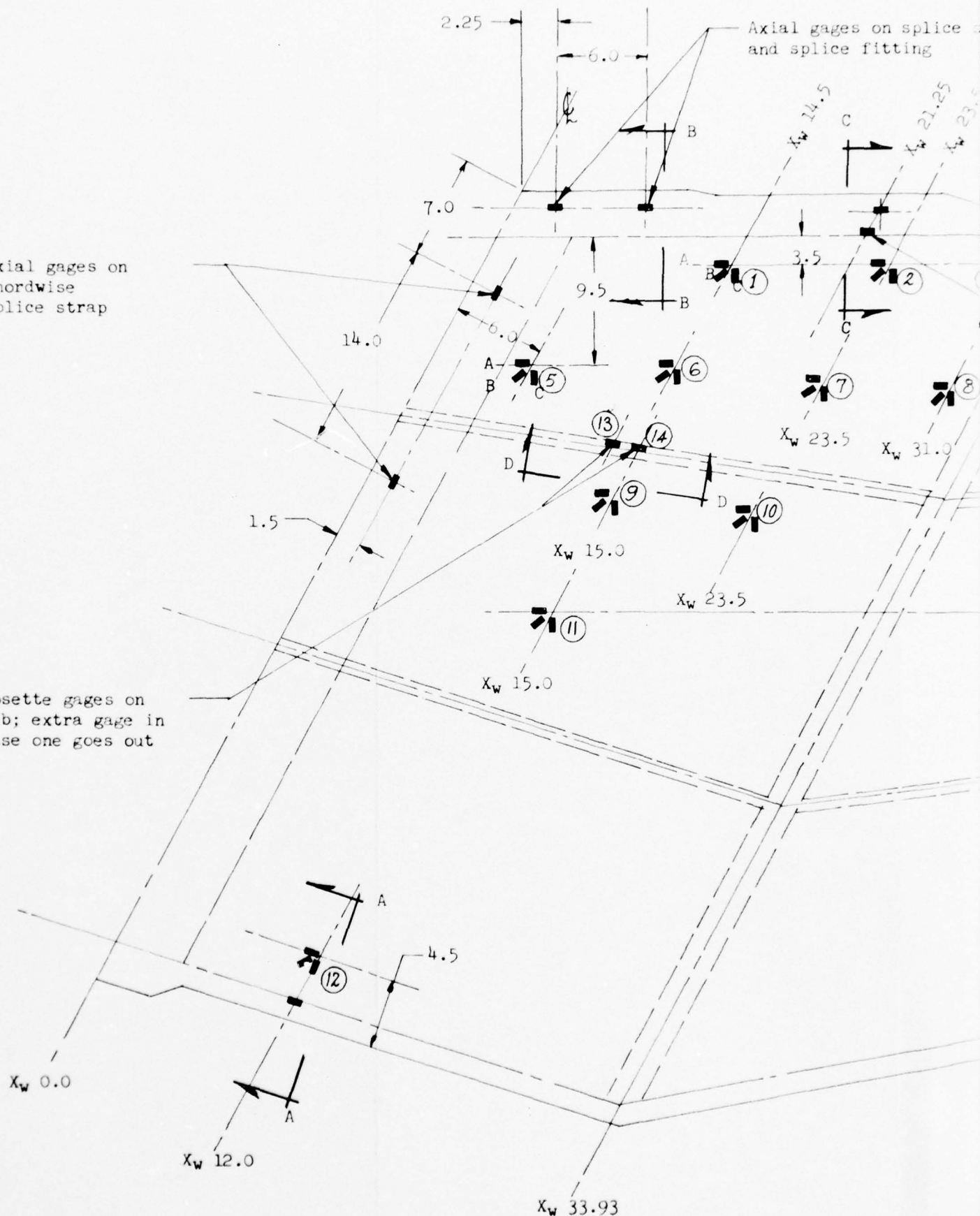


FIGURE 79 COMPOSITE WING STRUCTURAL TEST SETUP

Axial gages on  
chordwise  
splice strap

Rosette gages on  
web; extra gage in  
case one goes out



NOTE: All cover rosette gages oriented as shown with one leg parallel to rear spar plane except (12); typical upper and lower covers.

Gages (1) and (5) to be back-to-back gages, upper and lower covers.

gages on splice strap  
lice fitting

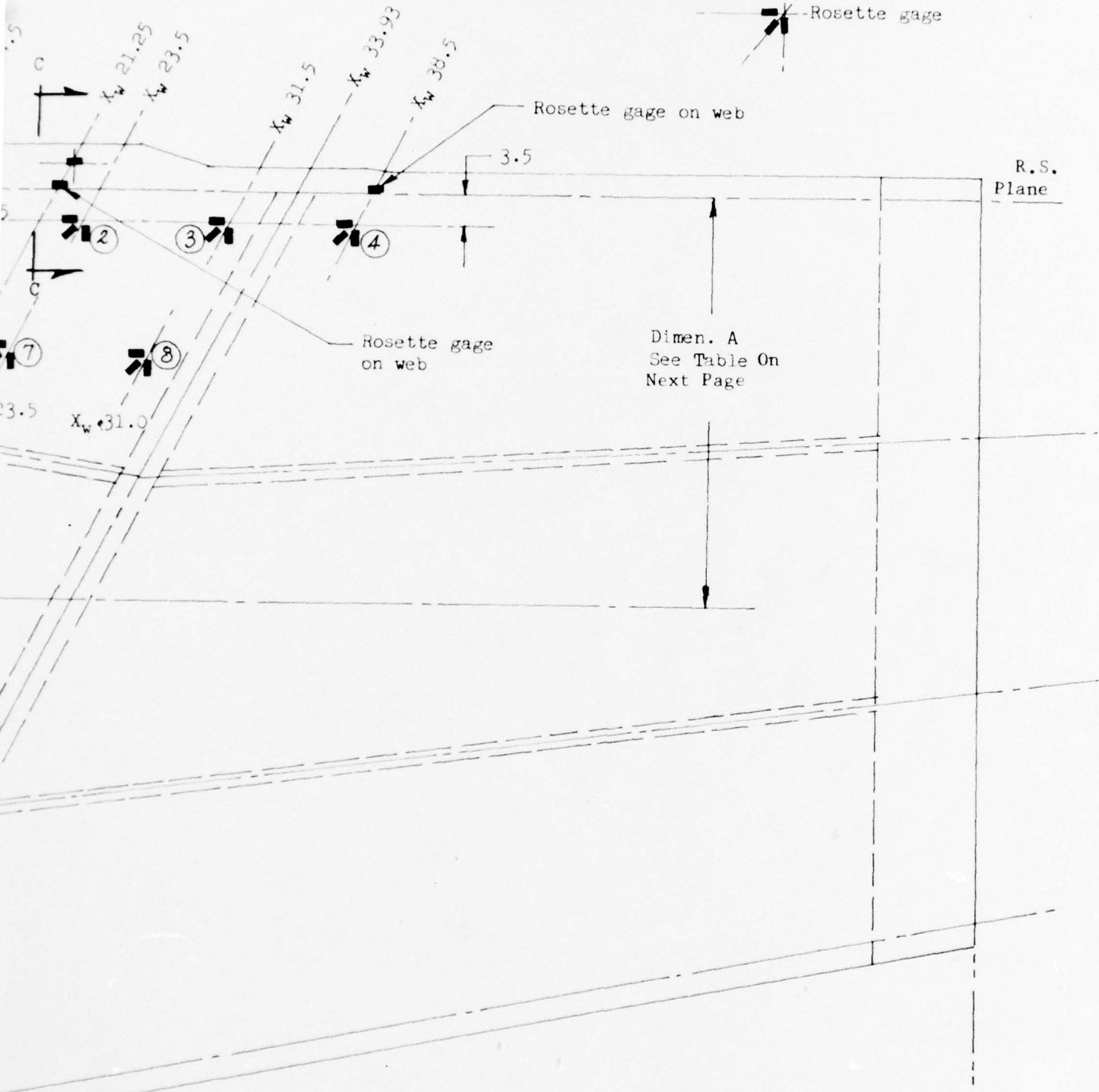
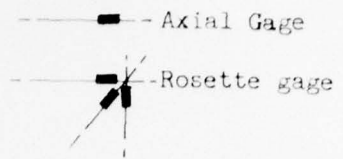
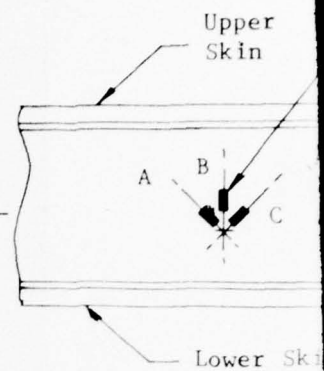
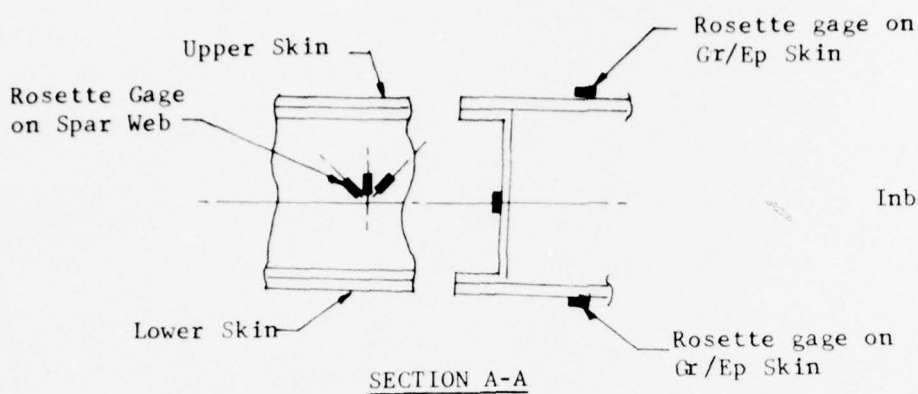


FIGURE 80  
STRAIN GAGE LOCATIONS

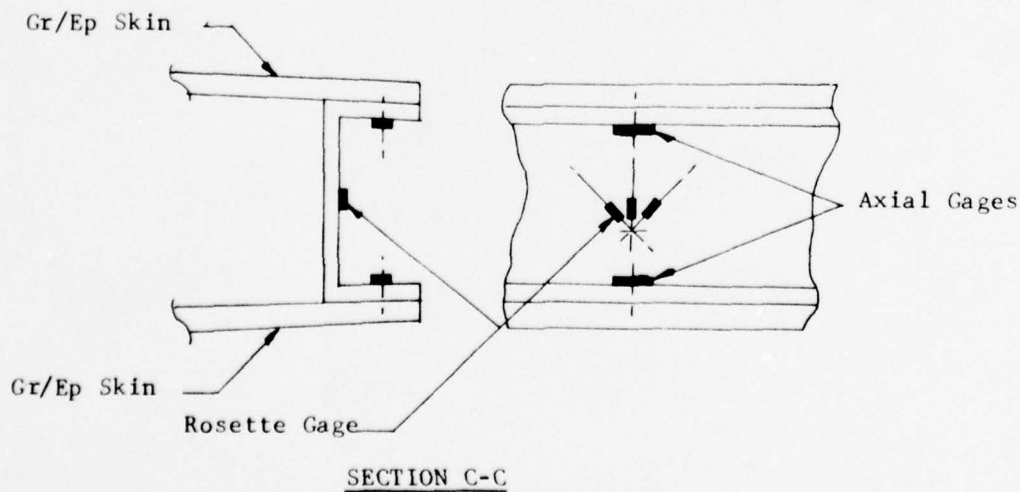
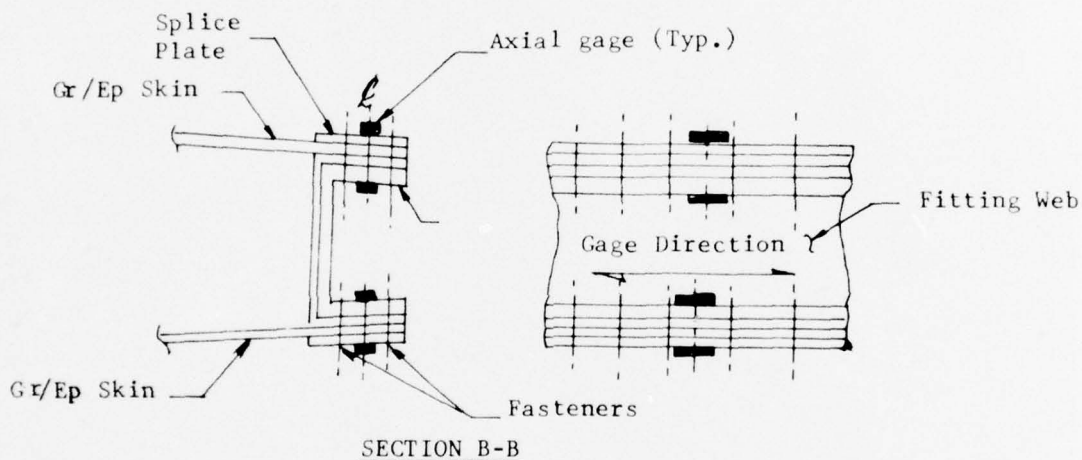
R.S. Sta.  
79.54

be back-to-back  
r covers.

2



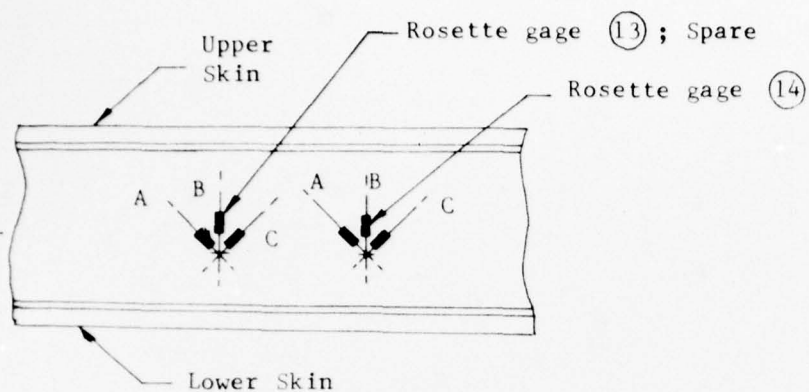
SECTION D-D



GAGE NO.	
1	UA*
1	UB
1	UC
1	LA
1	LB
1	LC
2	
3	
4	
5	UA
5	UB
5	UC
5	LA
5	LB
5	LC
6	
7	
8	
9	
10	
11	
12	
13SA	
13SB (S)	
13SC	
14SA	
14SB	
14SC	

\* UA denotes upper skin rosette leg A  
 LB denotes lower skin rosette leg B  
 SA denotes spar web rosette leg A



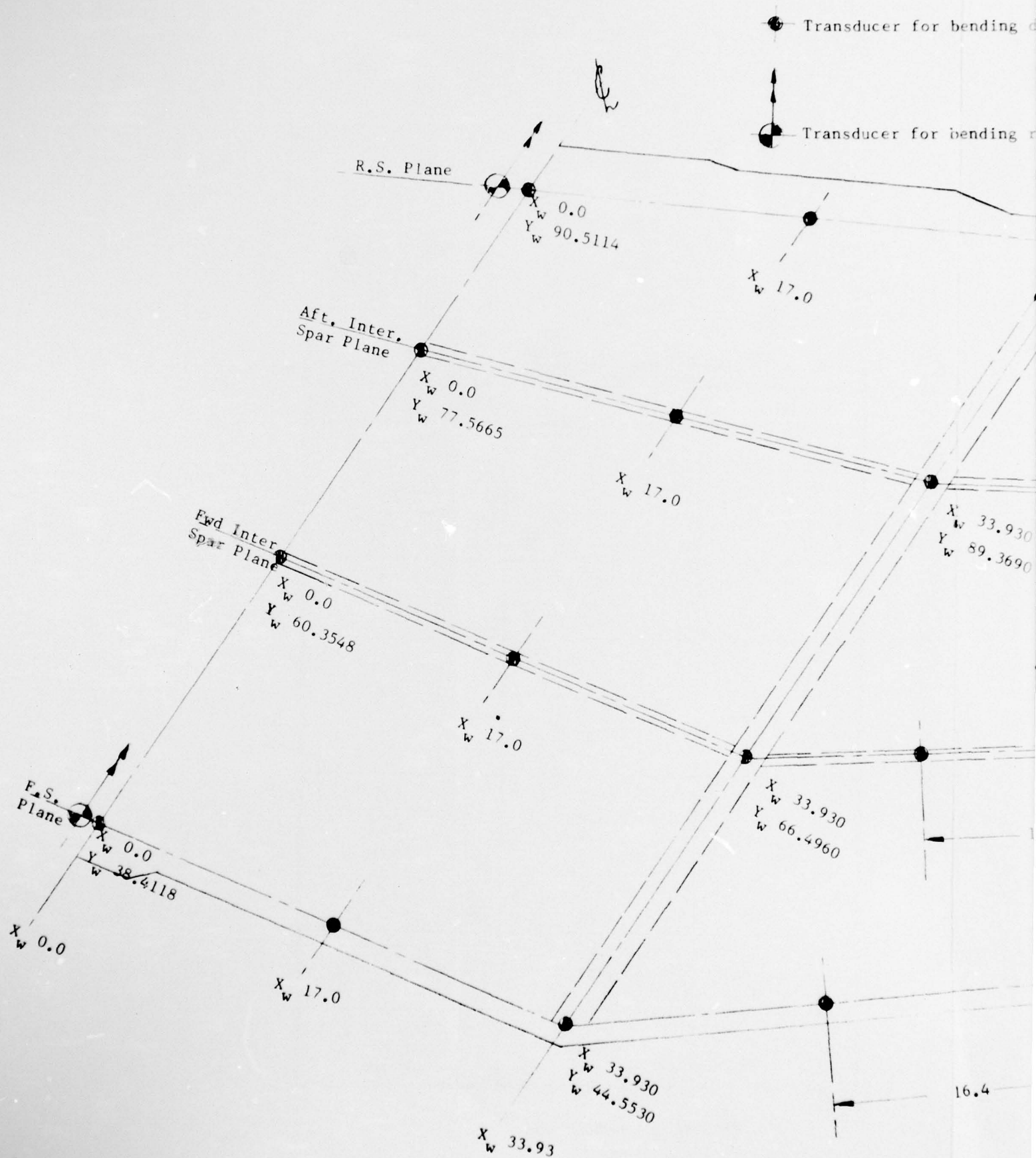


SECTION D-D

LOCATION DIMENSIONS FOR ROSETTE STRAIN GAGES		
GAGE NO.	$X_w$	DIMENSION A, inches
1 UA*	14.5	3.5
1 UB		
1 UC		
1 LA		
1 LB		
1 LC		
2	23.5	3.5
3	31.5	3.5
4	38.5	3.5
5 UA	6.0	9.5
5 UB		
5 UC		
5 LA		
5 LB		
5 LC		
6	14.5	9.5
7	23.5	10.5
8	31.0	11.0
9	15.0	18.0
10	23.5	19.0
11	15.0	25.5
12	12.0	See Prev. Page
13SA 13SB (Spare) 13SC	Just inboard of gage (14)	On aft intermediate spar web
14SA 14SB 14SC	14.5	On aft intermediate spar web

FIGURE 80 CONCLUDED  
STRAIN GAGE LOCATIONS

2

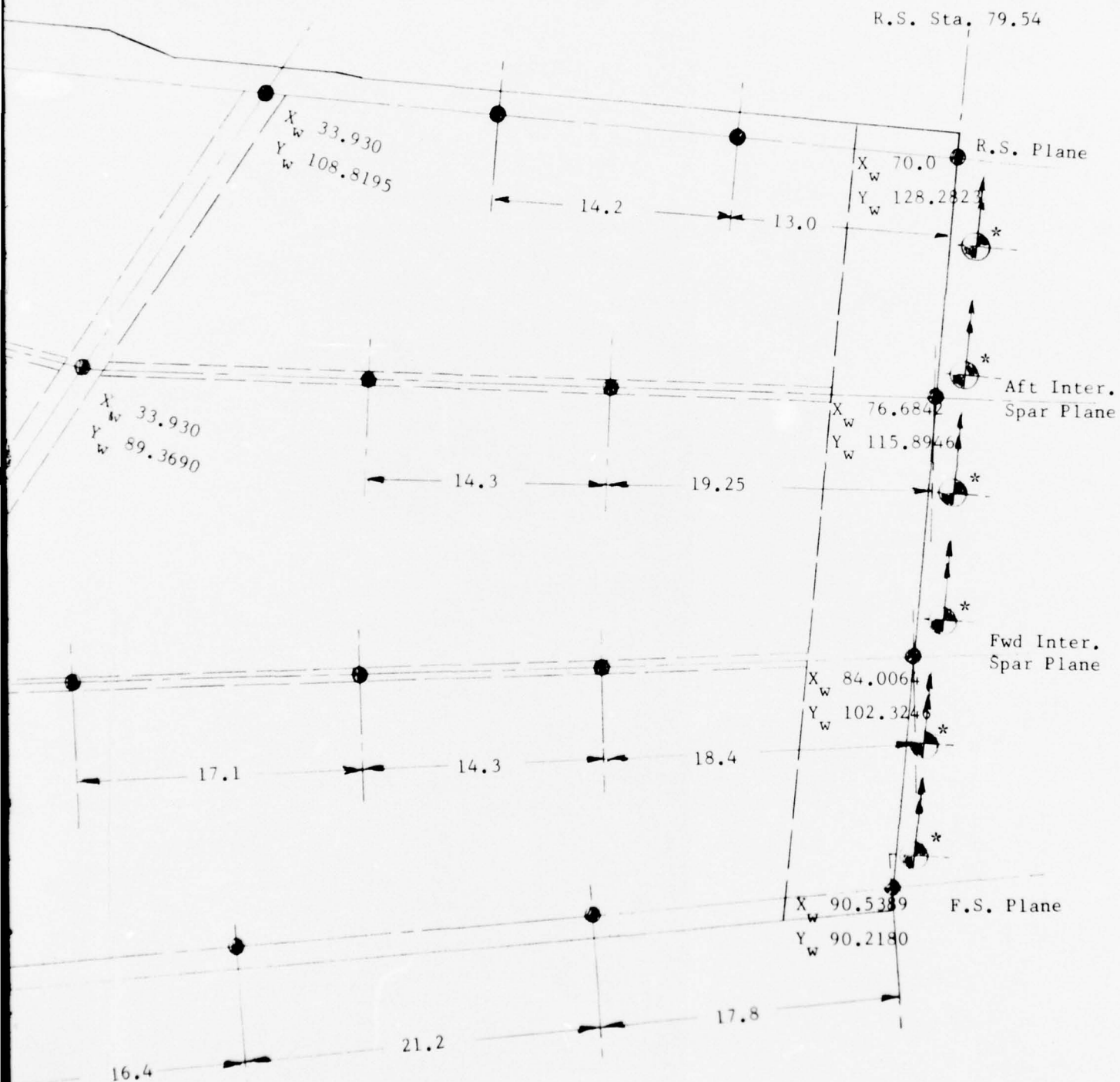


ducer for bending deflection

ducer for bending rotation

NOTES:

- 1 All deflection transducers are located on front spar, rear spar, or inter. spar lines and are located at NASTRAN node points.



\*Attach to I-Beams used for bending moment application.

FIGURE 81

PROPOSED DEFLECTION TRANSDUCER LOCATIONS

2

## 10.0 RECOMMENDATIONS

- It is recommended that future design of the composite wing baseline structural configuration include the following production improvements. Splice densified core into the upper cover skin panel and intermediate spar core blankets in the areas now filled with potting compound for stabilization during fastener installation. Integrate the intermediate spar webs with the lower spar caps to eliminate a Hi-Lok fastened joint. Incorporate a woven outer ply on all graphite skins to facilitate handling and reduce splintering at drilled holes and machined surfaces; limited fatigue test data warrants an evaluation of an exterior woven ply on surface delamination.
- Design and fabricate two flightworthy graphite/epoxy composite wing structural boxes that are compatible with the XFV-12A aircraft. Static test one wing box to demonstrate structural integrity; the other structural wing box to be installed on either Proto #1 or Proto #2 and flight tested to evaluate inflight characteristics of a composite wing. The wing design will be an extension of the center section specimen as modified to incorporate recommended changes and those resulting from testing of the specimen.

APPENDIX A  
STRUCTURAL ANALYSIS

PRECEDING PAGE BLANK-NOT FILMED



## APPENDIX A - STRUCTURAL ANALYSIS

This appendix includes internal load summaries as well as pertinent structural analyses of critical areas and stiffness data not presented in the main body of this report. The areas considered of importance for strength and stiffness assessment of the composite wing are as follows:

- (a) summaries of wing cover stresses for critical landing and flight conditions
- (b) wing cover panel stability analysis of honeycomb sandwich panels
- (c) wing spar shear flow summaries
- (d) free body diagrams of major structural elements
- (e) wing spar cap and attachment analyses
- (f) wing centerline splice analysis
- (g) wing-to-fuselage attachment analysis
- (h) deflections

## WING COVER STRESSES

Summaries of upper and lower wing cover stresses are presented for both the MAX. VERTICAL LANDING CONDITION and the critical symmetrical pull-up flight condition.

### MAX. VERTICAL LANDING CONDITION

Figures A-1 and A-2 summarize the upper cover stresses for the inboard and outboard areas, respectively, for the original configuration prior to increasing the aluminum spar cap area. Figure A-3 defines the inboard upper cover stress distribution after the aluminum spar cap areas were increased to reduce the cover stresses. The lower cover stress distributions for the inboard and outboard areas are shown in Figures A-4 and A-5, respectively, for the wing prior to increasing the rear spar cap area. The reduction in inboard lower cover stresses as a consequence of increasing the rear spar cap area is illustrated in the stress distribution shown in Figure A-6.

### SYMMETRICAL FLIGHT CONDITION 470303

The cover stress distributions shown in Figures A-7 through A-10 represent the stresses for the symmetrical flight condition as computed prior to increasing the rear spar cap area. Upper cover stresses are shown in Figures A-7 and A-8 and lower cover stresses shown in Figures A-9 and A-10. It should be noted that the stresses shown for the flight condition in the wing root area are significantly lower than those obtained for the MAX. VERTICAL LANDING CONDITION.

Figure A-11 shows the final aluminum rear spar cap areas used to obtain lower cover skin stresses ( $\sigma \approx 35000$  psi).

Maximum principal stress directions for the inboard end of the upper and lower covers are shown in Figures A-12 and A-13, respectively.

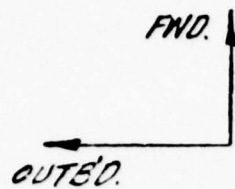
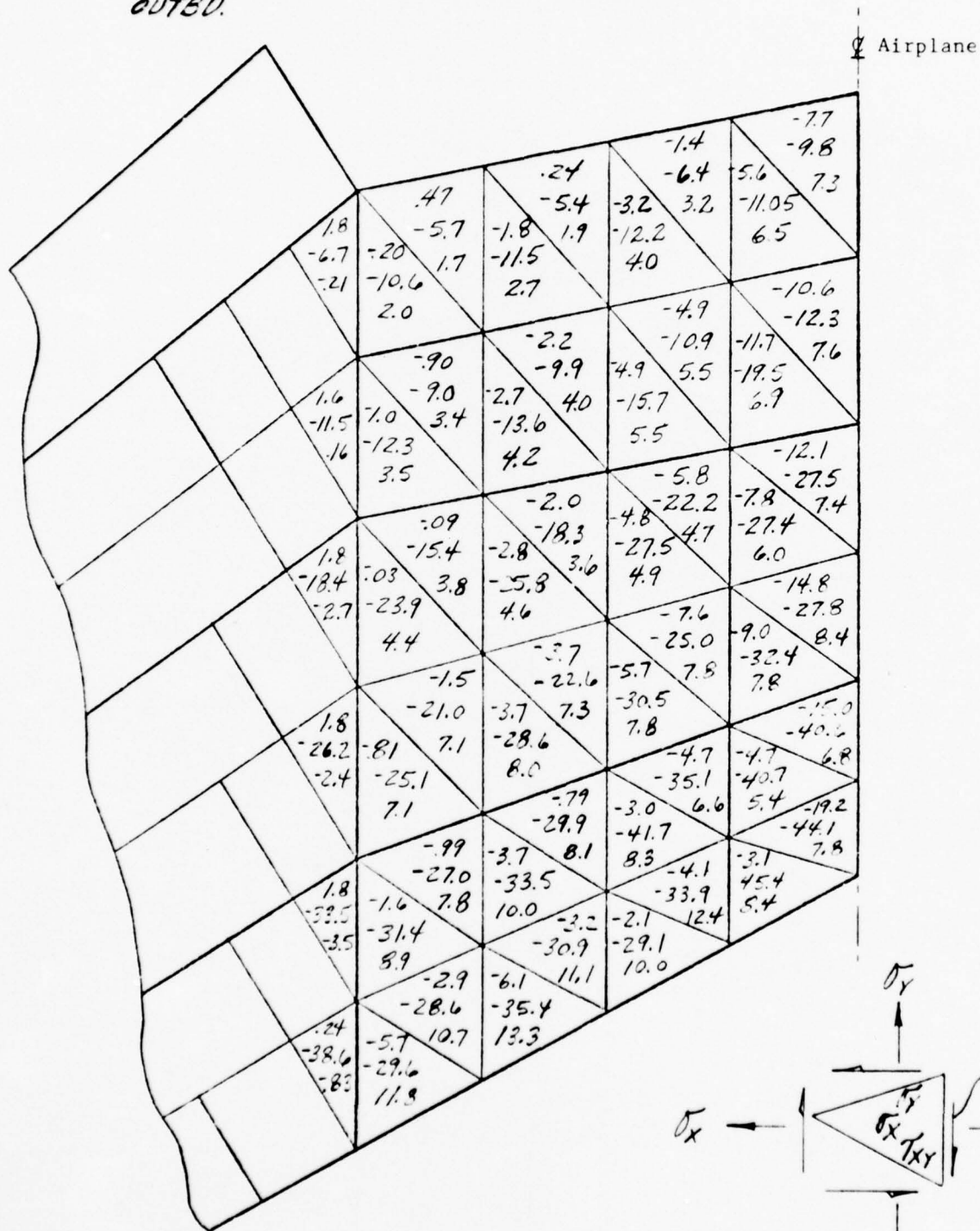


FIGURE A-1

WING UPPER COVER STRESSES

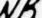
MAX. VERTICAL LOAD LANDING CONDITION

MAX. OPERATIONAL STRESSES ~ KSI



WING UPPER COVER STRESSES

INB'D.



FWD.

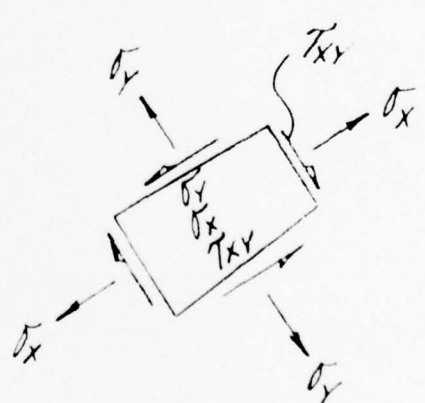
[illegible]

E A-2

VER STRESSES

LANDING CONDITION  
STRESSES ~ KSI

1.0	-17	-36.6	-29	-72	51	1.5	-1.4	-44	-27.9	-27.4	-13	-21	15	23
2.7	-36.6	-30.0	-29	-36.7	-36.0	-35.6	-28.8	-28.0	-27.9	-27.4	-25.6	-25.6	-23.5	-21.6
27	-35.1	-35.1	-35.1	-35.1	-35.1	-35.1	-35.1	-35.1	-35.1	-35.1	-35.1	-35.1	-35.1	-35.1
29.2	-29.2	-29.2	-29.2	-29.2	-29.2	-29.2	-29.2	-29.2	-29.2	-29.2	-29.2	-29.2	-29.2	-29.2
32	-25.9	-25.9	-25.9	-25.9	-25.9	-25.9	-25.9	-25.9	-25.9	-25.9	-25.9	-25.9	-25.9	-25.9
5.6	-2.2	-2.2	-2.2	-2.2	-2.2	-2.2	-2.2	-2.2	-2.2	-2.2	-2.2	-2.2	-2.2	-2.2
10	-17.4	-17.4	-17.4	-17.4	-17.4	-17.4	-17.4	-17.4	-17.4	-17.4	-17.4	-17.4	-17.4	-17.4
47	-0.2	-0.2	-0.2	-0.2	-0.2	-0.2	-0.2	-0.2	-0.2	-0.2	-0.2	-0.2	-0.2	-0.2
15	-11.9	-11.9	-11.9	-11.9	-11.9	-11.9	-11.9	-11.9	-11.9	-11.9	-11.9	-11.9	-11.9	-11.9
17	-1.1	-1.1	-1.1	-1.1	-1.1	-1.1	-1.1	-1.1	-1.1	-1.1	-1.1	-1.1	-1.1	-1.1
2	-3.6	-3.6	-3.6	-3.6	-3.6	-3.6	-3.6	-3.6	-3.6	-3.6	-3.6	-3.6	-3.6	-3.6
85	-3.9	-3.9	-3.9	-3.9	-3.9	-3.9	-3.9	-3.9	-3.9	-3.9	-3.9	-3.9	-3.9	-3.9
2.3	2.3	2.3	2.3	2.3	2.3	2.3	2.3	2.3	2.3	2.3	2.3	2.3	2.3	2.3



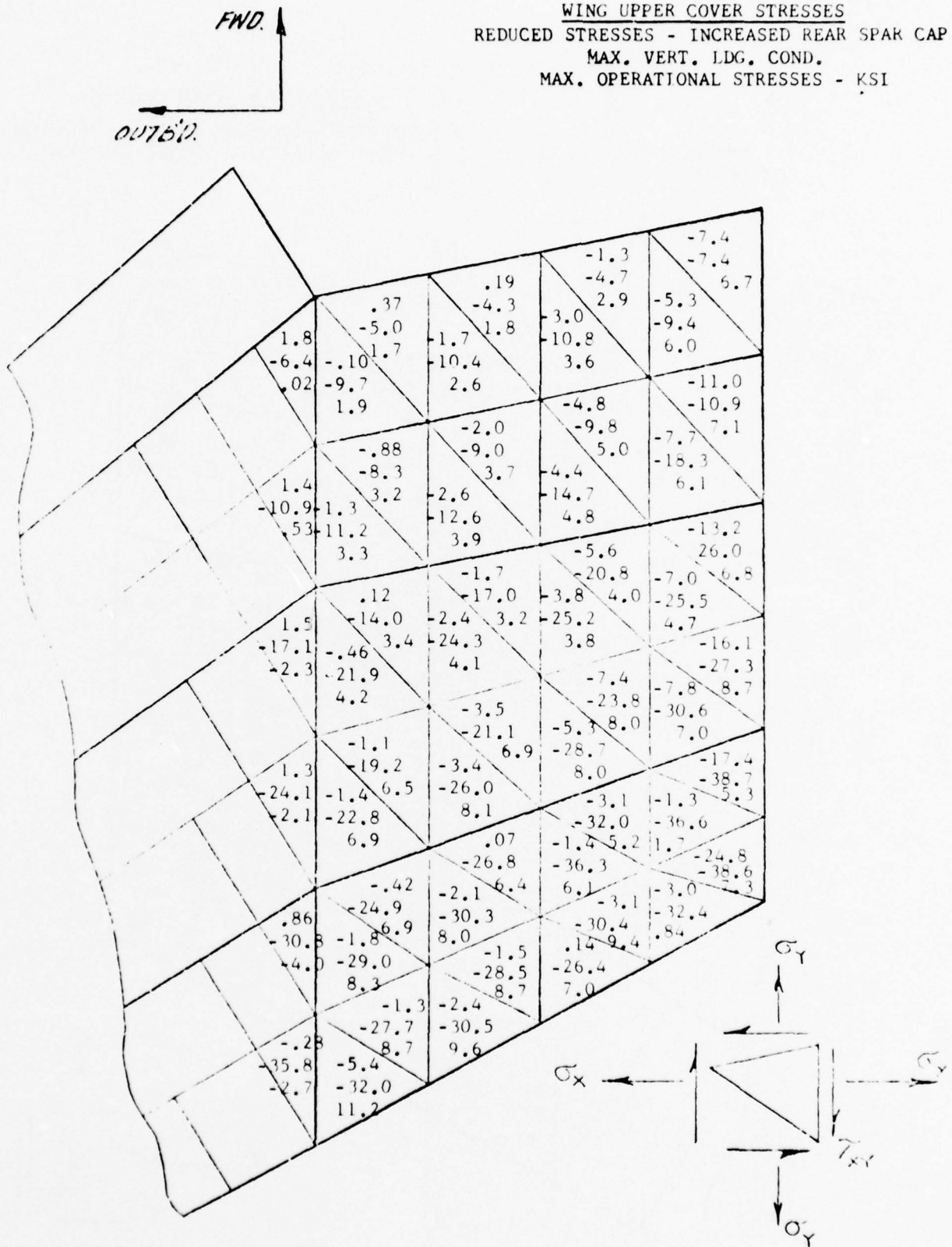
BEST AVAILABLE COPY

2



FIGURE A-3

WING UPPER COVER STRESSES  
 REDUCED STRESSES - INCREASED REAR SPAR CAP  
 MAX. VERT. LDG. COND.  
 MAX. OPERATIONAL STRESSES - KSI



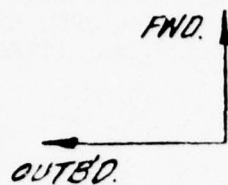
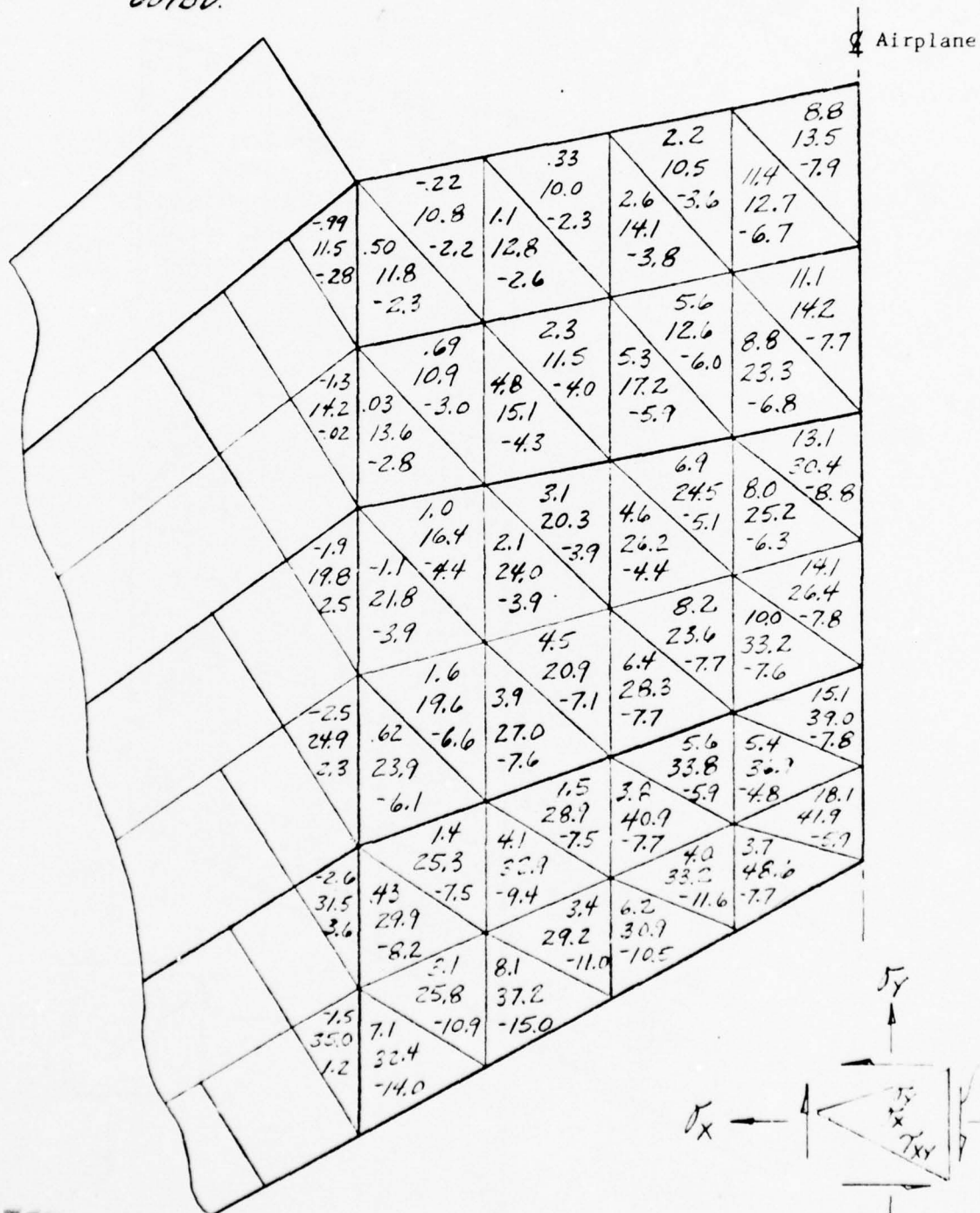


FIGURE A-4  
WING LOWER COVER STRESSES  
MAX. VERTICAL LOAD LANDING CONDITION  
MAX. OPERATIONAL STRESSES ~ KSI



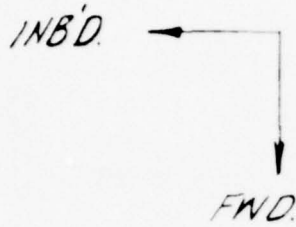
BEST AVAILABLE COPY

FIGURE A-5

WING LOWER COVER STRESSES

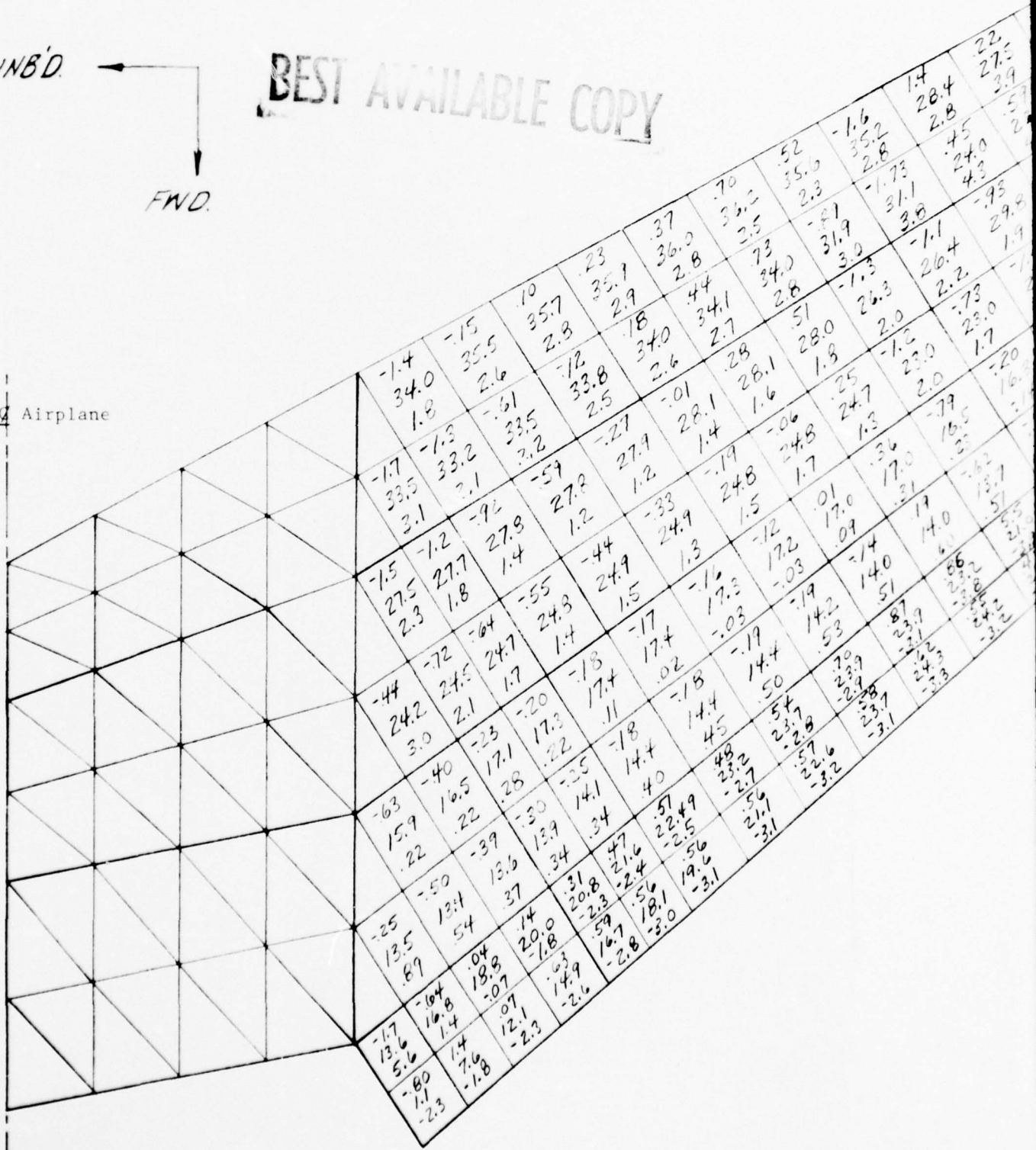
MAX. VERTICAL LOAD LANDING CONDITION

MAX. OPERATIONAL STRESSES - KSI

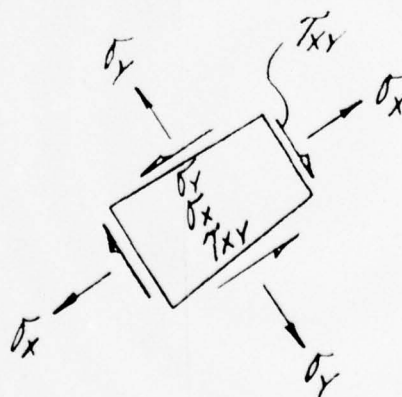
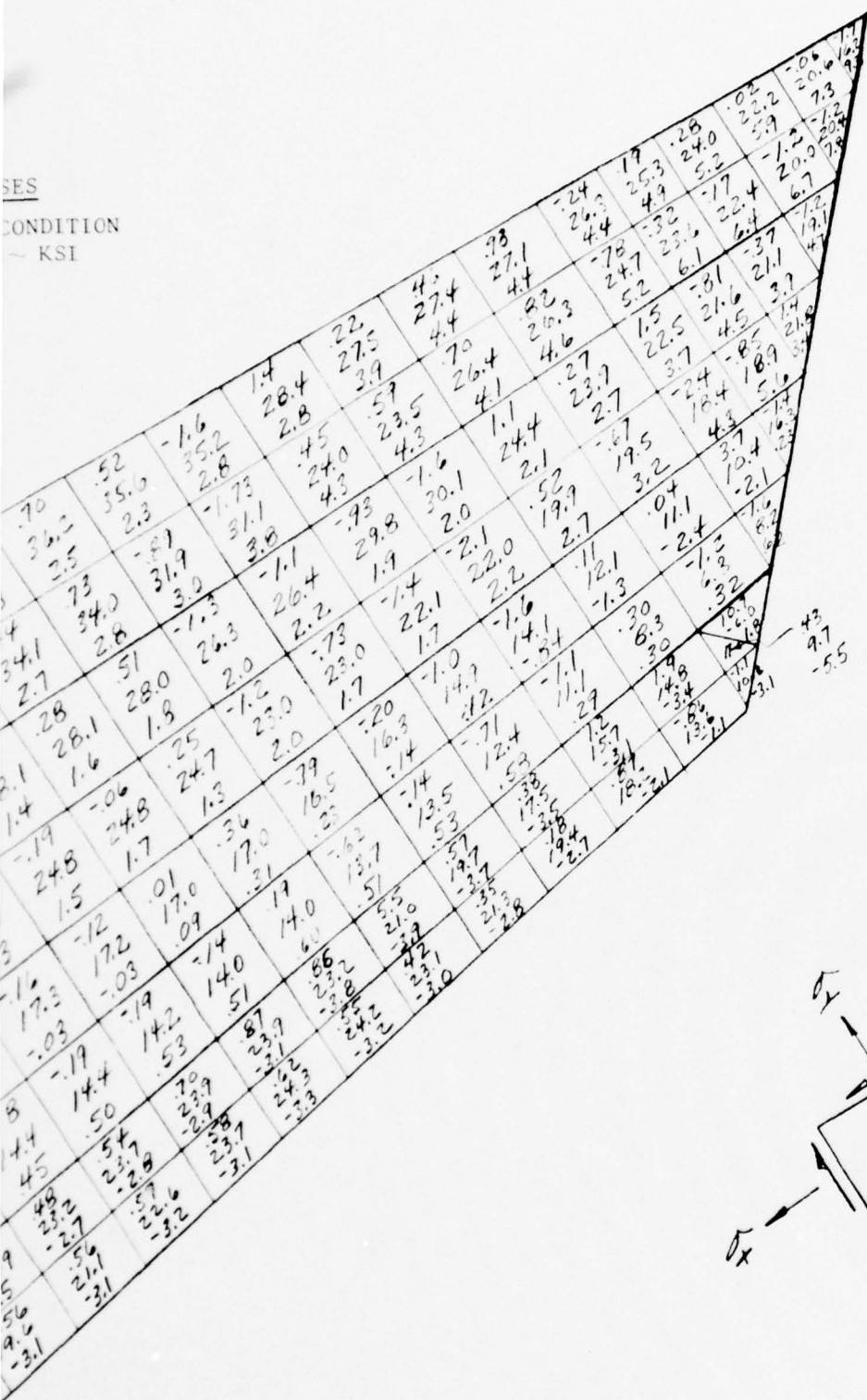


BEST AVAILABLE COPY

Airplane



SES  
CONDITION  
KSI

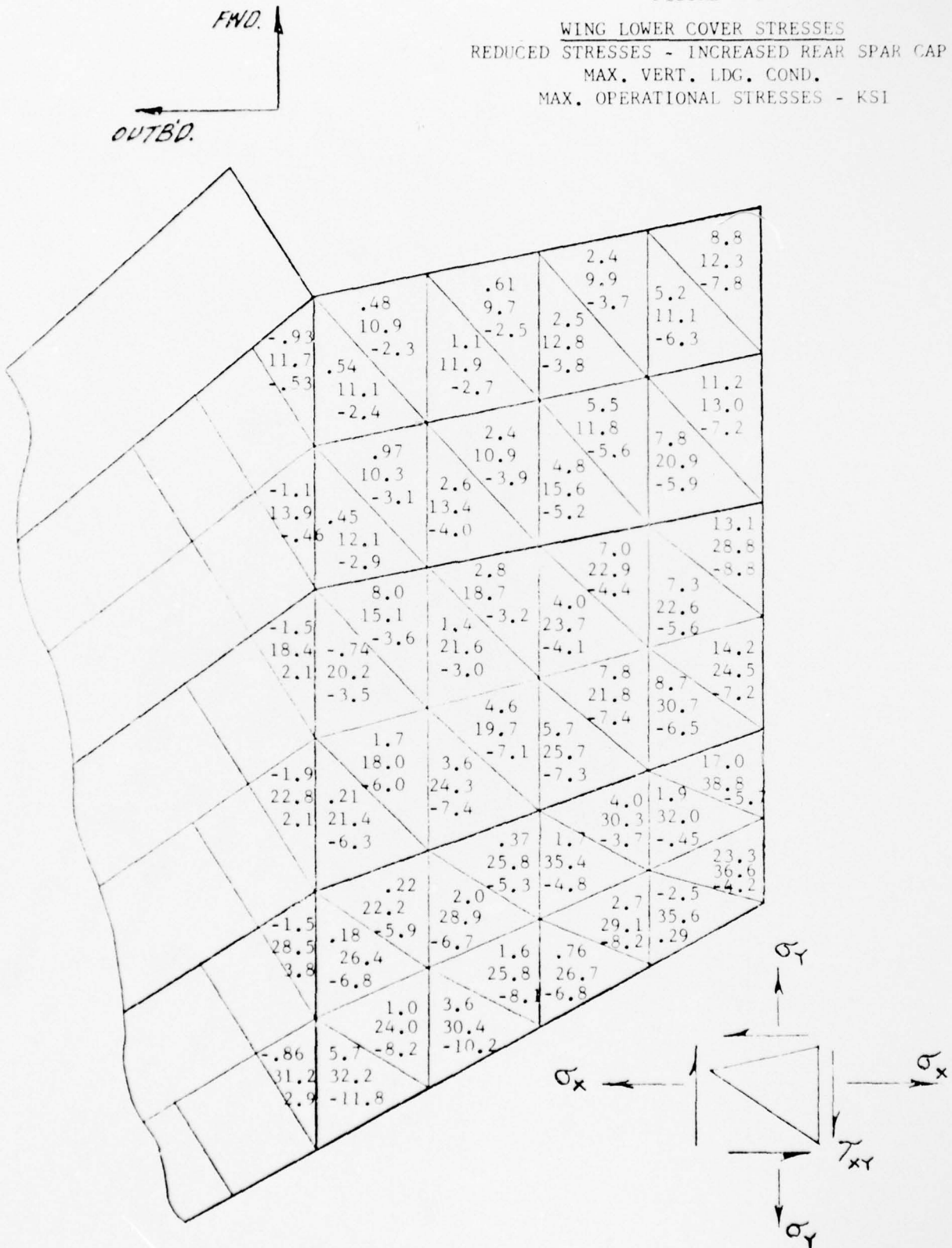


2



FIGURE A-6

WING LOWER COVER STRESSES  
REDUCED STRESSES - INCREASED REAR SPAR CAP  
MAX. VERT. LDG. COND.  
MAX. OPERATIONAL STRESSES - KSI





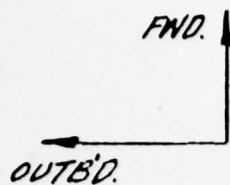
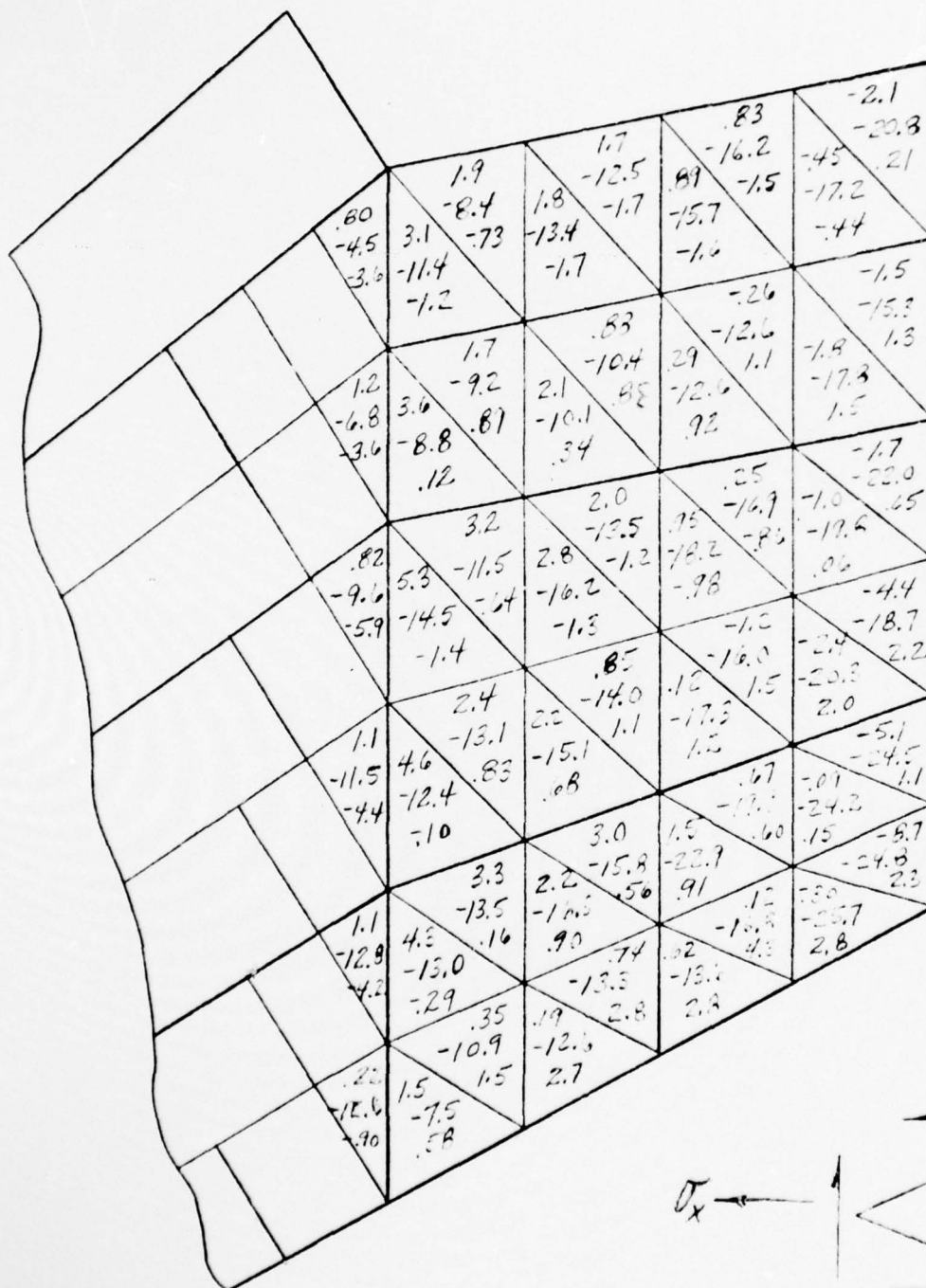


FIGURE A-7 WING UPPER COVER STRESSES

SYMMETRICAL FLIGHT CONDITION 470303  
ULTIMATE STRESSES - KSI

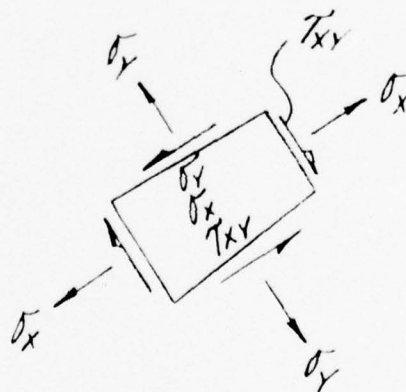
✈ Airplane



BEST AVAILABLE COPY

SYMMETRICAL FLIGHT CONDITION 470303  
ULTIMATE STRESSES - KSI





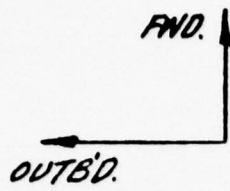


FIGURE A-9 WING LOWER COVER STRESSES

SYMMETRICAL FLIGHT CODITION 470303  
ULTIMATE STRESSES - KSI

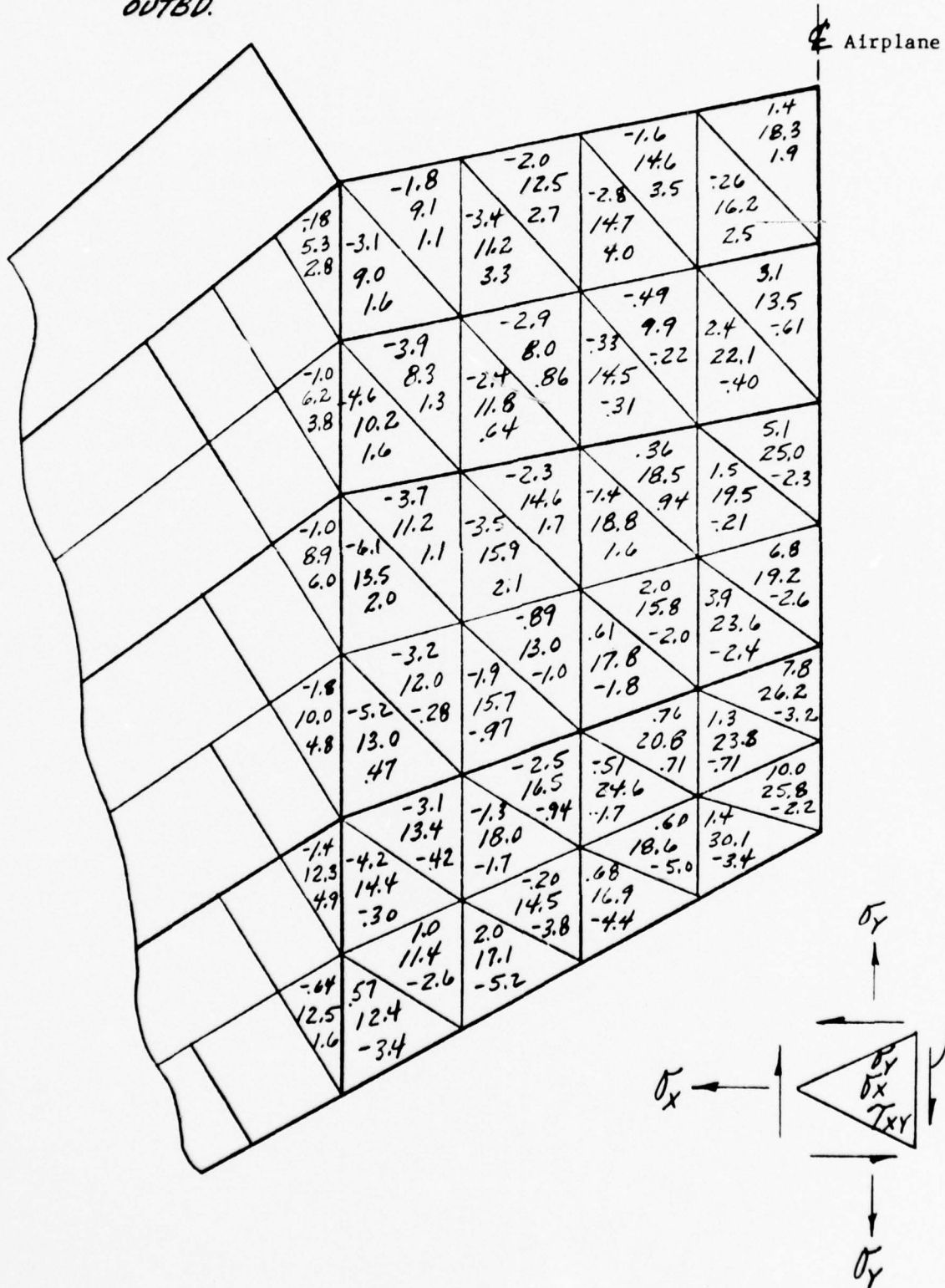
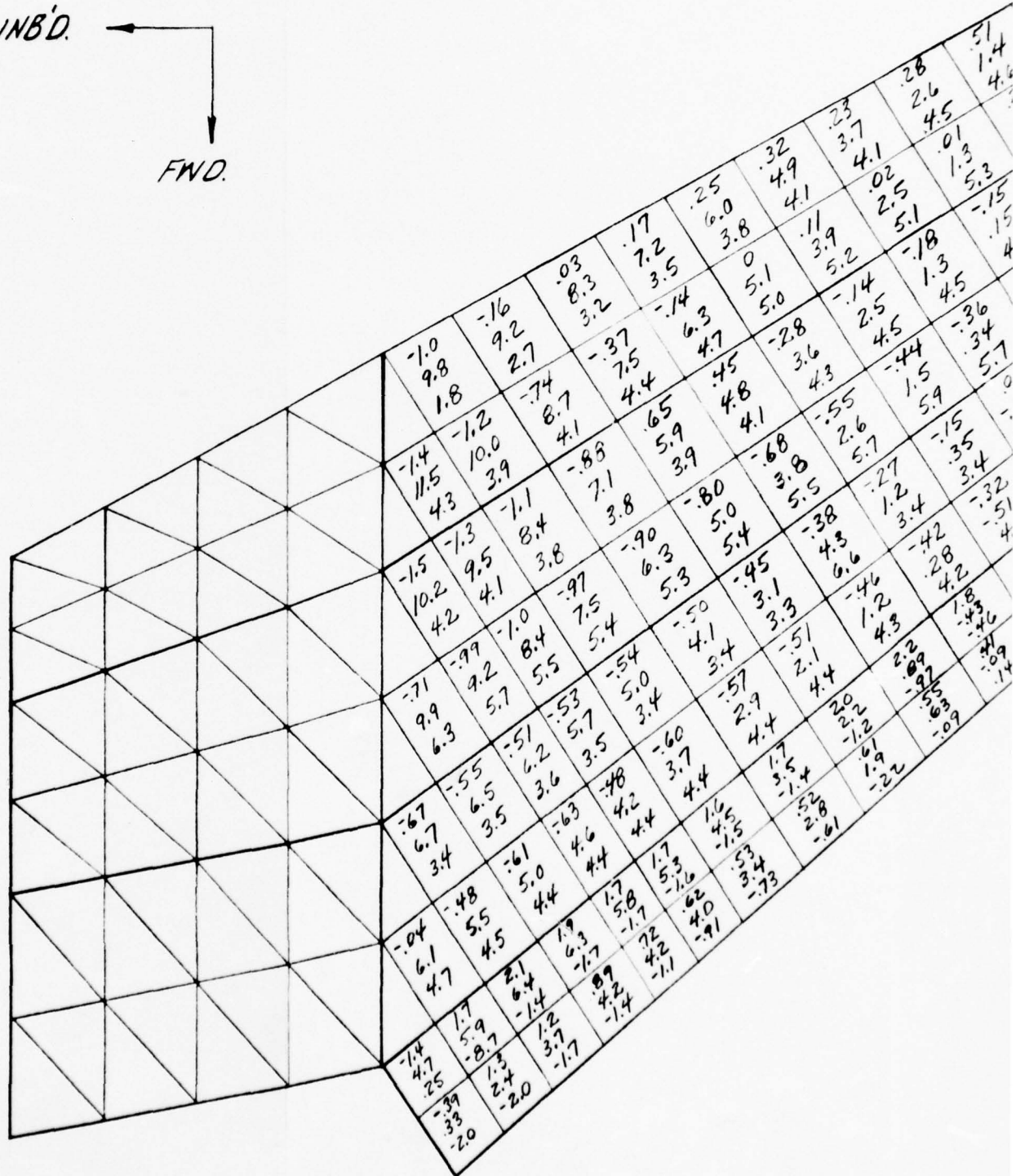
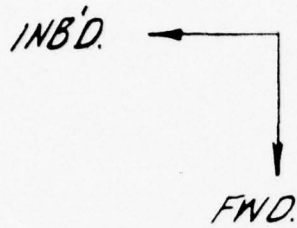


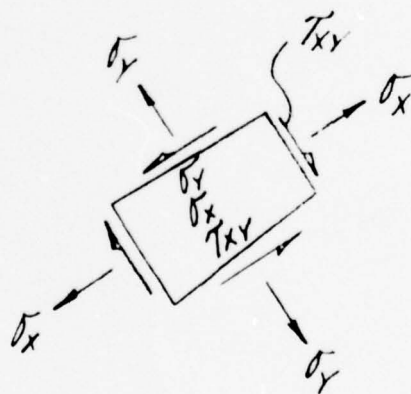
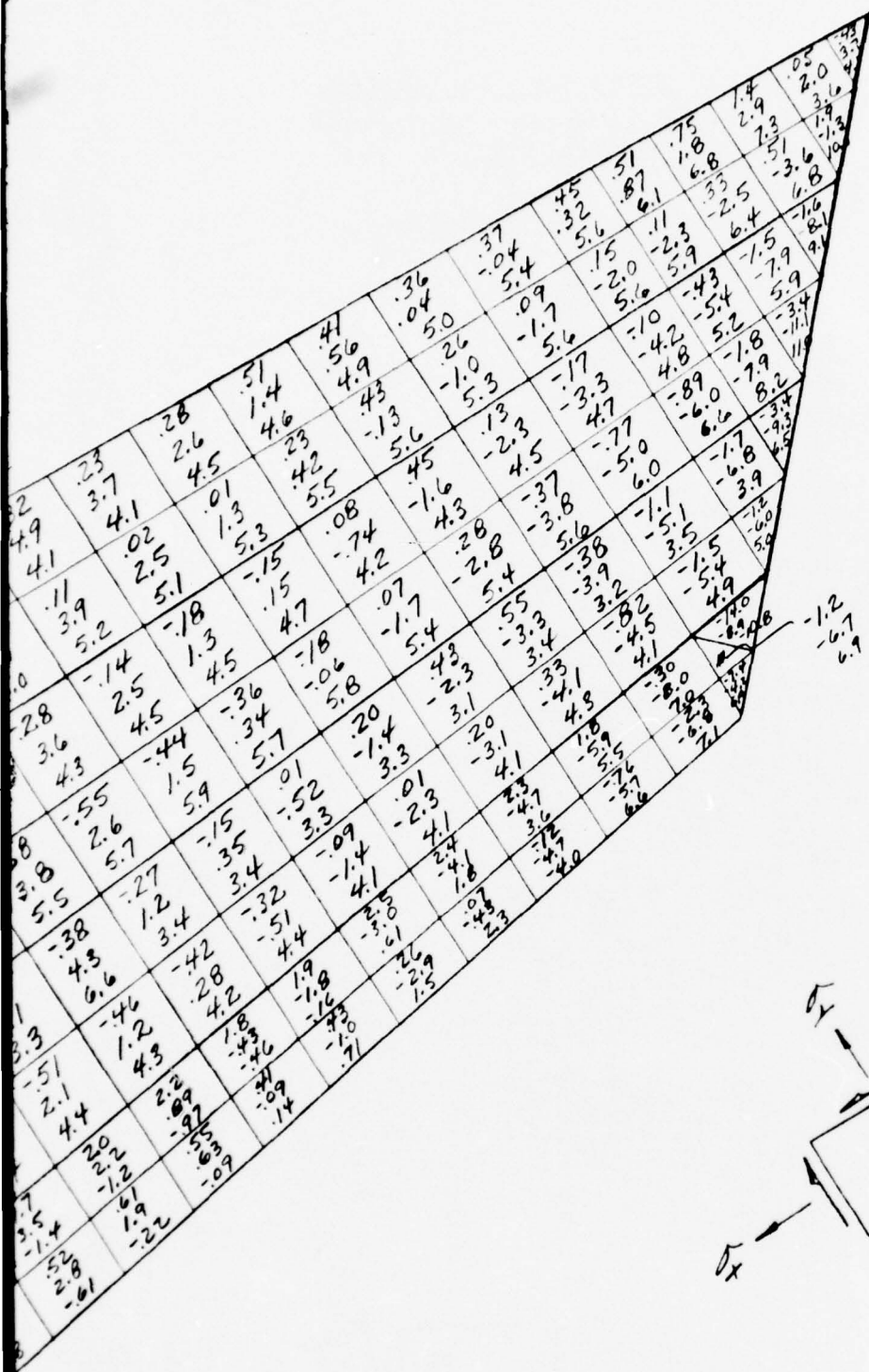


FIGURE A-10 WING LOWER COVER STRESSES

SYMMETRICAL FLIGHT CONDITION 470303  
ULTIMATE STRESSES - KSI



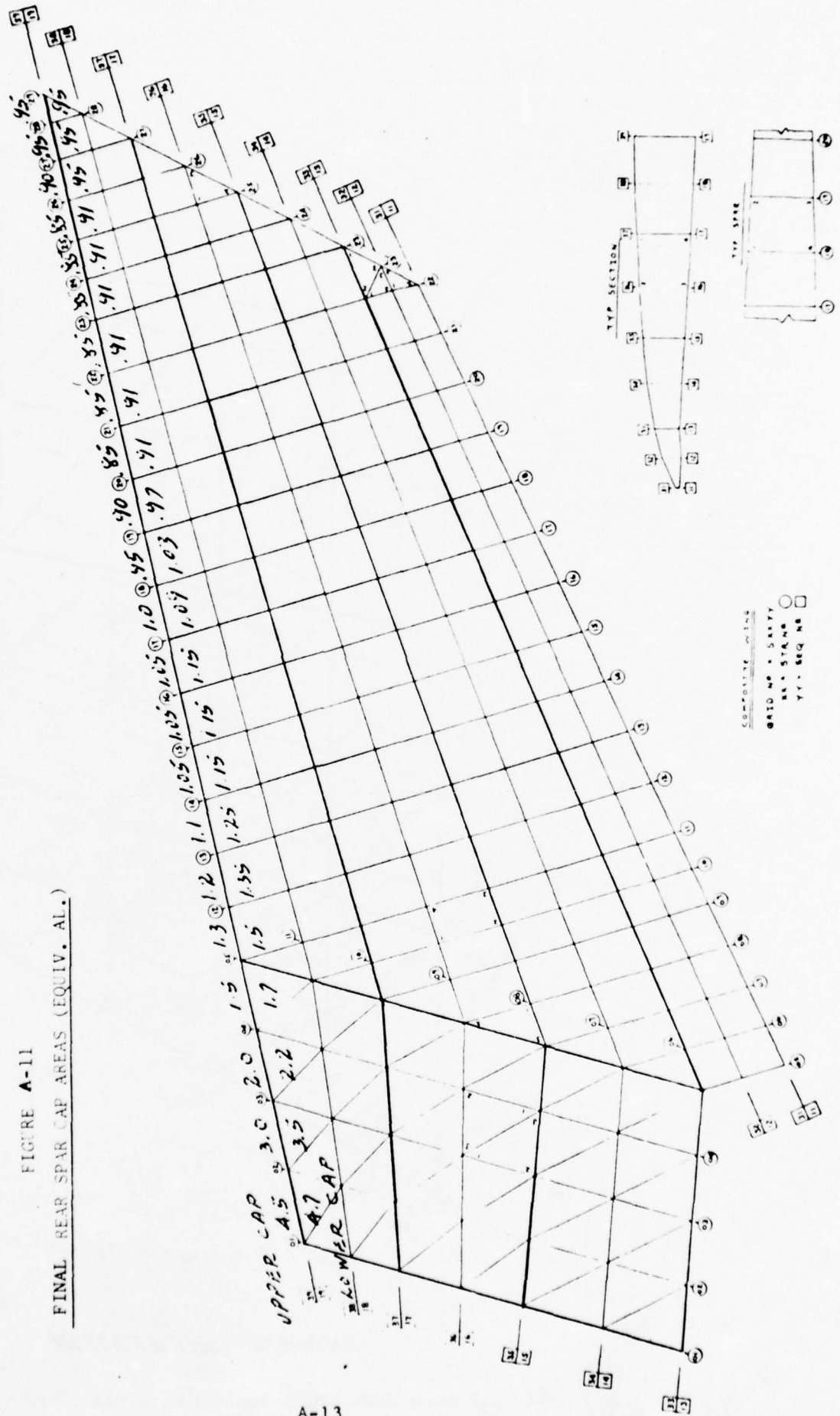


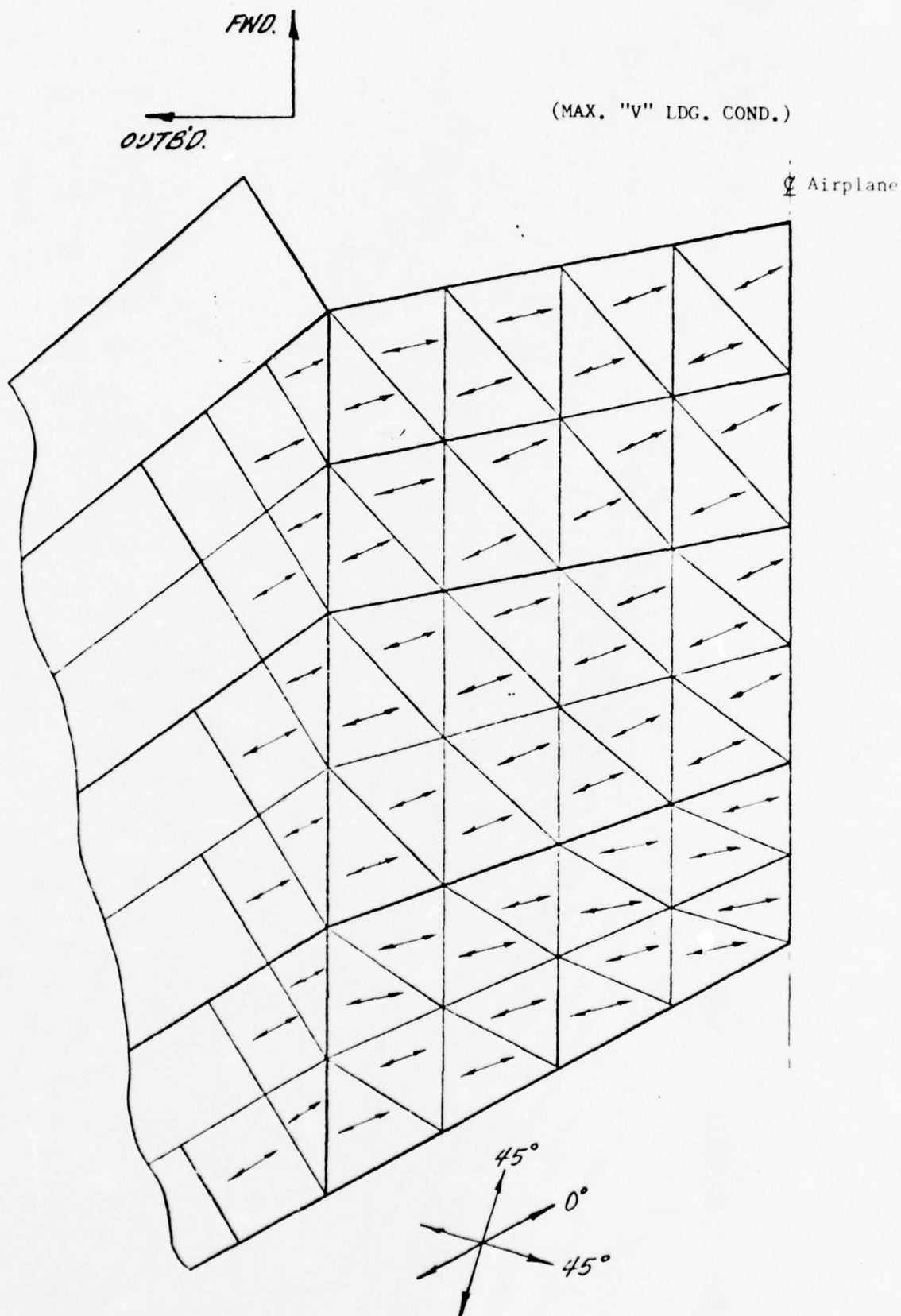


2

# NASTRAN MODEL FOR COMPOSITE WING

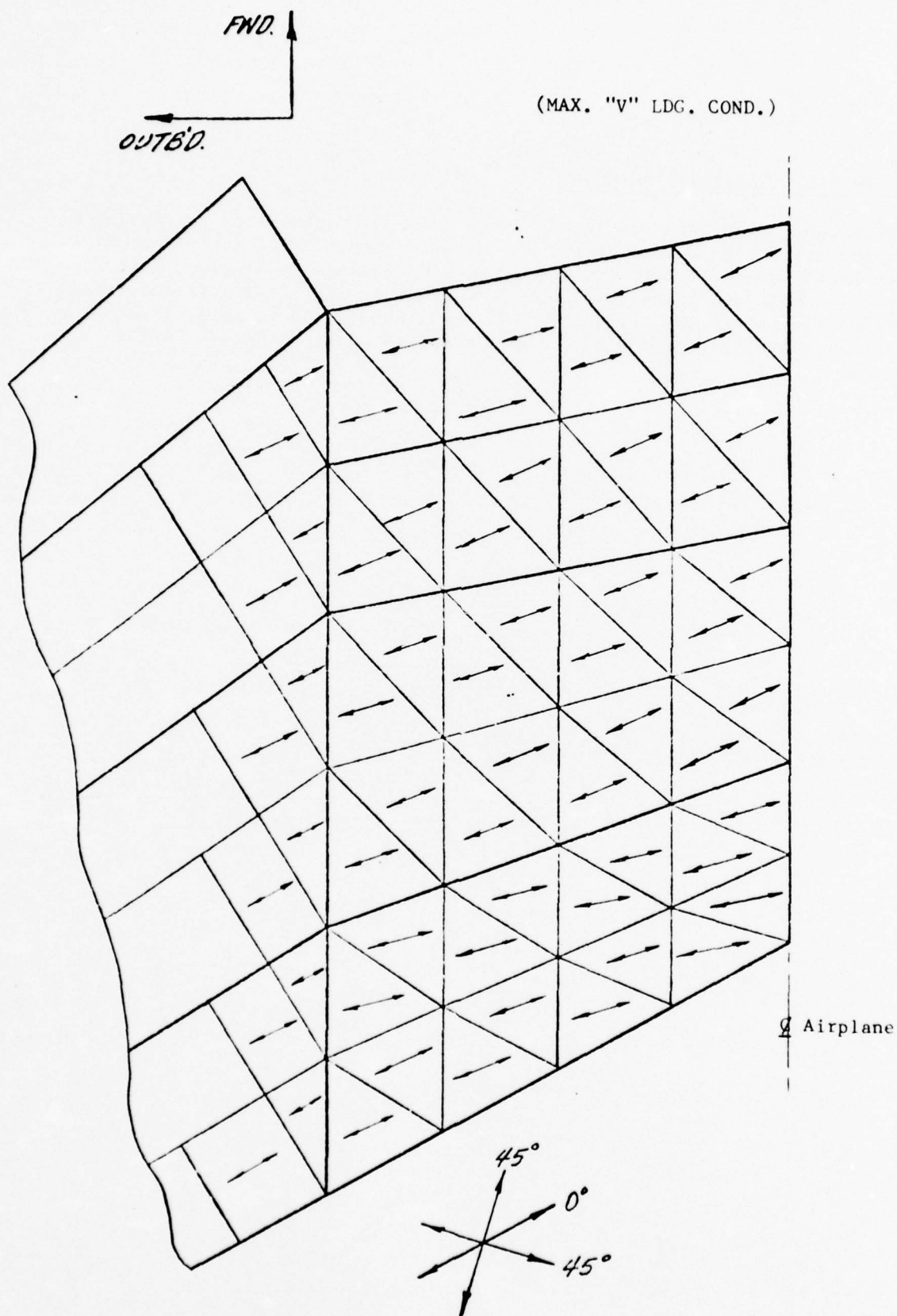
FIGURE A-11  
FINAL REAR SPAR CAP AREAS (EQUIV. AL.)





# LAMINATE ORIENTATION

FIGURE A-12 PRINCIPAL STRESS DIRECTION, UPPER COVER SKIN



### *LAMINATE ORIENTATION*

FIGURE A-13 PRINCIPAL STRESS DIRECTION, LOWER COVER SKIN

#### COVER PANEL STABILITY ANALYSIS

Cover panel stability was investigated using the methods of the Advanced Composites Design Guide and the AC5 computer program for definition of the buckling coefficient for the biaxially-loaded anisotropic critical panels. Both upper and lower covers were investigated for critical areas within the panels (K), (L), (M), (N), (O), and (P) as shown in Figure A-14. Stability analysis of these critical areas is shown on the following pages.



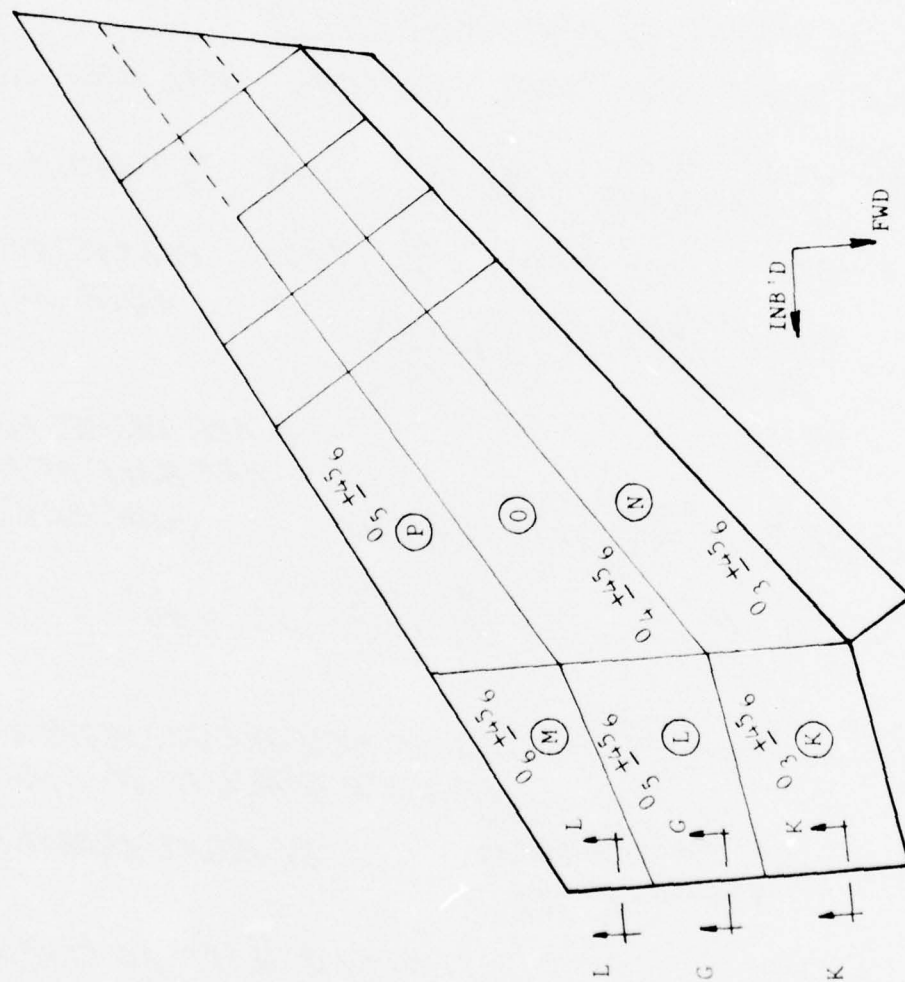


FIGURE A-14 PANEL IDENTIFICATION FOR STABILITY ANALYSIS



Columbus Aircraft Division  
Rockwell International

PREPARED BY: <u>REK</u>	REPORT NO.
CHECKED BY:	PAGE NO. OF
DATE	MODEL NO.

REF.

COMPOSITE WING UPPER COVER

CHECK PANEL (R) FOR INSTABILITY\*

MAX. VERT. LDG. COND. CRITICAL (MAX. OPER. LOADS)

$$\frac{N_y}{N_x} = \frac{-4900(.180)}{-13,000(.180)} = .38 \quad b = 21.6 \text{ IN.} \quad t_f = .090 \text{ IN.}$$

$$c = .42 \text{ IN.} \quad a = .34 \text{ IN.} \quad \frac{a}{b} = 1.57 \quad 80\% \pm 45^\circ, 20\% - 0^\circ$$

GR/EP MATL.

$$D_{11} = \frac{6.2 \times 10^6 (.090) (.42)^2}{2(.646)} \left( 1 + \frac{.090}{.42} \right)$$

$$= 92,511$$

Δ AVG. VALUES FOR  
AFT HALF OF PANEL  
(CONSERV.)

$$D_{22} = 92,511 \left( \frac{3.8 \times 10^6}{6.2 \times 10^6} \right) = 56,700$$

$$\lambda = \frac{a}{b} \sqrt{\frac{D_{22}}{D_{11}}} = 1.57 \sqrt{\frac{56,700}{92,511}} = 1.39$$

$$m = \lambda \sqrt{\frac{1 - b^2(N_y)}{\pi^2 D_{22}}} \quad \left( \text{NO. OF HALF WAVELENGTHS OF BUCKLED PANEL IN X-DIRECT.} \right)$$

$$= 1.39 \sqrt{\frac{1 - (21.6)^2(-.882)}{\pi^2 (56,700)}}$$

BI-AXIAL LOADING

$$= 1.29$$

$$\therefore m = 1.0 \text{ \& } n = 1.0 \text{ (Y-DIRECT.)}$$

FOR  $\frac{N_y}{N_x} = .38$ ,  $K_x = 2.4$  FROM AC5 COMPUTER PROGRAM

$$(N_x)_{CR} = \frac{2.4 (\pi)^2 \sqrt{92,511 (56,700)}}{(21.6)^2} = 3677 \text{ \#/IN.}$$

$$\therefore F_c = 20,426 \text{ \#/IN.}^2 \text{ ULT.}$$

ALLOW

$$M.S.D. = \frac{20,426}{13,000} - 1 = .57$$

\* SHEAR STRESS CONSIDERED NEGLIGIBLE



Columbus Aircraft Division  
Rockwell International

PREPARED BY <i>REK</i>	REPORT NO.
CHECKED BY:	PAGE NO. OF
DATE:	MODEL NO.

REF.

COMPOSITE WING UPPER COVER

CHECK PANEL ① FOR INSTABILITY\*

MAX. VERT. LDG. COND. CRITICAL (MAX. OPER. LOADS)

$$\frac{N_y}{N_x} = \frac{-5100(.204)}{-25,000(.204)} = .20 \quad b = 19.6 \text{ IN.} \quad t_f = .102 \text{ IN.}$$

$$C = .396 \text{ IN.} \quad a = 34 \quad \frac{a}{b} = 1.73 \quad 71\% \pm 45^\circ, 29\% \sim 0^\circ \text{ GR/EP MATL.}$$

$$D_{11} = \frac{7.8 \times 10^6 (.102) (.396)^2}{2(.726)} \left( 1 + \frac{.102}{.396} \right) = 108,057$$

$$D_{22} = 108,057 \left( \frac{3.9 \times 10^6}{7.8 \times 10^6} \right) = 54,029$$

$$\lambda = 1.73 \sqrt[4]{\frac{54,029}{108,057}} = 1.45$$

$$m = 1.45 \sqrt[4]{\frac{1 - (19.6)^2(-1040)}{\pi^2(54,029)}} = 1.35 \quad \therefore m = 1.0 \text{ \& } n = 1.0$$

405  
PROG.

FOR  $\frac{N_y}{N_x} = .20$ ,  $K_x = 2.68$

$$(N_x)_{CR} = \frac{2.68(\pi)^2 \sqrt{108,057(54,029)}}{(19.6)^2} = 5261 \text{ \#/IN.}$$

$$\therefore F_c = 25,789 \text{ \#/IN.}^2 \text{ ULT. ALLOW.} \quad \text{M.S.D.} = \frac{25,789}{25,000} - 1 = .03$$

Δ AVG. VALUES FOR ENTIRE PANEL

\* SHEAR STRESS CONSIDERED NEGLIGIBLE



Columbus Aircraft Division  
Rockwell International

PREPARED BY: <u>REK</u>		REPORT NO.
CHECKED BY:		PAGE NO. OF
DATE		MODEL NO.

REF.

COMPOSITE WING UPPER COVER

CHECK PANEL (M) FOR INSTABILITY\*

MAX. VERT. LDG. COND. CRITICAL (MAX. OPER. LOADS)

$$\frac{N_Y^{\Delta}}{N_X} = \frac{-5100(.216)}{-35,000(.216)} = .15 \quad b = 15.2 \text{ IN} \quad t_f = .108 \text{ IN.}$$

$$c = .384 \text{ IN.} \quad a = .34 \text{ IN.} \quad \frac{a}{b} = 2.24 \quad 67\% \pm 45^\circ, 33\% \sim 0^\circ$$

GR/EP MAT'L.

$$D_{11} = \frac{8.6 \times 10^6 (.108) (.384)^2}{2 (.758)} \left( 1 + \frac{.108}{.384} \right) = 115,750$$

$$D_{22} = 115,750 \left( \frac{3.8 \times 10^6}{8.6 \times 10^6} \right) = 51,145$$

$$\lambda = 2.24 \sqrt[4]{\frac{51,145}{115,750}} = 1.84$$

$$m = 1.84 \sqrt[4]{\frac{1 - (15.2)^2 (-1051)}{\pi^2 (51,145)}} = 1.53 \quad \therefore m = 1.0, \quad n = 1.0$$

QC5  
PROG.

FOR  $\frac{N_Y}{N_X} = .15, \quad K_X = 2.70$

$$(N_X)_{CR} = \frac{2.70 (\pi)^2 \sqrt{115,750 (51,145)}}{(15.2)^2} = 8874 \text{ #/IN.}$$

$$\therefore F_c = 41,085 \text{ #/IN.}^2 \text{ ULT.} \quad \text{M.S.} = \frac{41,085}{35,000} - 1 = .17$$

ALLOW.

\* SHEAR STRESS CONSIDERED NEGLIGIBLE  
Δ AVG. VALUES FOR ENTIRE PANEL



Columbus Aircraft Division  
Rockwell International

PREPARED BY: <u>REK</u>		REPORT NO.
CHECKED BY:		PAGE NO. OF
DATE		MODEL NO.

REF.

COMPOSITE WING UPPER COVER

CHECK PANEL (N) FOR INSTABILITY\*

MAX. VERT. LDG. COND. CRITICAL (MAX. OPER. LOADS)

$$\frac{N_y}{N_x} = \frac{-160(.180)}{-17,200(.180)} = .01 \quad b = 16 \text{ IN.} \quad t_f = .090 \text{ IN.}$$

$$c = .42 \text{ IN.} \quad a = 118 \text{ IN.} \quad \frac{a}{b} = 7.38 \quad 80\% \pm 45^\circ, 20\% \sim 0^\circ \text{ GR/EP MATL.}$$

$$\left. \begin{array}{l} D_{11} = 92,511 \\ D_{22} = 56,700 \end{array} \right\} \text{REF. PREV. CALC. FOR PANEL (R)}$$

$$\lambda = 7.38 \sqrt[4]{\frac{56,700}{92,511}} = 6.53$$

$$m = 6.53 \sqrt[4]{\frac{1 - (16)^2(-29)}{\pi^2(56,700)}} = 2.2 \quad \therefore m = 2.0 \neq n = 1.0$$

$$\text{FOR } \frac{N_y}{N_x} = .01, \quad K_x = 3.1 \text{ (CONSERV.)}$$

$$(N_x)_{cr} = \frac{3.0(\pi)^2 \sqrt{92,511(56,700)}}{(16)^2} = 8377 \text{ #/IN.}$$

$$\therefore F_c = \frac{46,539 \text{ #/IN.}^2 \text{ ULT.}}{\text{ALLOW.}} \quad M.S.U. = \frac{46,539}{17,200} - 1 = \text{HIGH}$$

\* SHEAR STRESS CONSIDERED NEGLIGIBLE  
Δ AVG OF AFT INBD. PORTION OF PANEL





Columbus Aircraft Division  
Rockwell International

PREPARED BY: <b>REK</b>		REPORT NO.
CHECKED BY:		PAGE NO. OF
DATE:		MODEL NO.

REF.

COMPOSITE WING UPPER COVER

CHECK PANEL ① FOR INSTABILITY\*

MAX. VERT. LDG. COND. CRITICAL (MAX. OPER. LOADS)

$$\frac{N_y}{N_x} = 0 \quad b = 17.5 \text{ IN.} \quad t_f = .096 \text{ IN.}$$

$$c = .408 \text{ IN.} \quad a = 117 \text{ IN.} \quad \frac{a}{b} = 6.69 \quad 75\% \pm 45^\circ, 25\% \sim 0^\circ$$

GR/EP MATL

$$D_{11} = \frac{7.0 \times 10^6 (.096) (.408)^2}{2(.6903)} \left(1 + \frac{.096}{.408}\right) = 100,090$$

$$D_{22} = 100,090 \left( \frac{3.85 \times 10^4}{7.0 \times 10^6} \right) = 55,050$$

$$m = 6.69 \sqrt[4]{\frac{55,050}{100,090}} = 5.76 \quad \text{FOR UNIAXIAL LOADING}$$

$$\therefore m = 5.0 \text{ \& } n = 1.0$$

ACS  
PROG.

$$\text{FOR } \frac{N_y}{N_x} = 0, \quad K_x = 3.0 \text{ (CONSERV.)}$$

$$(N_x)_{CR} = \frac{3.0 (\pi)^2 \sqrt{100,090 (55,050)}}{(17.5)^2} = 7177 \text{ \#/IN.}$$

$$\therefore F_c = 37,380 \text{ \#/IN.}^2 \text{ ULT. M.S.} = \frac{37,380}{29,400} - 1 = .27$$

ALLOW.

$$F_c^A = 29,400 \text{ \#/IN.}^2$$

\* SHEAR STRESS CONSIDERED NEGLIGIBLE

Δ AVG. VALUES FOR AFT INBD. PORTION OF PANEL



Columbus Aircraft Division  
Rockwell International

PREPARED BY: <u>REK</u>		REPORT NO.
CHECKED BY:		PAGE NO. OF
DATE:		MODEL NO.

REF.

COMPOSITE WING UPPER COVER

CHECK PANEL (D) FOR INSTABILITY\*

MAX. VERT. LDG. COND. CRITICAL (MAX. OPER. LOADS)

$$\frac{N_y}{N_x} \approx 0 \quad b = 16 \text{ IN.} \quad t_f = .102 \text{ IN.}$$

$$c = .396 \text{ IN.} \quad a = 116 \text{ IN.} \quad \frac{a}{b} = 7.25 \quad 71\% \pm 45^\circ, 29\% \sim 0^\circ$$

GR/EP MAT'L.

$$\left. \begin{array}{l} D_{11} = 108,057 \\ D_{22} = 54,029 \end{array} \right\} \text{REF. PREV. CALC. FOR PANEL (D)}$$

$$m = 7.25 \sqrt{\frac{54,029}{108,057}} = 6.10$$

$$\therefore m = 6.0 \text{ \& } n = 1.0$$

$$\text{FOR } \frac{N_y}{N_x} = 0, K_x = 2.9$$

$$(N_x)_{cr} = \frac{2.9 (\pi)^2 \sqrt{108,057 (54,029)}}{(16)^2} = 8542 \text{ \# / IN.}$$

$$\therefore F_c = 41,873 \text{ \# / IN.}^2$$

ALLOW.

$$M.S.D. = \frac{41,873}{36,500} - 1 = .14$$

$$f_c^A = 36,500 \text{ \# / IN.}^2$$

\* SHEAR STRESS CONSIDERED NEGLIGIBLE  
A AVG. VALUES



Columbus Aircraft Division  
Rockwell International

PREPARED BY: <i>REK</i>		REPORT NO.
CHECKED BY:		PAGE NO. OF
DATE:		MODEL NO.

REF.

COMPOSITE WING LOWER COVER

CHECK PANEL (K) FOR INSTABILITY\*

ASSUME DOWNBENDING STRESSES SAME AS 40%  
OF UPBENDING STRESSES FOR SYMM. FLT. COND. 470303  
(ULT. LOADS)

$$N_y^A = 1420(.180)(.40) = 102 \text{ \#/IN. (TENS.)} \quad b = 21.6 \text{ IN. } t_f = .090$$

$$N_x^A = -12,750(.180)(.40) = -918 \text{ \#/IN.} \quad c = .22 \text{ IN.}$$

$$a = 34 \text{ IN.} \quad \frac{a}{b} = 1.57 \quad 80\% \pm 45^\circ, 20\% \sim 0^\circ \text{ GR/EP}$$

SINCE  $N_y$  IS TENSION LOAD, THE PANEL LOADING  
WILL BE CONSIDERED AS UNIAXIAL -

$$D_{11} = \frac{6.2 \times 10^6 (.090)(.22)^2}{2(.646)} \left(1 + \frac{.090}{.22}\right) = 29,455$$

$$D_{22} = 29,455 \left( \frac{3.8 \times 10^6}{6.2 \times 10^6} \right) = 18,053$$

$$m = \frac{a}{b} \sqrt{\frac{D_{22}}{D_{11}}} = 1.57 \sqrt{\frac{18,053}{29,455}} = 1.39$$

$$\therefore m = 1.0 \neq n = 1.0$$

4C5  
PROG.

FOR  $\frac{N_y}{N_x} = 0$ ,  $K_x = 4.2$  (CONSERV.)

$$(N_x)_{cr} = \frac{4.2(\pi)^2 \sqrt{29,455(18,053)}}{(21.6)^2} = 2049 \text{ \#/IN.}$$

$$M.S.U. = \frac{2049}{918} - 1 = \underline{\underline{HIGH}}$$

\* SHEAR STRESS CONSIDERED NEGLIGIBLE

Δ AVG. VALUES



Columbus Aircraft Division  
Rockwell International

PREPARED BY: <b>REK</b>		REPORT NO.
CHECKED BY:		PAGE NO. OF
DATE:		MODEL NO.

REF.

COMPOSITE WING LOWER COVER

CHECK PANEL ④ FOR INSTABILITY\*

REF. PANEL ④ FOR ASSUMED LOADING FOR  
DOWNBENDING COND. ~ (ULT. LOADS)

$$N_y^A = 1130(.204)(.40) = 92 \text{ \#/IN. (TENS.) } b = 19.6 \text{ IN.}$$

$$N_x^A = -16,700(.204)(.40) = -1363 \text{ \#/IN. } t_f = .102 \text{ IN.}$$

$$a = 34 \text{ IN. } \frac{a}{b} = 1.73 \quad c = .196 \text{ IN. } 71\% \pm 45^\circ, 29\% \sim 0^\circ$$

GRIEP MATL.

SINCE  $N_y$  IS TENSION LOAD, THE PANEL LOADING  
WILL BE CONSIDERED AS UNIAXIAL ~

$$D_{11} = \frac{7.8 \times 10^6 (.102)(.196)^2}{2(.726)} \left(1 + \frac{.102}{.196}\right) = 32,004$$

$$D_{22} = 32,004 \left(\frac{3.9 \times 10^6}{7.8 \times 10^6}\right) = 16,002$$

$$m = 1.73 \sqrt[4]{\frac{16,002}{32,004}} = 1.45$$

$$\therefore m = 1.0 \neq n = 1.0$$

$$\text{FOR } \frac{N_y}{N_x} = 0, \quad K_x = 3.45 \text{ (CONSERV.)}$$

ACS  
PROG.

$$(N_x)_{cr} = \frac{3.45 (\pi)^2 \sqrt{32,004(16,002)}}{(19.6)^2} = 2006 \text{ \#/IN.}$$

$$M.S.U. = \frac{2006}{1363} - 1 = .47$$

\* SHEAR STRESS CONSIDERED NEGLIGIBLE  
Δ AVG. VALUES





Columbus Aircraft Division  
Rockwell International

PREPARED BY: <u>REK</u>		REPORT NO.
CHECKED BY:		PAGE NO. OF
DATE:		MODEL NO.

REF.

COMPOSITE WING LOWER COVER

CHECK PANEL (M) FOR INSTABILITY\*

REF. PANEL (R) FOR ASSUMED LOADING FOR  
DOWNBENDING COND. - (ULT. LOADS)

$$N_Y^a = -806(.216)(.40) = -70 \#/\text{IN.} \quad \therefore \frac{N_Y}{N_X} = .04$$

$$N_X = -19,000(.216)(.40) = -1642 \#/\text{IN.}$$

SINCE  $\frac{N_Y}{N_X} \approx 0$  CONSIDER AS UNIAXIAL LOADING

$$b = 15.2 \text{ IN.} \quad t_f = .108 \text{ IN.} \quad c = .184 \text{ IN.} \quad a = 34 \text{ IN.}$$

$$\frac{a}{b} = 2.24 \quad 67\% \pm 45^\circ, 33\% \sim 0^\circ \text{ GR/EP}$$

$$D_{11} = \frac{8.6 \times 10^6 (.108)(.184)^2}{2(.758)} \left( 1 + \frac{.108}{.184} \right) = 32,917$$

$$D_{22} = 32,917 \left( \frac{3.8 \times 10^6}{8.6 \times 10^6} \right) = 14,545$$

$$m = 2.24 \sqrt[4]{\frac{14,545}{32,917}} = 1.83$$

$$\therefore m = 1.0 \text{ \& } n = 1.0$$

QCS  
PROG.

$$\text{FOR } \frac{N_Y}{N_X} = 0, \quad K_X = 3.2 \text{ (CONSERV.)}$$

$$(N_X)_{CR} = \frac{3.2(\pi)^2 \sqrt{32,917(14,545)}}{(15.2)^2} = 2991 \#/\text{IN.}$$

$$\text{M.S.} = \frac{2991}{1642} - 1 = \underline{\underline{.82}}$$





Columbus Aircraft Division  
Rockwell International

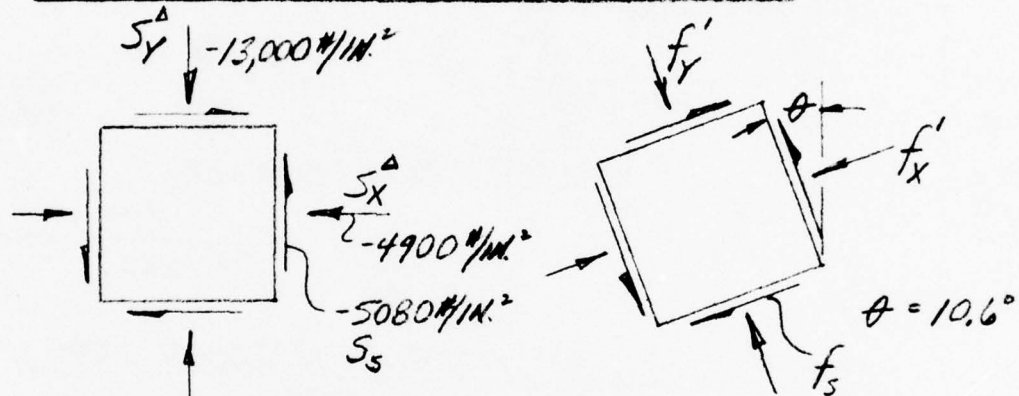
PREPARED BY: <i>REK</i>	REPORT NO.
CHECKED BY:	PAGE NO. OF
DATE:	MODEL NO.

REF.

COMPOSITE WING UPPER COVER

CHECK PANEL (B) FOR INSTABILITY UTILIZING NASTRAN STRESSES\* REORIENTED INTO PANEL AXIS

MECHS.  
OF  
MATHS.  
LAURSON  
& COX  
PGS.  
267 &  
268



$$f'_s = \left[ \frac{S_x - S_y}{2} \right] \sin 2\theta + S_s \cos 2\theta \quad (\text{MAX. VERT. LOG. COND.})$$

$$= \left[ \frac{-4900 + 13,000}{2} \right] \sin 21.2^\circ - 5080 \cos 21.2^\circ$$

$$= -3272 \text{ #/in.}^2$$

$$f'_x = \frac{S_x + S_y}{2} + \left[ \frac{S_x - S_y}{2} \right] \cos 2\theta - S_s \sin 2\theta$$

$$= \left[ \frac{-4900 - 13,000}{2} \right] + \left[ \frac{-4900 + 13,000}{2} \right] \cos 21.2^\circ + 5080 \sin 21.2^\circ$$

$$= -3337 \text{ #/in.}^2$$

$$f'_y = \frac{S_x + S_y}{2} + \left[ \frac{S_x - S_y}{2} \right] \cos 2\theta - S_s \sin 2\theta$$

$$= \left[ \frac{-4900 - 13,000}{2} \right] + \left[ \frac{-4900 + 13,000}{2} \right] \cos 201.2^\circ + 5080 \sin 201.2^\circ$$

$$= -14,563 \text{ #/in.}^2 \quad (\theta_1 = \theta + 90^\circ)$$

$\Delta f_x$  REIDENTIFIED AS ALGEBRAICALLY LARGER OF BIAXIAL STRESSES  
\* AVE. VALUES FOR AFT HALF OF PANEL (CONSERV.)



Columbus Aircraft Division  
Rockwell International

PREPARED BY: <u>REK</u>		REPORT NO.
CHECKED BY:		PAGE NO. OF
DATE:		MODEL NO.

REF.

COMPOSITE WING UPPER COVER

CHECK OF PANEL ① WITH REORIENTED NASTRAN STRESSES (CONT'D.)

ACS  
PROG.

PREV.  
CALC.  
FOR  
①

$$\frac{N_y}{N_x} = \frac{-3511(.180)}{-14,563(.180)} = .24 \quad K_x = 2.9$$

$$(N_x)_{CR} = \frac{2.9(3677)}{2.4} = 4443 \text{ \#/IN. ULT.}$$

$$M.S.D. = \frac{4443}{2622} - 1 = .69$$

CHECK PANEL ② UTILIZING NASTRAN STRESSES\*  
REORIENTED INTO PANEL AXIS

$$S_y^A = -25,000 \text{ \#/IN.}^2 \quad S_x^A = -5100 \text{ \#/IN.}^2 \quad S_z = -7270 \text{ \#/IN.}^2$$

$$\theta = 15.4^\circ \quad \theta_1 = 90 + 15.4 = 105.4^\circ$$

$$f'_s = \left[ \frac{-5100 + 25,000}{2} \right] \sin 30.8^\circ - 7270 \cos 30.8^\circ = -1150 \text{ \#/IN.}^2$$

$$f'_x = \left[ \frac{-5100 - 25,000}{2} \right] + \left[ \frac{-5100 + 25,000}{2} \right] \cos 30.8^\circ + 7270 \sin 30.8^\circ$$

$$= -2781 \text{ \#/IN.}^2$$

$$f'_y = \left[ \frac{-5100 - 25,000}{2} \right] + \left[ \frac{-5100 + 25,000}{2} \right] \cos 210.8^\circ + 7270 \sin 210.8^\circ$$

$$= -27,319 \text{ \#/IN.}^2$$

ACS  
PROG.

PREV.  
CALC.  
FOR  
②

$$\frac{N_y}{N_x} = \frac{-2781(.204)}{-27,319(.204)} = .10 \quad K_x = 3.2$$

$$(N_x)_{CR} = \frac{3.2}{2.68} (5261) = 6282 \text{ \#/IN. ULT.}$$

$$M.S.D. = \frac{6282}{5573} - 1 = .12$$

\*  $\Delta f_x$  REIDENTIFIED AS ALGEBRAICALLY LARGER OF BIAXIAL STRESSES  
\* AVG. VALUES FOR PANEL



Columbus Aircraft Division  
Rockwell International

PREPARED BY: <u>REK</u>		REPORT NO.
CHECKED BY:		PAGE NO. OF
DATE:		MODEL NO.

REF.

COMPOSITE WING UPPER COVER

CHECK PANEL (M) FOR REORIENTED NASTRAN STRESSES\*

$$S_y^A = -35,000 \text{ #/IN.}^2, S_x^A = -5100 \text{ #/IN.}^2, S_s = -9213 \text{ #/IN.}^2$$

$$\theta = 24.7^\circ \quad \theta_1 = 90 + 24.7 = 114.7^\circ$$

$$f_s' = \left[ \frac{-5100 + 35,000}{2} \right] \sin 49.4^\circ - 9213 \cos 49.4^\circ = 5356 \text{ #/IN.}^2$$

$$f_x' = \left[ \frac{-5100 - 35,000}{2} \right] + \left[ \frac{-5100 + 35,000}{2} \right] \cos 49.4^\circ + 9213 \sin 49.4^\circ$$

$$= -3326 \text{ #/IN.}^2$$

$$f_y' = \left[ \frac{-5100 - 35,000}{2} \right] + \left[ \frac{-5100 + 35,000}{2} \right] \cos 229.4^\circ + 9213 \sin 229.4^\circ$$

$$= -36,774 \text{ #/IN.}^2$$

QC5  
PROG.

$$\frac{N_y}{N_x} = \frac{-3326 (.216)}{-36,774 (.216)} = .09 \quad K_x = 3.0$$

$$(N_x)_{CR} = \frac{3.0}{2.7} (8874) = 9860 \text{ #/IN. ULT.}$$

$$M.S.D. = \frac{9860}{7943} - 1 = .24$$

\* AVG. VALUE FOR PANEL  
 $\Delta f_x$  REIDENTIFIED AS ALGEBRAICALLY LARGER OF  
BIAXIAL STRESSES

#### WING SPAR SHEAR FLOWS

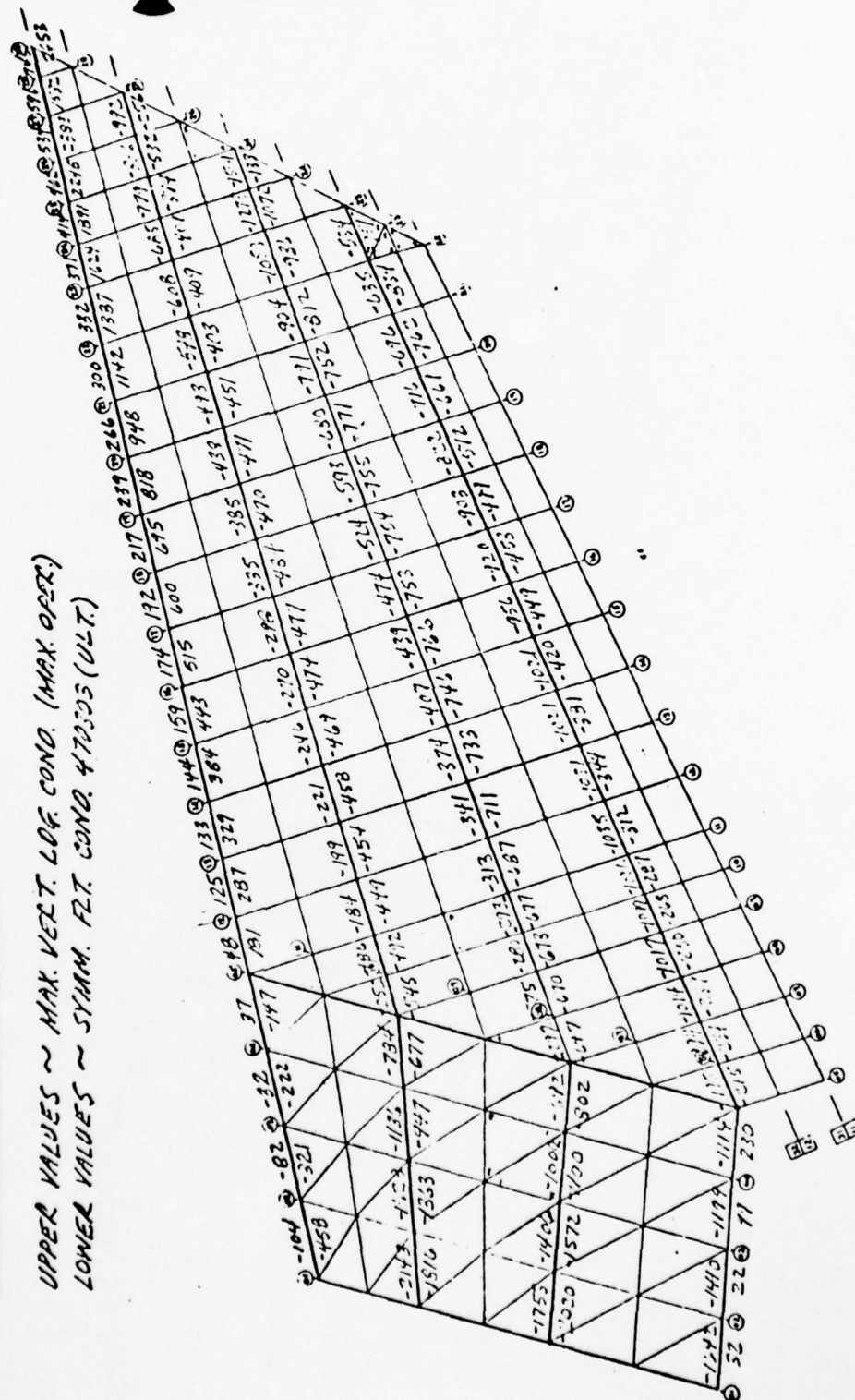
Two figures are presented to illustrate the wing spar web shear flow distribution as defined by the NASTRAN computer analysis. Figure A-15 shows the spar web shear flows for both the MAX. VERTICAL LANDING CONDITION and the critical symmetrical flight condition based on the original spar cap areas. The updated spar web shear flows for the MAX. VERTICAL LANDING CONDITION are shown in Figure A-16 based on the increased spar cap areas of the final configuration.





WING SPAR SHEAR FLOWS (N/IN)

UPPER VALUES ~ MAX. VERT. LOG. COND. (MAX. OPER.)  
LOWER VALUES ~ SYMM. FLT. COND. 47355 (ULT.)







#### FREE BODY DIAGRAMS

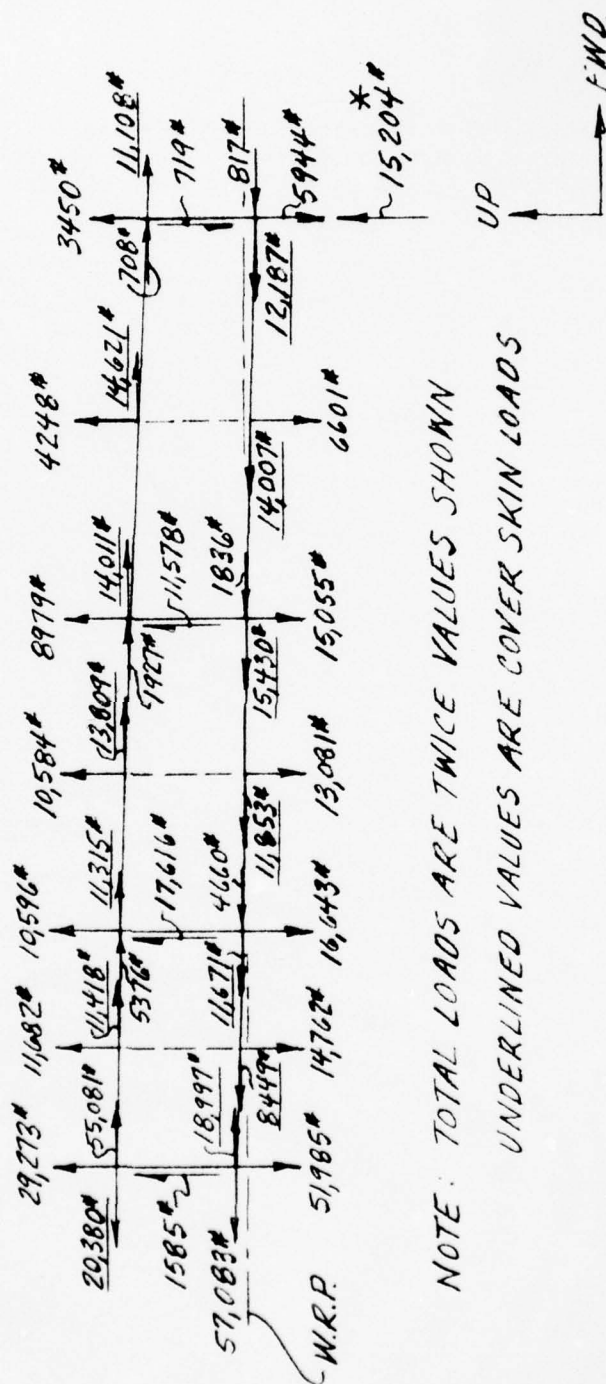
Free body diagrams are presented in Figures A-17, A-18, and A-19 for the centerline rib, B.P. 33.93 rib, and inboard end of the rear spar, respectively. The free body diagrams were obtained by utilizing the NASTRAN internal loads program, level 15.9.

FIGURE A-17

# FREE BODY DIAGRAM OF CENTERLINE RIB

NASTRAN EXTERNAL GRID POINT FORCES PER SIDE <sup>Δ</sup>

MAX. VERT. LANDING COND. ~ MAX OPER LOS.



AD-A041 208

ROCKWELL INTERNATIONAL. COLUMBUS OHIO COLUMBUS AIRCRA--ETC F/G 11/4  
EVALUATION OF COMPOSITE WING FOR XFV-12A AIRPLANE.(U)

DEC 76 D N ULRY, R W GEHRING, K J CLAYTON

N62269-74-C-0577

UNCLASSIFIED

NR76H-135

NADC-77183-30

NL

3 OF 4  
AD  
A041208

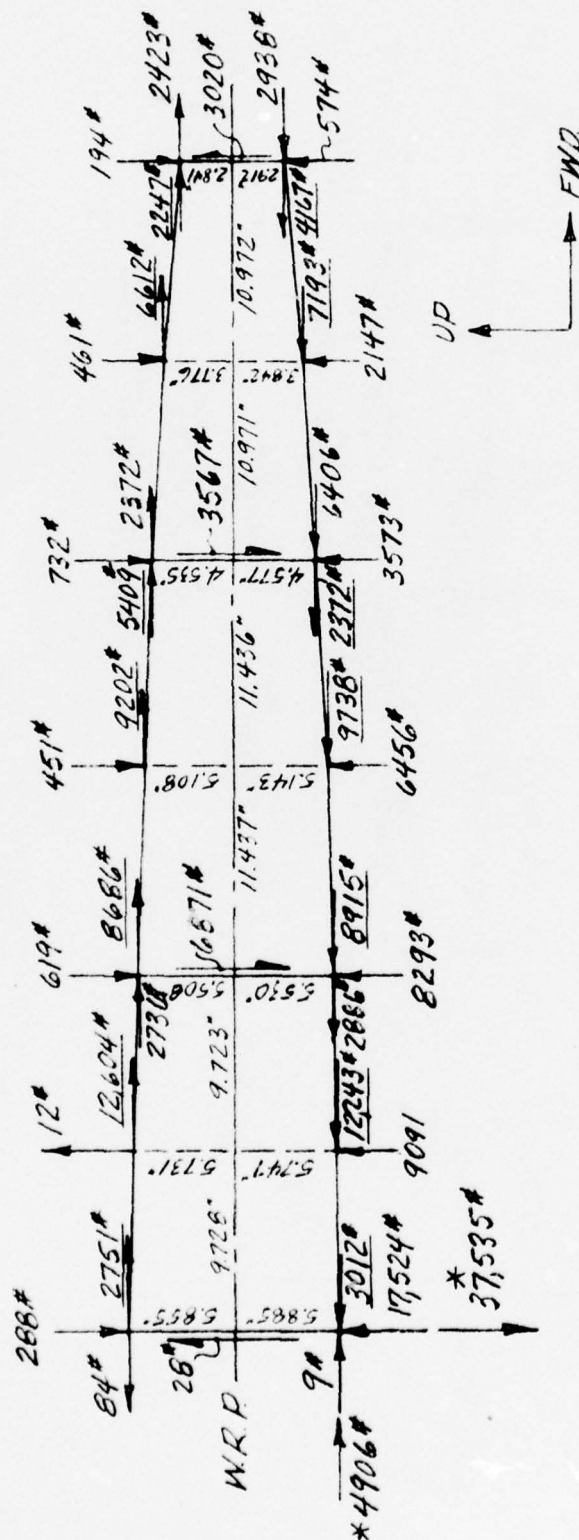


FIGURE A-15

FREE BODY DIAGRAM OF B.P. 33.93 RIB

NASTRAN EXTERNAL GRID POINT FORCES<sup>A</sup>

MAX. VERT. LANDING COND. MAX. OPER. LDS.



NOTE: UNDERLINED VALUES ARE COVER SKIN LOADS

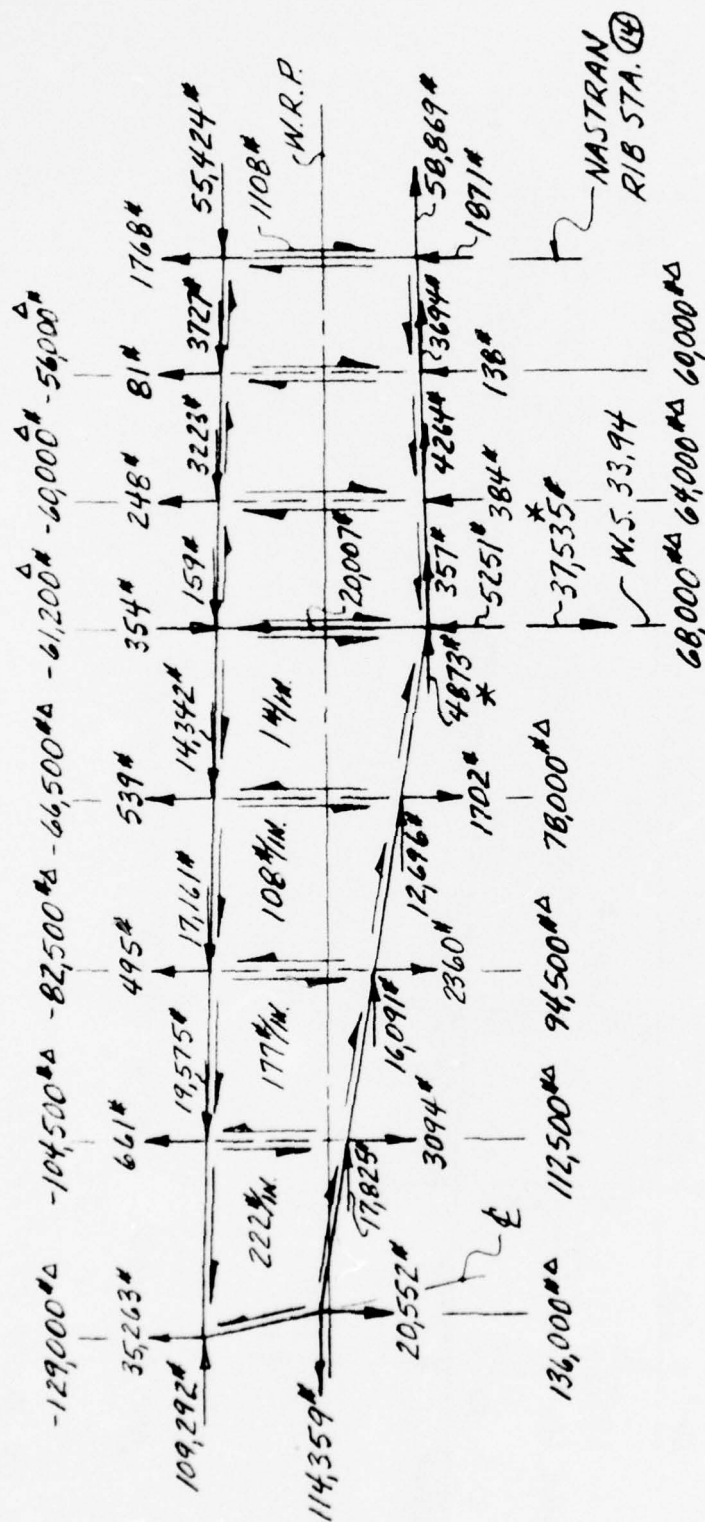
Δ WING REF. SYSTEM

\* AFT WING-TO-FUS. ATTACH LDS.



FREE BODY DIAGRAM OF REAR SPAR

NASTRAN EXTERNAL GRID POINT FORCES (REAR SPAR REF SYS.)



\* AFT WING-TO-FUS. ATTACH. LOADS

$\Delta$  INTERPOLATED SPAR CAP AXIAL LOADS

MAX. VERT. LOG. COND. ~ MAX. OPER. LOS.

#### WING SPAR ANALYSIS

Analysis of critical spar areas is shown on the following pages and includes skin attachment to the fwd spar, fwd spar upper cap, upper skin attachment to fwd intermediate spar, and lower skin attachment to fwd intermediate spar.



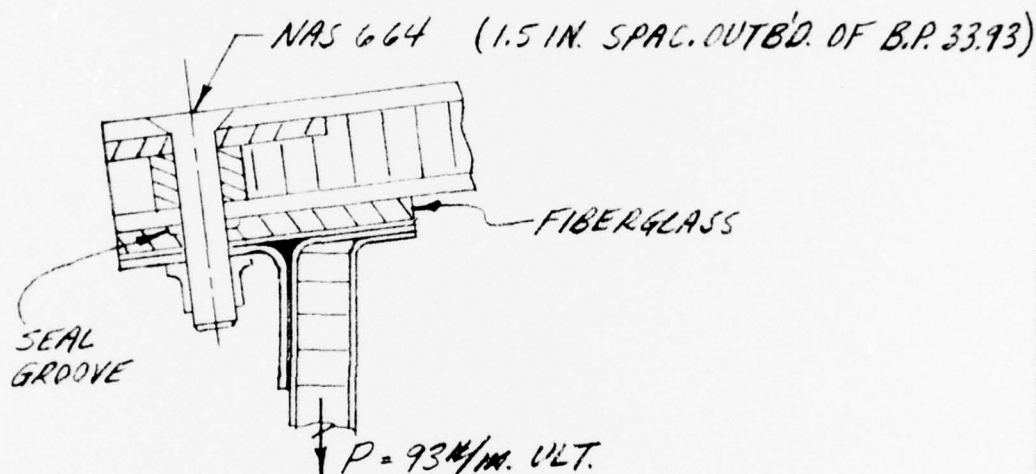
Columbus Aircraft Division  
Rockwell International

PREPARED BY: <u>REK</u>	REPORT NO.
CHECKED BY:	PAGE NO. OF
DATE	MODEL NO.

REF.

COMPOSITE WING FWD. SPAR

CHECK SKIN ATTACH. @ FWD. SPAR



LOADS @ NASTRAN RIB STA. (11) ~ SYMM. FLT. COND.

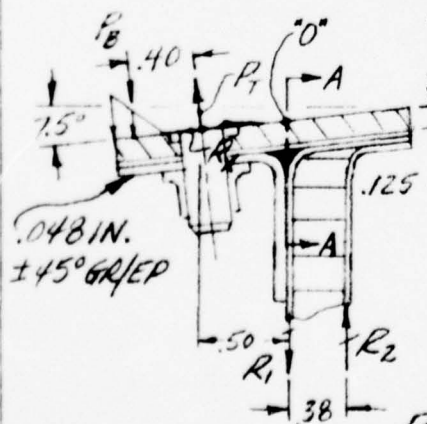
ASSUME INTERN. PRESS. = 9#/IN.<sup>2</sup> ULT. 470303

AERODYNAMIC LOADING + INTERN. LOADS = 21#/IN. ULT.  
(CONSERV.)

FWD. CHORDWISE SPAN = 16 IN.

TOTAL RUNNING LOAD = 21 + .50(16)(9) = 93#/IN. ULT.

CALC. LOS. BASED ON 1.50 FASTENER SPAC.



ASSUME 25% END FIXITY @ ATTACH.  
BETWEEN UPPER COVER SKIN &  
FWD. SPAR UPPER CAP ~

$$P_B = \frac{.25(1.5)(93)(.50)^2}{.40} = 20\#$$

$$P_T = 20 + 1.5(93) = 160\#$$

$$M_{A-A} = 1.5(93)(.50) - .25(1.5)(93)(.50)^2 = 61\#$$

$$R_2 = \frac{61}{.38} = 161\# \quad R_1 = 161 + 1.5(93) = 301\#$$



Columbus Aircraft Division  
Rockwell International

PREPARED BY: <u>REK</u>		REPORT NO.
CHECKED BY:		PAGE NO. OF
DATE:		MODEL NO.

REF.

COMPOSITE WING FWD. SPAR

CHECK OF FWD. SPAR UPPER CAP (CONTD.)

CHECK BENDING @ SECT. A-A ~ (ULT. LOADS)

NEGLECT .048 IN.  $\pm 45^\circ$  GR/EP ANGLE & ASSUME .50 IN EFFECTIVE WIDTH ~

$$f_b = \frac{6(61)}{.50(.125)^2} = 46,848 \text{ #/IN.}^2$$

MIL-  
HDBK-  
17

$$F_{bu} = 83,500 \text{ #/IN.}^2$$

$$M.S.U. = \frac{83,500}{46,848} - 1 = .78$$

CHECK NAS 664 IN UPPER CAP ~  
(.062 IN. DEEP SEAL GROOVE)

MIL-  
HDBK-  
17  
COMP  
MAN.

$$F_{brg} = 54,100 \text{ #/IN.}^2$$

FIBERGLASS

$$F_{arg} = 110,000 \text{ #/IN.}^2$$

GR/EP

$\therefore$  ULT. BRG. ALLOW./FASTENER ~

$$P_{ALLOW.} = .048(.25)(110,000) + .0625(.25)(54,100) = 2165 \text{ #}$$

$$q_{max} = 1035 \text{ #/IN. OUTED. OF B.P. 33.93} \quad M.S.U. = \frac{2165}{1.5(1035)} - 1 = .39$$

CHECK ADHESIVE FILLET AREA ~

MACDAG  
TESTS

LOCAL JOINT ALLOW. = 973 #/IN. ULT.

APPLIED LD. = 301 #

$$M.S.U. = \frac{973(.50)}{301} - 1 = .61$$

LOCAL SPAR WEB TENS. LOAD ~ (ASSUME .50 IN. EFFECT. WIDTH)

$$f_t = \frac{301}{.50(.048)} = 12,542 \text{ #/IN.}^2 \text{ (CONSERV.)}$$

COMP.  
MAN.

$$F_{tu} = 23,200 \text{ #/IN.}^2 \pm 45^\circ \text{ H.S. GR/EP} \quad M.S.U. = \frac{23,200}{12,542} - 1 = .84$$





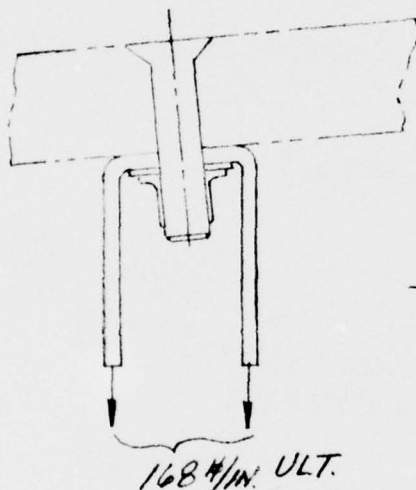
Columbus Aircraft Division  
Rockwell International

PREPARED BY: <i>REK</i>		REPORT NO.
CHECKED BY:		PAGE NO. OF
DATE:		MODEL NO.

REF.

COMPOSITE WING FWD. INTERM. SPAR

UPPER SKIN ATTACH. OUTBD. OF B.P. 33.93 RIB



LOADS @ NASTRAN RIB STA. ⑪

168 #/IN. ULT.

CALC. LOADS BASED ON SYMM. FLT. COND. 470303  
TRANSVERSE SPAR WEB LOADS COMBINED WITH  
INTERNAL PRESS. + AERODYNAMIC PRESS.

INTERN. PRESS. = 6 #/IN. LIMIT.

ASSUME UPPER COVER PRESS. LOADS DISTRIBUTED TO  
SPARS BY SIMPLY SUPPORTED BEAMS

FWD. SPAN = 16 IN. AFT SPAN = 18 IN.

NASTRAN  
RUN

AERODYNAMIC LOADING + INTERNAL LOADING = 15 #/IN. ULT.

TOTAL RUNNING LOAD =  $15 + .50(16 + 18)(6) = 168 \text{ #/IN. ULT.}$





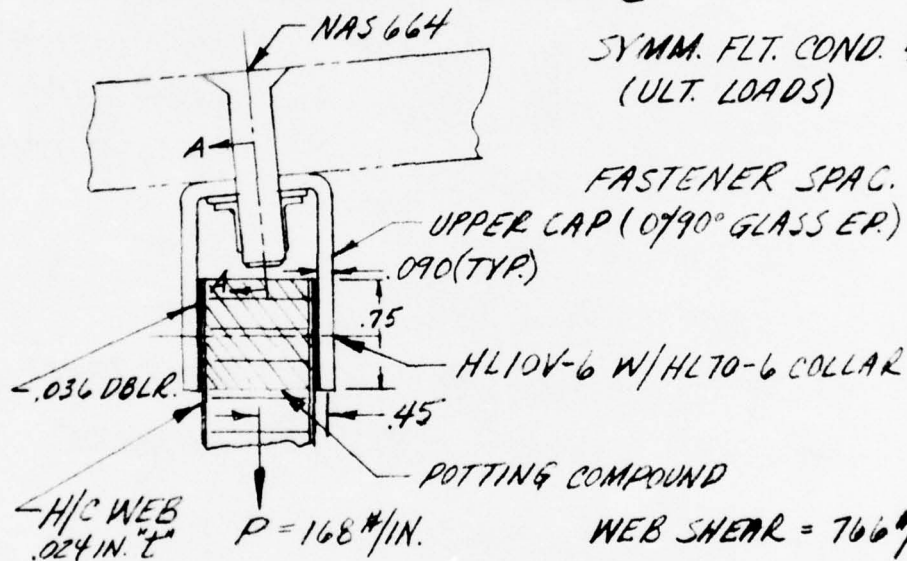
Columbus Aircraft Division  
Rockwell International

PREPARED BY: <i>REK</i>	REPORT NO.
CHECKED BY:	PAGE NO. OF
DATE:	MODEL NO.

REF.

COMPOSITE WING FWD. INTERM. SPAR  
UPPER SKIN ATTACH. OUTBD. OF B.P. 33.93 RIB

LOADS @ NASTRAN RIB STA. ⑪ ~



SYMM. FLT. COND. 470303  
(ULT. LOADS)

FASTENER SPAC. = 1.5 IN.

UPPER CAP (0°/90° GLASS EP.)

.090 (TYP.)

.75

H/L10V-6 W/ H/L70-6 COLLAR

.45

POTTING COMPOUND

H/C WEB  
.024 IN. THK

$P = 168 \text{ \#/IN.}$

WEB SHEAR =  $766 \text{ \#/IN.}$

CHECK BENDING @ SECT. A-A ~

(ASSUME 50% END FIXITY @ ATTACH. TO H/C WEB)

$$M_{A-A} = 168(.75)(.50)(.45)(1.5) = 42.5 \text{ \#}$$

ASSUME .50 IN. EFFECT. WIDTH (NEGLECT RETAINER STRIP)

$$f_{bt} = \frac{6(42.5)}{.50(.090)^2} = 62,963 \text{ \#/IN.}^2$$

MATL. ~ GLASS EPOXY PREPREG. FABRIC

$$F_{80} = 83,500 \text{ \#/IN.}^2$$

$$M.S.U. = \frac{83,500}{62,963} - 1 = .32$$

CHECK NAS 664 SHEAR ALLOW. IN UPPER CAP ~

$$f_{bsg} = \frac{1.5(766)}{.25(.090)} = 51,067 \text{ \#/IN.}^2 \quad F_{80} = 54,100 \text{ \#/IN.}^2 \quad M.S.U. = \frac{54,100}{51,067} - 1 = .05$$

MIL-  
HDBK-  
17  
Pg.  
4-51



Columbus Aircraft Division  
Rockwell International

PREPARED BY: <u>REK</u>		REPORT NO.
CHECKED BY:		PAGE NO. OF
DATE		MODEL NO.

REF.

COMPOSITE WING FWD. INTERM. SPAR

UPPER SKIN ATTACH. OUTBD. OF B.P. 33.93 RIB (CONT'D.)

CHECK ATTACH. OF H/C WEB TO UPPER CAP ~

SPAR SHEAR LOAD = 766 #/IN.

FLT. COND. 470303  
(ULT. LOADS)

TRANSVERSE LD. = 168 #/IN.

RESULTANT FASTENER LD. ~

1.50 FASTENER SPAC.

$$R = .50(1.5)(168 + 766) \\ = 588 \# \text{ (SINGLE SH'R.)}$$

ALLOW. HL10V-6 IN .090IN. GLASS EPOXY UPPER CAP ~

SHEAR OUT CHECK ~ 38IN. EDGE DISTANCE

$$f_s = \frac{588}{2(.090)(.38)} = 8596 \#/\text{IN.}^2$$

$$F_{su} = 13,900 \#/\text{IN.}^2$$

$$M.S.U. = \frac{13,900}{8596} - 1 = .61$$

BEARING CHECK ~

$$f_{brg} = \frac{588}{.090(.1875)} = 34,844 \#/\text{IN.}^2$$

$$F_{BRG} = 54,100 \#/\text{IN.}^2$$

$$M.S.U. = \frac{54,100}{34,844} - 1 = .55$$

NAS 664 BEARING IN INNER .090IN. GR/EP FACE SHEET  
NOT CRITICAL BY COMPARISON WITH FIBERGLASS UPPER  
SPAR CAP

MIL-  
HDBK-  
17  
PG.  
4-51



Columbus Aircraft Division  
Rockwell International

PREPARED BY: <u>REK</u>	REPORT NO.
CHECKED BY:	PAGE NO. OF
DATE:	MODEL NO.

REF.

COMPOSITE WING FWD. INTERM. SPAR

UPPER CAP ATTACH. TO H/C WEB OUTBD. OF B.P. 33.93 (CONTD.)

ALLOW. HL10V-6 IN GR/EP WEB FACE SH<sup>1</sup> ~

(.036 IN. DBLR. + .024 IN. WEB ~ ± 45° H.S. GR/EP)

$$\frac{D}{t} = \frac{.1875}{.060} = 3.13$$

EQUIV. BRG. STRESS = 59,000 #/IN.<sup>2</sup>

$$P_{ALLOW.} = 59,000 (.1875) (.060) = 664 \text{ #/IN.} \quad M.S.U. = \frac{664}{588} - 1 = .12$$

CHECK SHEAR ALLOW. OF ± 45° H.S. GR/EP WEB ~

$$q = 391 \text{ #/IN. @ NASTRAN RIB STA. (13)}$$

$$f_s = \frac{391}{.048} = 8146 \text{ #/IN.}^2$$

$$F_{SCR} > F_{SU} = 52,000 \text{ #/IN.}^2$$

$$M.S.U. = \frac{52,000}{8146} - 1 = \text{HIGH}$$

CHECK HL10V-6 INSTALL. CRUSHING LD. ON SPAR WEB CORE ~

$$P = 2\pi T P K$$

$$= 2\pi (35) (32) (.08)$$

$$= 563 \text{ #}$$

T = 35 # INSTALL. TORQUE W/ HL70-6 COLLARS

P = 32 THRD'S./IN.

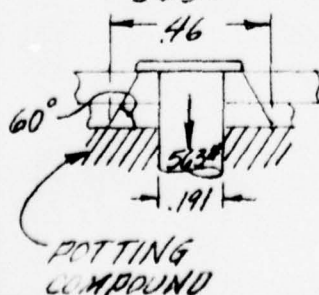
K = .08 ASSUMED FRICT. FACTOR

$$A_{brg} = \frac{\pi}{4} (.46^2 - .191^2) = .137 \text{ IN.}^2$$

$$f_{brg} = \frac{563}{.137} = 4109 \text{ #/IN.}^2$$

$$F_{BRG. ALLOW.} = 4500 \text{ #/IN.}^2 \quad M.S.U. = \frac{4500}{4109} - 1 = .09$$

\* 80% OF COMP. MAN. VALUE (1.2.2-16)



LAB TESTS



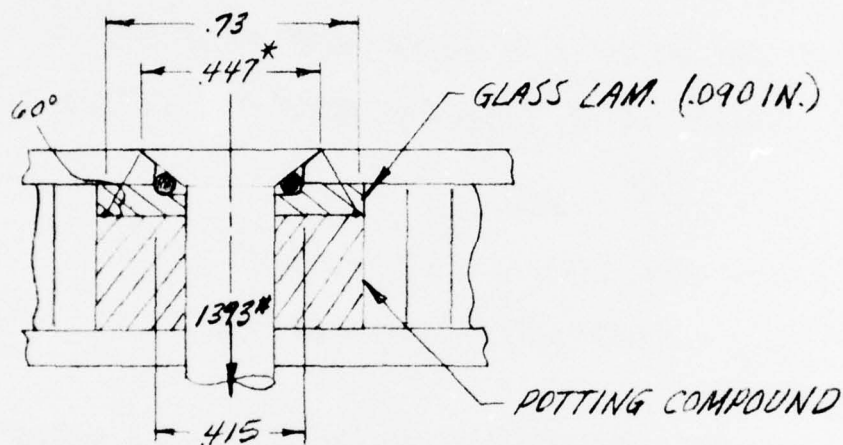
Columbus Aircraft Division  
Rockwell International

PREPARED BY: <i>REK</i>	REPORT NO.
CHECKED BY:	PAGE NO. OF
DATE	MODEL NO.

REF.

COMPOSITE WING FWD. INTERM. SPAR

CHECK NAS 654 INSTALL IN UPPER SKIN



FASTENER INSTALL. PRE-LO. ~

$$P = 2\pi TPK$$

$$T = 99'' \text{ MAX.}$$

PRE-LO.

$$P = 28 \text{ THRS./IN.}$$

$$= 2(\pi)(99)(28)(.08)$$

$$K = .08 \text{ ASSUMED FRICT. FACTOR}$$

$$= 1393 \#$$

$$A_{brg} = \frac{\pi}{4} [ .447^2 - .415^2 ] = .0217 \text{ IN.}^2$$

$$f_{brg} = \frac{1393}{.0217} = 64,194 \#/\text{IN.}^2$$

$$M.S.D. = \frac{115,000}{(64,194)} - 1 = .79$$

$$F_{brg} = 115,000 \#/\text{IN.}^2 \text{ H.S. GR/EP MATL.}$$

CHECK POTTING COMPOUND FOR 1393# PRE-LO. ~

$$A_{brg} = \frac{\pi}{4} [ .73^2 - .25^2 ] = .369 \text{ IN.}^2$$

$$f_{brg} = \frac{1393}{.369} = 3775 \#/\text{IN.}^2$$

$$F_{brg} = 4500 \#/\text{IN.}^2 \text{ ALLOW.}$$

$$M.S.D. = \frac{4500}{3775} - 1 = .19$$

\* NAS 654 HD. DIA.

COMP.  
MAN.  
Pg.  
12.2-22





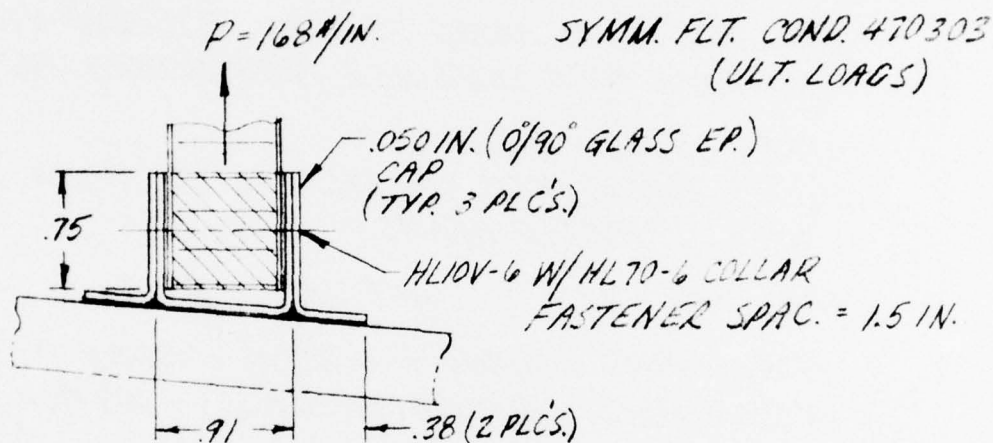
Columbus Aircraft Division  
Rockwell International

PREPARED BY: <b>REK</b>		REPORT NO.
CHECKED BY:		PAGE NO. OF
DATE:		MODEL NO.

REF.

COMPOSITE WING FWD. INTERM. SPAR

LOWER SKIN ATTACH. OUTBD. OF B.P. 33.93 RIB



CHECK BONDED JOINT FOR  $168 \text{ \#}/\text{IN.}$  LOAD

MDAC  
TESTS

ASSUME NORMAL L.D. TENS. ALLOW. =  $950 \text{ \#}/\text{IN.}$  ULT.  
(CAP TESTS 788 - 1020 LBS./IN.)

CONSIDER FASTENER LOAD IS CONCENTRATED ALONG  
.50 IN. LENGTH ~

$$P = \frac{1.5(168)}{.50} = 504 \text{ \#}/\text{IN.}$$

$$M.S.D. = \frac{788}{504} - 1 = .56$$

(MIN.)

LAB  
TESTS

BOND SHEAR STRENGTH =  $1500 \text{ \#}/\text{IN.}$  (CONSERV.)

$$P_s = 1.65(1500) = 2475 \text{ \#}/\text{IN. ULT.}$$

ALLOW

$$Q = 766 \text{ \#}/\text{IN. (NOT CRITICAL)}$$

HL10V-6 NOT CRITICAL IN LOWER CAP BY COMPARISON  
WITH UPPER CAP INSTALL.

COMPOSITE WING AFT INTERM. SPAR OUTBD. OF B.P. 33.93  
RIB NOT CRITICAL BY COMPARISON





Columbus Aircraft Division  
Rockwell International

PREPARED BY: <u>REK</u>		REPORT NO.
CHECKED BY:		PAGE NO. OF
DATE		MODEL NO.

REF.

COMPOSITE WING FWD. INTERM. SPAR

UPPER SKIN ATTACH. INBD. OF B.P. 33.93 RIB

CALCULATE LOADS BASED ON SYMM. FLT. COND. 470303  
TRANSVERSE LOAD COMBINED WITH INTERN. PRESS. ~

INTERN. PRESS. =  $9 \text{ \#/IN.}^2$  ULT.

ASSUME COVER PRESS. LDS. DISTRIBUTED TO SPARS BY  
SIMPLY SUPPORTED BEAMS ~

FWD. SPAN = 22 IN. AFT SPAN = 20 IN.

NASTRAN  
PROG.

AERODYNAMIC LOADING + INTERN. LOADING =  $100 \text{ \#/IN.}$  ULT.  
INTERN. PRESS. LD. =  $.50(9)(20+22) = 189 \text{ \#/IN.}$  ULT.

FASTENER SPACING = 1.0 IN. TOTAL LD. =  $289 \text{ \#/IN.}$  ULT.

LOADS @ NASTRAN RIB STA. (03) ~ FLT. COND. 470303

CHECK BENDING @ SECT. A-A OF UPPER CAP CHANNEL ~  
(REF. FWD. INTERM. SPAR CALC. OUTBD. OF B.P. 33.93 RIB)

MOM. ARM FOR TRANSVERSE LD. = 45 IN.

(ASSUME 50% END FIXITY @ ATTACH. TO H/C WEB AND  
.50 IN. EFFECT. WIDTH @ SECT. A-A)

$$M_{A-A} = 289(.75)(.45)(.50) = 49 \text{ \#}$$

$$f_{bL} = \frac{6(49)}{50(.160)^2} = 20851 \text{ \#/IN.}^2 \text{ ULT.}$$

COMP.  
MAN.  
PS.  
1.2.2-14

$F_{TU} = 86,000 \text{ \#/IN.}^2$  FOR  $60\% \pm 45^\circ$ ,  $40\% \sim 90^\circ$  H.S. GR/EP  
MAT'L.

$$M.S._0 = \frac{86,000}{20851} - 1 = 3.12$$



Columbus Aircraft Division  
Rockwell International

PREPARED BY: <u>REK</u>		REPORT NO.
CHECKED BY:		PAGE NO. OF
DATE		MODEL NO.

REF

COMPOSITE WING AFT INTERM. SPAR

UPPER SKIN ATTACH. INB'D. OF B.P. 33.93 RIB

CHECK NAS 664 IN .168 IN. UPPER SPAR CAP ~  
MAT'L. ~ 60% ±45°, 40% 90° H.S. GR/EP

$$Q_3 = 2458 \text{ \#/IN.} \quad \text{AVERAGE VALUE @ INB'D. END FOR MAX. VERT. LOF. COND.}$$

$$f_{brg} = \frac{2458}{.25(.168)} = 58523 \text{ \#/IN.}^2 \quad \text{BRG. IN .102 IN. GR/EP INNER FACE SH'T. NOT CRITICAL}$$

$$F_{brg} = 60,000 \text{ \#/IN.}^2 \text{ (CONSERV.)} \quad M.S.D. = \frac{60,000}{58523} - 1 = .02$$

CHECK ATTACH. OF H/C WEB TO UPPER CAP CHANNEL ~  
HL10V-6 @ 1.0 IN. SPAC.

ASSUME FWD. INTERM. SPAR TRANSVERSE LD. (CONSERV.)  
∴ TRANSVERSE LD. = 289 \#/IN. ULT.

$$\text{SPAR SHL. LD.} = 2393 \text{ \#/IN. (MAX.)}$$

$$\text{RESULTANT FASTENER LD.} = .50(289 + 2458) = 1237 \text{ \# SINGLE SH'R.}$$

BRG. CHECK HL10V-6 IN .168 IN. GR/EP UPPER CAP ~

$$f_{brg} = \frac{1237}{.168(.1875)} = 39270 \text{ \#/IN.}^2$$

$$F_{brg} = 60,000 \text{ \#/IN.}^2$$

$$M.S.D. = \frac{60,000}{39270} - 1 = .52$$

BRG. CHECK HL10V-6 IN .048 IN. + .072 DBLR. ±45° GR/EP WEB ~

$$f_{brg} = \frac{1237}{.120(.1875)} = 54978 \text{ \#/IN.}^2$$

$$F_{brg} = 60,000 \text{ \#/IN.}^2 \text{ (CONS.)}$$

$$M.S.D. = \frac{60,000}{54978} - 1 = .09$$



Columbus Aircraft Division  
Rockwell International

PREPARED BY: <u>REK</u>	REPORT NO.
CHECKED BY:	PAGE NO. OF
DATE:	MODEL NO.

REF.

COMPOSITE WING AFT INTERM. SPAR  
LOWER SKIN ATTACH. INBD. OF B.P. 33.93 RIB

CHECK BOND FOR  $q = 2393 \text{ #/IN.}$  LOADING

(REF. CALC. FOR FWD. INTERM. SPAR ATTACH. TO LOWER SKIN OUTBD. OF B.P. 33.13 RIB)

BOND AREA WIDTH =  $2(38) + .91 = 1.66 \text{ IN.}$

$$f_s = \frac{2393}{1.66} = 1442 \text{ #/IN.}^2$$

LAE  
TESTS

$F_{su} = 1500 \text{ #/IN.}^2$   
ADHESIVE

$$M.S.D. = \frac{1500}{1442} - 1 = .04$$

CHECK AFT INTERM. SPAR H/C PANEL STABILITY

o OUTBD. END ~ TAPERED PANEL

$$q^* = 912 \text{ #/IN.}$$

MATL. ~  $t_f = .048 \text{ IN. } \pm 45^\circ \text{ GR/EP}$   
 $6 \text{ #/FT.}^3 \text{ PHENOLIC CORE}$

$$f_s = \frac{912}{.096} = 9500 \text{ #/IN.}^2$$

ACH  
PROX.

$$F_{scr} > F_{su} = 52,000 \text{ #/IN.}^2$$

$$M.S.D. = \frac{52,000}{9500} - 1 = \text{HIGH}$$

o MID-SPAN ~

$$q^* = 1685 \text{ #/IN.}$$

$$f_s = \frac{1685}{.096} = 17,552 \text{ #/IN.}^2$$

$$M.S. = \frac{52,000}{17,552} - 1 = \text{HIGH}$$

$$F_{scr} > F_{su} = 52,000 \text{ #/IN.}^2 \quad \Delta 80\% \text{ OF COMP. MAN. VALUE (1.2.2-16)}$$

o INBD. END ~

$$q^* = 2458 \text{ #/IN.} \quad f_s = \frac{2458}{.096} = 25,604 \text{ #/IN.}^2$$

$$F_{scr} > F_{su} = 52,000 \text{ #/IN.}^2$$

$$M.S.D. = \frac{52,000}{25,604} - 1 = \text{HIGH}$$

\* MAX. VERT. LFG. COND. (MAX. OPER. LD.)

#### WING CENTERLINE SPLICE ANALYSIS

Analysis of the critical centerline splice areas for the centerline rib area are presented on the following pages. These analyses include the lower cover splice fwd of the rear spar, upper cover splice fwd of the rear spar, lower cover splice at section G-G (Reference Figure A-14), lower cover splice at section K-K (Reference Figure A-14), and the lower cover splice at section L-L (Reference Figure A-14).



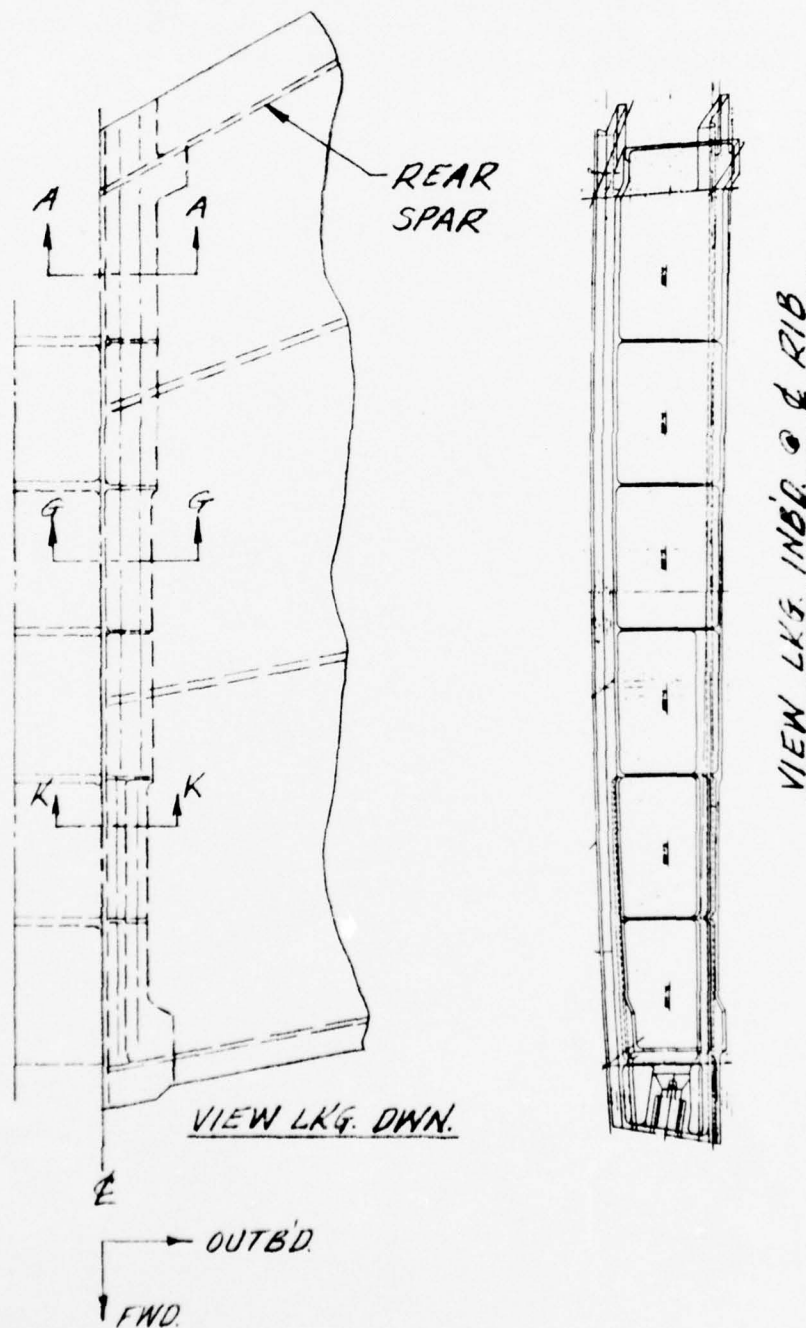


Columbus Aircraft Division  
Rockwell International

PREPARED BY: <i>REK</i>		REPORT NO.
CHECKED BY:		PAGE NO. OF
DATE		MODEL NO.

REF.

COMPOSITE WING CENTERLINE SPLICE







Columbus Aircraft Division  
Rockwell International

PREPARED BY: *REK*

CHECKED BY:

DATE:

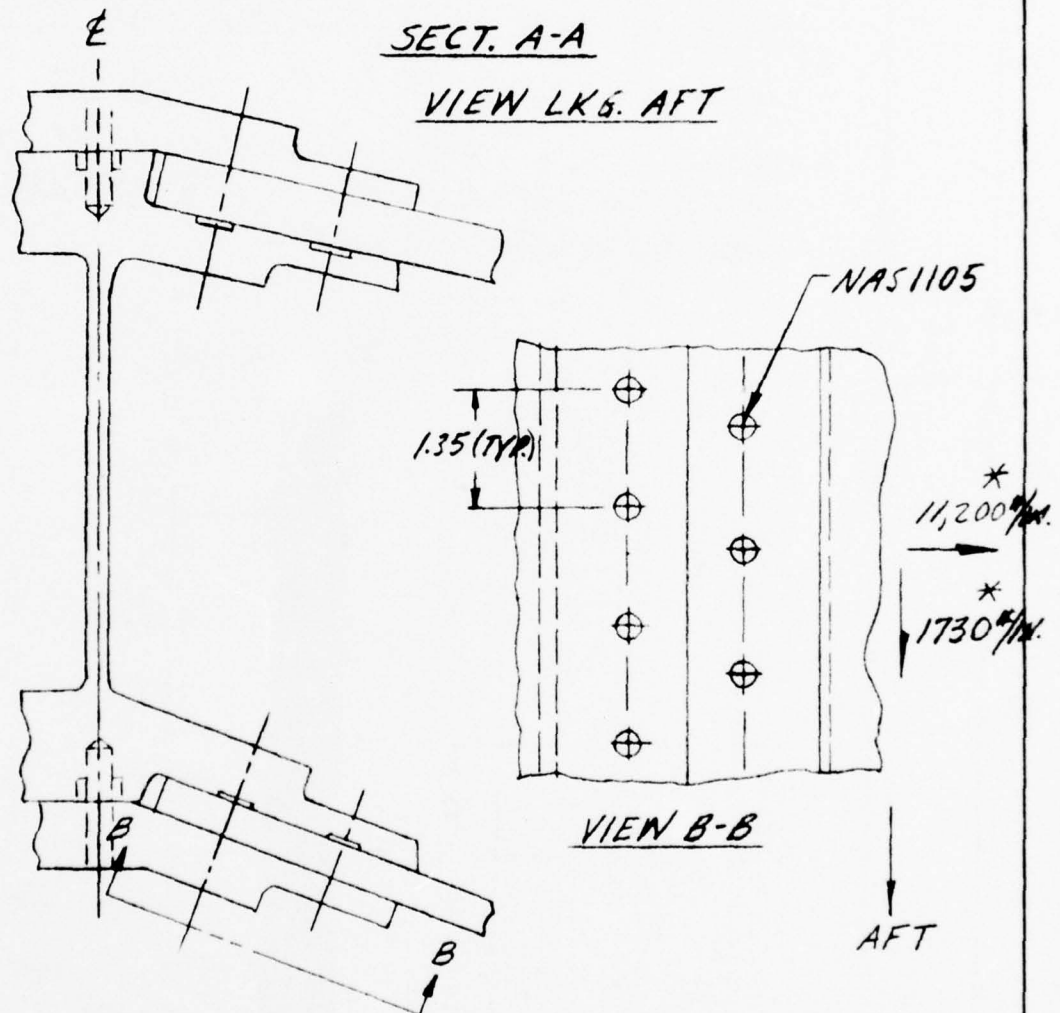
REPORT NO.

PAGE NO. OF

MODEL NO.

REF.

COMPOSITE WING CENTERLINE SPLICE



\* EXTRAPOLATED MAX. LOWER COVER MAX. OPERATIONAL  
LOADS FOR CRITICAL HIGH SINK LANDING COND.



Columbus Aircraft Division  
Rockwell International

PREPARED BY: <i>REK</i>	REPORT NO.
CHECKED BY:	PAGE NO. OF
DATE	MODEL NO.

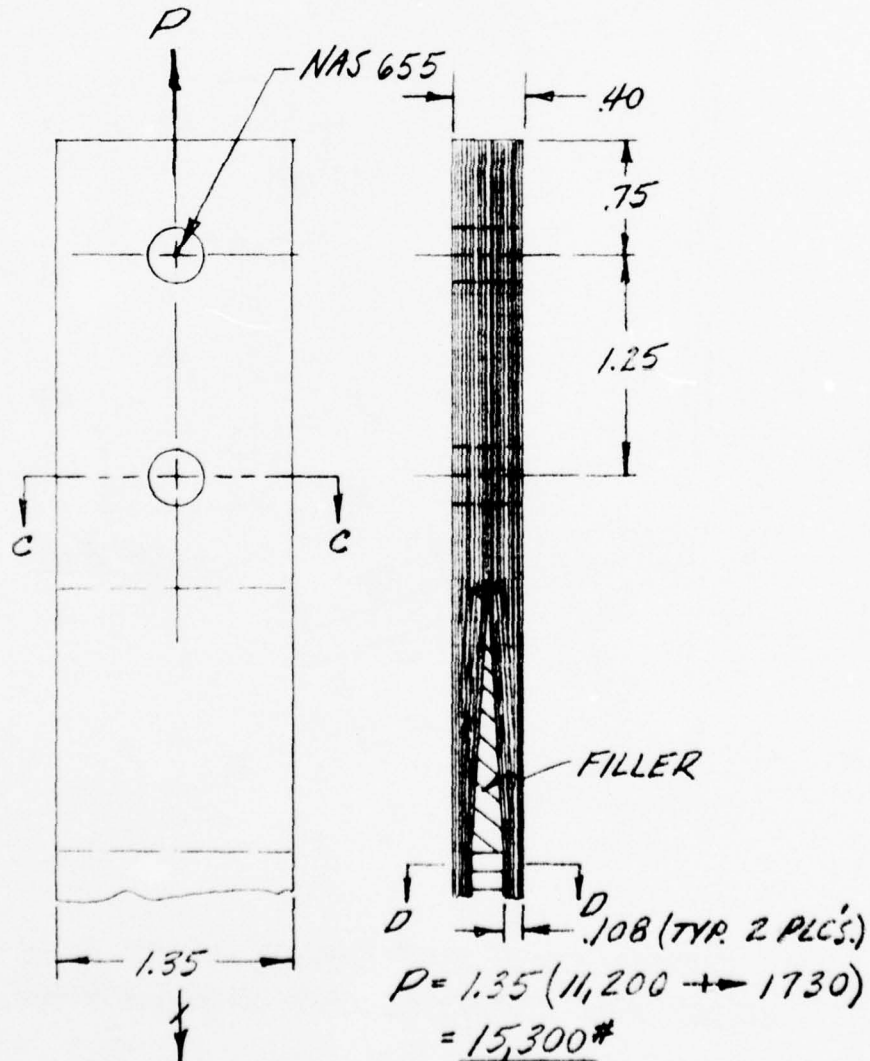
REF.

COMPOSITE WING CENTERLINE SPLICE

CHECK OF LOWER COVER SPLICE FWD. OF REAR SPAR

MAX. VERT. LANDING COND. (MAX. OPER. LDS.)

CHECK COVER SKIN IN SPLICE AREA USING  
FASTENER SPACING UNIT WIDTH AND RESULTANT  
LOAD FROM BIAXIAL LOADS





Columbus Aircraft Division  
Rockwell International

PREPARED BY: <b>REK</b>	REPORT NO.
CHECKED BY:	PAGE NO. OF
DATE:	MODEL NO.

REF.

COMPOSITE WING CENTERLINE SPLICE

CHECK OF LOWER COVER SPLICE FWD. OF R.S. (CONT'D.)

TENSION STRENGTH CHECK @ SECT. C-C ~

MAT'L. ~ 49% ± 45°, 27% ~ 0°, 24% ~ 90° H.S. GR/EP

$e = 1.25 \text{ IN.}$   $W = 1.35 \text{ IN.}$   $D = .313 \text{ IN.}$   $t = .40 \text{ IN.}$

$$\frac{e}{W} = .93$$

COMP.  
MAN.

FIG.  
1.3.2-31

FIG.  
1.2.2-14

$K_{t_c} = 1.5$  NET TENS. STRESS CONCENTRATION FACTOR

$$F_{TU} = 76,000 \text{ #/IN.}^2$$

$$P_{\text{ALLOW.}} = (1.35 - .313)(.40) \left( \frac{76,000}{1.5} \right)$$
$$= 21,017 \text{ # ULT.}$$

$$M.S.O. = \frac{21,017}{15,300} - 1 = .37$$

CHECK SECT. D-D FOR 11,333 #/IN. LOAD ~

MAT'L. ~ 67% ± 45°, 33% ~ 0° GR/EP (HIGH-STRENGTH)

$$f_t = \frac{11,333}{.216} = 52,468 \text{ #/IN.}^2$$

"

$$F_{TU} = 75,000 \text{ #/IN.}^2$$

$$M.S.O. = \frac{75,000}{52,468} - 1 = .42$$



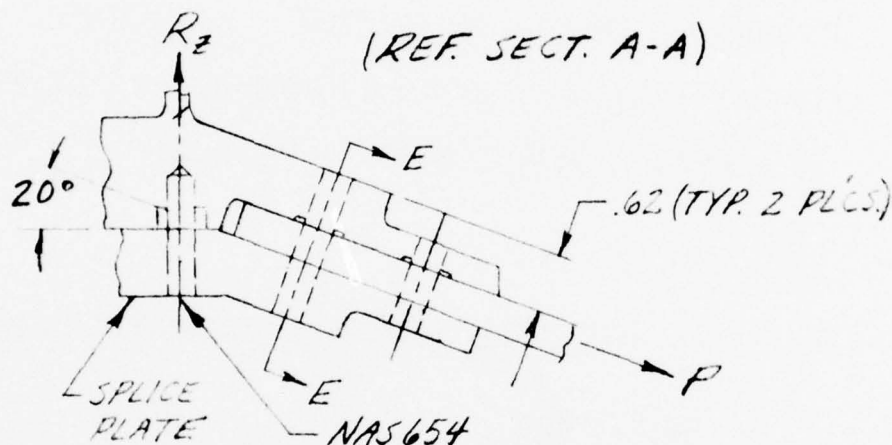
Columbus Aircraft Division  
Rockwell International

PREPARED BY: <i>REK</i>	REPORT NO.
CHECKED BY:	PAGE NO. OF
DATE:	MODEL NO.

REF:

COMPOSITE WING CENTERLINE SPLICE

CHECK OF LOWER COVER SPLICE FWD OF R.S. (CONT'D.)



CHECK SPLICE PLATE @ SECT. E-E FOR  $P = 11,333 \text{ \#/IN.}$   
LOAD ~ MAX. VERT. LG. COND. (MAX. OPER. LOS.)

FASTENER SPACING  $"b" = 1.35 \text{ IN.}$   $q = .313$   $C = 1.25$

$A_{NET} = .42 \text{ IN.}^2 / \text{IN. WIDTH}$

$\theta = 90^\circ$   $\frac{q}{b} = .23$

$K_T = 2.32$

$$f_t = \frac{.50(11,333)(2.32)}{.42} = 31,300 \frac{\text{\#}}{\text{IN.}} (\text{NOT CRITICAL})$$

MAT'L ~ 7075-T73 AL. BAR  $F_{TU} = 65,000 \text{ \#/IN.}^2$

CHECK LOAD ON NAS654 BOLT FOR  $P = 11,200 \text{ \#/IN.}$   
\$ SHEAR LOAD =  $1730 \text{ \#/IN.}$  (AIRPLANE CONFIG)\*

$R_2 = 2(11,200)(.50) \sin 20^\circ = 3831 \text{ \#/IN.}$   $R_3 = 1730 \text{ \#/IN.}$

FASTENER SPACING =  $1.0 \text{ IN.}$

TENSION ALLOW. =  $4800 \text{ \#ULT.}$

WHEN COMBINED WITH  $1730 \text{ \# SHR. LD.}$

$$M.S.D. = \frac{4800}{3831} - 1 = .25$$

\* TEST ARTICLE LOADING IS 50% OF A/P CONFIG. LOAD

BRUHN  
FIG.  
C13.19

MIL-  
HDBK-  
5B

NAG-  
44  
PG.  
02-1-2



Columbus Aircraft Division  
Rockwell International

PREPARED BY: <u>REK</u>	REPORT NO.
CHECKED BY:	PAGE NO. OF
DATE:	MODEL NO.

<u>REF.</u>	<u>COMPOSITE WING CENTERLINE SPLICE</u> <u>CHECK OF LOWER COVER SPLICE FWD. OF R.S. (CONT'D.)</u>  SHEAR-BEARING STRENGTH OF NAS 655 BOLT IN 40 IN. 49% ± 45°, 27% - 0°, 24% - 90° H.S. GR/EP  $\frac{D}{t} = \frac{.313}{.40} = .78$ $\frac{e}{D} = \frac{.75}{.313} = 2.4$  $\frac{S}{D} = \frac{1.35}{.313} = 4.3$ CONSIDER AS DOUBLE SHEAR COMBINATION  COMP MAN. FIG. 1.3.2-26  $F_{brg} = 105,000 \text{ #/IN.}^2$ ALLOW.  $P_{brg} = 105,000 (.313) (.40) = 13,146 \text{ # ULT.}$ ALLOW.  APPLIED LD. = .50 (15,300) = 7650 #  $M.S.U. = \frac{13,146}{7650} - 1 = .71$  <u>CHECK DOUBLE SHEAR STRENGTH OF NAS 655 -</u>  NAG- 644 PG. 14-1-1  $P_{ALLOW.} = 14,600 \text{ # ULT.}$  $M.S.U. = \frac{14,600}{.50 (15,300)} - 1 = .90$
-------------	--





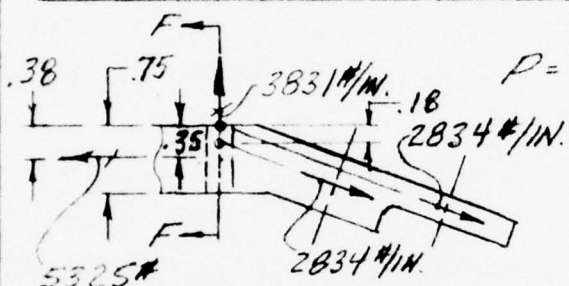
Columbus Aircraft Division  
Rockwell International

PREPARED BY: <i>REK</i>	REPORT NO.
CHECKED BY:	PAGE NO. OF
DATE:	MODEL NO.

REF.

COMPOSITE WING CENTERLINE SPLICE

CHECK OF LOWER COVER SPLICE FWD. OF R.S. (CONT'D.)



$P = 5667 \text{ #/IN. (MAX. OPER. LOADS)}$

MAT'L. ~ 7075-T73 AL.  
BAR

BENDING  $\sigma$  SECT. F-F ~ FASTENER SPAC. = 1.0 IN.

$$M = 2834 (.35 + .11) = 1474 \text{ #}$$

$$A_{NET} = (.75)^2 = .562 \text{ IN.}^2$$

$$f_b = \frac{6(1474)}{(.75)^3} = 20,964 \text{ #/IN.}^2$$

$$F_{BU} = 93,000 \text{ #/IN.}^2$$

$$R_b = \frac{20,964}{93,000} = .23$$

$$f_t = \frac{5325}{.562} = 9475 \text{ #/IN.}^2$$

$$F_{TU} = 65,000 \text{ #/IN.}^2$$

$$R_T = \frac{9475}{65,000} = .15$$

STRESS CONCENTRATION FACTOR ~

$$a = .25 \quad b = 2.0 \quad \theta = 0^\circ$$

$$\frac{a}{b} = .125 \quad K_t = 2.2$$

$$M.S.O. = \frac{1}{2.2(.23 + .15)} - 1 = .19$$

MIL-  
HDBK-  
5B

BRUNN  
FIG.  
C13.19



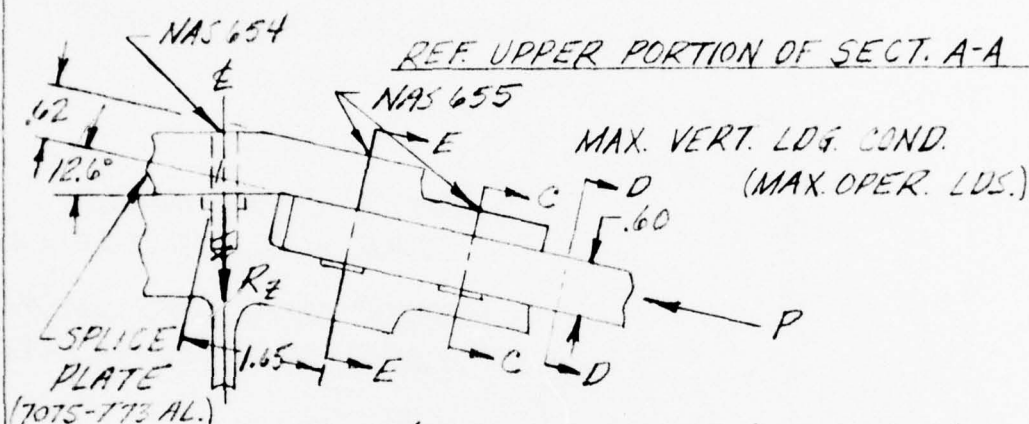
Columbus Aircraft Division  
Rockwell International

PREPARED BY: <i>REK</i>	REPORT NO.
CHECKED BY:	PAGE NO. OF
DATE	MODEL NO.

REF.

COMPOSITE WING CENTERLINE SPLICE

CHECK OF UPPER COVER SPLICE FWD OF REAR SPAR



$$\text{UPPER COVER INBD. LD.} = 49,000(.216) = 10,584 \text{ \#/IN.}$$

$$\text{UPPER COVER FWD. SHR. LD.} = 8000(.216) = 1728 \text{ \#/IN.}$$

$$\therefore P = 10,584 + 1728 = 10,724 \text{ \#/IN. RESULTANT LD.}$$

CHECK LOAD ON NAS 654 & BOLT FOR  $P = 10,724 \text{ \#/IN.}$

& SHEAR LOAD = 1728 \#/IN. (AIRPLANE CONFIG.)\*

FASTENER SPACING = 1.0 IN.

$$R_2 = 2(10,724)(.50) \sin 12.6^\circ = 2339 \text{ \#} \quad R_3 = 1728 \text{ \#}$$

NAS 654 BOLT NOT CRITICAL BY COMPARISON WITH LOWER COVER SPLICE

SPLICE PLATE @ SECT. E-E AND UPPER COVER @ SECT'S. C-C & D-D NOT CRITICAL BY COMPARISON WITH LOWER COVER.

INTER-RIVET BUCKLING CHECK OF SPLICE PLATE ~

ASSUME .60 IN. EFFECTIVE WIDTH FOR 5362 \# LD. ~

$$S/E = 5.3 \text{ FOR PINNED ENDS (CONSERV.)} \quad f_c = \frac{5362}{.60(.62)} = 14,415 \text{ \#/IN.}^2 \text{ (NOT CRIT.)}$$

$$F_{IR} = 65,000 \text{ \#/IN.}^2$$

\* TEST ARTICLE LOADING IS 50% OF A/P CONFIG. LOAD

BROUHN  
FIG.  
07.18



Columbus Aircraft Division  
Rockwell International

PREPARED BY: <u>REK</u>	REPORT NO.
CHECKED BY:	PAGE NO. OF
DATE:	MODEL NO.

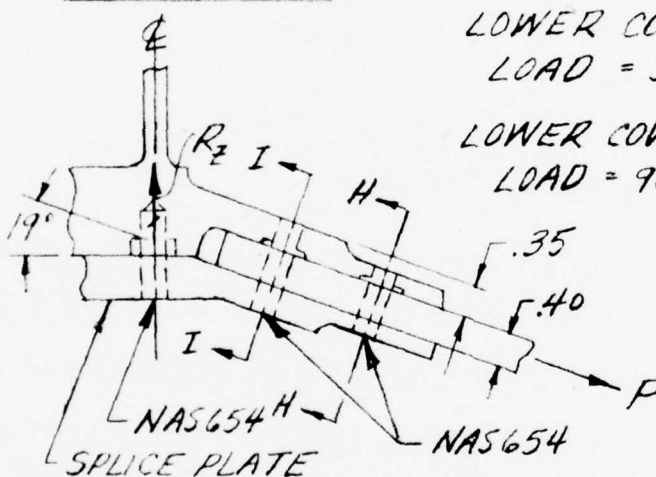
REF.

COMPOSITE WING CENTERLINE SPLICE

CHECK OF LOWER COVER SPLICE @ SECT. G-G

MAX. VERT. LDG. COND. (MAX. OPER. LOADS)

LOWER PORTION  
OF SECT. G-G



LOWER COVER OUTBD.

$$LOAD = 32,500(.204) = 6630 \#/IN.$$

LOWER COVER AFT SHEAR

$$LOAD = 9000(.204) = 1836 \#/IN.$$

$$P = (6630 + 1836) \\ = 6880 \#/IN. \\ \text{RESULTANT LD.}$$

LOWER COVER SKIN @ SECT. H-H NOT CRITICAL BY  
COMPARISON WITH SECT. C-C CALC.

CHECK SHEAR-BEARING STRENGTH OF NAS654 IN  
40 IN. 49%  $\pm 45^\circ$ ; 27%  $\sim 0^\circ$ ; 24%  $\sim 90^\circ$  H.S. GR/EP

$$\frac{D}{t} = \frac{.25}{.40} = .625 \quad \frac{e}{D} = \frac{.60}{.25} = 2.4$$

$$\frac{S}{D} = \frac{1.20}{.25} = 4.8 \quad \text{CONSIDER AS DOUBLE SHEAR} \\ \text{COMBINATION}$$

$$F_{bry} = 105,000 \#/IN.^2 \quad F_{bry} = 105,000(.40)(.25) = 10,500 \#/ULT. \\ \text{ALLOW.} \quad \text{ALLOW.}$$

$$\text{APPLIED LD.} = .50(6880)(1.20) \\ = 4128 \#$$

$$M.S.U. = \frac{10,500}{4128} - 1 = \text{HIGH}$$

COMP.  
MAN.  
176.  
1.3.2-26



Columbus Aircraft Division  
Rockwell International

PREPARED BY: <b>REK</b>	REPORT NO.
CHECKED BY:	PAGE NO. OF
DATE:	MODEL NO.

REF.	<p><u>COMPOSITE WING CENTERLINE SPLICE</u></p> <p><u>CHECK OF LOWER COVER SPLICE @ SECT. G-G (CONTD.)</u></p> <p>DOUBLE SHEAR STRENGTH CHECK OF NAS655 FASTENERS ~ MAX. VERT. LDG. COND. (MAX. OPER. LOADS)</p> <p><math>P_{ALLOW.} = 9300 \# \text{ULT.}</math></p> <p>APPLIED LOAD = 4128# <math>M.S.U. = \frac{9300}{4128} - 1 = \text{HIGH}</math></p> <p>CHECK SPLICE PLATE @ SECT. I-I FOR <math>P = 6880 \#/\text{IN.}</math></p> <p>FASTENER SPACING <math>b = 1.20 \text{ IN.}</math> <math>a = .25</math> <math>c = 1.10</math> <math>\theta = 90^\circ</math></p> <p><math>A_{NET} = .227 \text{ IN.}^2/\text{IN. WIDTH}</math> <math>\frac{a}{b} = .21</math> <math>K_t = 2.36</math></p> <p><math>f_t = \frac{.50(6880)(2.36)}{.227} = 35,764 \#/\text{IN.}^2</math></p> <p>MAT'L. ~ 7075-T73 AL. BAR <math>F_{T0} = 65,000 \#/\text{IN.}^2</math></p> <p>CHECK LOAD ON NAS654 &amp; BOLT FOR <math>P = 6880 \#/\text{IN.}</math></p> <p>\$ SHEAR LOAD = 1836#/\text{IN. (AIRPLANE CONFIG.)*</p> <p><math>R_z = 2(6880)(.50) \sin 19^\circ = 2239 \#/\text{IN.}</math></p> <p><math>R_s = 1836 \#/\text{IN.}</math> FASTENER SPAC. = 1.25 IN.</p> <p>TENSION ALLOW. = 4000# \text{ULT. WHEN COMBINED WITH 2295# SHR. LD.}</p> <p><math>M.S.U. = \frac{4000}{2799} - 1 = .42</math></p> <p>*TEST ARTICLE LOADING IS 50% OF A/P CONFIG. LOAD</p>
------	---





Columbus Aircraft Division  
Rockwell International

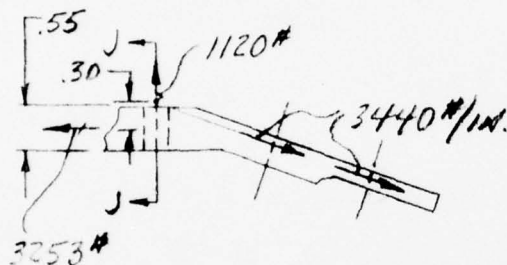
PREPARED BY: <b>REK</b>		REPORT NO.
CHECKED BY:		PAGE NO. OF
DATE:		MODEL NO.

REF.

COMPOSITE WING CENTERLINE SPLICE

CHECK OF LOWER COVER SPLICE @ SECT. G-G (CONTD.)

BENDING @ SECT. J-J ~



MATL. - 7075-T73 AL. BAR

FASTENER SPAC. = 1.20 IN.  
@  $\phi$

$$M = .30(3253)(1.2) = 1171 \text{ "IN.}^2 \text{ (CONSERV)}$$

$$A_{NET} = .95(.50) = .475 \text{ IN.}^2$$

$$f_b = \frac{6(1171)}{.95(.55)^2} = 24,448 \text{ #/IN.}^2$$

MIL-  
HDBK-  
5B

$$F_{BU} = 93,000 \text{ #/IN.}^2$$

$$R_b = \frac{24,448}{93,000} = .26$$

$$f_t = \frac{3253(1.2)}{.475} = 8218 \text{ #/IN.}^2$$

$$F_{TU} = 65,000 \text{ #/IN.}^2$$

$$R_T = \frac{8218}{65,000} = .13$$

STRESS CONCENTRATION FACTOR ~

$$a = .25 \quad b = 2.4 \quad \theta = 0^\circ$$

BRUHN  
FIF.  
C13.19

$$\frac{a}{b} = .104 \quad K_t = 2.3$$

$$M.S. = \frac{1}{2.3(.26 + .13)} - 1 = .11$$





Columbus Aircraft Division  
Rockwell International

PREPARED BY: <b>REK</b>	REPORT NO.
CHECKED BY:	PAGE NO. OF
DATE:	MODEL NO.

REF.

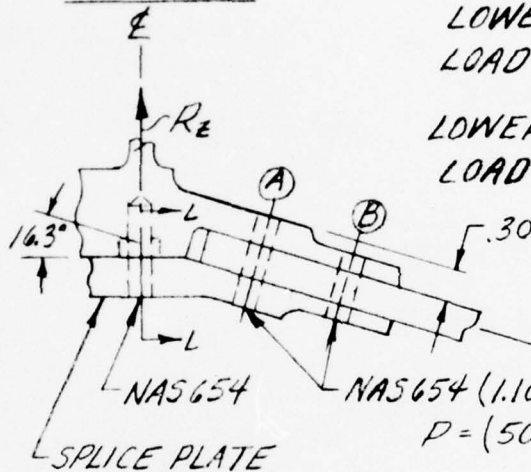
COMPOSITE WING CENTERLINE SPLICE

CHECK OF LOWER COVER SPLICE @ SECT. K-K

MAX. VERT. LANDING COND.

(MAX. OPER. LOADS)

LOWER PORTION OF  
SECT. K-K



LOWER COVER OUTBD.

$$\text{LOAD} = 28,000(.180) = 5040 \#/\text{IN.}$$

LOWER COVER AFT SHEAR

$$\text{LOAD} = 8000(.180) = 1440 \#/\text{IN.}$$

$$P = (5040 + 1440) = 5242 \#/\text{IN.}$$

RESULTANT LOAD

COVER SKIN NOT CRITICAL @ HOLE (B) BY COMPARISON

CHECK SPLICE PLATE @ HOLE (A) --  $a = .25$   $c = 1.0$   $\theta = 90^\circ$

$$A_{\text{NET}} = .25 \text{ IN.} / 1.10 \text{ IN. WIDTH}$$

$$b = 1.10 \quad \frac{a}{b} = .23$$

$$K_t = 2.32$$

$$f_t = \frac{5242(.50)(2.32)(1.1)}{.25} = 26,755 \#/\text{IN.}^2 \text{ (NOT CRIT.)}$$

CHECK LOAD ON NAS 654 & BOLT FOR  $P = 5040 \#/\text{IN.}$   
& SHEAR LOAD =  $1440 \#/\text{IN.}$  (AIRPLANE CONFIG.)

$$R_z = 2(5040)(.50) \sin 16.3^\circ = 1415 \#/\text{IN.}$$

$$R_s = 1440 \#/\text{IN.} \quad \text{FASTENER SPAC.} = 1.50 \text{ IN.}$$

TENSION ALLOW. =  $3600 \#/\text{ULT.}$

$$M.S.D. = \frac{3600}{2123} - 1 = .67$$

MIL-  
HDBK-  
58



Columbus Aircraft Division  
Rockwell International

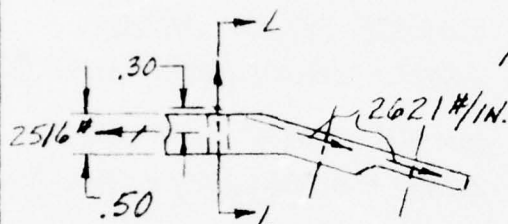
PREPARED BY: <i>REK</i>		REPORT NO.
CHECKED BY:		PAGE NO. OF
DATE:		MODEL NO.

REF.

COMPOSITE WING CENTERLINE SPLICE

CHECK OF LOWER COVER SPLICE @ SECT. L-L

BENDING @ SECT. L-L ~



MATL. ~ 7075-T73 AL. BAR

FASTENER SPAC. = 1.50 IN.  
@  $\perp$

$$M = .30(2516)(1.5) = 1132 \text{ IN.}$$

$$A_{NET} = 1.25(.50) = .62 \text{ IN.}^2$$

$$f_b = \frac{6(1132)}{1.25(.50)^2} = 21,734 \text{ #/IN.}^2$$

$$F_{80} = 93,000 \text{ #/IN.}^2$$

$$R_b = \frac{21,734}{93,000} = .23$$

$$f_t = \frac{2516(1.5)}{.62} = 6087 \text{ #/IN.}^2$$

$$F_{T0} = 65,000 \text{ #/IN.}^2$$

$$R_T = \frac{6087}{65,000} = .09$$

STRESS CONCENTRATION FACTOR ~

$$a = .25 \quad b = 3.0 \quad \theta = 0^\circ$$

$$\frac{a}{b} = .08 \quad K_t = 2.4$$

$$M.S.D. = \frac{1}{2.4(.23 + .09)} - 1 = .30$$

MIL-  
HDBK-  
5B

BRUNN  
F14  
C13.11

#### WING-TO-FUSELAGE ATTACHMENT

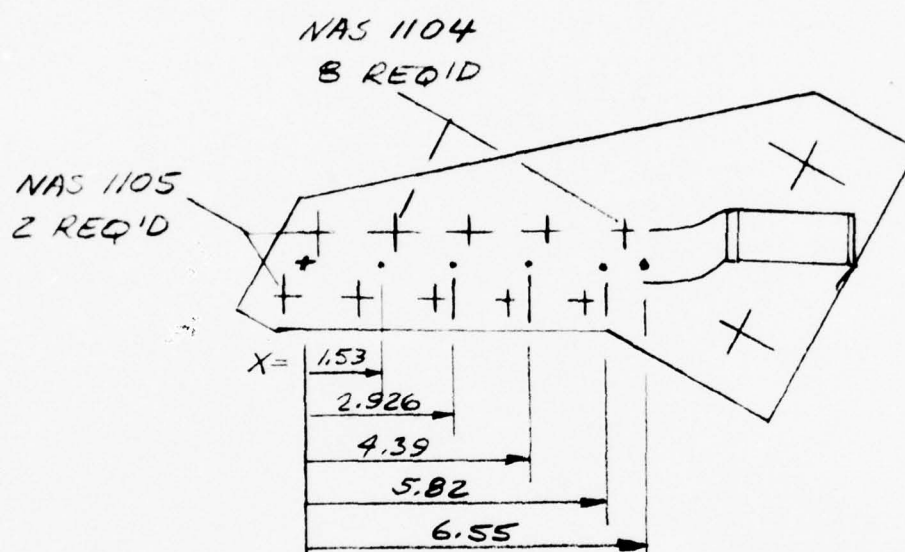
The critical wing-to-fuselage attachment fitting and attachment of the fitting to the rear spar of the wing are analyzed in this section. The critical mode is shearout of the attachment lug for the net load of 38165 lbs. produced by the MAX. VERTICAL LANDING CONDITION.



Columbus Aircraft Division  
Rockwell International

PREPARED BY: <i>HR</i>		REPORT NO.
CHECKED BY:		PAGE NO. OF
DATE:		MODEL NO.

FITTING ASSY - COMPOSITE WING, CENTER SECTION,  
WING TO FUSELAGE ATTACH, AFT 8679-110113

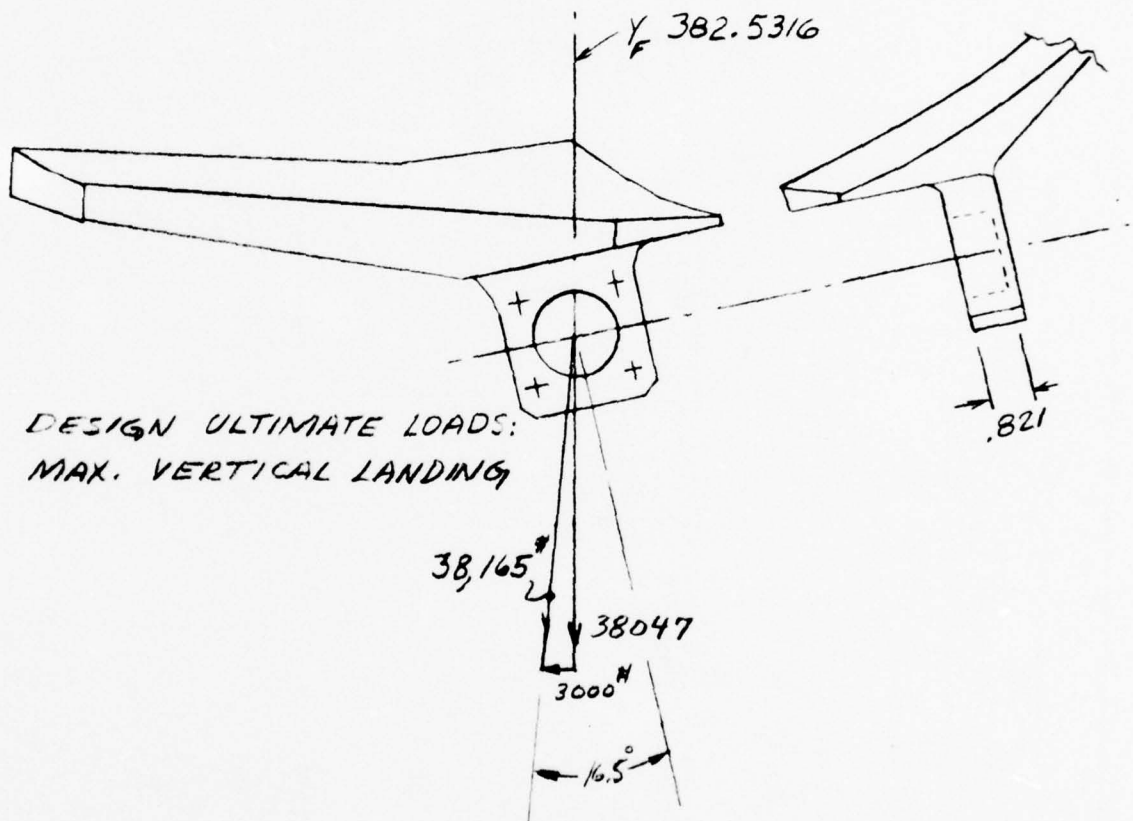




Columbus Aircraft Division  
Rockwell International

PREPARED BY: <i>HR</i>		REPORT NO.
CHECKED BY:		PAGE NO. OF
DATE:		MODEL NO.

FITTING ASSY - COMPOSITE WING, CENTER SECTION,  
WING TO FUSELAGE ATTACH, AFT 8679-110113



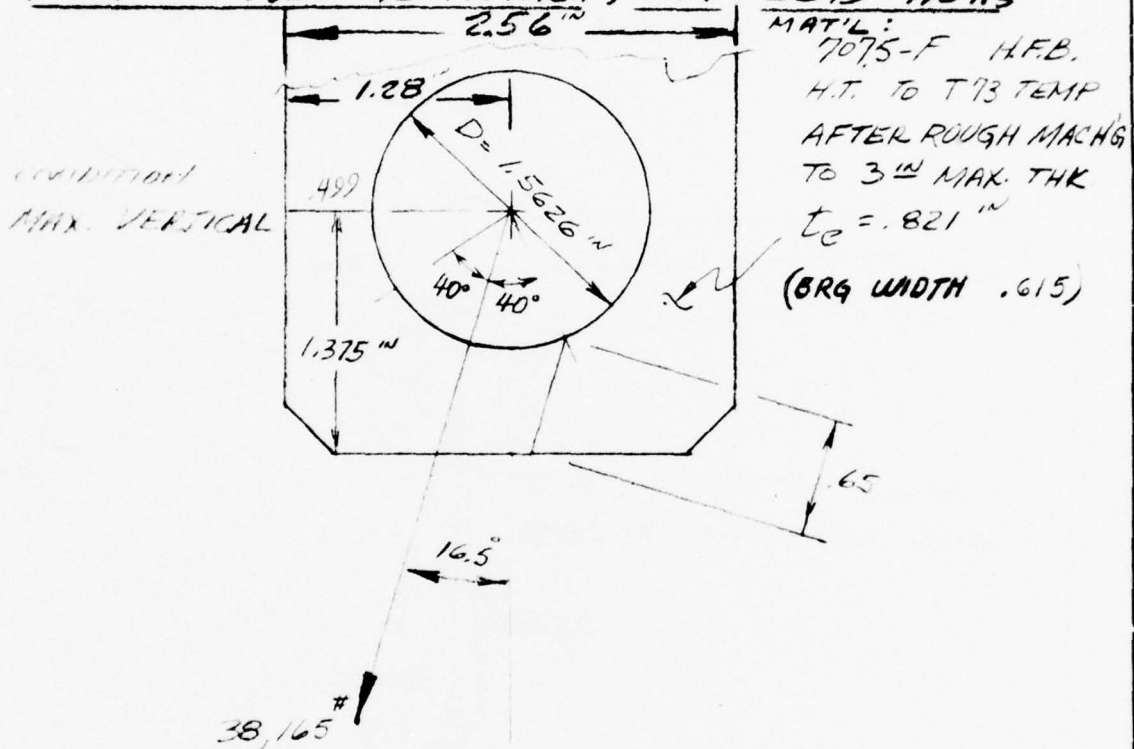




Columbus Aircraft Division  
Rockwell International

PREPARED BY: <i>HR</i>	REPORT NO.
CHECKED BY:	PAGE NO. OF
DATE:	MODEL NO.

REF FITTING ASSY - COMPOSITE WING, CENTER SECTION,  
WING TO FUSELAGE ATTACH, AFT B679-110113



SHEAR-OUT

$$f_s = \frac{38165}{2(.821)(.65)} = 35,758 \text{ psi}$$

$$F_{SO} = 39000 \text{ psi}$$

$$M.S. = \frac{39000}{35758} - 1 = .09$$

TENSION CHECK

$$f_t = \frac{38165}{2(.821).499} = 46,579$$

$$F_{T0} = 61,000 \text{ psi S.T. CONSERVATIVE}$$

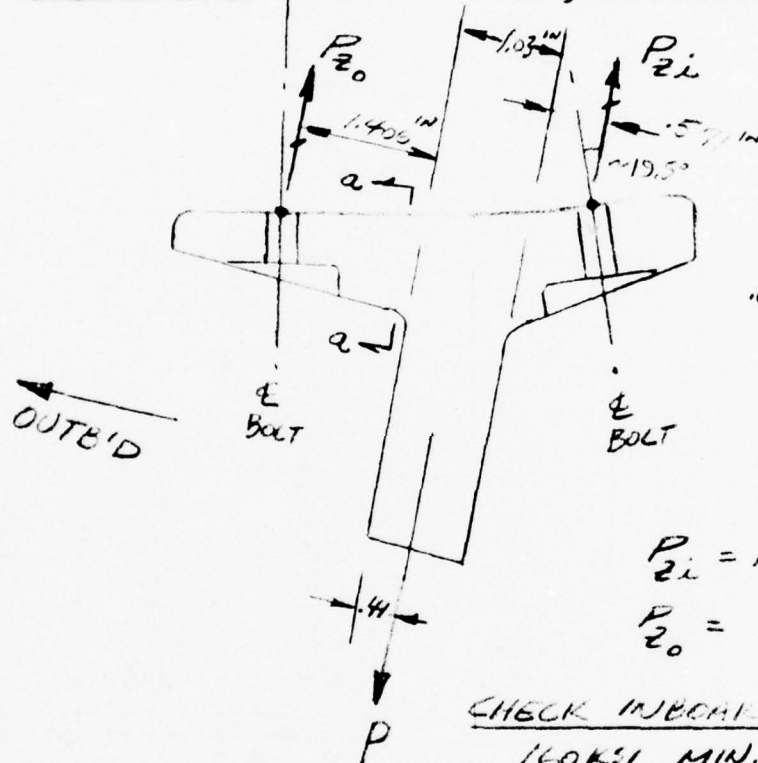
$$M.S. = \frac{61000}{46579} - 1 = .30$$



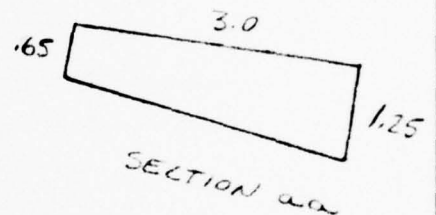
Columbus Aircraft Division  
Rockwell International

PREPARED BY: <i>HR</i>		REPORT NO.
CHECKED BY:		PAGE NO. OF
DATE:		MODEL NO.

FITTING ASSY - COMPOSITE WING, CENTER SECTION;  
WING TO FUSELAGE ATTACH, AFT 8679 - 110113



MAT'L  
7075-F  
HAND FORGED BILLET  
HT TO TEMP T13



$$P_{2i} = 1.816/3.007 P = .6039 P$$

$$P_{20} = .3961 P$$

CHECK INBOARD BOLT 5/8 DIA.  
160KSI MIN. (NAS1310-34)  
 $P_{ULT} = 39520 \text{ LBS}$

$$P_{BOLT} = P_{2i} / \sin 19.5 = .6406 P = 24343 \text{ #}$$

$$M.S. = \frac{39520}{24343} - 1 = .62$$

NAS 577-10A (CARNEL NUT)  
578-10B  
 $P_{ULT ALL} = 48700 \text{ #}$

CHECK SECTION aa

$$M = .3961 P (1.406) = .5569 P \text{ (CANTILEVER)}$$

$$f_{AU} = \frac{6M}{3(.9)^2} = 2.47M \text{ OR } 1.375P = 52,250 \text{ psi}$$

$$F_{10} = F_{10} = 64,000 \text{ psi CONSV.}$$

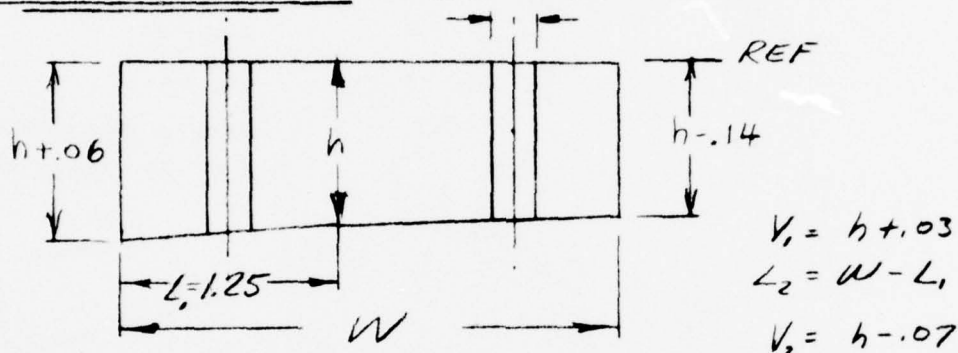
$$M.S. = \frac{64000}{52250} - 1 = .22$$



**Columbus Aircraft Division**  
Rockwell International

PREPARED BY: <i>HR</i>		REPORT NO.
CHECKED BY:		PAGE NO. OF
DATE:		MODEL NO.

FITTING ASSY - COMPOSITE WING, CENTER SECTION,  
WING TO FUSELAGE ATTACH, AFT 8679-110113  
IDEALIZED SECTION .260 2 PL



X	h	W	V <sub>2</sub>	L <sub>2</sub>	V <sub>1</sub>	L <sub>1</sub>
1.53	.93	2.83	.86	1.58	.96	1.25
2.926	1.064	3.18	.99	1.93	1.09	↑ ↓ 1.25
4.39	1.203	3.48	1.13	2.23	1.23	
5.82	1.34	3.89	1.27	2.64	1.37	
6.55	1.408	4.14	1.34	2.89	1.44	

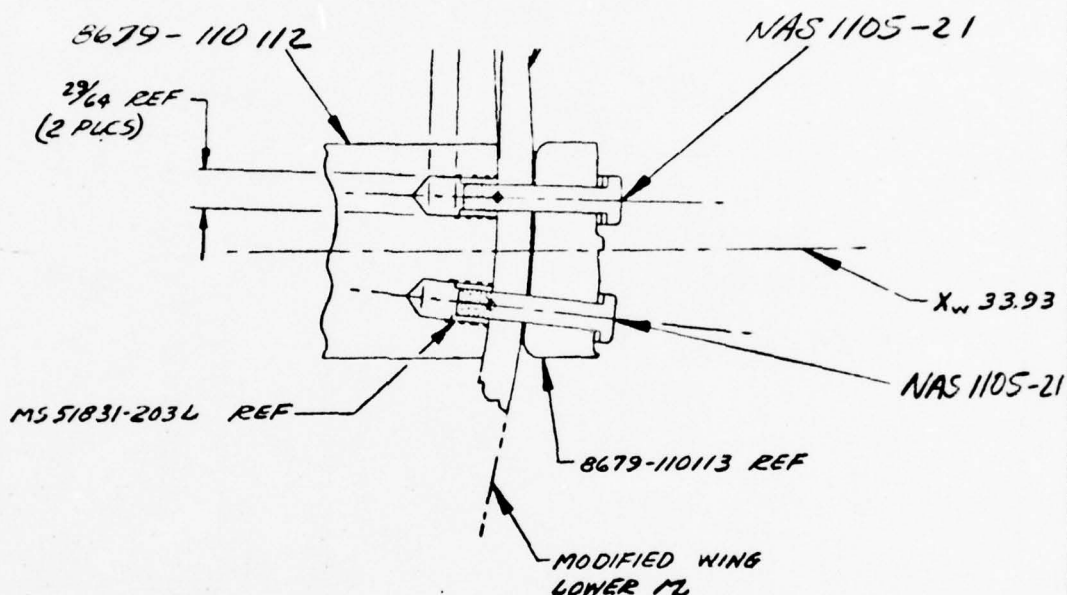
X	L <sub>1</sub> (NET)	L <sub>2</sub> (NET)	I	$\bar{I}$	A	C <sub>MAX</sub>
1.53	.99	1.32	.144	.453	2.086	.537
2.926		1.67	.242	.499	2.732	.621
4.39		1.97	.392	.583	3.444	.677
5.82		2.38	.621	.650	4.379	.75
6.55		2.89	.828	.683	5.298	.787

X	M=8985X*	F <sub>B</sub>	F <sub>B</sub> =1.5 F <sub>T0</sub>	M.S.	(CONSERVATIVE)
1.53	13747	51265	99000	.93	
2.926	26290	67463	↑ ↓ 99000	.47	
4.39	39444	68121		.45	
5.82	52293	63156		.56	
6.55	58851	55937		.77	



Columbus Aircraft Division  
Rockwell International

PREPARED BY: <i>HR</i>		REPORT NO.
CHECKED BY:		PAGE NO. OF
DATE:		MODEL NO.



$$P = 8985 \div 2 = 4492 \text{ \#/BOLT}$$

PULLOUT STRENGTH OF INSERT IN 8679-110112

$$P_{ALL} = (.3588) 39000 = 13993 \text{ \#}$$

TENSION STRENGTH OF NAS 1105-21

$$P_{ALL} = 8780$$

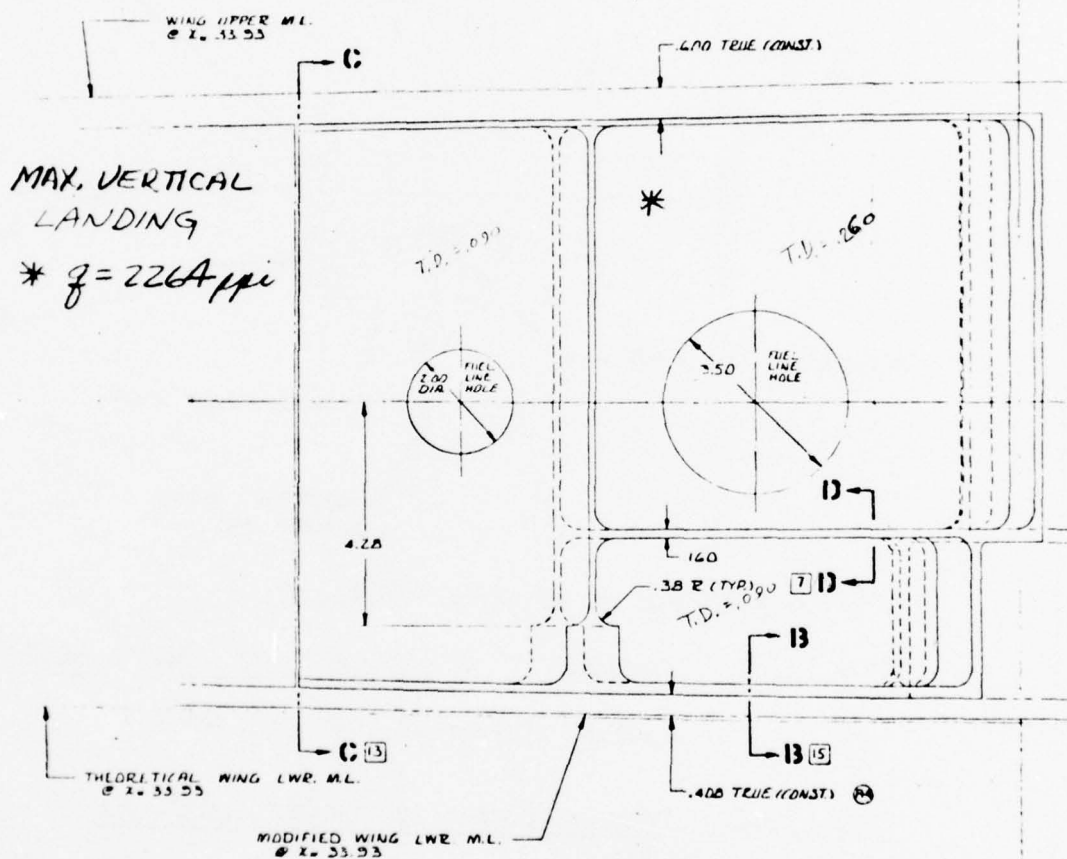
$$M.S. = \frac{8780}{4492} - 1 = \underline{\underline{.95}}$$



Columbus Aircraft Division  
Rockwell International

PREPARED BY: <i>HR</i>	REPORT NO.
CHECKED BY:	PAGE NO. OF
DATE:	MODEL NO.

RIB-COMPOSITE WING, CENTER SECTION,  $X_w$  33.93 AFT  
8679-110112



$$F_{su} = (K_1 - K_2 \frac{D}{b}) F_{Tu} = (.46 - .395 \frac{3.5}{7.68}) 66,000$$

$$= 18,479 \text{ psi OR } 4805 \text{ psi}$$

$$M.S. = \frac{4805}{2264} - 1 = \underline{\underline{1.0}}$$



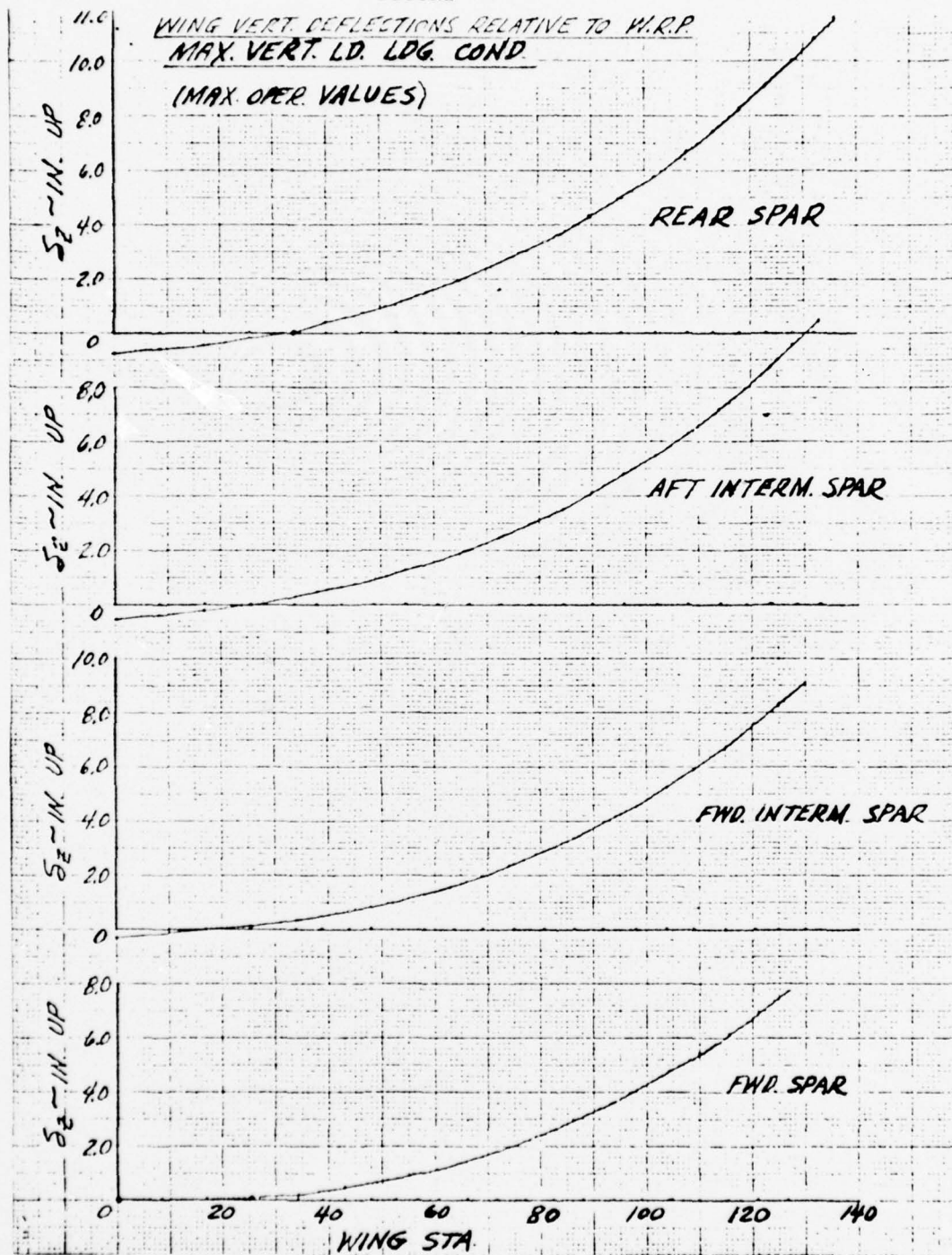
#### WING DEFLECTIONS

Figures A-20 and A-21 present the wing vertical deflection for each spar for the MAX. VERTICAL LANDING CONDITION and the critical flight condition, respectively. Deflections were defined by the NASTRAN computer program.



Columbus Aircraft Division  
Rockwell International

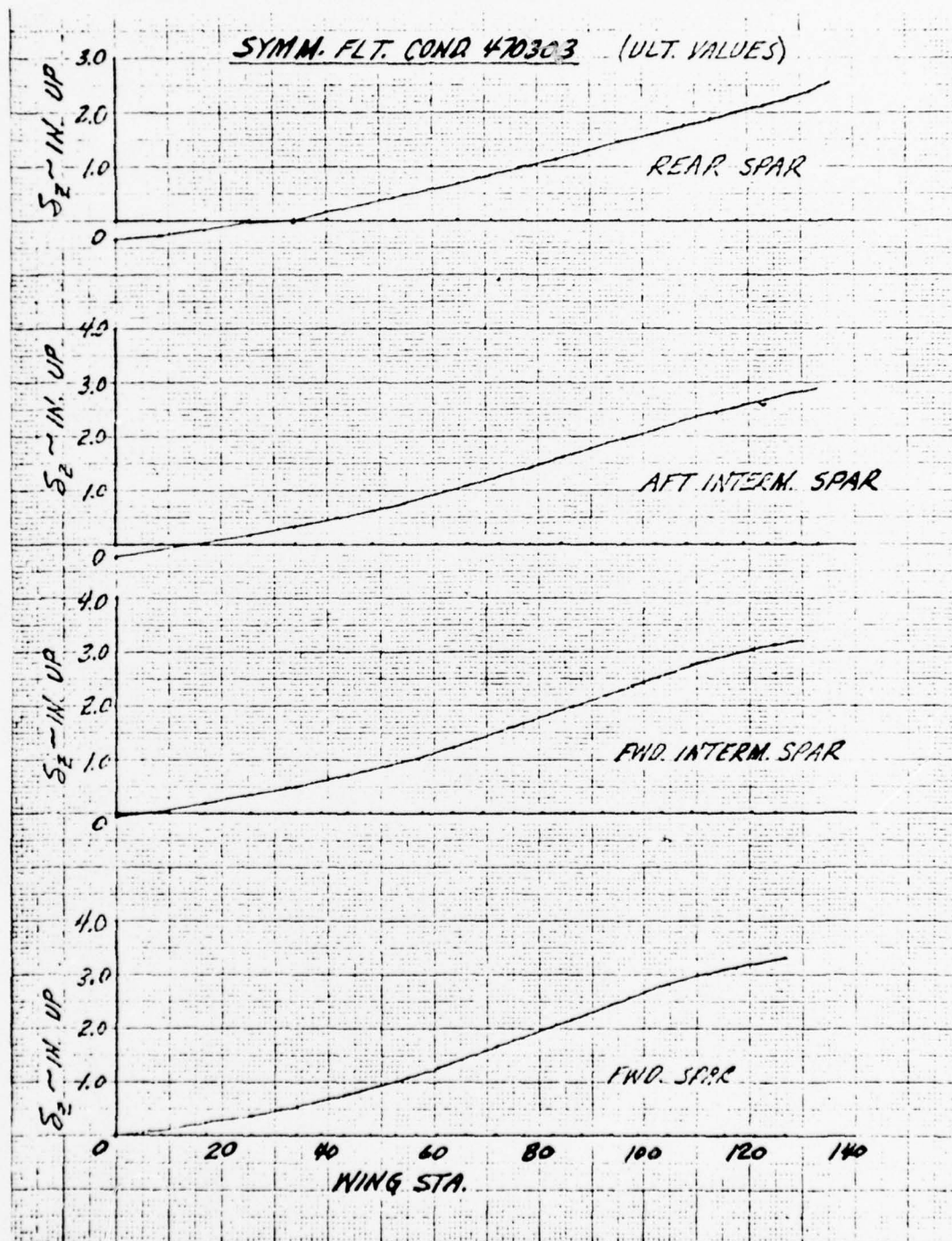
FIGURE A-20





Columbus Aircraft Division  
Rockwell International

FIGURE A-21 WING VERT. DEFLECTIONS RELATIVE TO W.R.P.



APPENDIX B  
COMPOSITE WING DRAWINGS

PRECEDING PAGE BLANK NOT FILMED

B-1 COMPOSITE WING TEST SECTION DRAWINGS

The drawings presented in this section include the structural assembly of the composite wing center section test specimen (8679-110100), upper and lower skin panels of the center section test specimen (8679-110101 and 8679-110102), and a production flow diagram for the test section. These drawings reflect the configuration fabricated and delivered to the Naval Air Development Center for test. Figure B-1 (8 sheets) describes the structural assembly, and Figures B-2 and B-3 illustrate the fabrication and assembly of the upper and lower skin panels, respectively. The production flow diagram for the test section is shown in Figure B-4.



20

20

19

18

17

16

15

8679-11018-023 1 REQD (UPPER SURFACE)  
 8679-11018-023 1 REQD (LOWER SURFACE)  
 8679-11017-005 1 REQD

HE111-0011-0608 4 REQD  
 HE111-0011-0609 2 REQD  
 HE114-0032-0006 6 REQD  
 8679-110101 REF

.56 (TYP LOWER SURFACE)

.75 (TYP LOWER SURFACE)

X<sub>W</sub> 33.930

.75 (TYP LOWER SURFACE)

8679-11011 REF

8679-11018-019 REF

8679-11018-019 1 REQD (UPPER SURFACE)  
 8679-11018-019 1 REQD (LOWER SURFACE)

WING UPPER PL

HE111-0011-0608 4 REQD  
 HE111-0011-0609 2 REQD  
 HE114-0032-0006 6 REQD

8679-11017-003 1 REQD

OUTER FRONT SPARE PLANE (B.75 R)

.915 REF

.50

.62

1.53

HE111-0011-0605 6 REQD  
 HE114-0032-0006 6 REQD

VIEW A  
 SCALE 1/1

9

SECTION B-B  
 SCALE 1/1

18

8679-110100

REV

A

1

20

19

18

17

16

15

2

15

14

13

12

11

W.R.P.

WING LOWER M.

8679-11011 REF

8679-11017-003 REF

8679-11018-013 REF

.56 REF

OUTBD FRONT SPAR PLANE

1.75

3.81

8679-110102 REF

HE111-0011-0609 REF  
(TYP THRU 8679-11017-005)

8679-110103 REF

HE111-0011-0608 REF  
(TYP THRU 8679-11017-005)SECTION 13-13  
SCALE 1/16

NAS158046T25  
LD153-0011-0018  
MS2104266  
NAS1106-24  
LD153-0011-0018  
LD153-0011-0018  
MS2104266

1 REQD UPPER  
1 REQD SURFACE  
1 REQD  
1 REQD  
1 REQD (UNDER BOLT HEAD)  
1 REQD (UNDER NUT)  
1 REQD

LOWER SURFACE

NAS158046T25 2 REQD  
LD153-0011-0018 2 REQD  
MS2104266 2 REQD  
NAS1106-24 2 REQD  
LD153-0011-0018 2 REQD  
LD153-0011-0018 2 REQD  
MS2104266 2 REQD

867

INBD AFT  
SPAR PLANE

NAS1104-15  
NAS1598-4R  
MS2107564  
MS20426403 (FLUSH IN 8679-11018-035)

10 REQD UPPER  
10 REQD SURFACE  
10 REQD ONLY  
20 REQD

NAS158044T14  
MS29513-010  
MS2107564  
MS20426403 (FLUSH IN 8679-11018-035)

15 REQD UPPER  
15 REQD SURFACE  
15 REQD ONLY  
30 REQD

INBD FWD INTRD  
SPAR PLANE

NAS1104-15  
NAS1598-4R  
MS2107564  
MS20426403 (FLUSH IN 8679-11018-023)

10 REQD UPPER  
10 REQD SURFACE  
10 REQD ONLY  
20 REQD

NAS158044T14  
MS29513-010  
MS2107564  
MS20426403 (FLUSH IN 8679-11018-023)

14 REQD UPPER  
14 REQD SURFACE  
14 REQD ONLY  
28 REQD

INBD FRONT  
SPAR PLANE

8679-110110 REF

X=0.000

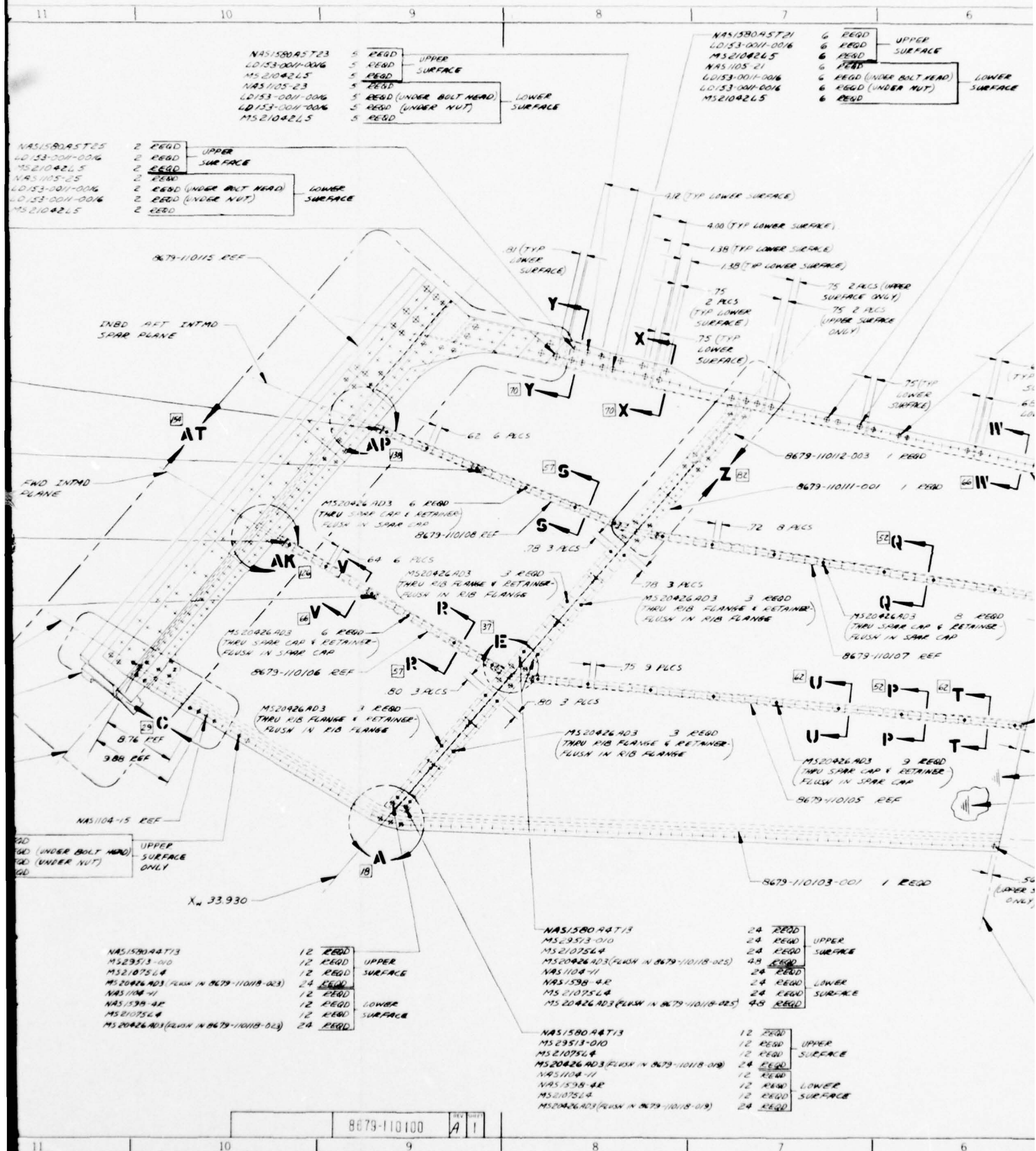
NAS1104-15 REF

NAS1104-15  
LD153-0011-0018  
LD153-0011-0018  
MS2104266

4 REQD UPPER  
4 REQD (UNDER BOLT HEAD) SURF  
4 REQD (UNDER NUT) ONLY  
4 REQD

NAS158044T14  
MS29513-010  
MS2107564  
MS20426403  
NAS1104-15  
NAS1598-4R  
MS2107564  
MS20426403

BEST AVAILABLE COPY









8679-11010

H

G

F

E

D

C

B

A

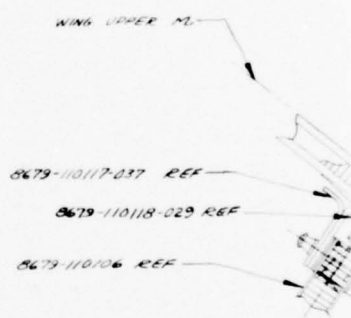
48

47

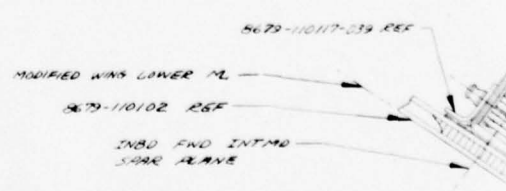
46

45

44

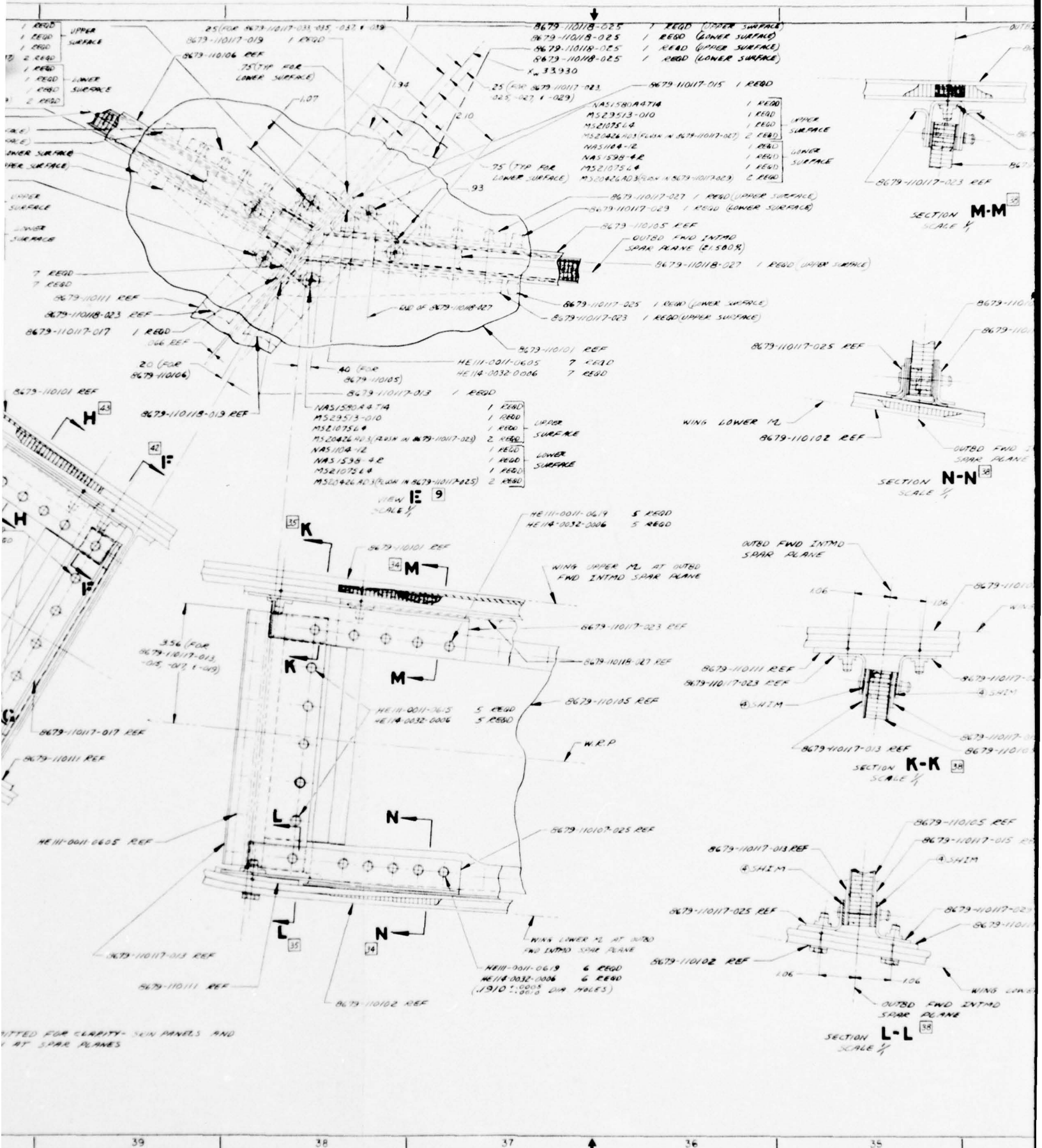


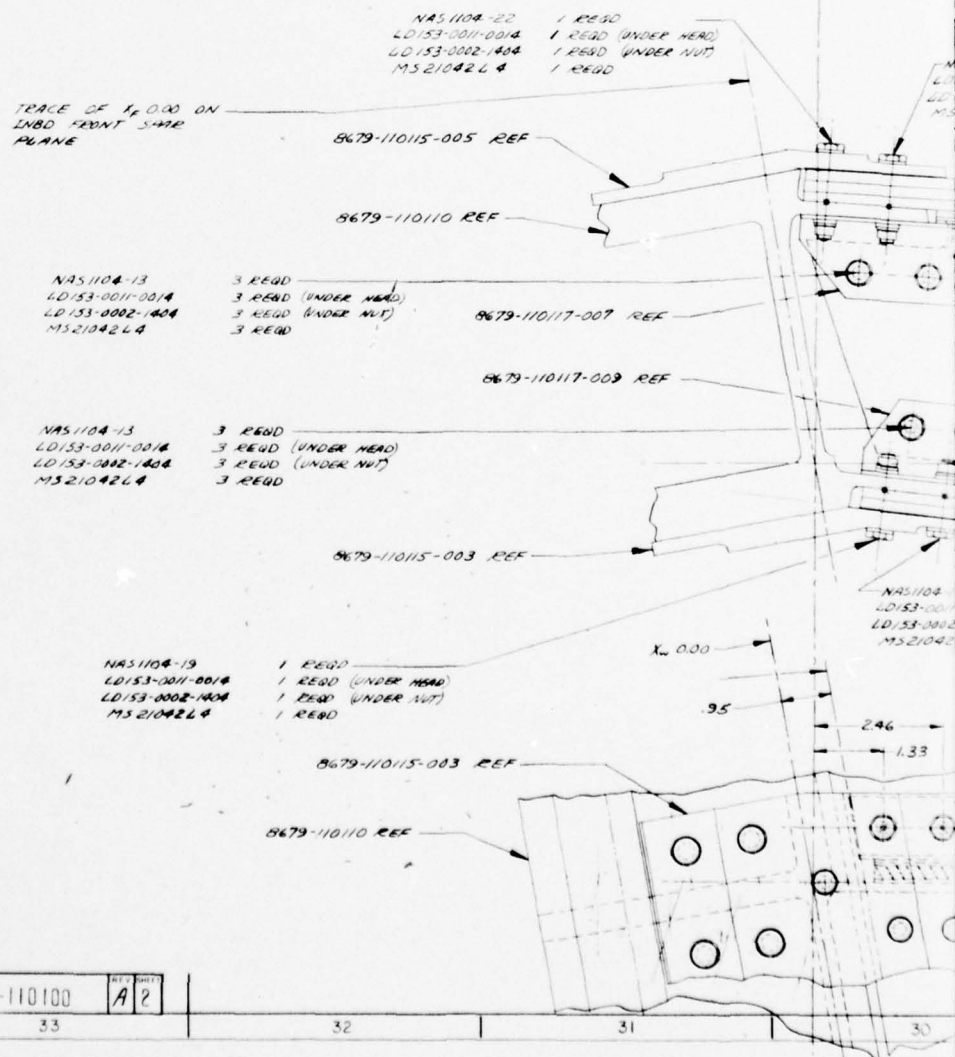
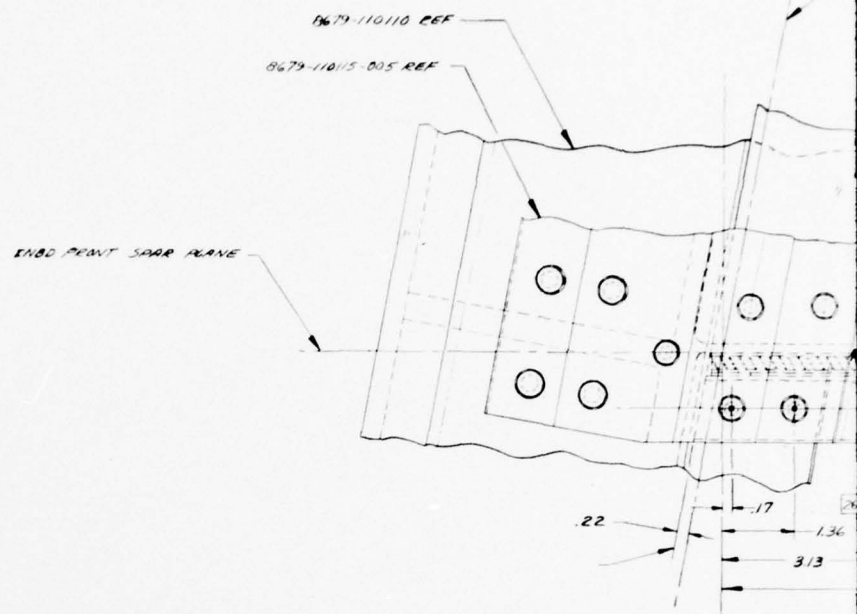
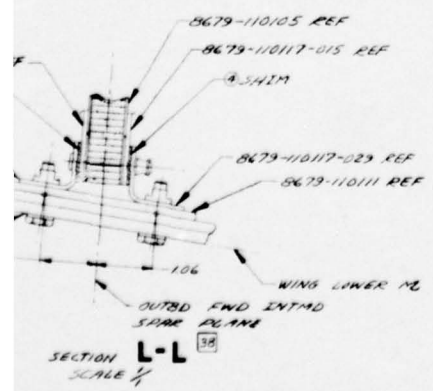
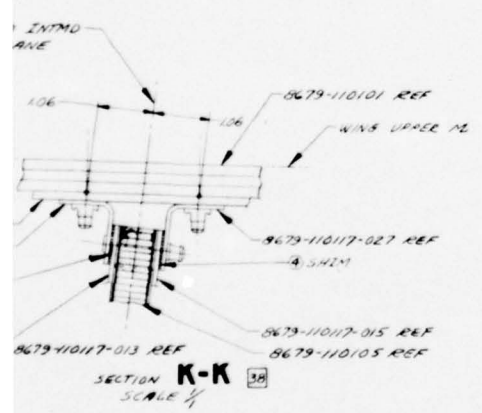
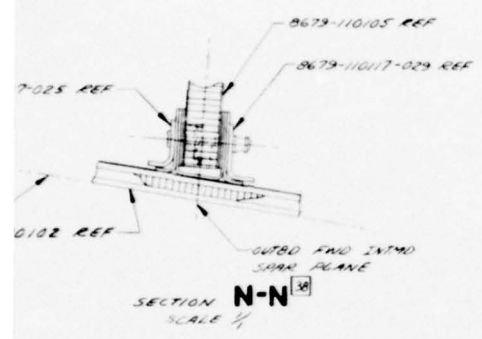
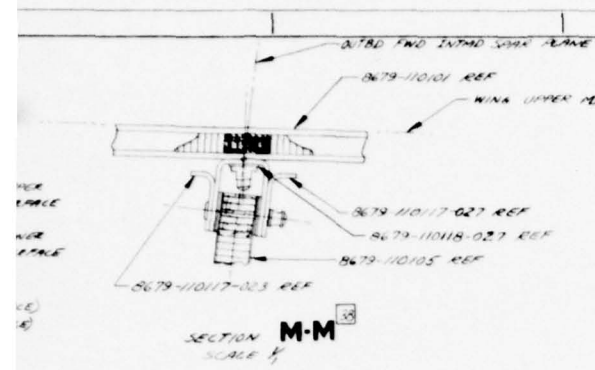
SECTION H  
SCALE



SECTION J  
SCALE 1/4



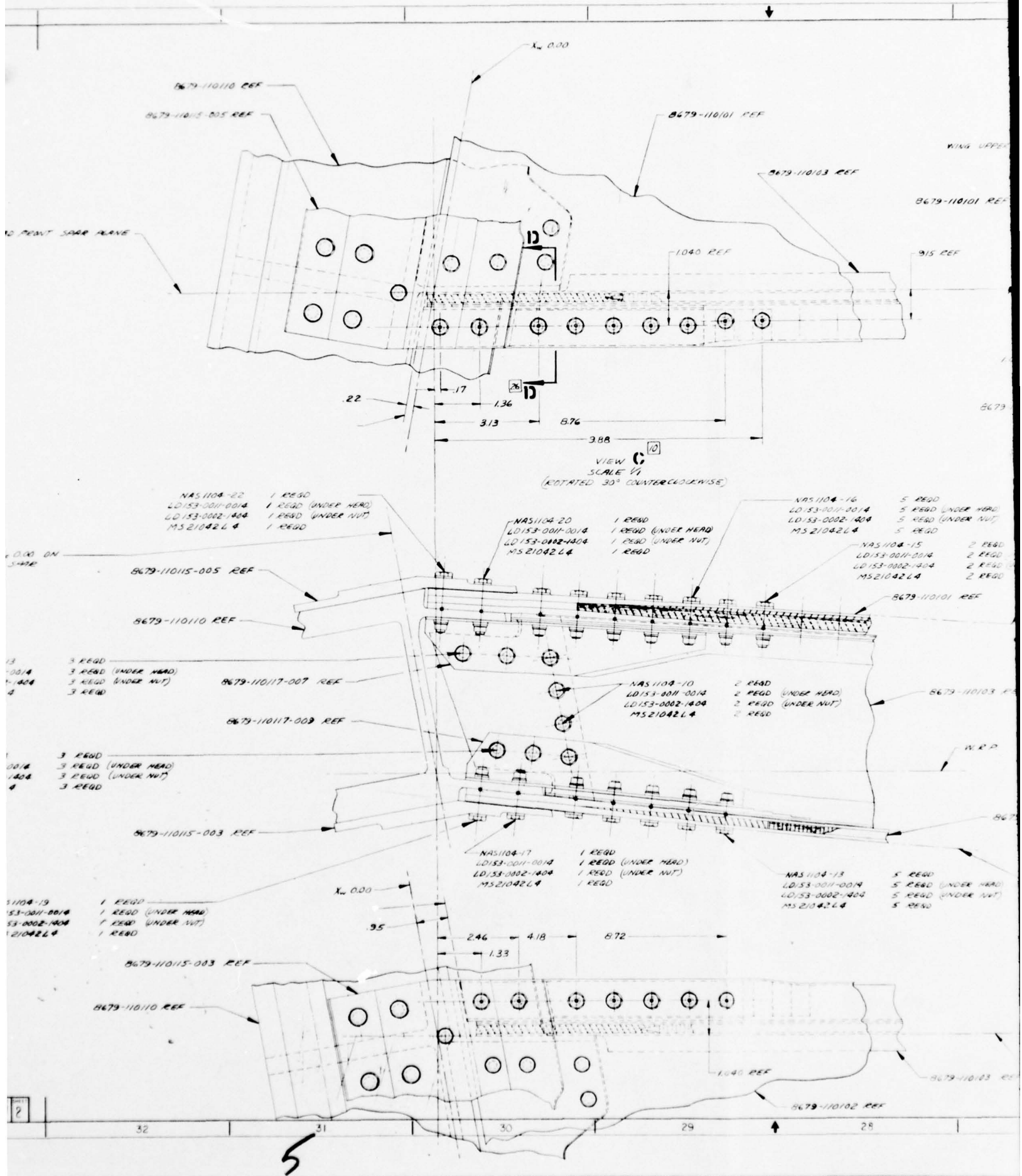




8679-110100  
A 2

4

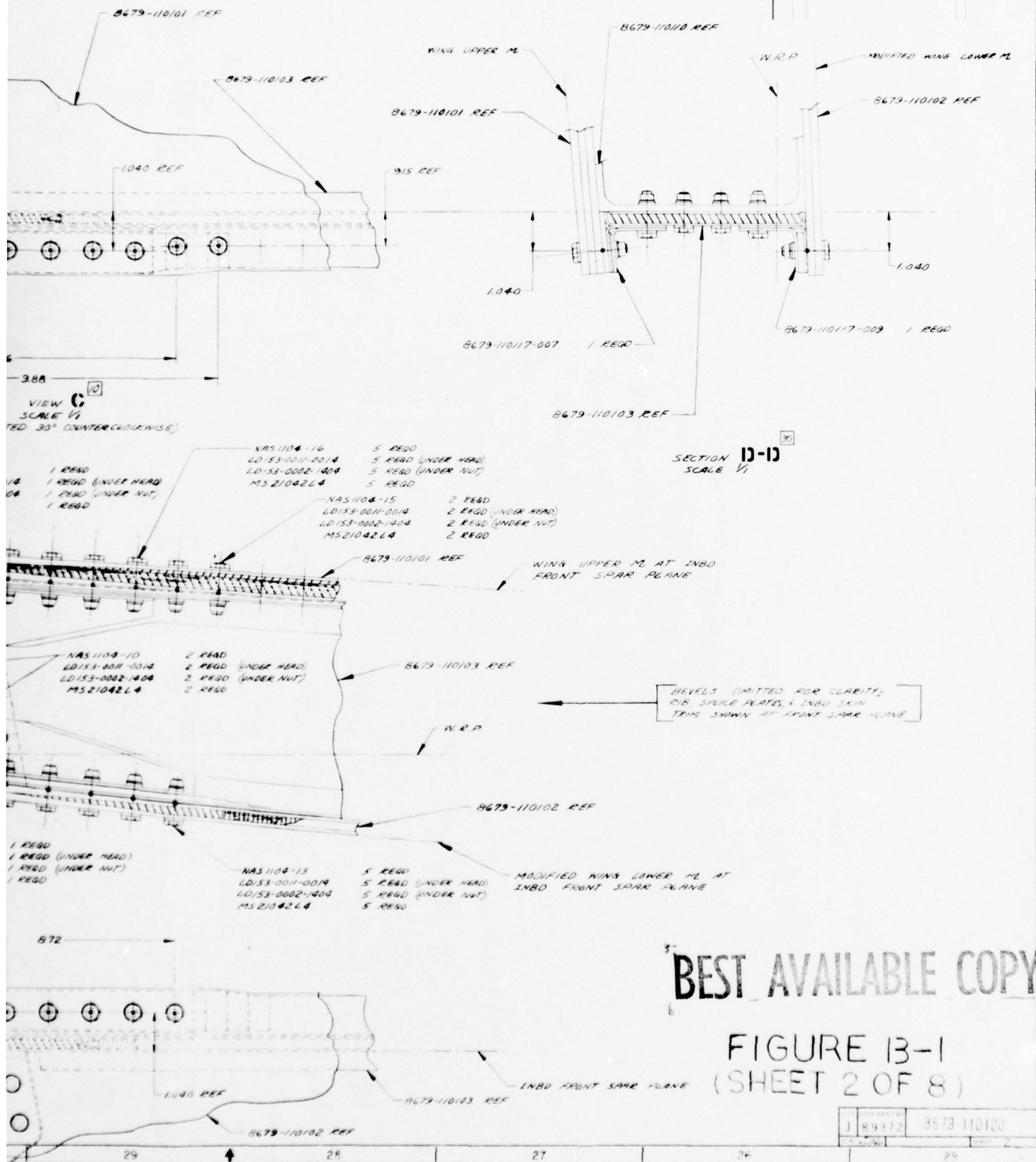






NR 76H 135  
PG B-4

REVISIONS		DATE	APPROVED
1	MAY BE REWORKED 2 CANNOT BE REWORKED		
2	REWORK CHANGES 3 NEW DATA PRACTICE		
3	REWORK CHANGES 4 NEW DATA PRACTICE		
4	REWORK CHANGES 5 NEW DATA PRACTICE		
5	REWORK CHANGES 6 NEW DATA PRACTICE		
6	REWORK CHANGES 7 NEW DATA PRACTICE		
7	REWORK CHANGES 8 NEW DATA PRACTICE		
8	REWORK CHANGES 9 NEW DATA PRACTICE		
9	REWORK CHANGES 10 NEW DATA PRACTICE		
10	REWORK CHANGES 11 NEW DATA PRACTICE		
11	REWORK CHANGES 12 NEW DATA PRACTICE		
12	REWORK CHANGES 13 NEW DATA PRACTICE		
13	REWORK CHANGES 14 NEW DATA PRACTICE		
14	REWORK CHANGES 15 NEW DATA PRACTICE		
15	REWORK CHANGES 16 NEW DATA PRACTICE		
16	REWORK CHANGES 17 NEW DATA PRACTICE		
17	REWORK CHANGES 18 NEW DATA PRACTICE		
18	REWORK CHANGES 19 NEW DATA PRACTICE		
19	REWORK CHANGES 20 NEW DATA PRACTICE		
20	REWORK CHANGES 21 NEW DATA PRACTICE		
21	REWORK CHANGES 22 NEW DATA PRACTICE		
22	REWORK CHANGES 23 NEW DATA PRACTICE		
23	REWORK CHANGES 24 NEW DATA PRACTICE		
24	REWORK CHANGES 25 NEW DATA PRACTICE		
25	REWORK CHANGES 26 NEW DATA PRACTICE		
26	REWORK CHANGES 27 NEW DATA PRACTICE		
27	REWORK CHANGES 28 NEW DATA PRACTICE		
28	REWORK CHANGES 29 NEW DATA PRACTICE		
29	REWORK CHANGES 30 NEW DATA PRACTICE		
30	REWORK CHANGES 31 NEW DATA PRACTICE		
31	REWORK CHANGES 32 NEW DATA PRACTICE		
32	REWORK CHANGES 33 NEW DATA PRACTICE		
33	REWORK CHANGES 34 NEW DATA PRACTICE		
34	REWORK CHANGES 35 NEW DATA PRACTICE		
35	REWORK CHANGES 36 NEW DATA PRACTICE		
36	REWORK CHANGES 37 NEW DATA PRACTICE		
37	REWORK CHANGES 38 NEW DATA PRACTICE		
38	REWORK CHANGES 39 NEW DATA PRACTICE		
39	REWORK CHANGES 40 NEW DATA PRACTICE		
40	REWORK CHANGES 41 NEW DATA PRACTICE		
41	REWORK CHANGES 42 NEW DATA PRACTICE		
42	REWORK CHANGES 43 NEW DATA PRACTICE		
43	REWORK CHANGES 44 NEW DATA PRACTICE		
44	REWORK CHANGES 45 NEW DATA PRACTICE		
45	REWORK CHANGES 46 NEW DATA PRACTICE		
46	REWORK CHANGES 47 NEW DATA PRACTICE		
47	REWORK CHANGES 48 NEW DATA PRACTICE		
48	REWORK CHANGES 49 NEW DATA PRACTICE		
49	REWORK CHANGES 50 NEW DATA PRACTICE		
50	REWORK CHANGES 51 NEW DATA PRACTICE		
51	REWORK CHANGES 52 NEW DATA PRACTICE		
52	REWORK CHANGES 53 NEW DATA PRACTICE		
53	REWORK CHANGES 54 NEW DATA PRACTICE		
54	REWORK CHANGES 55 NEW DATA PRACTICE		
55	REWORK CHANGES 56 NEW DATA PRACTICE		
56	REWORK CHANGES 57 NEW DATA PRACTICE		
57	REWORK CHANGES 58 NEW DATA PRACTICE		
58	REWORK CHANGES 59 NEW DATA PRACTICE		
59	REWORK CHANGES 60 NEW DATA PRACTICE		
60	REWORK CHANGES 61 NEW DATA PRACTICE		
61	REWORK CHANGES 62 NEW DATA PRACTICE		
62	REWORK CHANGES 63 NEW DATA PRACTICE		
63	REWORK CHANGES 64 NEW DATA PRACTICE		
64	REWORK CHANGES 65 NEW DATA PRACTICE		
65	REWORK CHANGES 66 NEW DATA PRACTICE		
66	REWORK CHANGES 67 NEW DATA PRACTICE		
67	REWORK CHANGES 68 NEW DATA PRACTICE		
68	REWORK CHANGES 69 NEW DATA PRACTICE		
69	REWORK CHANGES 70 NEW DATA PRACTICE		
70	REWORK CHANGES 71 NEW DATA PRACTICE		
71	REWORK CHANGES 72 NEW DATA PRACTICE		
72	REWORK CHANGES 73 NEW DATA PRACTICE		
73	REWORK CHANGES 74 NEW DATA PRACTICE		
74	REWORK CHANGES 75 NEW DATA PRACTICE		
75	REWORK CHANGES 76 NEW DATA PRACTICE		
76	REWORK CHANGES 77 NEW DATA PRACTICE		
77	REWORK CHANGES 78 NEW DATA PRACTICE		
78	REWORK CHANGES 79 NEW DATA PRACTICE		
79	REWORK CHANGES 80 NEW DATA PRACTICE		
80	REWORK CHANGES 81 NEW DATA PRACTICE		
81	REWORK CHANGES 82 NEW DATA PRACTICE		
82	REWORK CHANGES 83 NEW DATA PRACTICE		
83	REWORK CHANGES 84 NEW DATA PRACTICE		
84	REWORK CHANGES 85 NEW DATA PRACTICE		
85	REWORK CHANGES 86 NEW DATA PRACTICE		
86	REWORK CHANGES 87 NEW DATA PRACTICE		
87	REWORK CHANGES 88 NEW DATA PRACTICE		
88	REWORK CHANGES 89 NEW DATA PRACTICE		
89	REWORK CHANGES 90 NEW DATA PRACTICE		
90	REWORK CHANGES 91 NEW DATA PRACTICE		
91	REWORK CHANGES 92 NEW DATA PRACTICE		
92	REWORK CHANGES 93 NEW DATA PRACTICE		
93	REWORK CHANGES 94 NEW DATA PRACTICE		
94	REWORK CHANGES 95 NEW DATA PRACTICE		
95	REWORK CHANGES 96 NEW DATA PRACTICE		
96	REWORK CHANGES 97 NEW DATA PRACTICE		
97	REWORK CHANGES 98 NEW DATA PRACTICE		
98	REWORK CHANGES 99 NEW DATA PRACTICE		
99	REWORK CHANGES 100 NEW DATA PRACTICE		



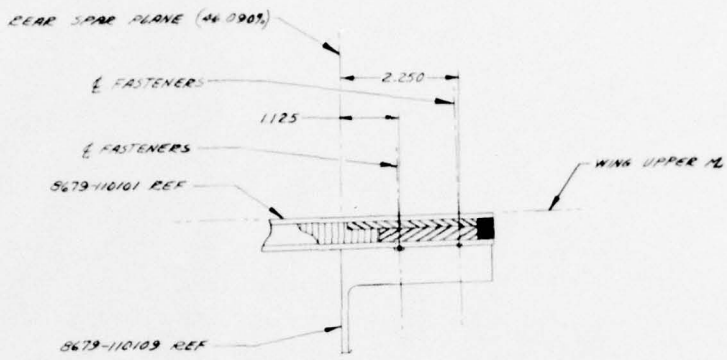
BEST AVAILABLE COPY

FIGURE B-1  
(SHEET 2 OF 8)

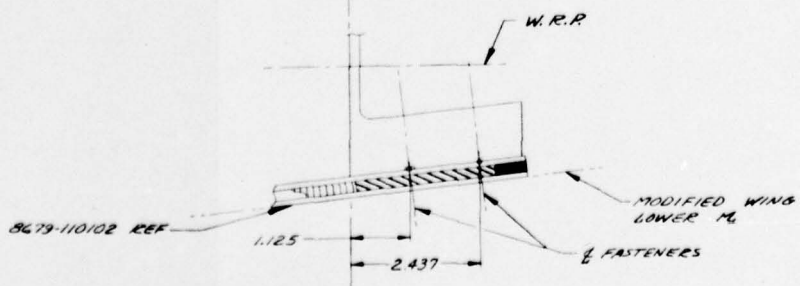
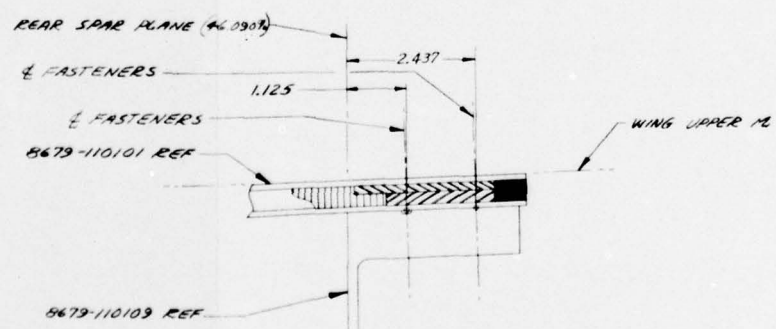
1	89372	8679-110100
2		
3		
4		
5		
6		
7		
8		
9		
10		
11		
12		
13		
14		
15		
16		
17		
18		
19		
20		
21		
22		
23		
24		
25		
26		
27		
28		
29		
30		
31		
32		
33		
34		
35		
36		
37		
38		
39		
40		
41		
42		
43		
44		
45		
46		
47		
48		
49		
50		
51		
52		
53		
54		
55		
56		
57		
58		
59		
60		
61		
62		
63		
64		
65		
66		
67		
68		
69		
70		
71		
72		
73		
74		
75		
76		
77		
78		
79		
80		
81		
82		
83		
84		
85		
86		
87		
88		
89		
90		
91		
92		
93		
94		
95		
96		
97		
98		
99		
100		

6

8679-110100

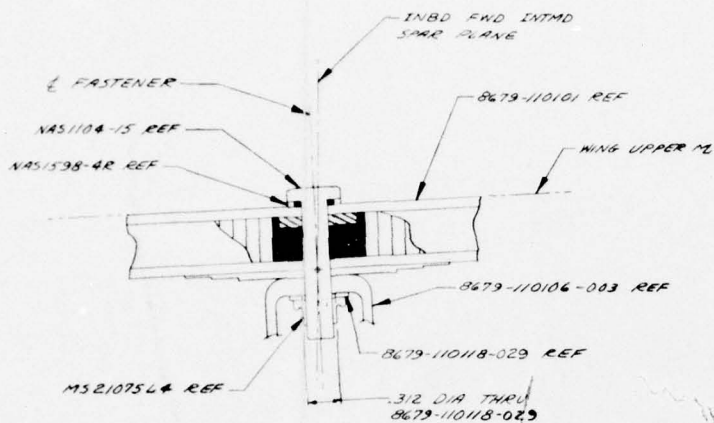


SECTION X-X  
SCALE 1/2  
(ROTATED 79° CLOCKWISE)

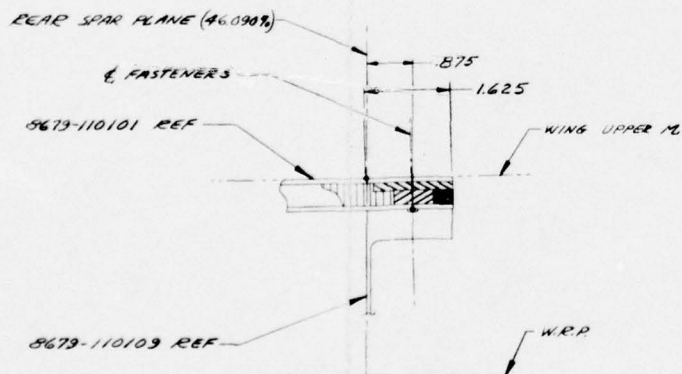


SECTION Y-Y  
SCALE 1/2  
(ROTATED 79° CLOCKWISE)

8679-110100



SECTION **V-V**  
 SCALE  $\frac{1}{4}$   
 (TYP NAS1598 WASHER INSTALLATION)  
 (ROTATED 60° CLOCKWISE)



SECTION **W-W**  
 SCALE  $\frac{1}{4}$   
 (ROTATED 75° CLOCKWISE)

415 ± .005  
 63/

125 REF

.031 ± .005 R 63/

.28 (TYP FOR ALL NUTPLATE RETAINERS IN INTMD SPAR CAPS)

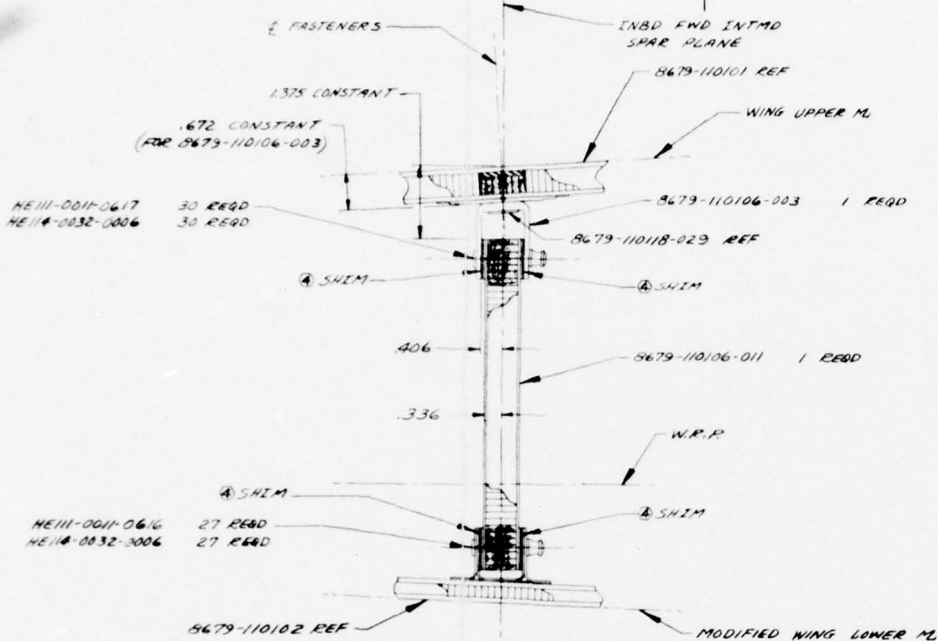
.312 DIA 8679-110101 REF  
 (DIA. TYP FOR ALL FASTENERS)  
 OUTBD FWD INTMD SPAR PLANE (21.500 ± .005)

FASTENERS

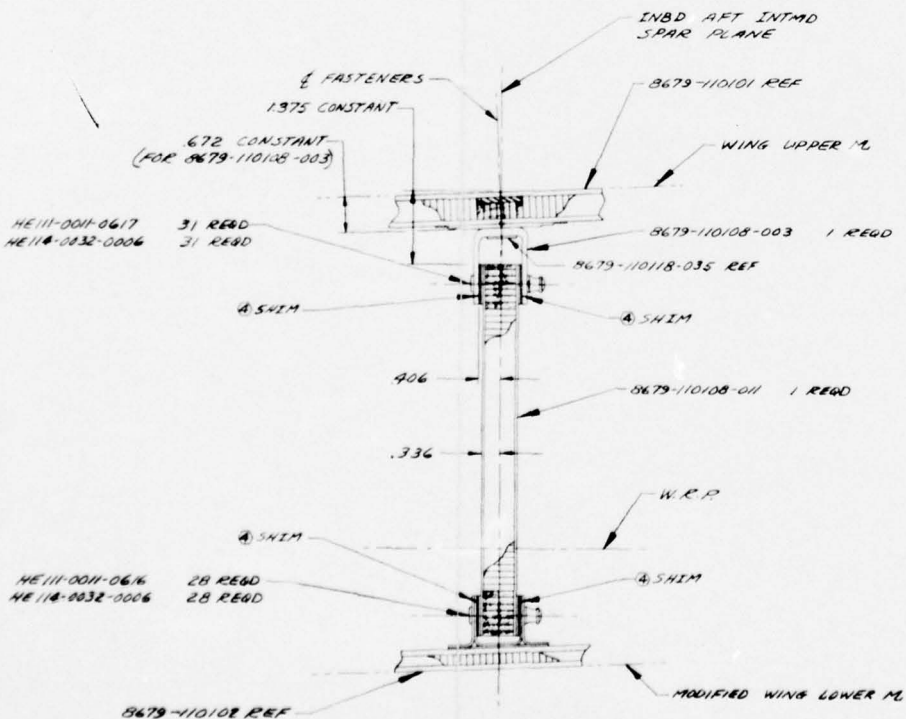
8679-110101 REF

MS21075L4 REF





SECTION **R-R**  
SCALE 1/2  
(ROTATED 60° CLOCKWISE)

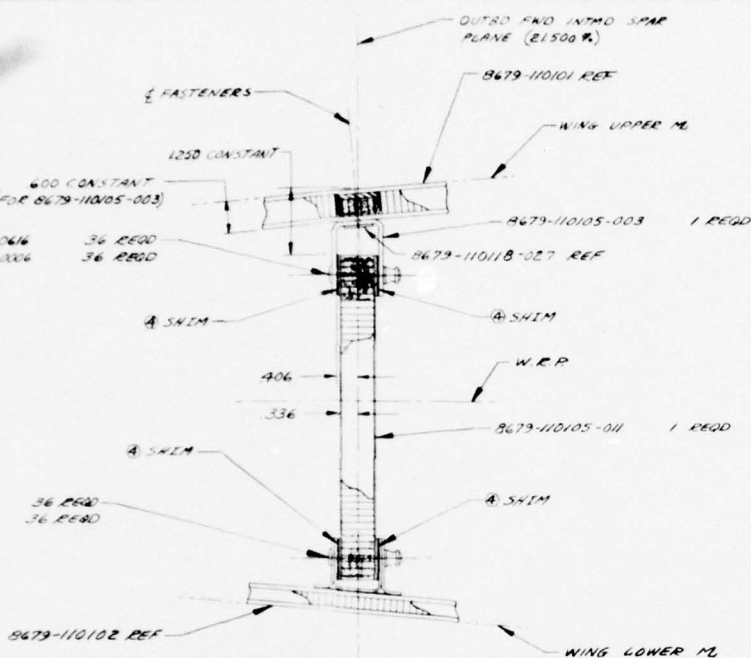


SECTION **S-S**  
SCALE 1/2  
(ROTATED 60° CLOCKWISE)

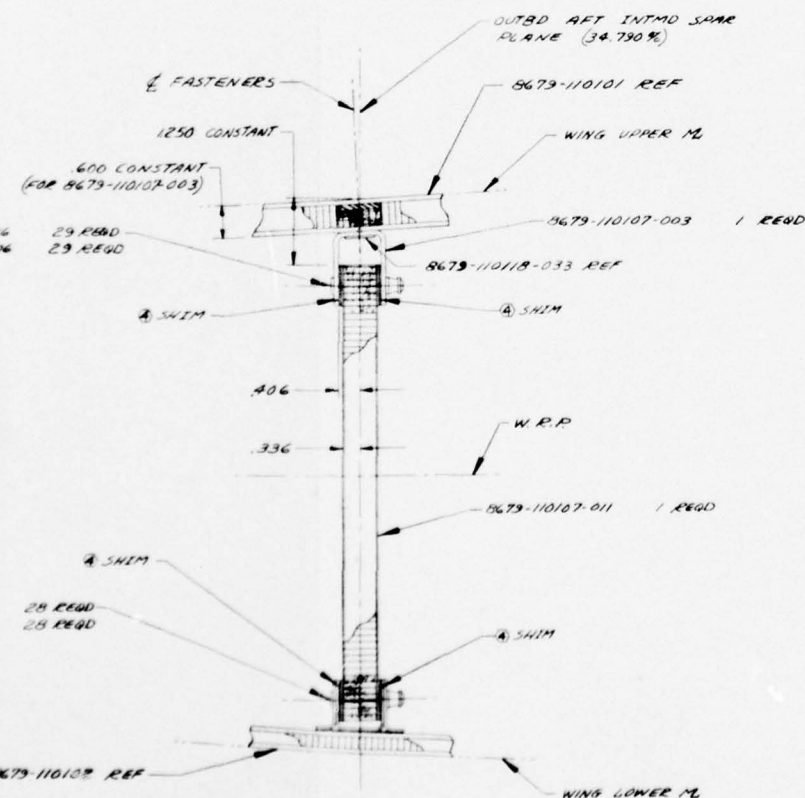


REVISIONS			
NO.	DESCRIPTION	DATE	APPROVED
1	MAY BE REWORKED 2 CANNOT BE REWORKED 3 REWORK CHANGE 4 NEW TECH PRACTICE 5 PARTS MADE IN		
1	FOR REVISIONS SEE PAGE 8679-110100	1-5-76	

NR76H-135  
PG 13-5



SECTION P-P  
SCALE 1/2  
(ROTATED 85° CLOCKWISE)



SECTION Q-Q  
SCALE 1/2  
(ROTATED 80° CLOCKWISE)

BEST AVAILABLE COPY

FIGURE 13-1  
(SHEET 3 OF 8)

DATE	893372	8679-110100
BY		
CHECKED		
APPROVED		

8679-110100

H

G

F

E

D

C

B

A

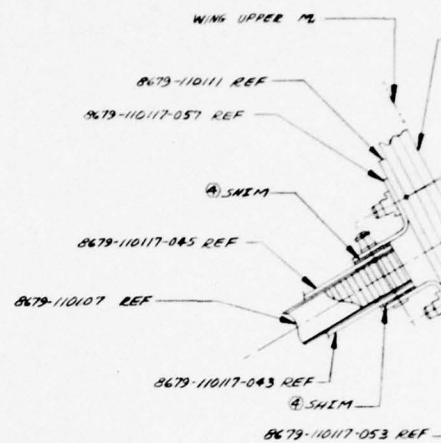
96

95

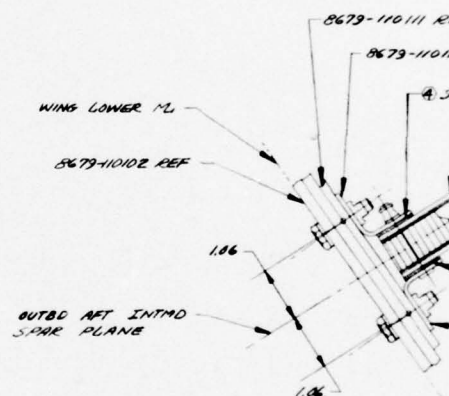
94

93

92



SECTION AC-



SECTION AD-

8679-110111 REF

8679-110117-057 REF

④ SHIM

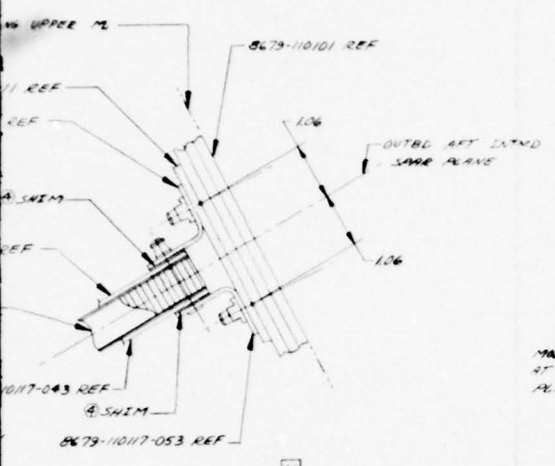
WING LOWER PL

8679-110102 REF

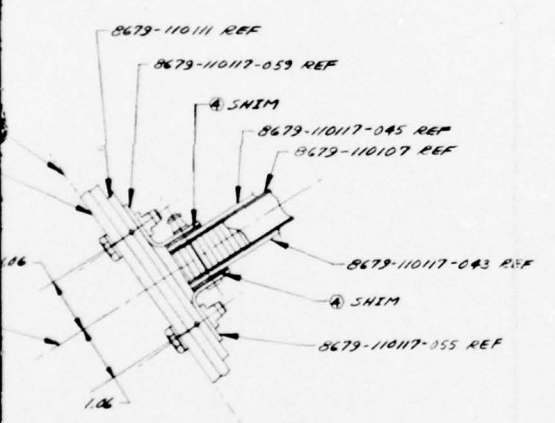
1.06

OUTBD AFT INTMD SPAR PLANE

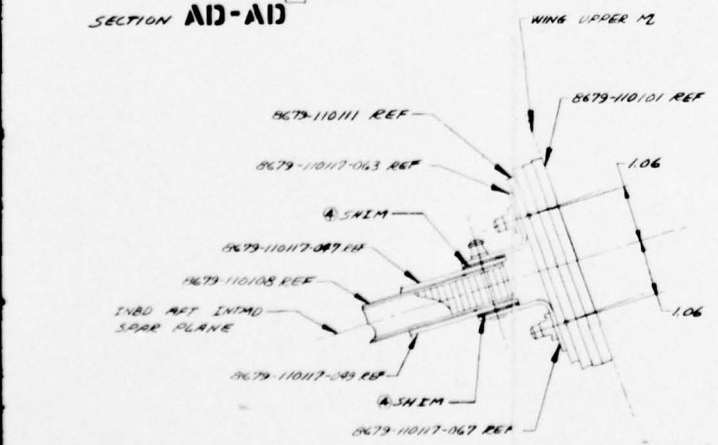
1.06



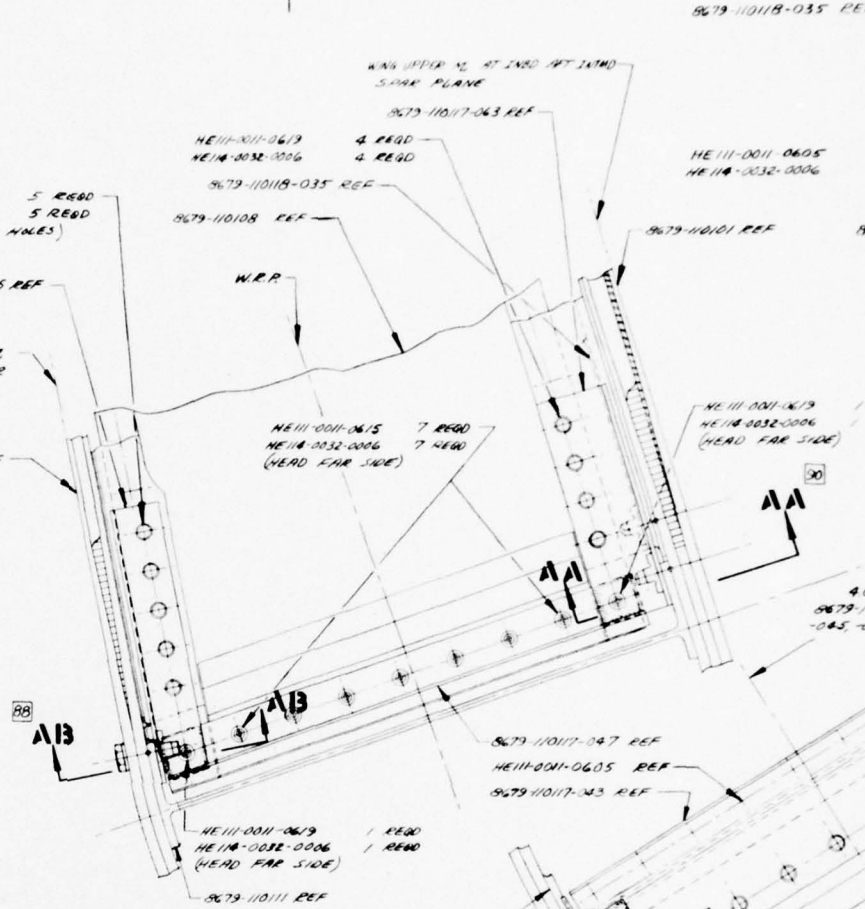
SECTION AC-AC



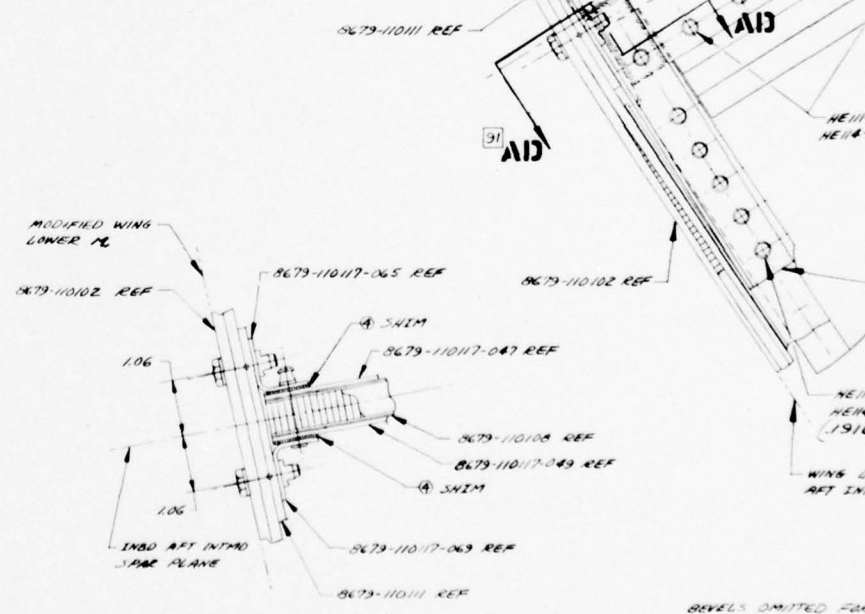
SECTION AD-AD



SECTION AA-AA

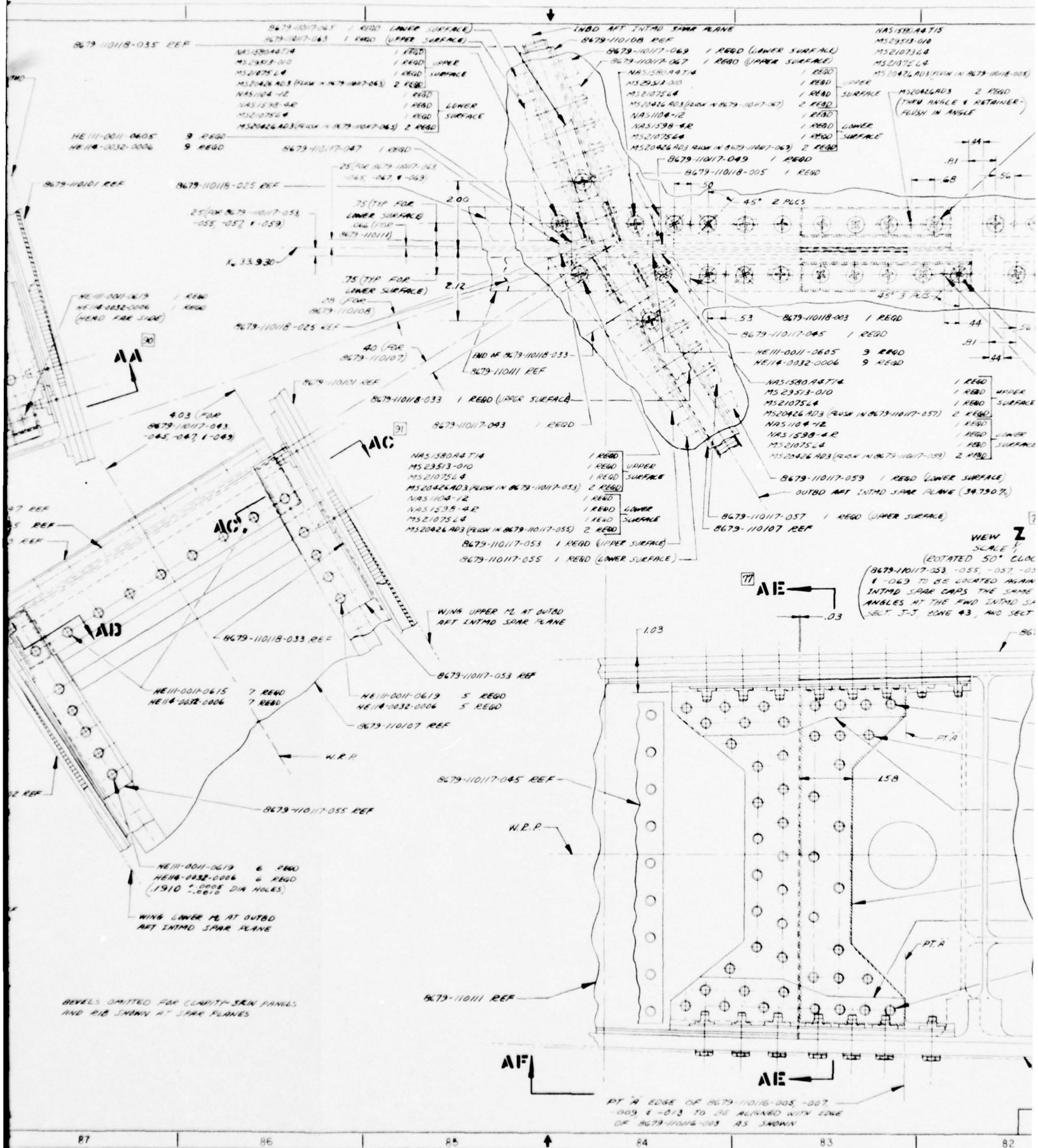


SECTION AB-AB



REVELS OMITTED FOR AND RIB SHOWN AT

8679-110100	REV SHEET
	A 4





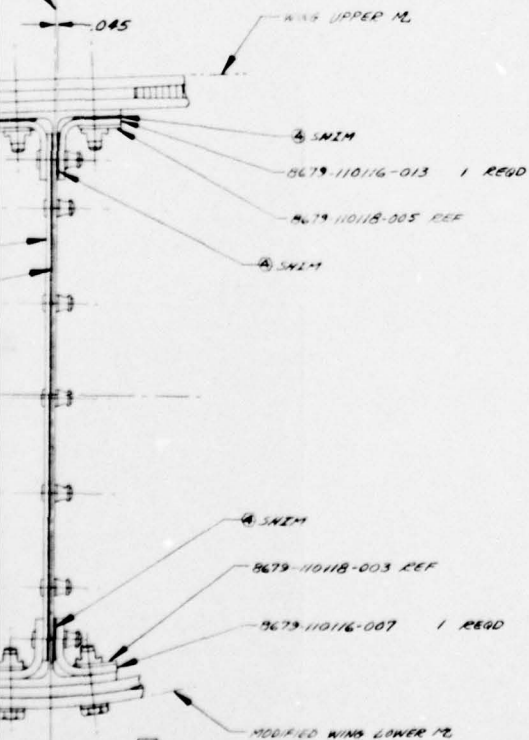




REVISIONS			
NO.	DESCRIPTION	DATE	APPROVED
MAY BE DELETED 2 CANNOT BE DELETED			
1 RECORD CHANGES 2 NEW SHEET PRACTICE			
3 RIGHTS MADE IN			
A	FOR REVISIONS, SEE AL 5679-110100	1-5-76	H. M. PALLOCK

NR 76H-135  
PG 13-6

33.930



BEST AVAILABLE COPY

FIGURE B-1

(SHEET 4 OF 8)

WING AIE-AIE  
AGE 1  
116-003, -007, & -013 TO 08  
8679-110111

89372	8679-110-00
4	4

5

001010100

H

G

F

E

D

C

B

A

120

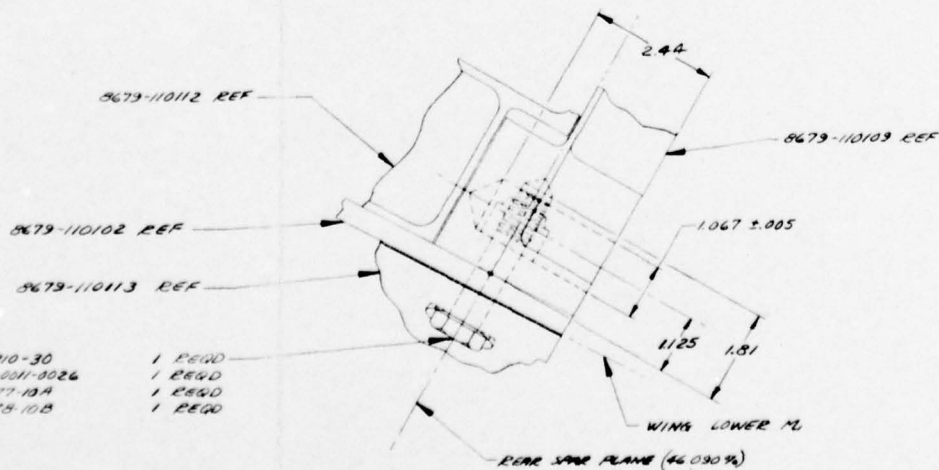
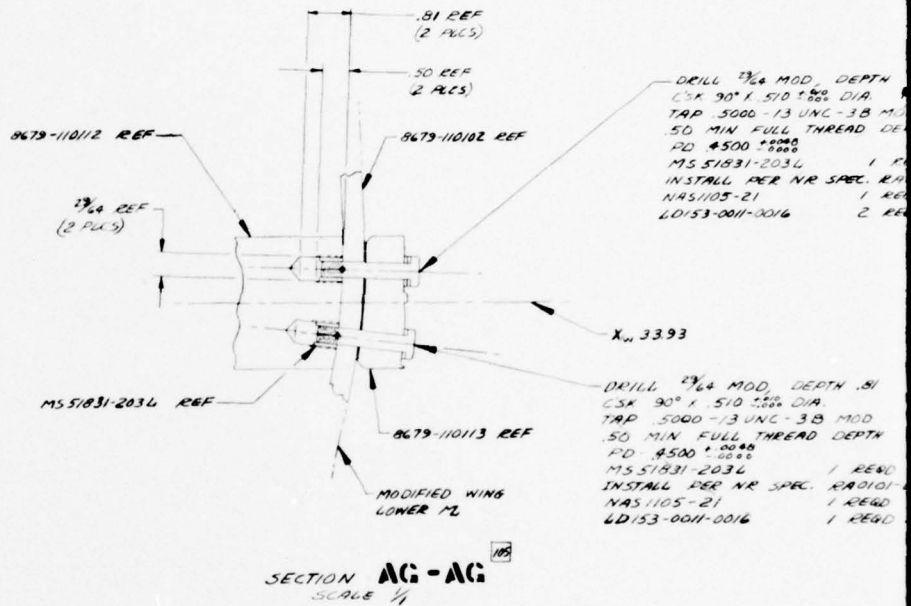
119

118

117

116

NAS 1310-3  
L0153-0001  
NAS 1777-10  
NAS 178-10



SECTION AJ-AJ  
SCALE  $\frac{1}{1}$   
(CENTERS OF INTERSECTING HOLES  
SHALL COINCIDE WITHIN .010)

8679-110100

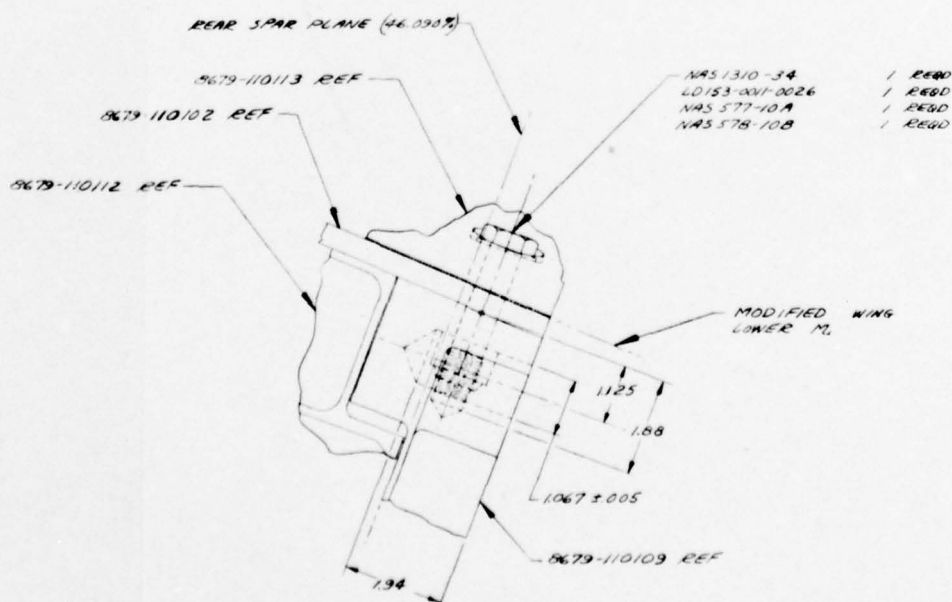
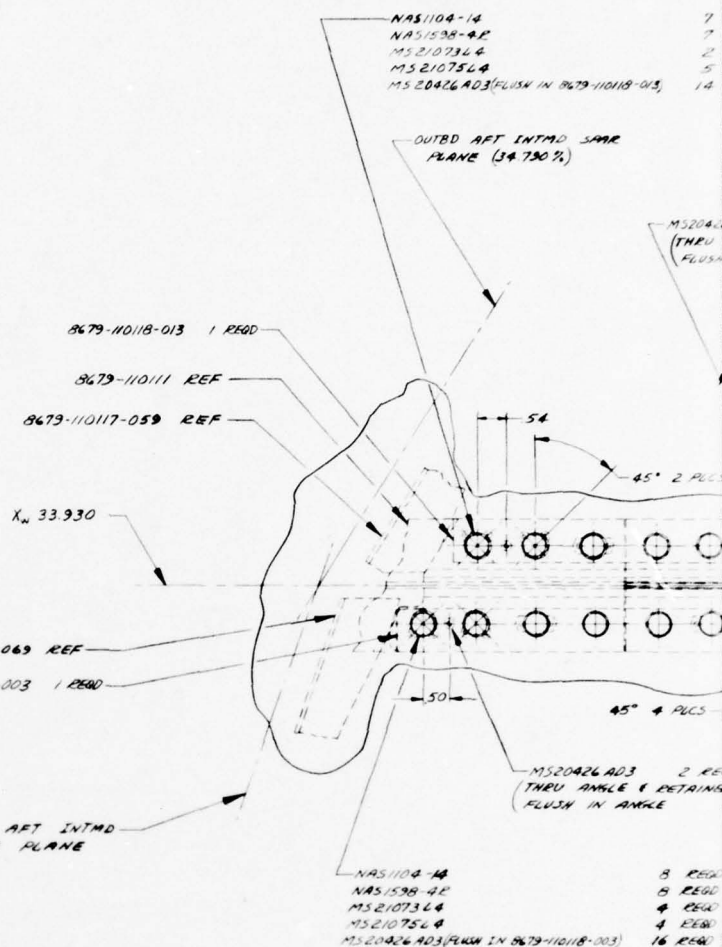
REV. SHEET  
A 5

2

DRILL  $\frac{7}{8}$  MOD. DEPTH .81  
 CSK 90° X .510  $\pm .005$  DIA.  
 TAP .5000 -13 UNC -3B MOD  
 .50 MIN FULL THREAD DEPTH  
 RD  $\pm .0005$   
 MS 51831-2034 1 REQD  
 INSTALL PER NR SPEC. RAD101-003  
 NAS1105-21 1 REQD  
 LD153-0011-0016 2 REQD

X<sub>w</sub> 33.93

DRILL  $\frac{7}{8}$  MOD. DEPTH .81  
 CSK 90° X .510  $\pm .005$  DIA.  
 TAP .5000 -13 UNC -3B MOD  
 .50 MIN FULL THREAD DEPTH  
 RD  $\pm .0005$   
 MS 51831-2034 1 REQD  
 INSTALL PER NR SPEC. RAD101-003  
 NAS1105-21 1 REQD  
 LD153-0011-0016 1 REQD



SECTION AH-AH  
 SCALE  $\frac{1}{4}$   
 (CENTERS OF INTERSECTING HOLES  
 SHALL COINCIDE WITHIN .010)

3



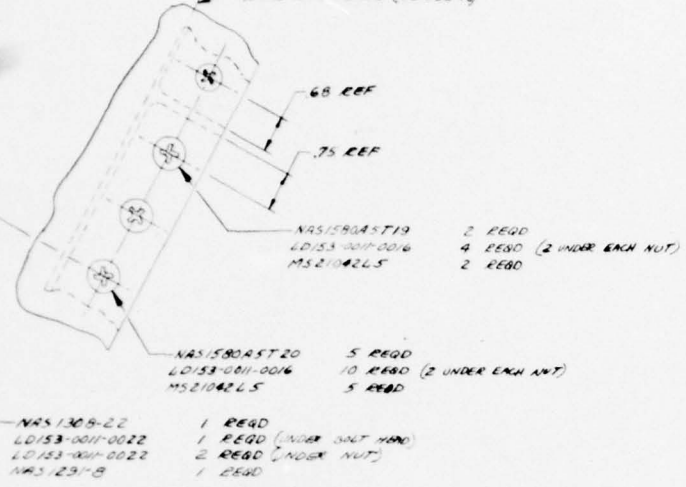




REAR SPAR PLANE (86.090 P)

REVISIONS		DATE	APPROVED
1	MAY BE REWORKED		
2	CANNOT BE REWORKED		
3	REWORK CHANGE		
4	NEW SHOP PRACTICE		
5	PARTS MADE IN		
FOR REVISIONS SEE		8679-110100	J. M. ANGLICK
PL 8679-110100			1-5-76

NR76H-135  
PG B-7



BEST AVAILABLE COPY

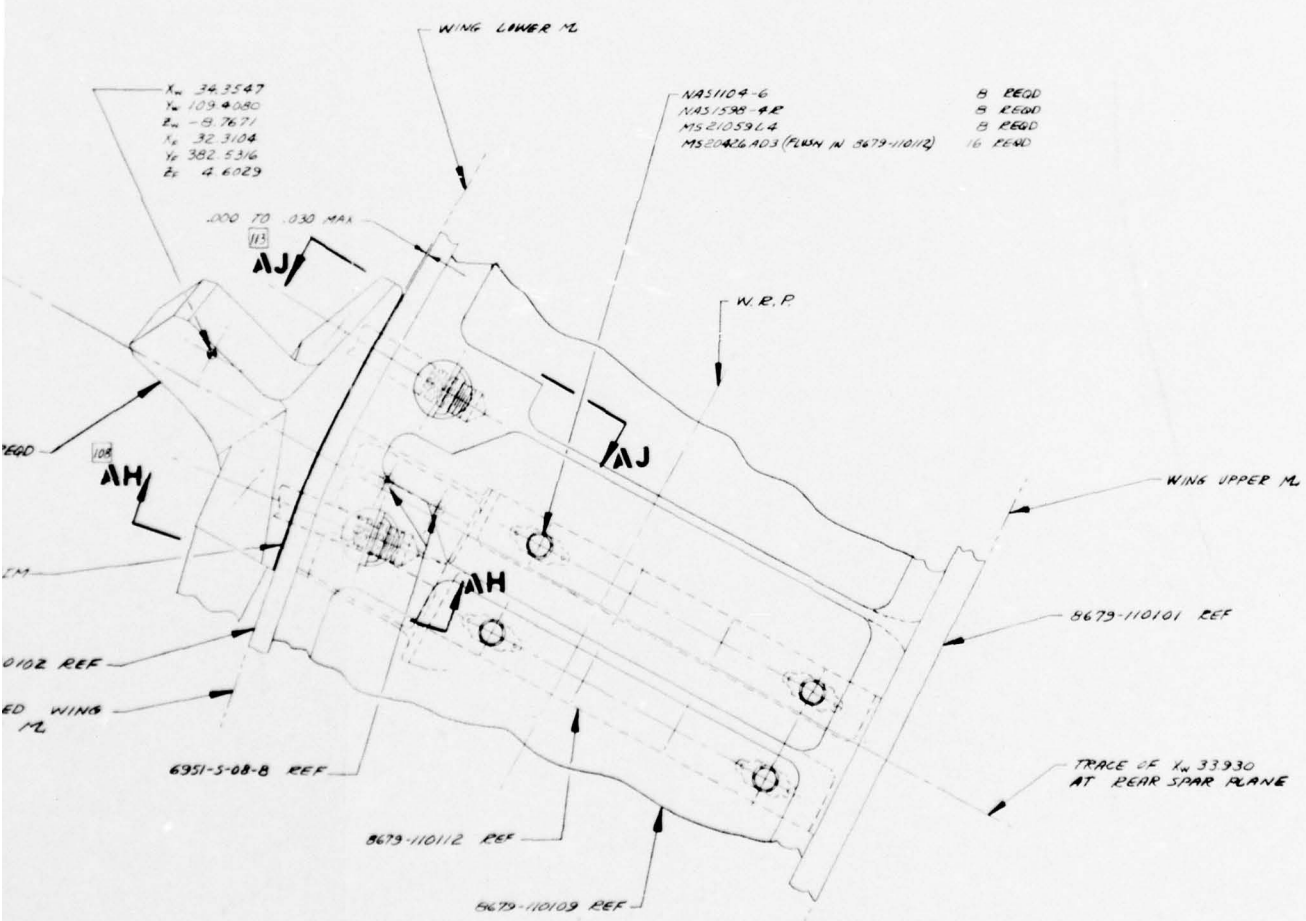


FIGURE B-1  
(SHEET 5 OF 8)

DATE	DEL. DATE	8679-110100
J 89372		
SCALE	SHEET	5

A

8679-110117-089 es

NAS1105-23  
NAS1105-27  
60153-001-0016  
MS2107545  
MS20426A04 (PLWN IN 8679-11017-099)

178

A(2)

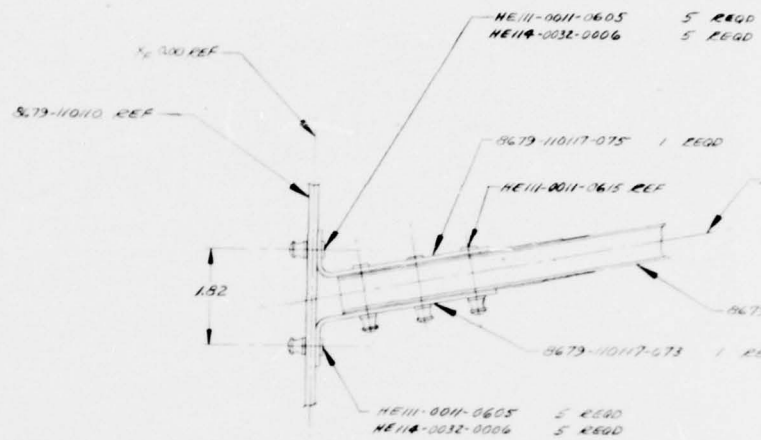
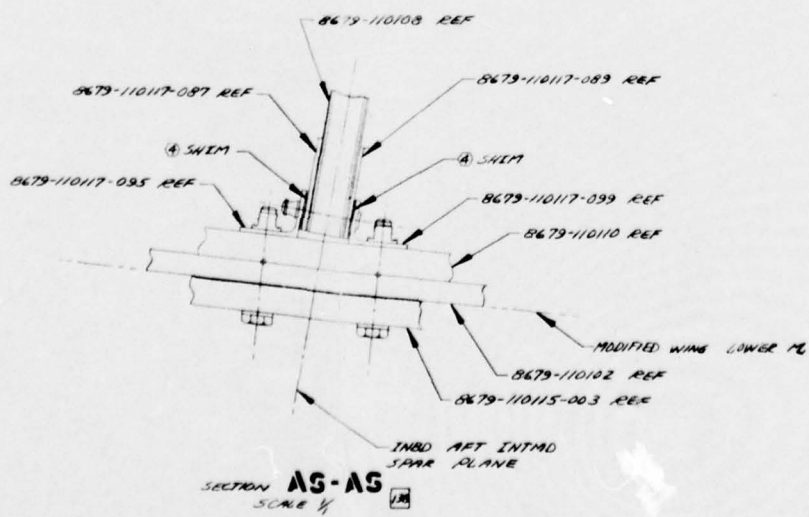
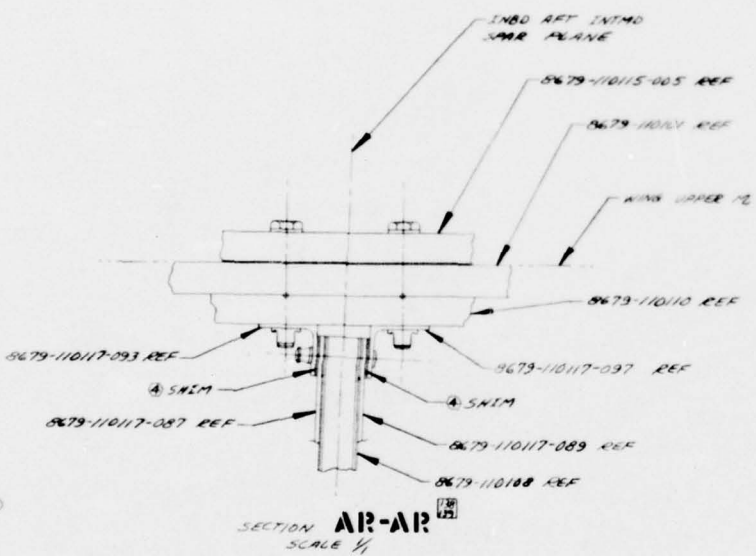


94E)

93)

REF

1 REQD  
INST VERT  
93-021



BEVE  
PLA  
SHA  
PLA



0605 5 RECD  
0606 5 RECD

0705 1 RECD

0615 REF

INBD FWD INTMD SPAR PLANE

8679-110106 REF

8679-110117-073 1 RECD

RECD  
RECD

END OF 8679-110117-083

X<sub>N</sub> 0.00

.33

.322

8679-110110 REF

8679-110115-005 REF

8679-110117-075 REF

8679-110117-073 REF

END OF 8679-110118-029

.38

END OF 8679-110117-077

TRACE OF X<sub>N</sub> 0.00 ON INBD FWD INTMD SPAR PLANE

8679-110115-005 REF

8679-110110 REF

HE111-0011-0615 9 RECD  
HE114-0032-0006 9 RECD  
(HEAD FAR SIDE) (19101.0005 DIA HOLES)

8679-110117-073 REF

HE111-0011-0605 REF

8679-110115-003 REF

X<sub>N</sub> 0.00

END OF 8679-110117-079 & 8679-110117-085

.81

8679-110117-073 REF

8679-110110 REF

8679-110115-003 REF

8679-110117-075 REF

8679-110102 REF

BEVELS OMITTED FOR CLARITY, RIB, SPICE PLATES, & INBD SKIN TRIM SHOWN AT INBD FWD INTMD SPAR PLANE

NAS 1104-18  
NAS 1104-21  
LD153-0014-0004  
MS 21075-24  
MS 20426-AD3 (FLUSH IN 8679-110117-085)

1 RECD  
1 RECD  
2 RECD  
2 RECD  
4 RECD

NAS 1104-18  
NAS 1104-21  
LD153-0014-0004  
MS 21075-24  
MS 20426-AD3 (FLUSH IN 8679-110117-085)

8679-110100

REV A 6

130

129

128

127

126

125

4



- NAS 1104-22 1 REQD
- NAS 1104-24 1 REQD
- LD 153-001-0014 2 REQD
- MS 2107564 2 REQD
- MS 20426AD3 (RWIN IN 8679-11017-083) 4 REQD

REVISIONS		DATE	APPROVED
NO.	DESCRIPTION		
1	MAY BE REWORKED 2 CANNOT BE REWORKED		
2	SHOULD CHANGE A NEW DASH PRACTICE		
3	PARTS MADE OK		
4	FOR REVISIONS SEE PG 8679-110100		

NR76H-135  
PG B-8

BEST AVAILABLE COPY

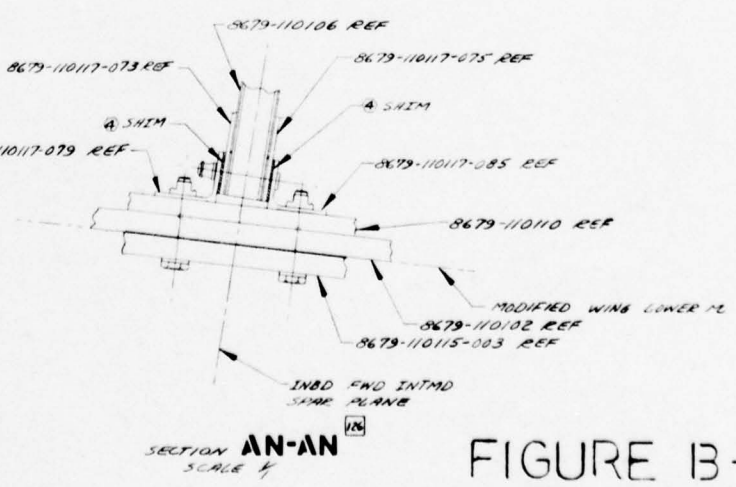
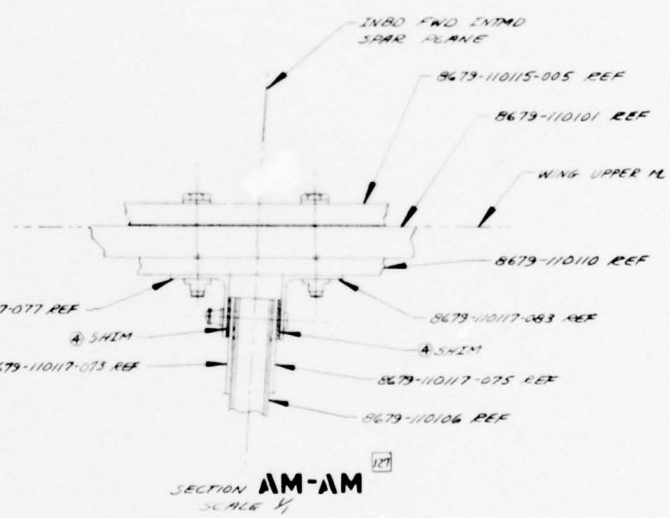
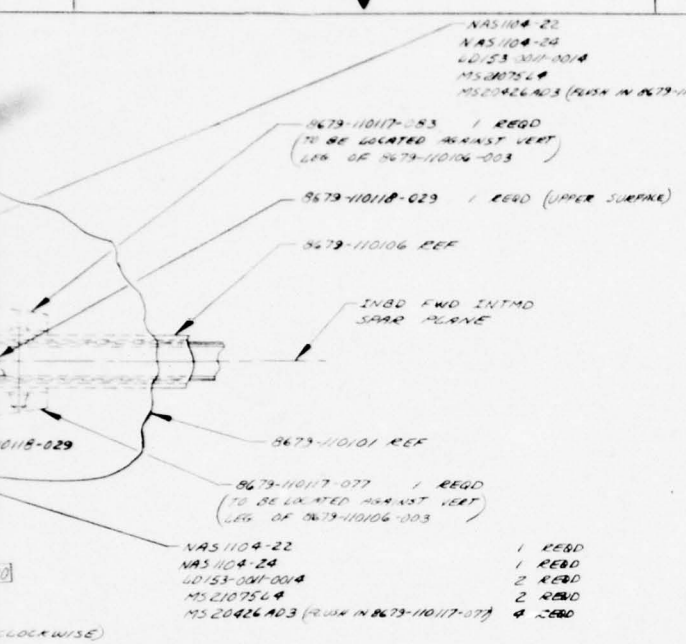


FIGURE B-1  
(SHEET 6 OF 8)

FIG. NO. IDENT.	8679-110100
J 89372	
DATE	
BY	
CHKD	
APPROVED	

001011-2528

H

G

F

E

D

C

B

A

168

167

166

165

164

.344<sup>±.004</sup> DIA 7 OVERSIZE HOLES  
 IN 8679-110115-003 ONLY  
 DRILL .54 MOD  
 DEPTH .81 THICKES  
 CSK .30 X .510<sup>±.010</sup> DIA 12 PLACES  
 TAP .5000-314K 3B MOD  
 .50 MIN FULL THD DEPTH  
 PD .4500<sup>±.0048</sup> 7 PLACES  
 MS 51831-203L 7 REQD  
 INSTALL PER SEE SPEC RAD101-003  
 NAS6605-13 7 REQD  
 LD153-001-0016 7 REQD

8679-110110-003 1 REQD

8679-110115-003 REF

8679-110102-001 REF

MODIFIED WING  
 LOWER ML

SECTION AX-AX  
 SCALE 1/4

.281<sup>±.004</sup> DIA 24 OVERSIZE HOLES  
 IN 8679-110115-003 ONLY  
 DRILL X (.397) MOD  
 DEPTH .72 24 HOLES  
 CSK .90 X .447<sup>±.010</sup> DIA 24 PLACES  
 TAP .4375-140M 3B MOD  
 .44 MIN FULL THD DEPTH  
 PD .3911<sup>±.0046</sup> 24 PLACES  
 MS 51831-202L 24 REQD  
 INSTALL PER SEE SPEC RAD101-003  
 NAS6604-9 8 REQD  
 NAS6604-11 9 REQD  
 NAS6604-12 6 REQD  
 NAS6604-13 1 REQD  
 LD153-001-0014 24 REQD

8679-110110-003 REF

8679-110115-003 REF

8679-110102-001 REF

MODIFIED WING  
 LOWER ML

63 (FOR 8679-110118-039 1-043)  
 (TIP LOWER SURFACE)

8679-110118-043 REF

.45 EDGE OF SKIN  
 AT Y 310.00 AND  
 Y 365.00

.78 EDGE OF SKIN  
 AT Y 310.00 &  
 Y 365.00  
 .50 (FOR 8679-110118-049  
 -049 -053 -057 1-059)  
 .50 (FOR 8679-110118-075  
 -049 -073 -083 1-059)  
 .44 (FOR 8679-110118-047  
 -053 1-048)  
 .38 (FOR 8679-110118-072  
 -053 1-048)

SECTION AII-AII  
 SCALE 1/4

8679-110100

REV  
 A 1

163

162

161

160

159

2

.344 ±.000 DIA 7 OVERSIZE HOLES  
IN B679-11015-005 ONLY  
DRILL .38 MOD  
DEPTH .181 7 HOLES  
CSK .90° X .510 ±.000 DIA 20 PLACES  
TAP .5000-13-38 MOD  
.50 MIN FULL THD DEPTH  
PD .4500 ±.000 7 PLACES  
MS S1831-202L 7 REQD  
INSTALL PER DR SPEC RAG101-003  
NAS6605-12 7 REQD  
LD153-0011-0016 7 REQD

NAS1105-19 1 REQD  
NAS1105-21 1 REQD  
LD153-0011-0016 2 REQD  
MS21075L5 2 REQD  
MS20426AD3 (FLUSH IN B679-11018-039) 4 REQD  
B679-11018-037 1 REQD  
MS20426AD3 (FLUSH IN RIB FLANGE) 2 REQD

NAS1105-19 1 REQD  
NAS1105-22 1 REQD  
LD153-0011-0016 2 REQD  
MS21075L5 2 REQD  
MS20426AD3 (FLUSH IN B679-11018-043) 4 REQD  
B679-11018-043 1 REQD  
MS20426AD3 (FLUSH IN RIB FLANGE) 2 REQD

NAS1105-19 3 REQD  
NAS1105-22 3 REQD  
LD153-0011-0016 6 REQD  
MS21075L5 6 REQD  
MS20426AD3 (FLUSH IN B679-11018-039) 12 REQD  
B679-11018-039 1 REQD  
MS20426AD3 (FLUSH IN RIB FLANGE) 2 REQD

NAS1105-20 3 REQD  
NAS1105-24 3 REQD  
LD153-0011-0016 6 REQD  
MS21075L5 6 REQD  
MS20426AD3 (FLUSH IN B679-11018-04) 12 REQD  
B679-11018-043 1 REQD  
MS20426AD3 (FLUSH IN RIB FLANGE) 2 REQD

SECTION AX-AX  
SCALE 1/2

VIEW AT

VIEW AT

INSD FRONT SPAR PLANE

INSD FWD INTD SPAR PLANE

NAS1104-23 7 REQD  
LD153-0011-0014 7 REQD  
MS21075L4 7 REQD  
MS20426AD3 (FLUSH IN B679-11018-043) 14 REQD  
B679-11018-043 1 REQD  
MS20426AD3 (FLUSH IN RIB FLANGE) 2 REQD

NAS1104-26 7 REQD  
LD153-0011-0014 7 REQD  
MS21075L4 7 REQD  
MS20426AD3 (FLUSH IN B679-11018-043) 14 REQD  
B679-11018-043 1 REQD  
MS20426AD3 (FLUSH IN RIB FLANGE) 2 REQD

NAS1104-18 8 REQD  
LD153-0011-0014 8 REQD  
MS21075L4 2 REQD  
MS21075L4 6 REQD  
MS20426AD3 (FLUSH IN B679-11018-053) 16 REQD  
B679-11018-053 1 REQD  
MS20426AD3 (FLUSH IN RIB FLANGE) 2 REQD

NAS1104-19 8 REQD  
LD153-0011-0014 8 REQD  
MS21075L4 2 REQD  
MS21075L4 6 REQD  
MS20426AD3 (FLUSH IN B679-11018-053) 16 REQD  
B679-11018-053 1 REQD  
MS20426AD3 (FLUSH IN RIB FLANGE) 2 REQD

NAS1104-15 3 REQD  
NAS1104-18 6 REQD  
LD153-0011-0014 9 REQD  
MS21075L4 1 REQD  
MS21075L4 8 REQD  
MS20426AD3 (FLUSH IN B679-11018-047) 18 REQD  
B679-11018-047 1 REQD  
MS20426AD3 (FLUSH IN RIB FLANGE) 3 REQD

NAS1104-21 3 REQD  
NAS1104-24 6 REQD  
LD153-0011-0014 9 REQD  
MS21075L4 1 REQD  
MS21075L4 8 REQD  
MS20426AD3 (FLUSH IN B679-11018-057) 18 REQD  
B679-11018-057 1 REQD  
MS20426AD3 (FLUSH IN RIB FLANGE) 3 REQD

NAS1104-23 7 REQD  
LD153-0011-0014 7 REQD  
MS21075L4 7 REQD  
MS20426AD3 (FLUSH IN B679-11018-045) 14 REQD  
B679-11018-045 1 REQD  
MS20426AD3 (FLUSH IN RIB FLANGE) 2 REQD

NAS1104-21 7 REQD  
NAS1104-24 7 REQD  
LD153-0011-0014 7 REQD  
MS21075L4 7 REQD  
MS20426AD3 (FLUSH IN B679-11018-055) 14 REQD  
B679-11018-055 1 REQD  
MS20426AD3 (FLUSH IN RIB FLANGE) 2 REQD

.281 ±.000 DIA 20 OVERSIZE HOLES  
IN B679-11015-005 ONLY  
DRILL .397 MOD  
DEPTH .72 20 HOLES  
CSK .90° X .447 ±.010 DIA 20 PLACES  
TAP .4375-14-38 MOD  
.44 MIN FULL THD DEPTH  
PD .3911 ±.000 20 PLACES  
MS S1831-202L 20 REQD  
INSTALL PER DR SPEC RAG101-003  
NAS6604-8 7 REQD  
NAS6604-10 12 REQD  
NAS6604-12 1 REQD  
LD153-0011-0014 20 REQD

VIEW AT  
SCALE 1/2  
(FASTENER HEADS SHOWN AT A/2 -  
NUTPLATES & NUTPLATE RETAINERS  
SHOWN AT INSIDE SURFACE)

SECTION AII'-AII'  
SCALE 1/2



19 3 REQD  
 20 3 REQD  
 21 006 6 REQD  
 22 6 REQD  
 23 12 REQD  
 24 1 REQD  
 25 2 REQD

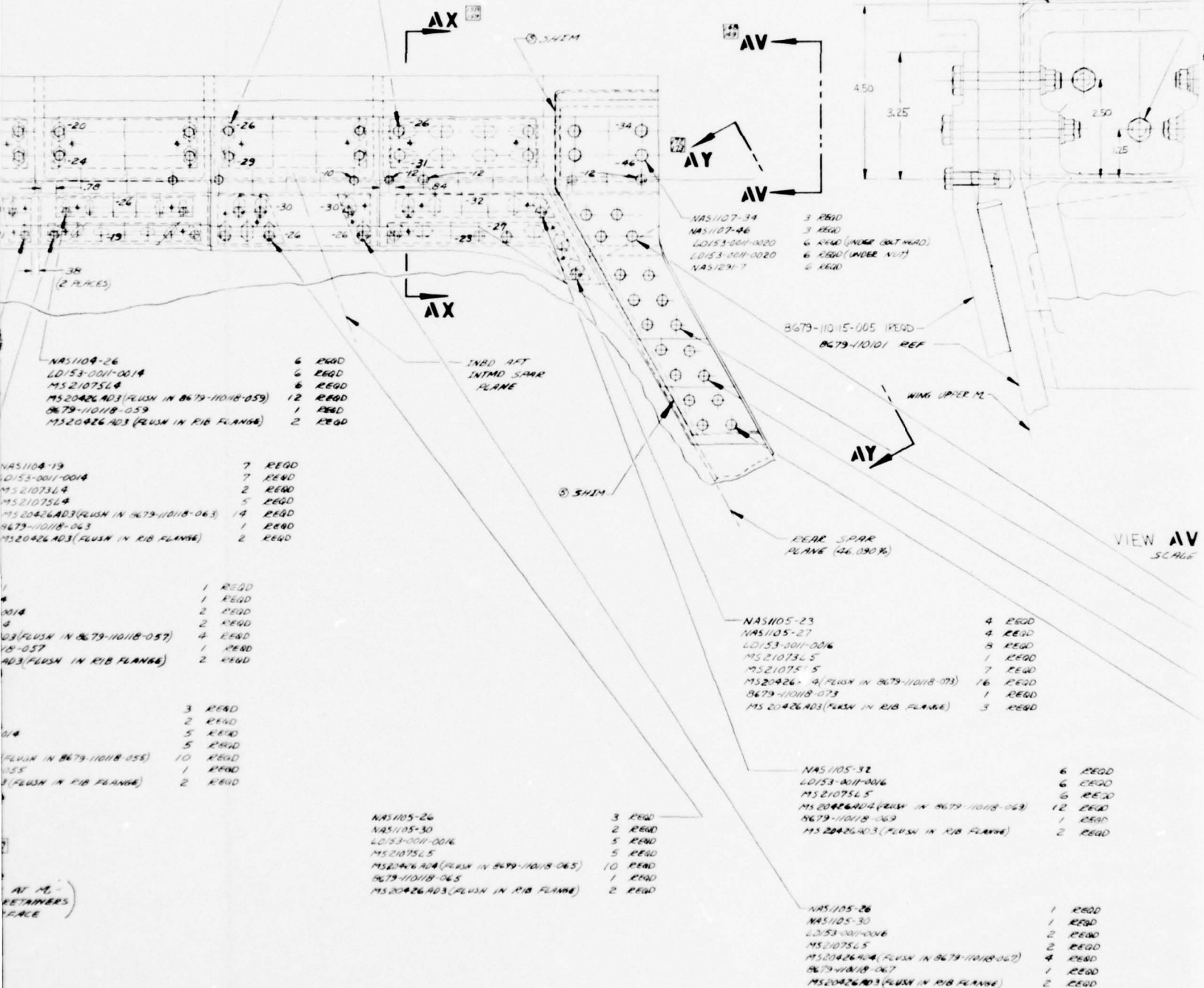
6 REQD  
 6 REQD  
 12 REQD  
 12 REQD  
 24 REQD  
 2 REQD  
 4 REQD

NAS105-26 4 REQD  
 NAS105-27 4 REQD  
 LD153-001-0016 8 REQD  
 MS21075L5 8 REQD  
 MS20426AD3 (FLUSH IN 8679-11018-043) 16 REQD  
 8679-11018-043 1 REQD  
 MS20426AD3 (FLUSH IN RIB FLANGE) 2 REQD

NAS1106-26 4 REQD  
 NAS1106-31 4 REQD  
 LD153-001-0018 8 REQD  
 F2000-6 4 REQD  
 MS21059L6 4 REQD  
 MS20426AD3 (FLUSH IN 8679-11018-039) 16 REQD  
 8679-11018-039 1 REQD  
 MS20426AD3 (FLUSH IN RIB FLANGE) 2 REQD

8679-11014-003  
 1 REQD

ZF 25.335  
 REF







00101 00100

H

G

F

E

D

C

B

A

NAS1107-46 3 REQD  
LD153-0011-0020 3 REQD  
LD153-0011-0020 3 REQD  
NAS1291-7 3 REQD

NAS1106-42 4 REQD  
LD153-0011-0018 4 REQD (1 UNDER EACH BOLT HEAD)  
LD153-0011-0018 8 REQD (2 UNDER EACH NUT)  
MS21042L6 4 REQD

NAS1106-42 4 REQD  
LD153-0011-0018 4 REQD (1 UNDER EACH BOLT HEAD)  
LD153-0011-0018 8 REQD (2 UNDER EACH NUT)  
MS21042L6 4 REQD

NAS1106-38 4 REQD  
LD153-0011-0018 4 REQD (1 UNDER EACH BOLT HEAD)  
LD153-0011-0018 4 REQD (1 UNDER EACH NUT)  
MS21042L6 4 REQD

NAS1106-36 4 REQD  
LD153-0011-0018 4 REQD (1 UNDER EACH BOLT HEAD)  
LD153-0011-0018 8 REQD (2 UNDER EACH NUT)  
MS21042L6 4 REQD

192

191

190

189

188

NAS1107-46 3 REQD  
 LD153-0011-0020 3 REQD (UNDER BOLT HEAD)  
 LD153-0011-0020 3 REQD (UNDER NUT)  
 NAS1291-7 3 REQD

NAS1107-36 3 REQD  
 LD153-0011-0020 3 REQD (1 UNDER EACH BOLT HEAD)  
 LD153-0011-0020 6 REQD (2 UNDER EACH NUT)  
 NAS1291-7 3 REQD

NAS1106-28 4 REQD  
 NAS1106-30 4 REQD  
 LD153-0011-0018 8 REQD  
 F2000-6 4 REQD  
 MS21075L6 4 REQD  
 MS20426AD4 (FLUSH IN 8679-110118-039) 16 REQD  
 8679-110118-039 1 REQD  
 MS20426AD4 (FLUSH IN RIB FLANGE) 2 REQD

NAS1105-26 4 REQD  
 NAS1105-30 4 REQD  
 LD153-0011-0016 8 REQD  
 MS21075L5 8 REQD  
 MS20426AD4 (FLUSH IN 8679-110118-043) 16 REQD  
 8679-110118-043 1 REQD  
 MS20426AD4 (FLUSH IN RIB FLANGE) 2 REQD

BOLT HEAD  
 (7)

BOLT HEAD  
 (7)

BOLT HEAD  
 (NUT)

BOLT HEAD  
 (NUT)

REAR SPAR  
 PLANE 46.090%

NAS1105-19 4 REQD  
 NAS1105-24 4 REQD  
 LD153-0011-0016 8 REQD  
 MS21075L5 1 REQD  
 MS21075L5 7 REQD  
 MS20426AD4 (FLUSH IN 8679-110118-093) 16 REQD  
 8679-110118-093 1 REQD  
 MS20426AD3 (FLUSH IN RIB FLANGE) 3 REQD

NAS1105-30 6 REQD  
 LD153-0011-0016 6 REQD  
 MS21075L5 6 REQD  
 MS20426AD4 (FLUSH IN 8679-110118-093) 12 REQD  
 8679-110118-093 1 REQD  
 MS20426AD3 (FLUSH IN RIB FLANGE) 2 REQD

NAS1105-22 1 REQD  
 NAS1105-26 1 REQD  
 LD153-0011-0016 2 REQD  
 MS21075L5 2 REQD  
 MS20426AD4 (FLUSH IN 8679-110118-087) 4 REQD  
 8679-110118-087 1 REQD  
 MS20426AD3 (FLUSH IN RIB FLANGE) 2 REQD

INBD AFT  
 INTMD SPAR  
 PLANE

INBD FWD  
 INTMD SPAR  
 PLANE

NAS1104-22 6 REQD  
 LD153-0011-0014 6 REQD  
 MS21075L4 6 REQD  
 MS20426AD3 (FLUSH IN 8679-110118-059) 12 REQD  
 8679-110118-059 1 REQD  
 MS20426AD3 (FLUSH IN RIB FLANGE) 2 REQD

NAS1104-16 7 REQD  
 LD153-0011-0014 7 REQD  
 MS21075L4 2 REQD  
 MS21075L4 5 REQD  
 MS20426AD3 (FLUSH IN 8679-110118-063) 14 REQD  
 8679-110118-063 1 REQD  
 MS20426AD3 (FLUSH IN RIB FLANGE) 2 REQD

NAS1105-22 3 REQD  
 NAS1105-26 2 REQD  
 LD153-0011-0016 5 REQD  
 MS21075L5 5 REQD  
 MS20426AD4 (FLUSH IN 8679-110118-085) 10 REQD  
 8679-110118-085 1 REQD  
 MS20426AD3 (FLUSH IN RIB FLANGE) 2 REQD

VIEW AU-AU

SCALE 1/2

(FASTENER HEADS SHOWN AT  
 NATURAL PLATE & NATURAL PLATE RETAIN  
 SHOWN AT INSIDE SURFACE  
 (LOOKING UP AT LOWER SURFACE)

8679-110100

REV A

187

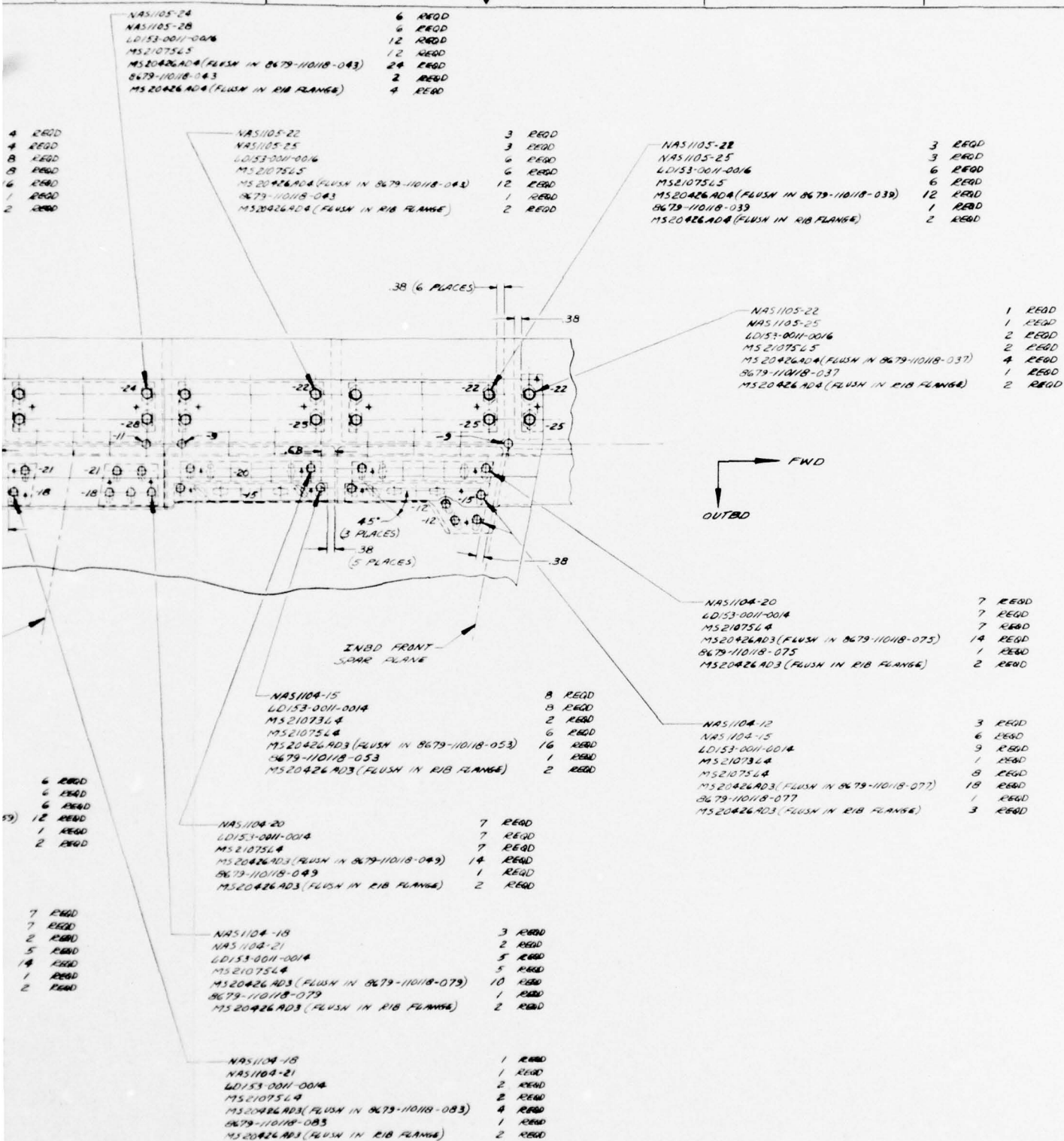
186

185

184

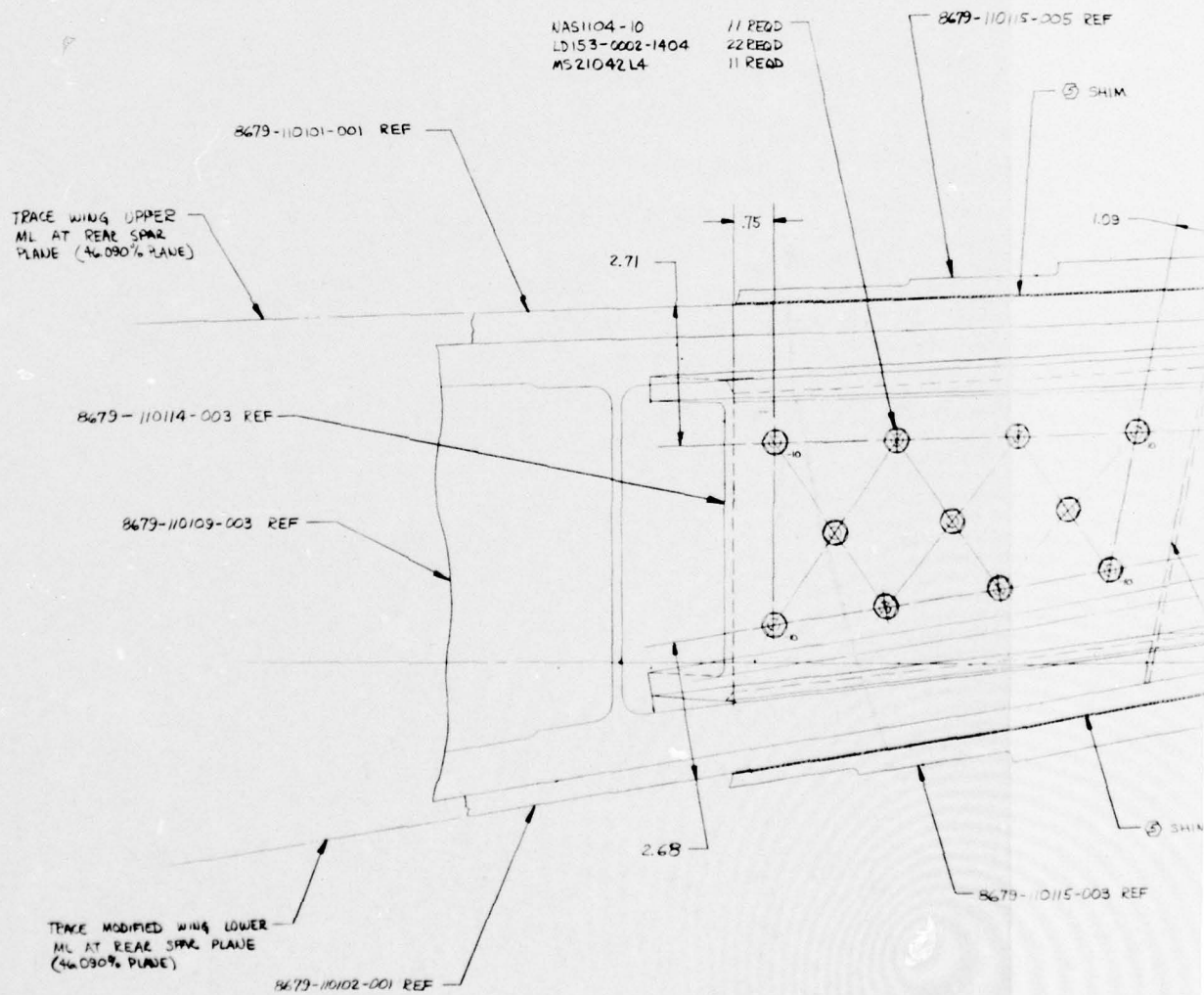
183

2



AU  
 HOWN AT PL  
 RETAINERS  
 SURFACE  
 OR SURFACE





SECTION AY-AY  
VIEW LOOKING NORMAL TO WING  
SECTION ROTATED 118° CLO

8679-110100

A 8

177

176

175

174

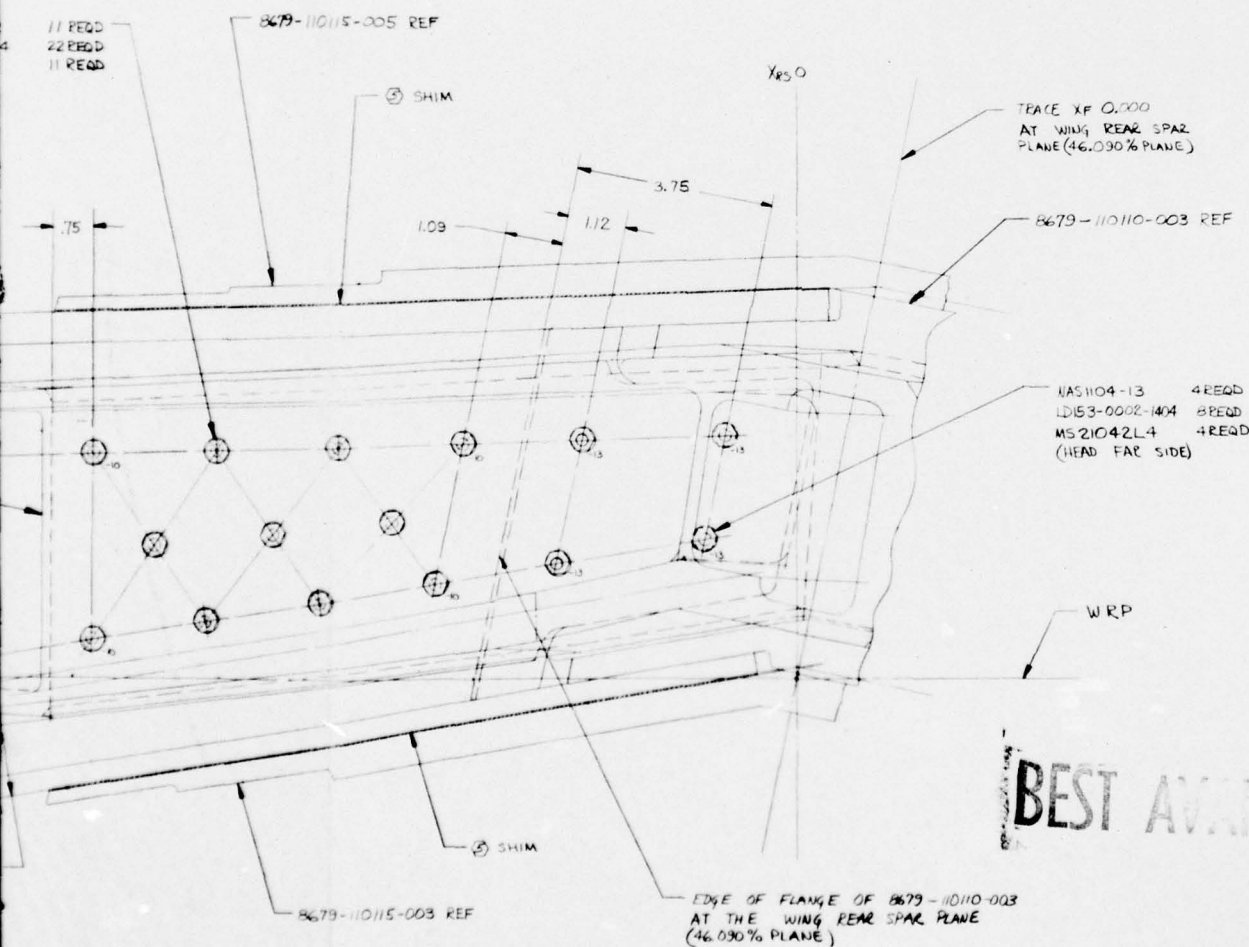
173

4



REVISIONS		
NO.	DESCRIPTION	DATE
1	MADE BY REVISIONS: 2. LAMINATE BY REVISIONS: 3. DRILLING CHANGE: 4. NEW TAP PRACTICE: 5. SHORTS MADE ON:	1-5-76
FOR REVISIONS, SEE PL 8679-110100		G.M. PALLOCK

NR76H-135  
PG B-10



BEST AVAILABLE COPY

SECTION **AY-AY**

VIEW LOOKING NORMAL TO WING REAR SPAR  
SECTION ROTATED 118° COUNTERCLOCKWISE

FIGURE B-1

(SHEET 8 OF 8)

8679-110100	8679-110100
J 89372	169

173

172

171

170

169

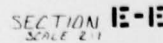
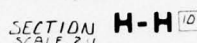
15

367973 TOWN 311 G. 4 REV 2 70

80-111010













REVISIONS		DATE	APPROVED
1	MAY BE REWORKED 2 CANNOT BE REWORKED 1 RECORD CHANGE 4 NEW SHOP PRACTICE 5 PARTS MADE OK		
A	FOR REVISIONS SEE PL 8679-110101	3 KOP/ITER 8-21-75	

NR76H-135  
PG B-11

TABLE I  
LAMINATE ORIENTATION FOR -003 & -005

LAMINATION NO.	ORIENTATION 1	ORIENTATION 4
L1	-45°	
L2	0°	-45°
L3	-45°	
L4	30° ②	
L5	0°	+45°
L6	-45°	
L7	+45°	
L8	0°	
L9	+45°	-45°
L10	30° ②	
L11	-45°	
L12	0°	-45°
L13	+45°	
L14	-45°	
L15	0°	+45°
L16	-45°	
L17	+45°	
L18	0°	+45°
L19	30° ②	
L20	0°	+45°
L21	+45°	
L22	-45°	
L23	0°	+45°
L24	-45°	
L25	+45°	
L26	0°	-45°
L27	-45°	
L28	30° ②	
L29	+45°	-45°
L30	0°	
L31	+45°	
L32	-45°	
L33	0°	+45°
L34	30° ②	
L35	-45°	-45°
L36	0°	
L37	+45°	

② ORIENTATION FOR LAMINATES L4, L10, L19, L28 & L34

$K = 0.000, K = 33.33$  (REF)  
 $K_{max} = 73.54$  (REF)

30°

BEST AVAILABLE COPY

FIGURE B-2

NOTES UNLESS OTHERWISE NOTED

FOR PARTS LIST SEE PL 8679-110101				Rockwell International Corporation Columbus Aircraft Division	
UNLESS OTHERWISE SPECIFIED: DIMENSIONS ARE IN INCHES MFG TOLERANCES ON: DIMENSIONS ARE: XX (DECIMALS) XXX (DECIMALS) ANGLES HOLE NOTED D12 THRU .040 ± .001 .001 D14 THRU .120 ± .002 .001 D16 THRU .220 ± .003 .001 D20 THRU .500 ± .004 .001 D30 THRU .750 ± .005 .001 D36 THRU 1.000 ± .007 .001 D40 THRU 2.000 ± .010 .001				CONTR NO DRAWN BY KOP/ITER 7/24/75 CHK BY APVD	
ITEM QTY NEXT ASSY USED ON END ITEM NO. THRU				PANEL UPPER SKIN COMPOSITE WING CENTER SECTION ASSY OF	
WROG FIG END ITEM APPLICATION EFFECTIVITY				J 89372 8679-110101	
DO NOT SCALE PRINT				DATE 7-27-75	

24

23

22

21

20

H

G

F

E

D

C

B

A

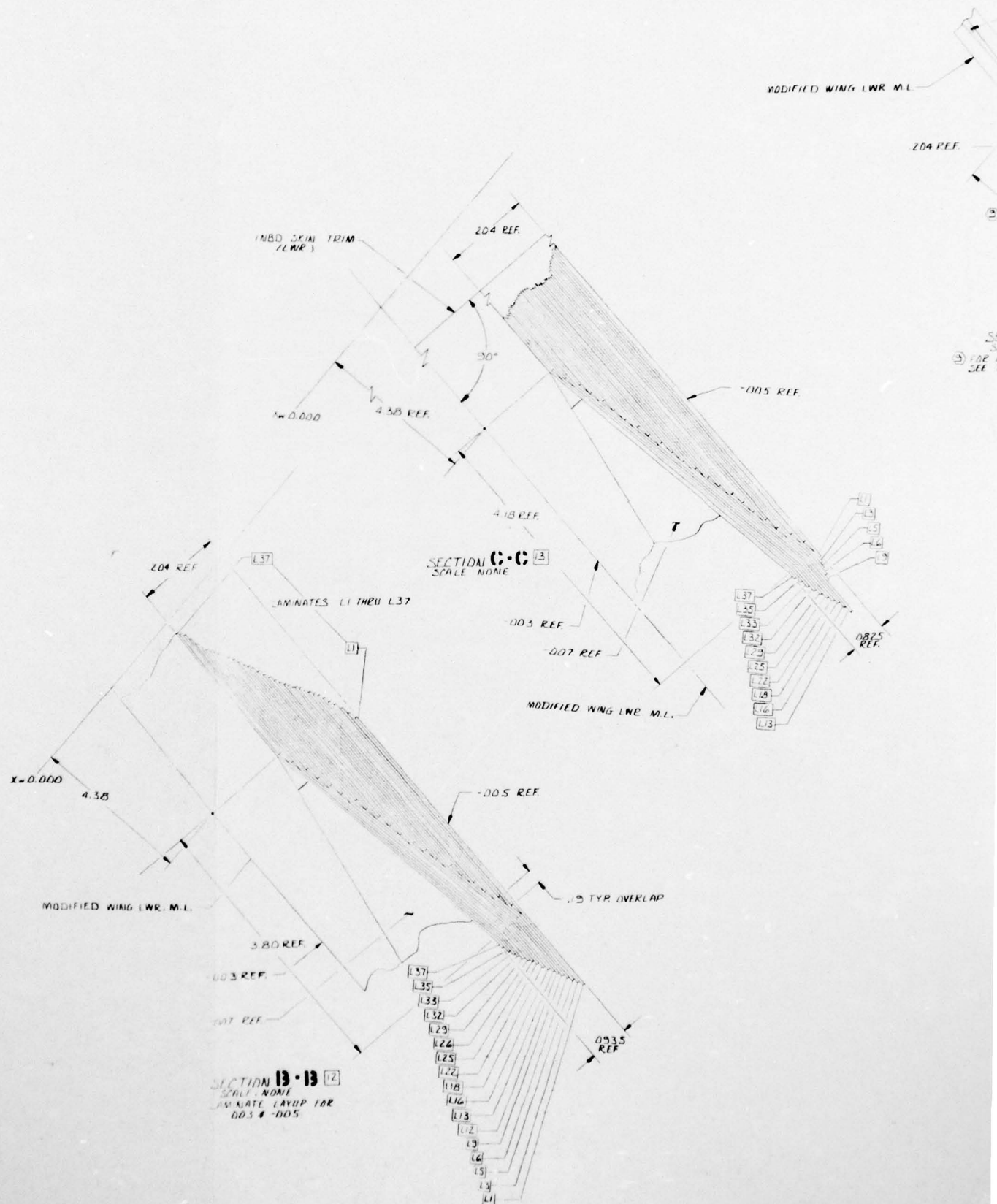
24

23

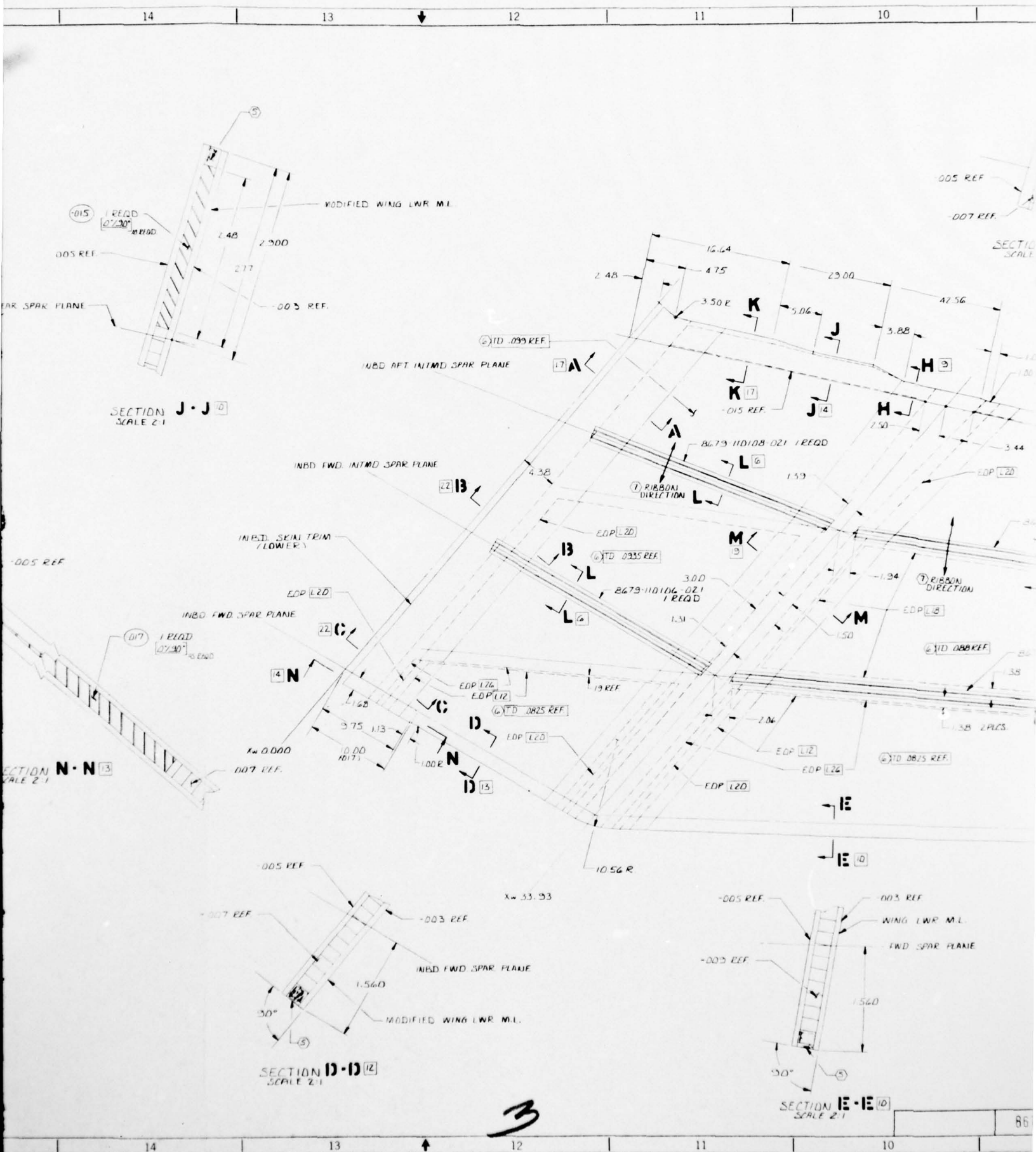
22

21

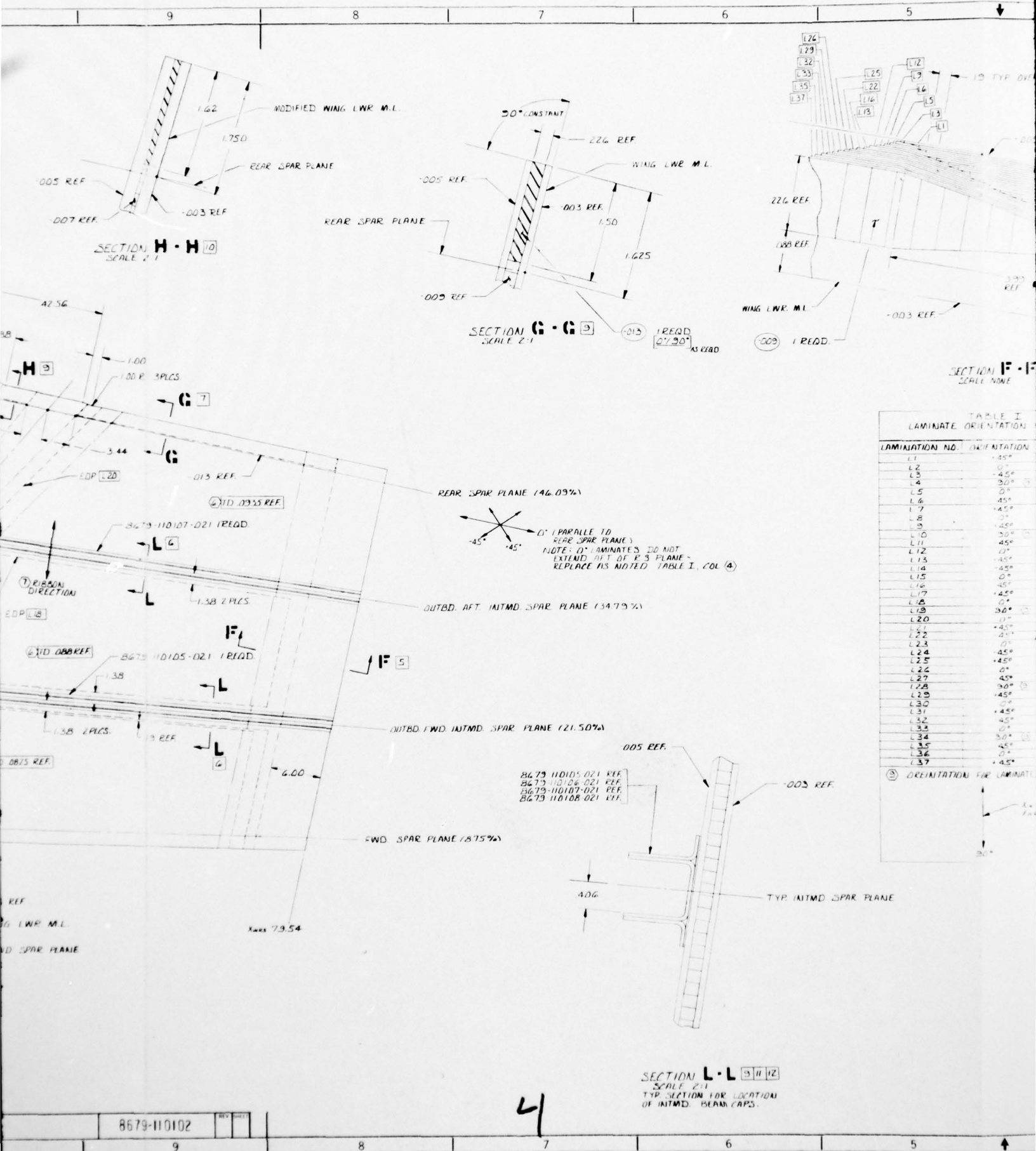
20





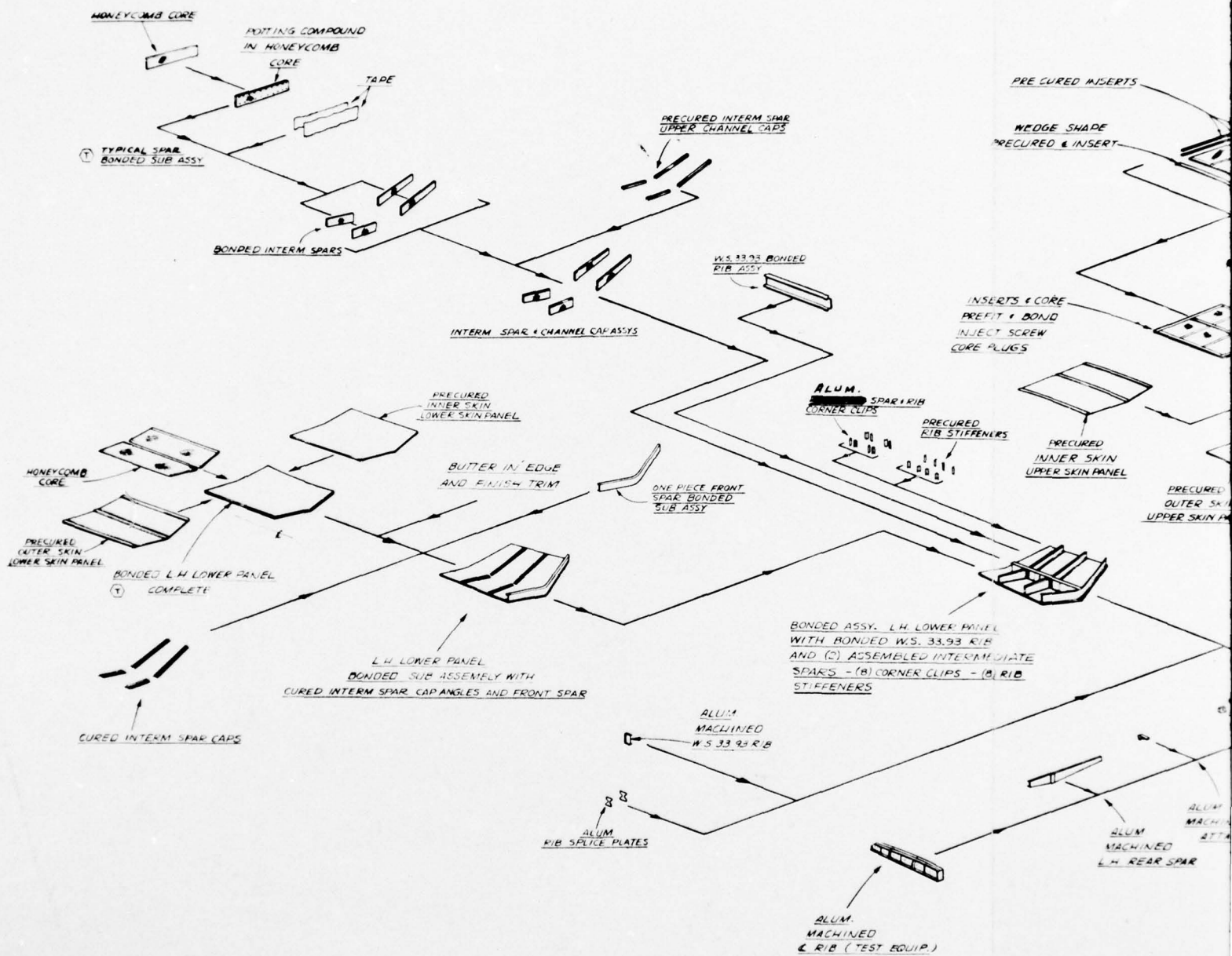


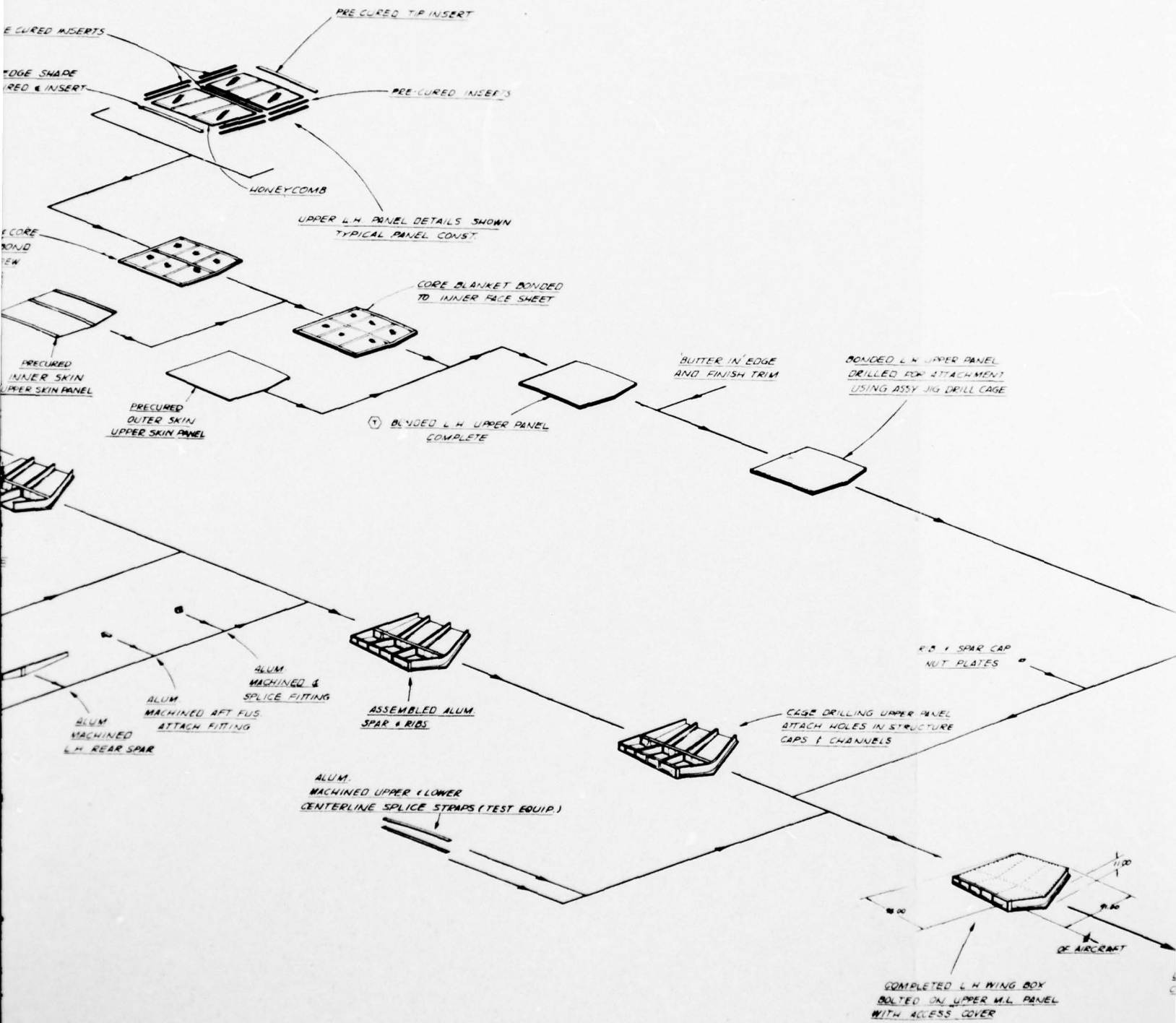






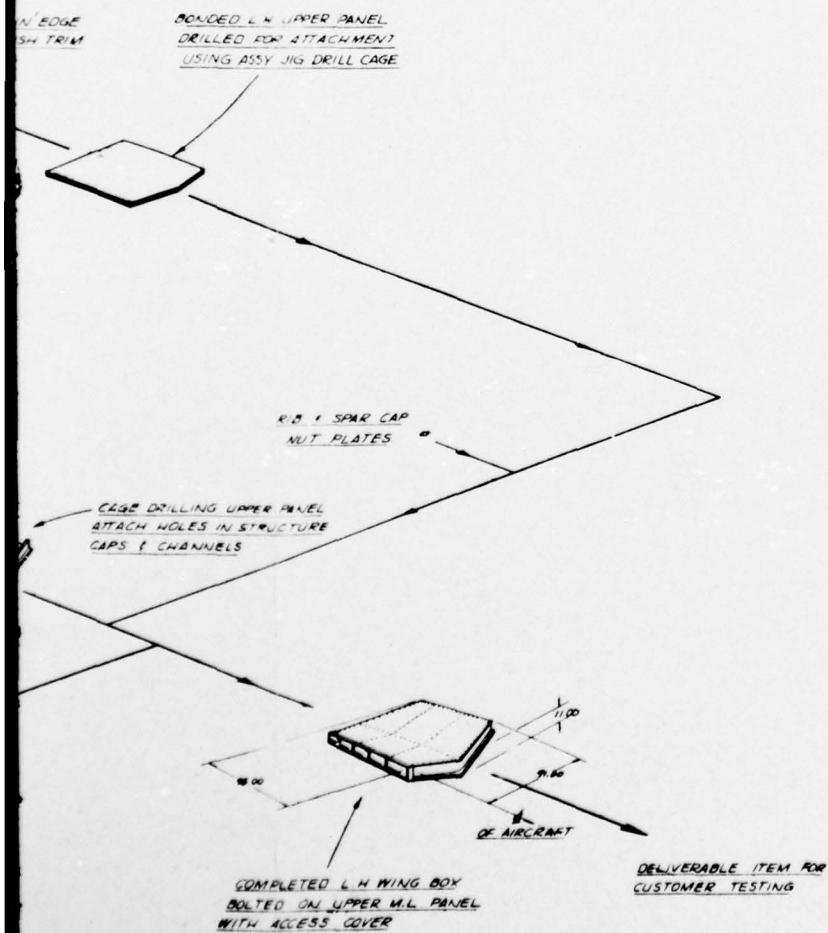






NR76H-135  
PG B-13

BEST AVAILABLE COPY



⑦ BONDED TEST ARTICLE WITH  
BONDED PART

FIGURE B-4

PRODUCTION FLOW DIAGRAM  
GO 8679

PRODUCTION FLOW DIAGRAM, HSK 1167-2  
GO 8679 GRAPHITE COMPOSITE WING BOX  
CONFIGURATION, REMOVABLE UPPER SKINS

REVISION	DATE	BY	APPROVED
1	11/10	1	
 Columbus Aircraft Division North American Rockwell COLUMBUS, OHIO 43016 MANUFACTURING ENGINEER			

REVISED 1-18-80 REVISED 8-24-80 REVISED 10-17-80 REVISED 11-20-80

3



B-2 COMPLETE WING STRUCTURAL ARRANGEMENT

Figure B-5 (Dwg. 8679-100001, 3 sheets) illustrates the complete wing structural arrangement as an extension of the test section described in Section B-1. These drawings illustrate the complete wing including access doors, tip rib, and provisions for attaching leading and trailing edge structure.



AD-A041 208

ROCKWELL INTERNATIONAL COLUMBUS OHIO COLUMBUS AIRCRA--ETC F/G 11/4  
EVALUATION OF COMPOSITE WING FOR XFV-12A AIRPLANE.(U)

DEC 76 D N ULRY, R W GEHRING, K I CLAYTON

N62269-74-C-0577

UNCLASSIFIED

NR76H-135

NADC-77183-30

NL

4 OF 4  
AD  
A041208



END

DATE  
FILMED

7-77

82.2-10000

24

23

22

21

20

H

G

F

E

D

C

B

A

24

23

22

21

20

TRACE OF REAR SPAR  
PLANE AT  $X_{w} 33.93$

FUEL LINE HOLES

TRACE OF 34.79%  
PLANE AT  $X_{w} 33.93$

WRP

SKIN PANEL

FOAM TYPE ADHESIVE

FIBER GLASS INSERT

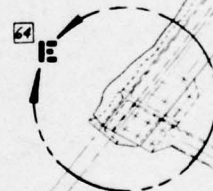
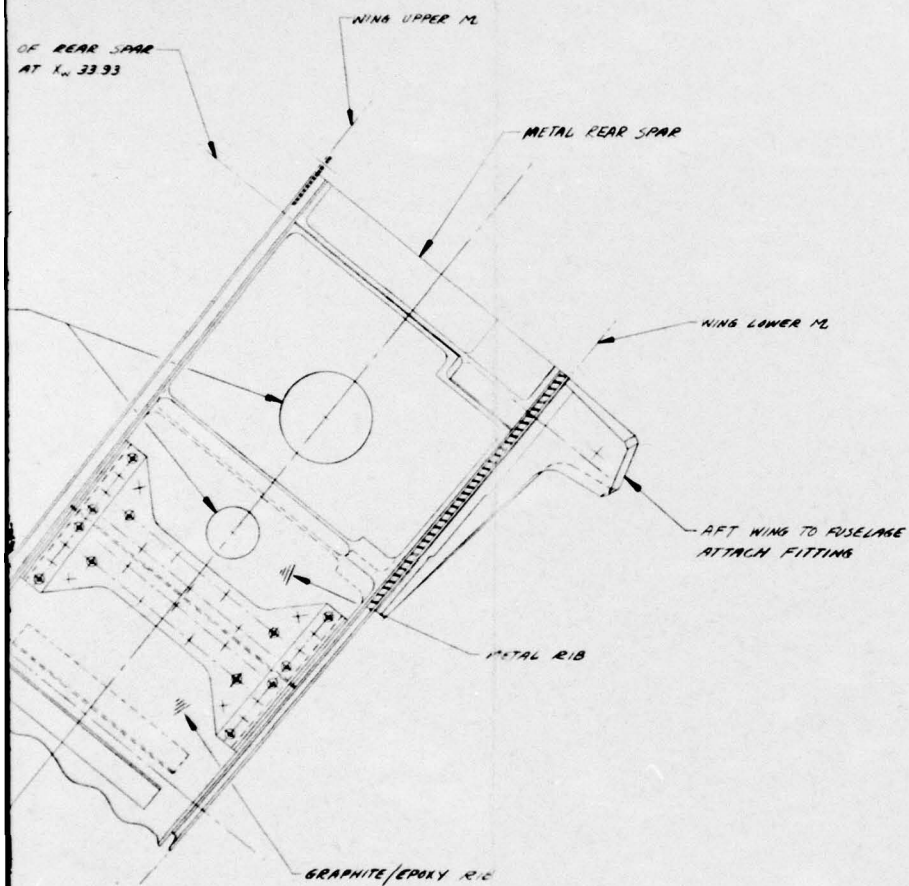
SEALS

ACCESS DOOR

SECTION **N-N**  
SCALE  $\frac{1}{1}$

VIEW **A-A**  
SCALE  $\frac{1}{2}$

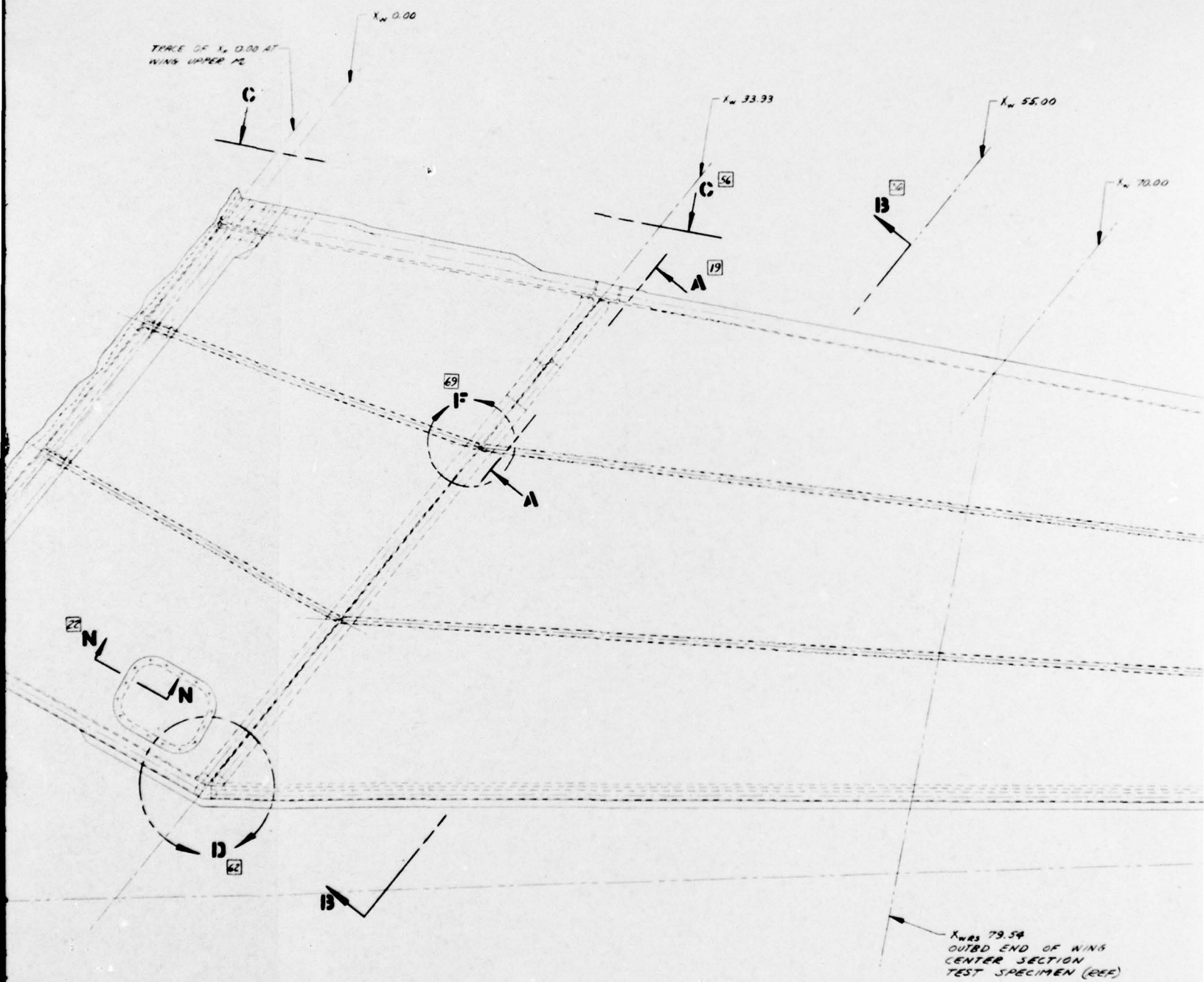
20 19 18 17 16 15



20 19 18 17 16 15

8679-100001

REV	DATE
A	1

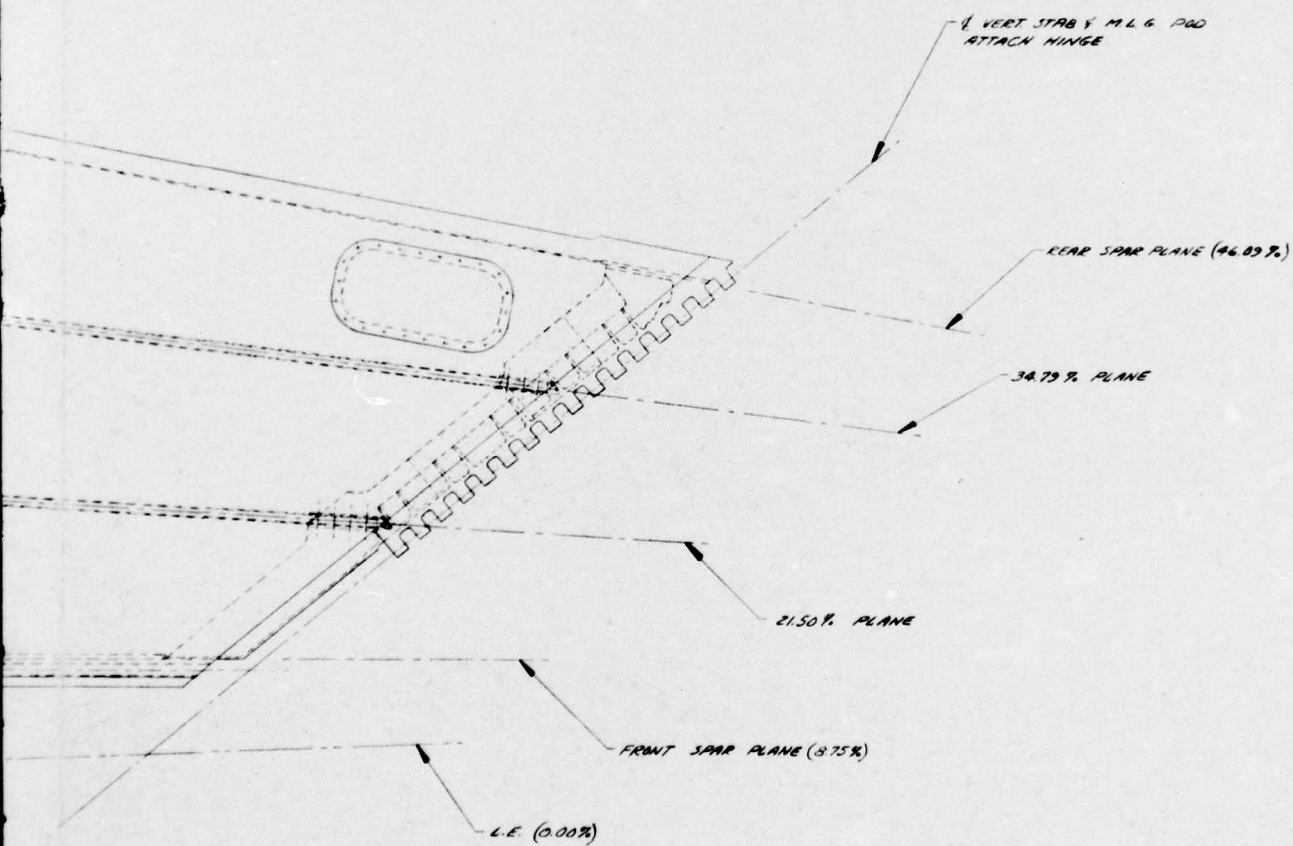


PLAN VIEW

SCALE  $\frac{1}{8}$

3





4



NR 76H - 135  
PAGE B-15

REVISIONS	
NO.	DESCRIPTION
1	MAY BE REWORKED - CANNOT BE REWORKED
2	REWORKED - CANNOT BE REWORKED
3	REWORKED - CANNOT BE REWORKED
4	REWORKED - CANNOT BE REWORKED
5	REWORKED - CANNOT BE REWORKED
6	REWORKED - CANNOT BE REWORKED
7	REWORKED - CANNOT BE REWORKED
8	REWORKED - CANNOT BE REWORKED
9	REWORKED - CANNOT BE REWORKED
10	REWORKED - CANNOT BE REWORKED

BEST AVAILABLE COPY

FIGURE B-5  
(SHEET 1 OF 3)

NOTES UNLESS OTHERWISE NOTED

				FOR PARTS LIST SEE PL	
				Rockwell International Corporation Columbus Aircraft Division	
				COMPOSITE WING CONCEPT	
				CONFIGURATION BASE LINE	
				J 89372 8679-100001	
				DO NOT SCALE PRINT	

000001-100001

H

G

F

E

D

C

B

A

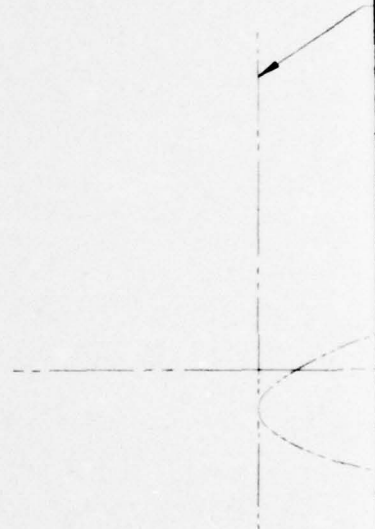
43

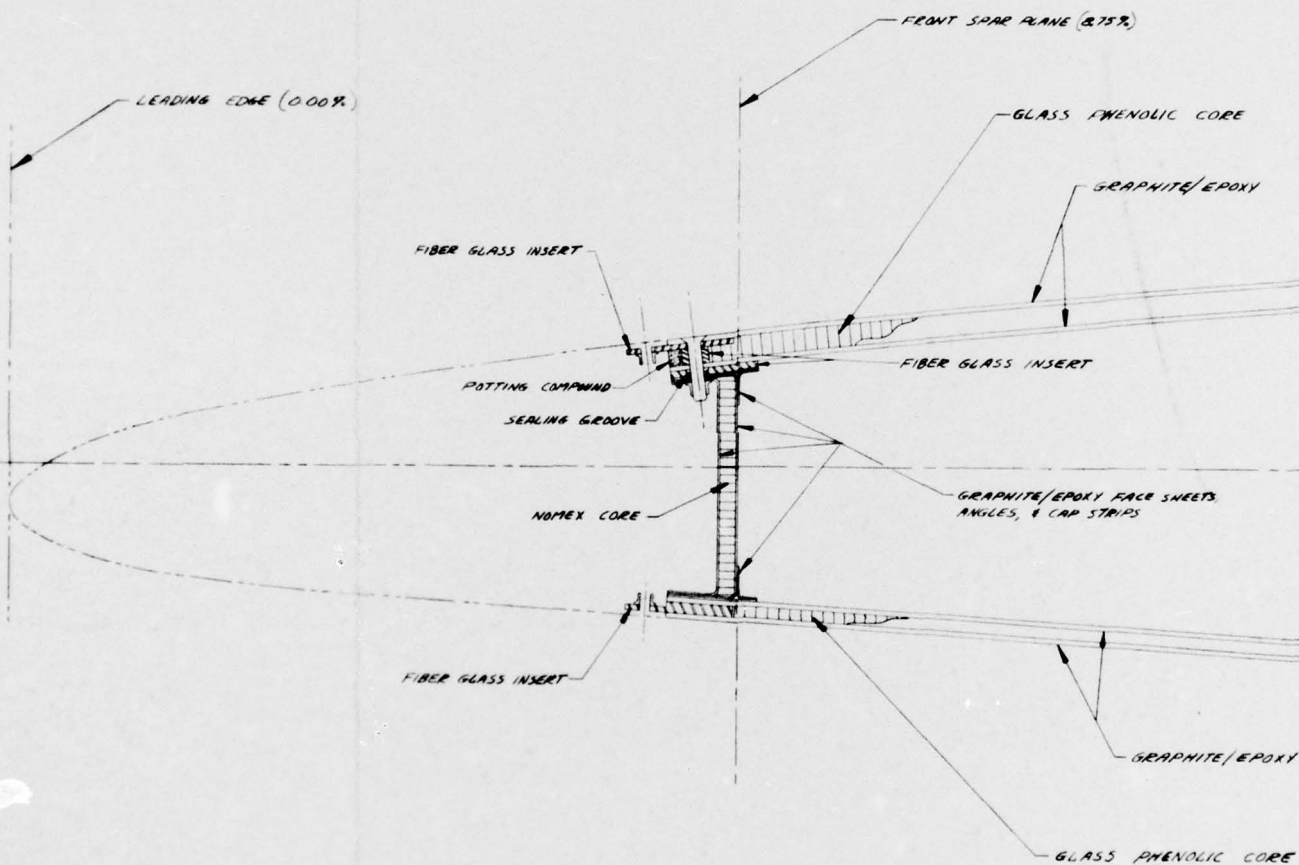
47

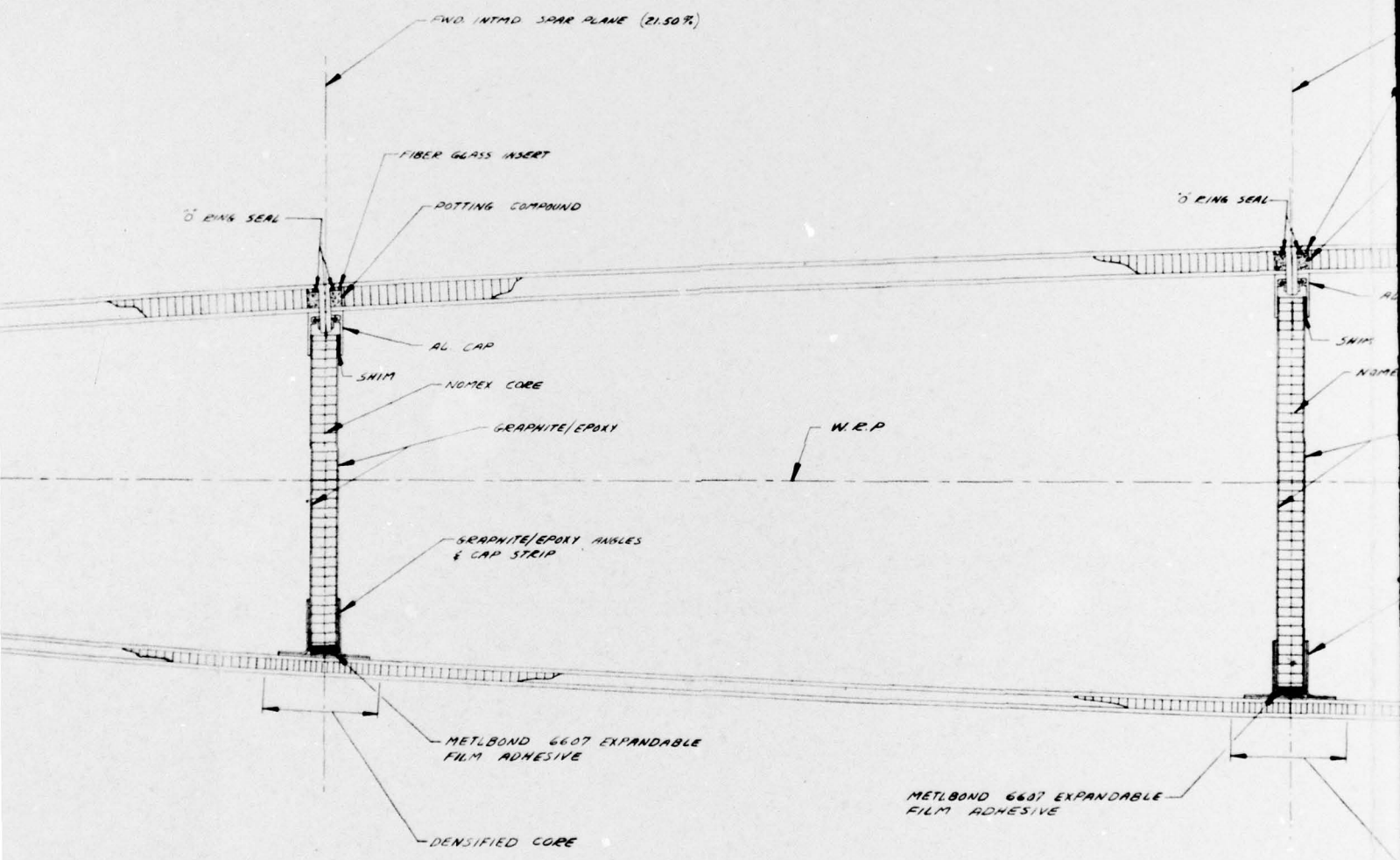
46

45

44

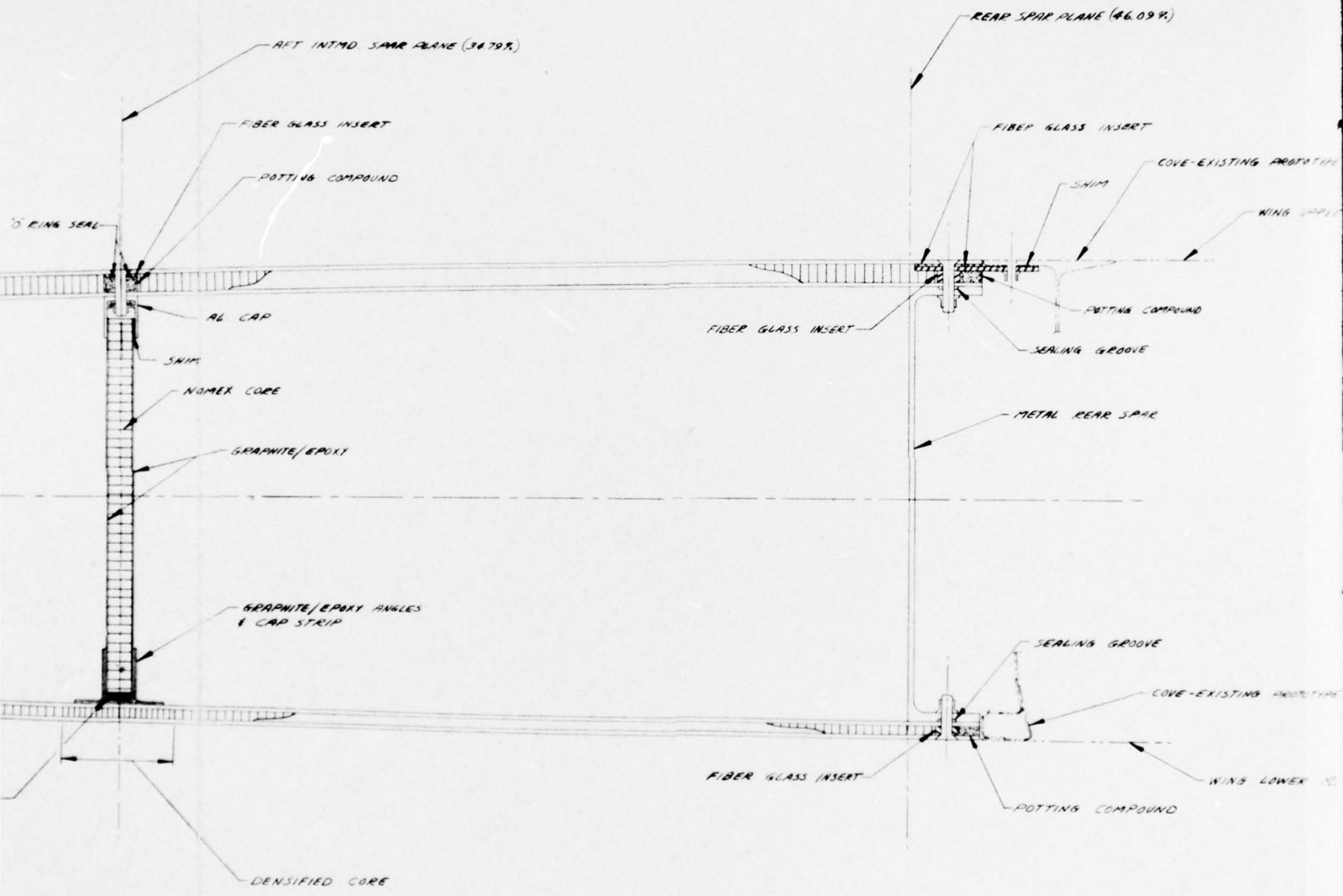






SECTION **B-B**  
 SCALE  $\frac{1}{2}$   
 (ROTATED 50° CLOCKWISE)





8679-100001

A 2

41



NR76H-135  
PAGE B-16

REVISIONS			
NO.	DESCRIPTION	DATE	APPROVED
1	MAY BE REWORKED 2 CANNOT BE REWORKED		
2	RECORD CHANGE 4 NEW SHOP PRACTICE		
3	PARTS MADE ON		
4			
5	SEE SHIP '71 FOR REVISIONS		

BEST AVAILABLE COPY

FIGURE B-5  
(SHEET 2 OF 3)

SIZE	CODE IDENT NO	8679-100001
J	89372	
SCALE	NOTES	SHEET 2

5

823-100001

H

G

F

E

D

C

B

A

TENSION BOLTS  
UPPER & LOWER  
MESHED HOLES IN SPLICE STRAPS  
HELICOIDS INSTALLED IN 4 RIB

UPPER SKIN PANEL

2 BA SCREWS - O-RING SEALED  
20/200 4 4 NUT - 4 PANE CO.  
INSTALLED INTO 4L KLEINER STRIP

UPPER SKIN PANEL

WING UPPER M.L.

VIEW L-L  
SCALE 1:1

WRP

WR SKIN PANEL

LWR SPLICE STRAP

1,000

SECTION K-K  
SCALE 1:1

FWD.

SCREWS - O-RING SEALED

A8D

DETAIL F-13

SCALE 1:2  
(TYP. 21.50% 34.79% 1  
ROTATED 180°)

34.73%

34.33.03

GRAPHITE/EPOXY RIB

UPPER SKIN PANEL

WING UPPER M.L.

INTERM. BEAM (MODIFIED)

MODIFIED INTERM. BEAM (MODIFIED)

WRP

MODIFIED WING LWR M.L.

LWR SKIN PANEL

GRAPHITE/EPOXY CLIPS  
CUTTED TO 34.55.83 RIB  
& TO INTERMEDIATE BEAMS

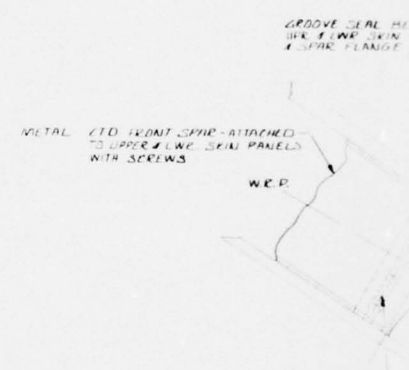
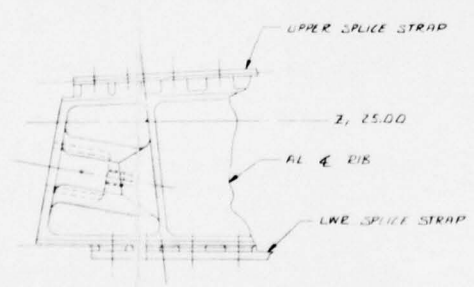
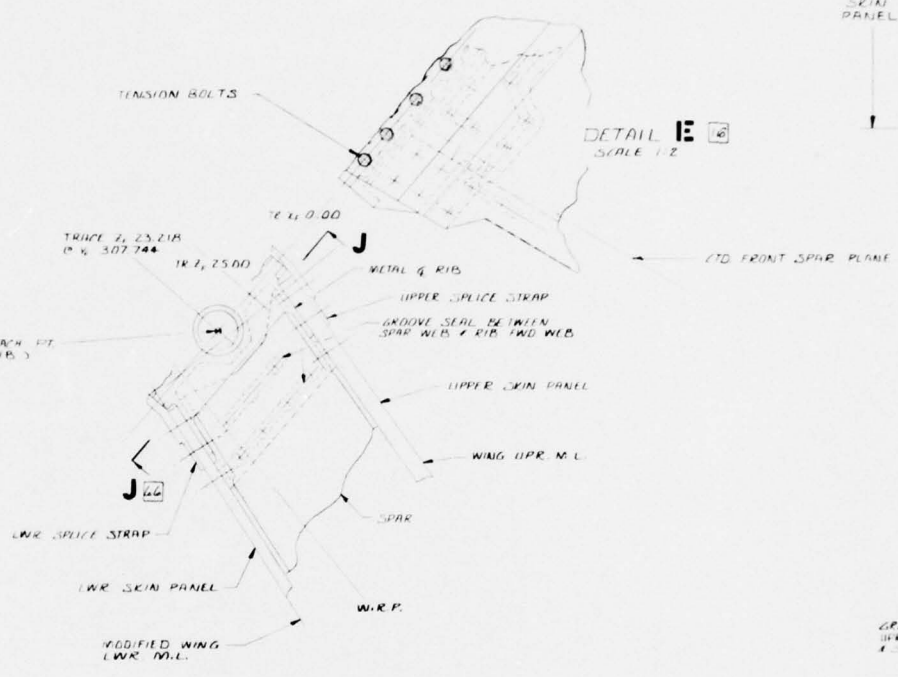
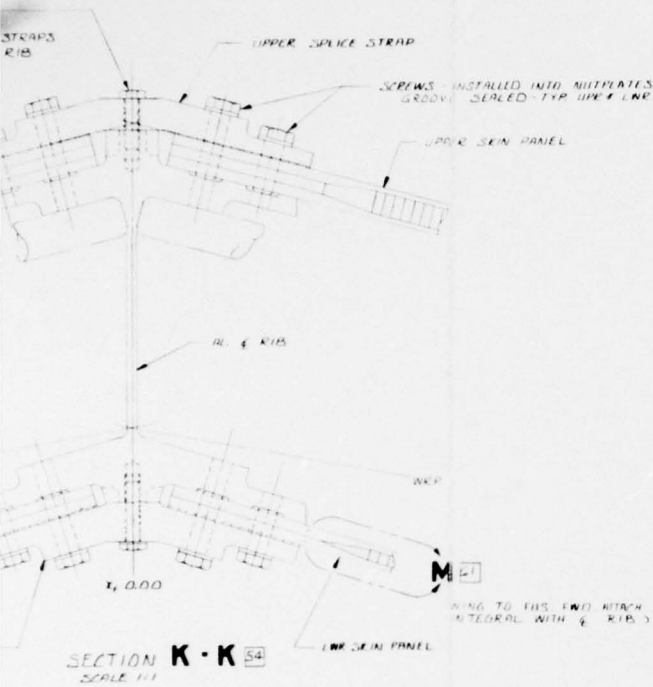
72

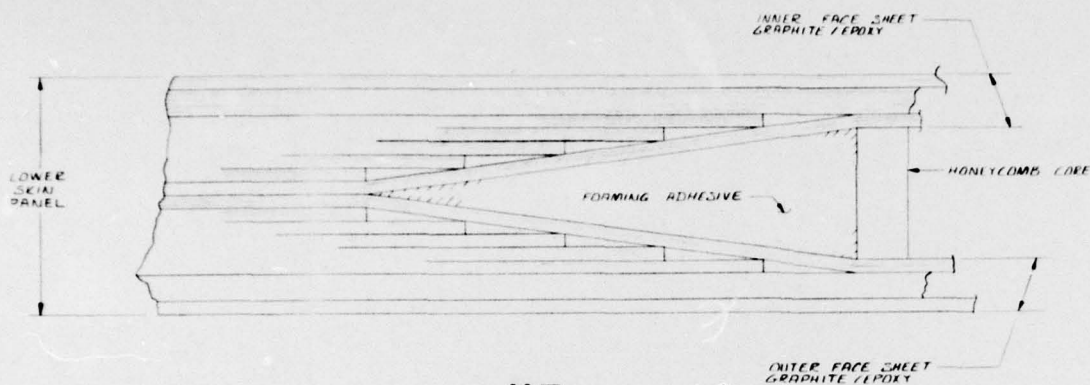
71

70

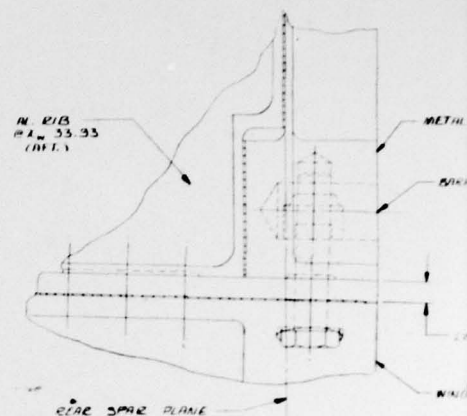
69

68



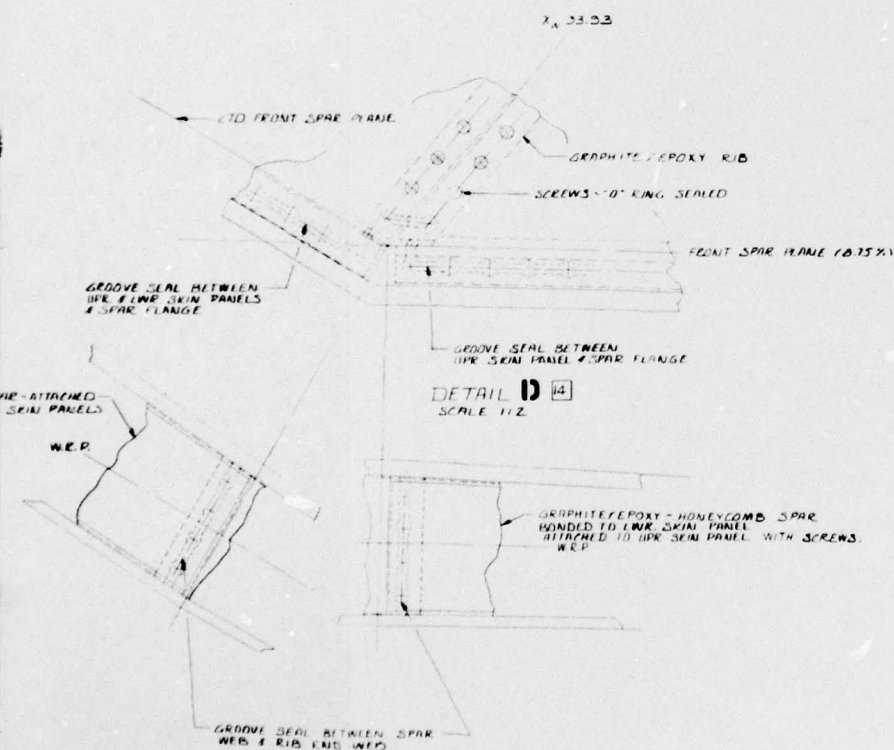


DETAIL M  $\frac{1}{2}$   
(UPPER SKIN PANEL SIMILAR)  
SCALE 10:1  
ROTATED



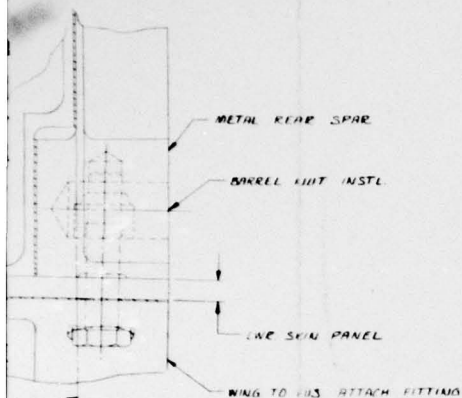
SECTION H-H  $\frac{1}{2}$   
SCALE 1:1

SPAR PLANE

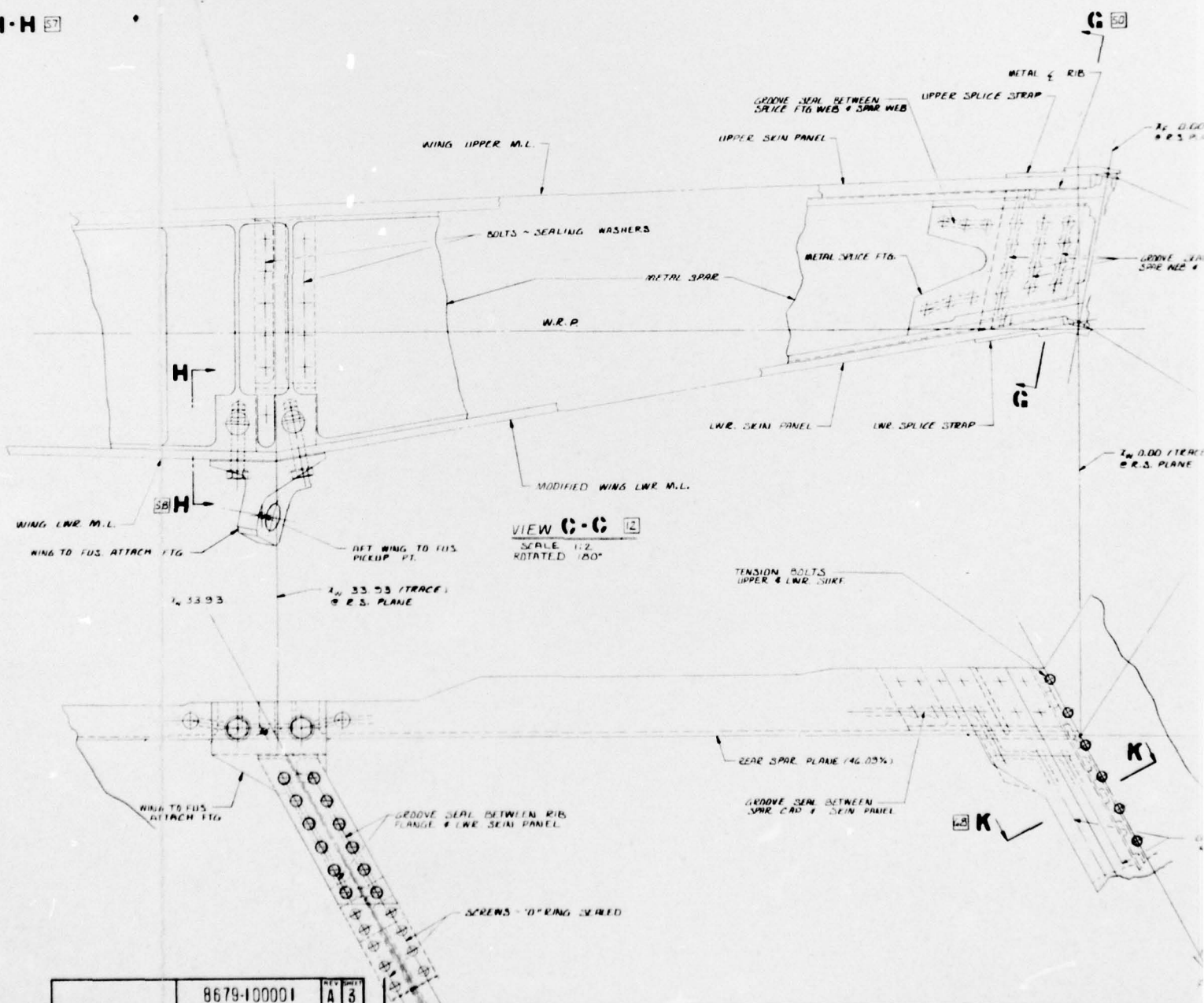


WING LOWER M.L.  
HING TO FUS. ATT.





SECTION H-H 57  
FILE 13



VIEW C-C 12  
SCALE 1:2  
ROTATED 180°

8679-100001

REV A 3

58

57

56

55

54

53

4

REVISIONS			
LINE	IN	DESCRIPTION	DATE APPROVED
		MAY BE REWORKED 2. CANNOT BE REWORKED	
		3. REWORK CHANGE 4. NEW TAPING PRACTICE	
		5. PARTS MADE IN	
A		SEE SHT 1 FOR REVISIONS	

BEST AVAILABLE COPY

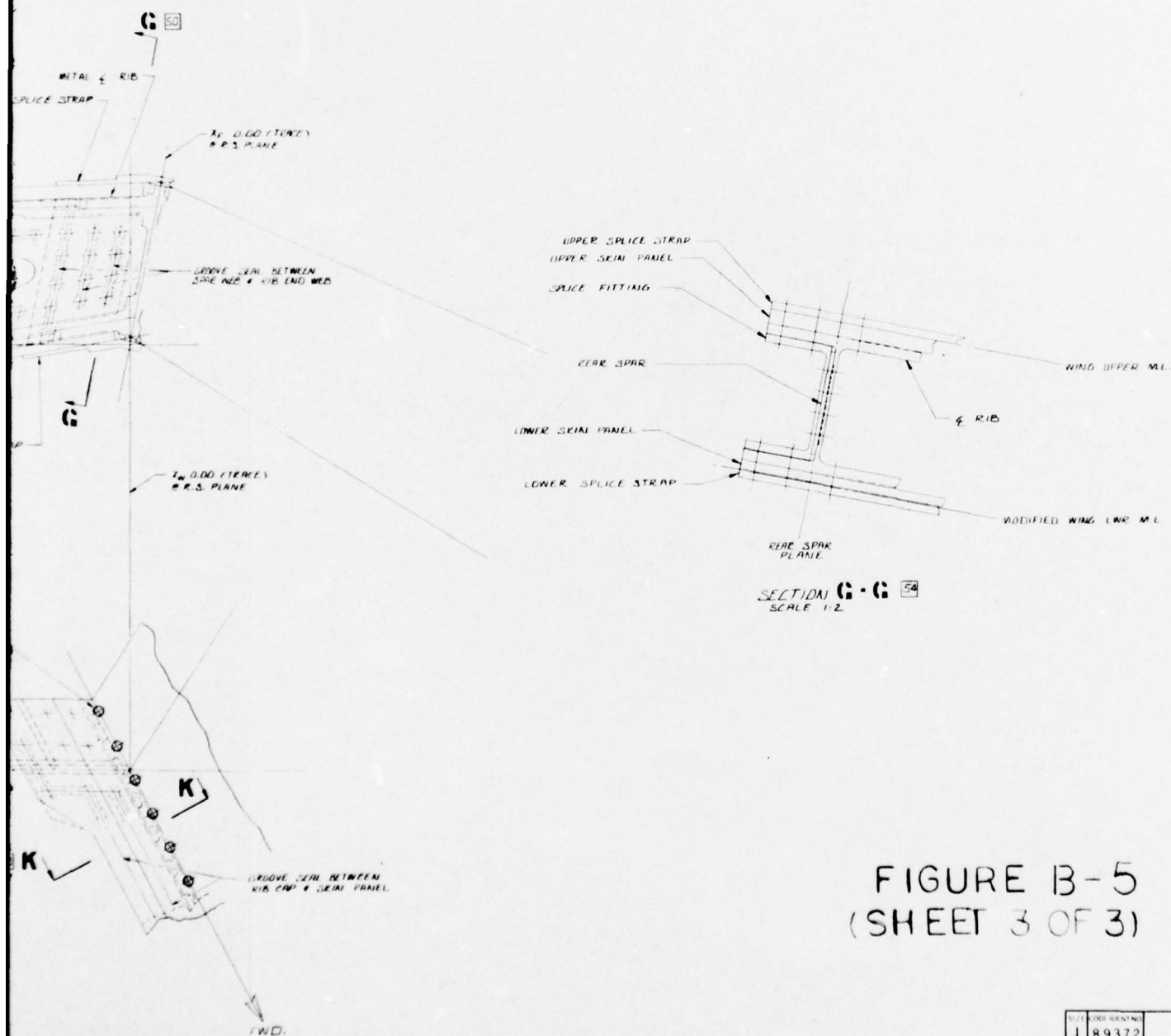


FIGURE B-5  
(SHEET 3 OF 3)

SIZE	CODE IDENT NO	
J	89372	8679-100001
SCALE	NOTE	SHEET 3

B-3 ALTERNATE DESIGN CONCEPT DRAWINGS

Figures B-6 and B-7 illustrate the "Configuration C" concept which is presented as an alternate design. This design utilizes a multi-cell precured substructure outboard of X 33.93 and full depth Trussgrid core inboard of X 33.93. A production flow diagram for this configuration is shown in Figure B-8.

46.09% PLANE  
(EXISTING R. SPAR PLANE ON PROTO)

FULL DEPTH  
TRUSS GRID CORE

33.00% PLANE

SEE FIGURE B-7

19.56% PLANE  
(EXISTING F. SPAR PLANE ON PROTO)

ACCESS  
REQ'D  
AREA

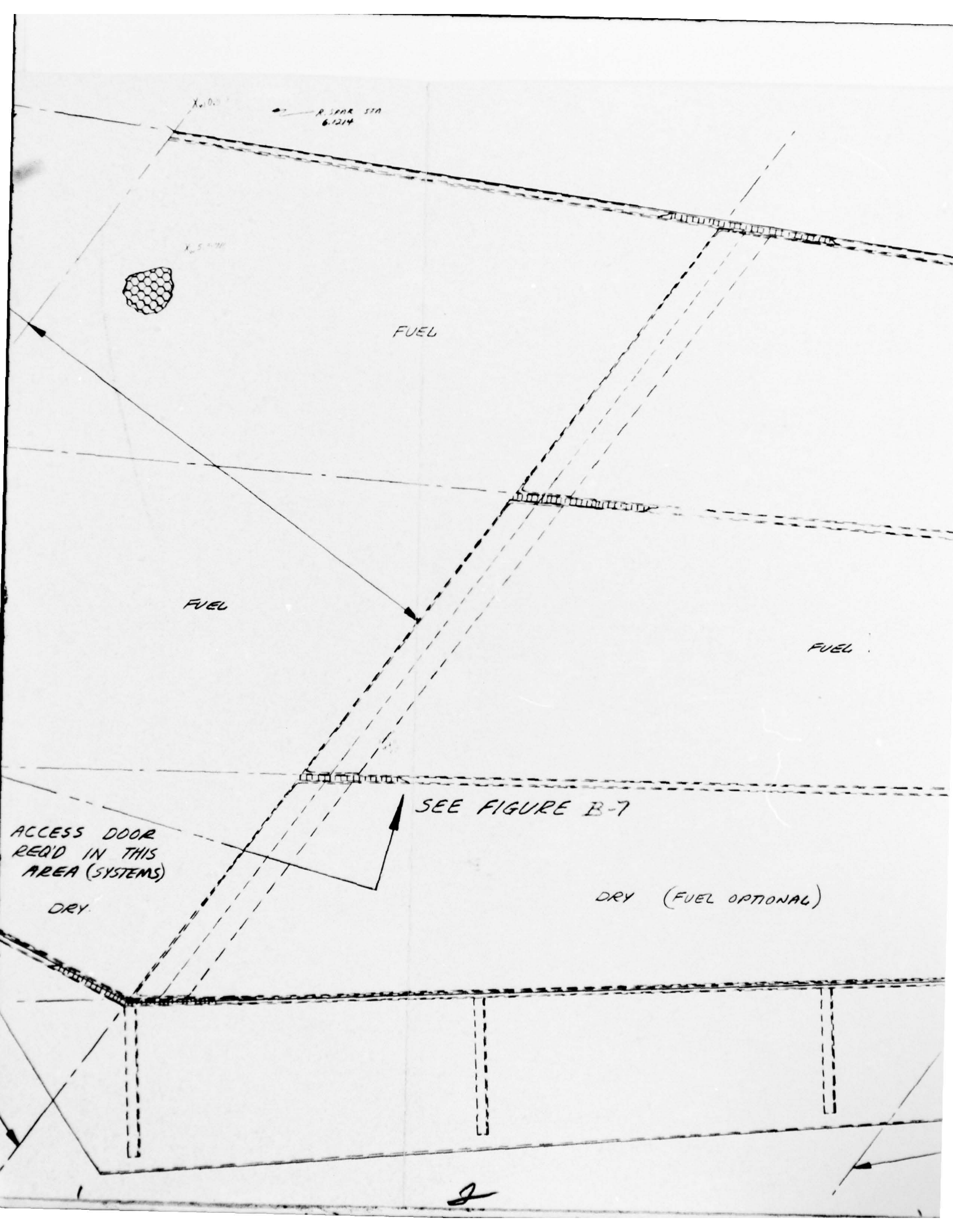
OR

8.75% PLANE

$X_w$  33.9300

$X_w$  0.00 ( $\neq$  AIRPLANE REF)





FUEL

FUEL

DRY (FUEL OPTIONAL)

DRY

$X_w 77.000$

•  $X_w 89.3575$

$X_w 120.000$

3

X<sub>w</sub> 120.00

FUEL

FUEL

NAL)

SKIN TRIM  
(EXISTING LOCATION)

⊥ FOLD HINGE

EXISTING  
OUTBD OF

4

NR76H-135  
PAGE B-19

BEST AVAILABLE COPY

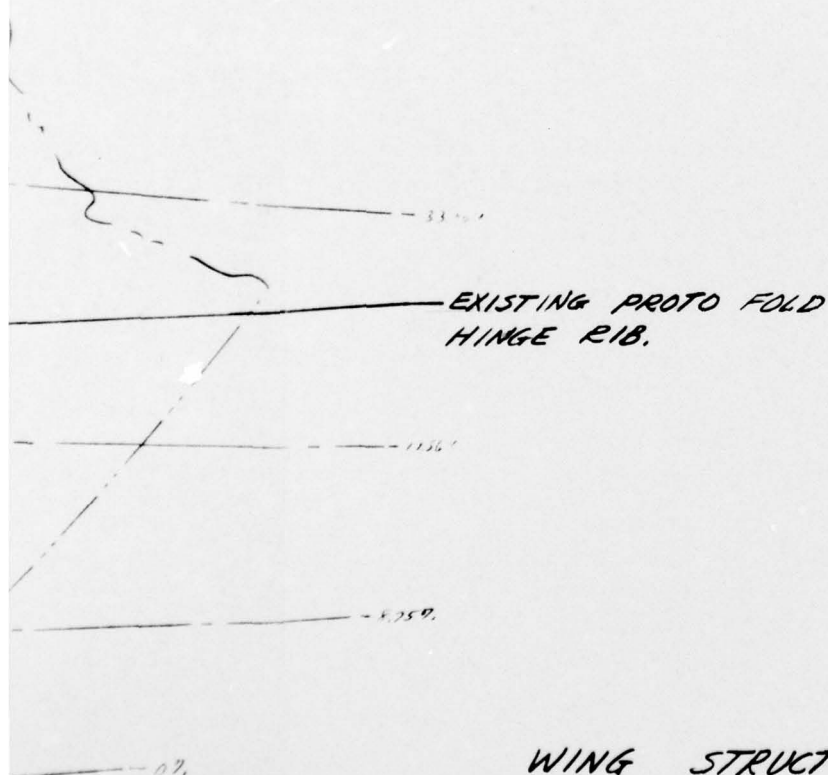


FIGURE B-6  
BASELINE " CONFIGURATION C

WING STRUCTURAL CONCEPT

SCALE  $\frac{1}{4}$

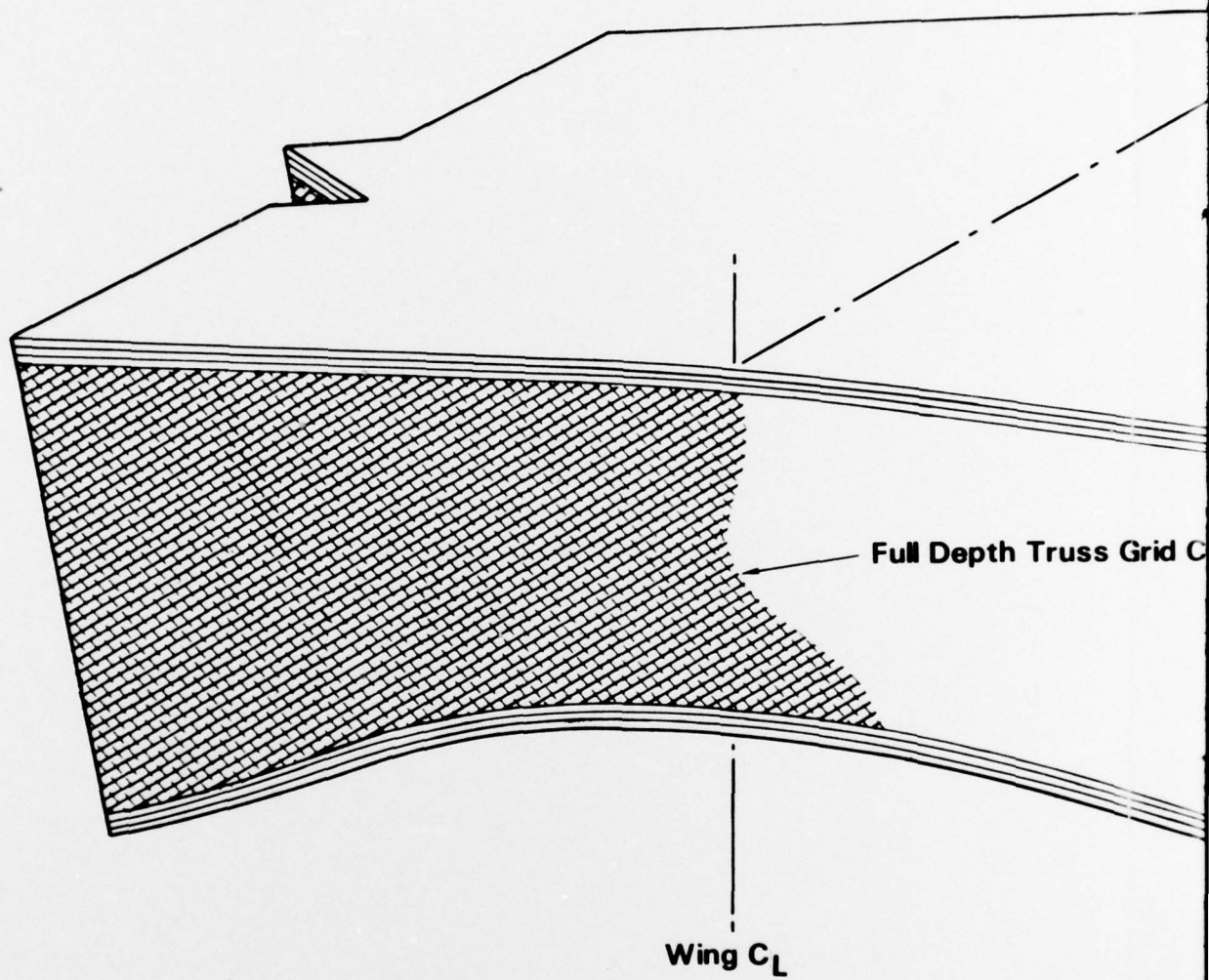
(FULL DEPTH CORE  
IN CTR BOX)

G.M. POLLOCK  
9-17-74

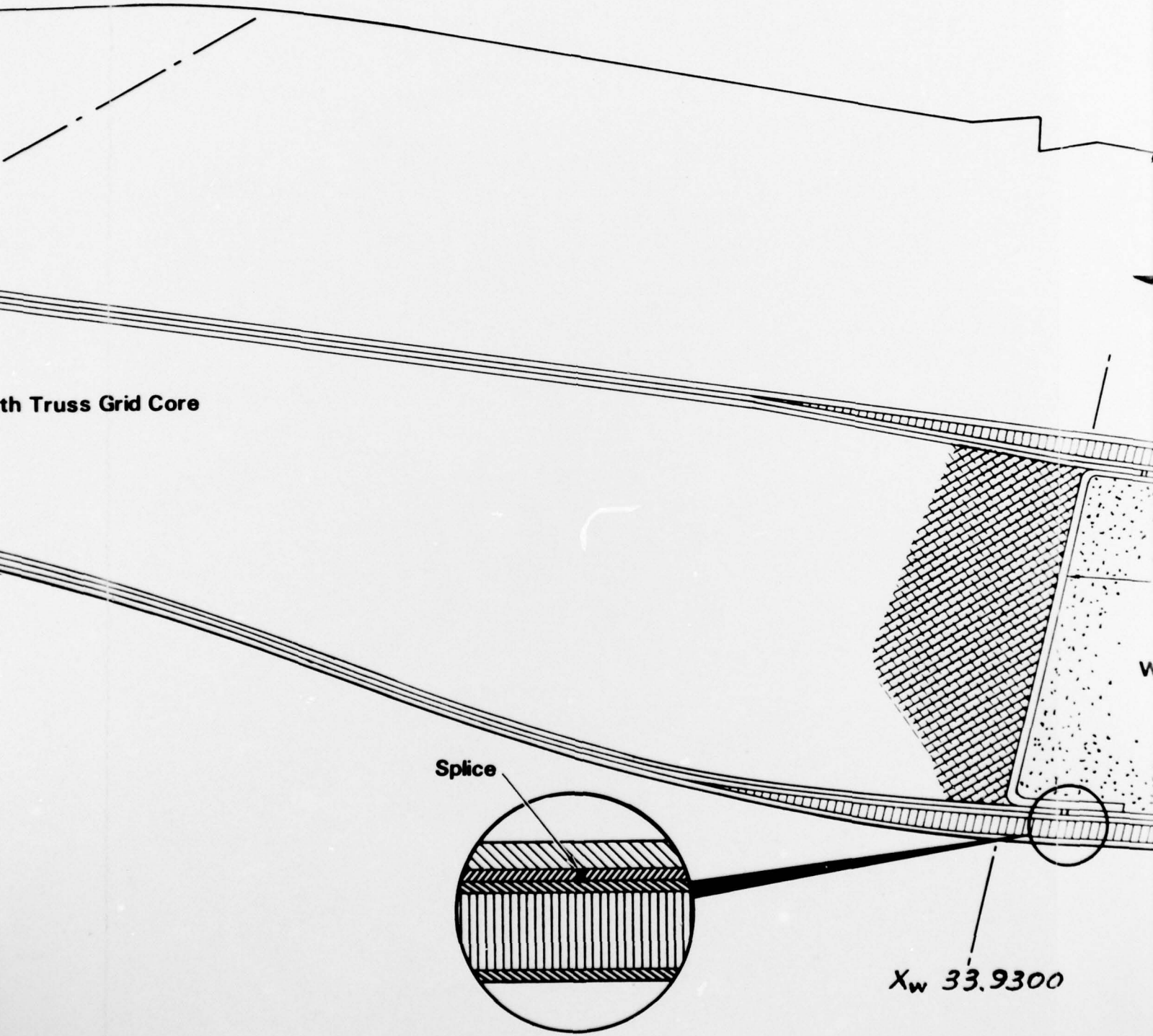
PROTO STRUCTURE  
SKIN TRIM

5





**SECTION LOOKING AFT**



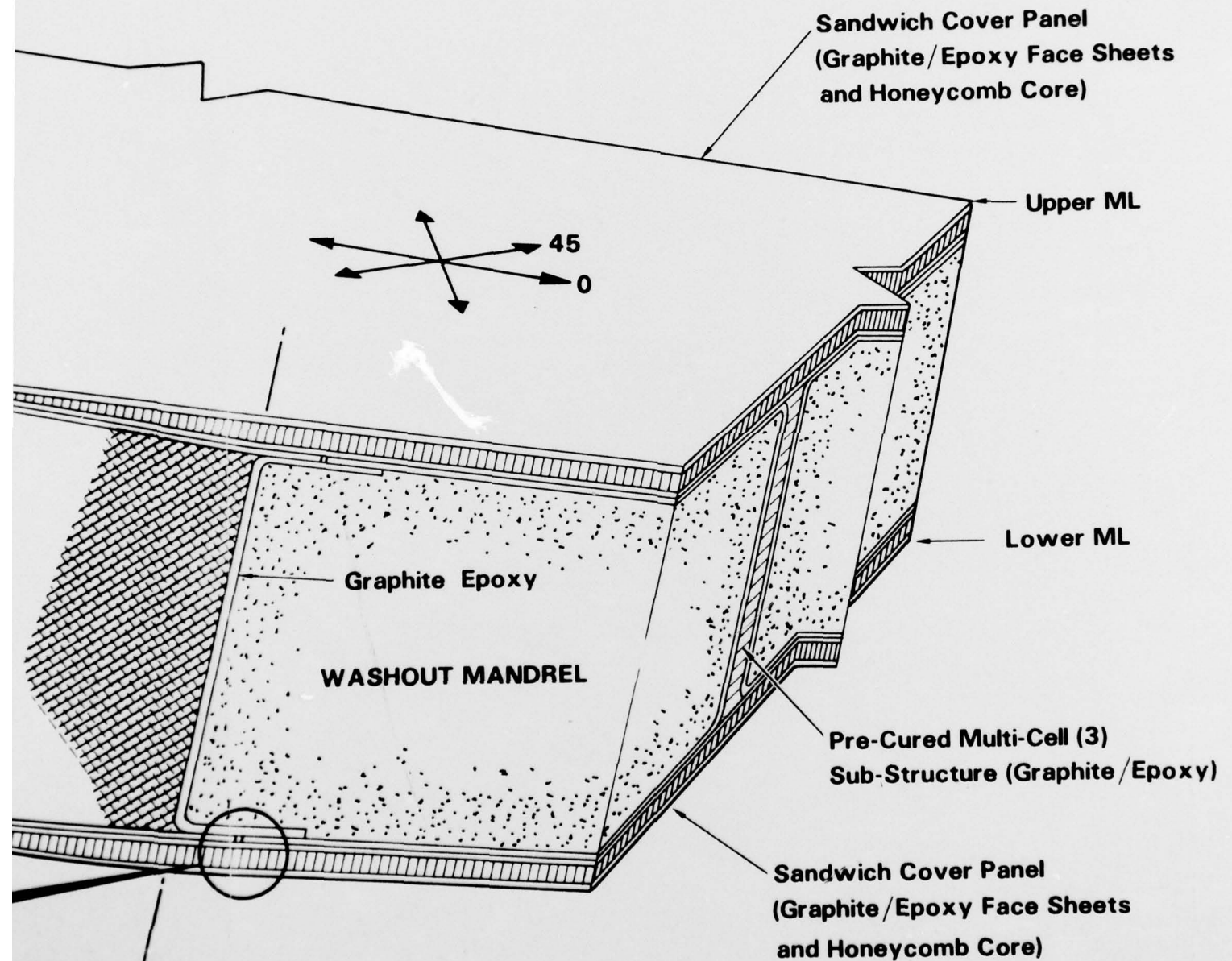
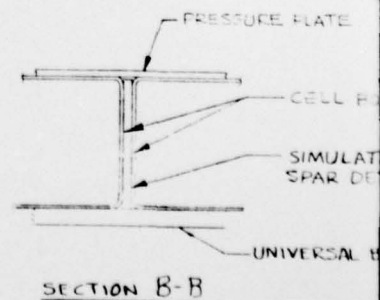
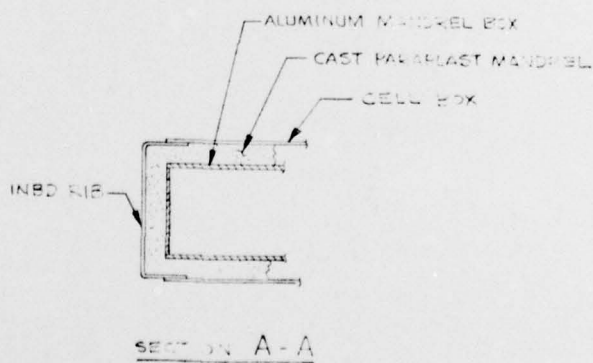
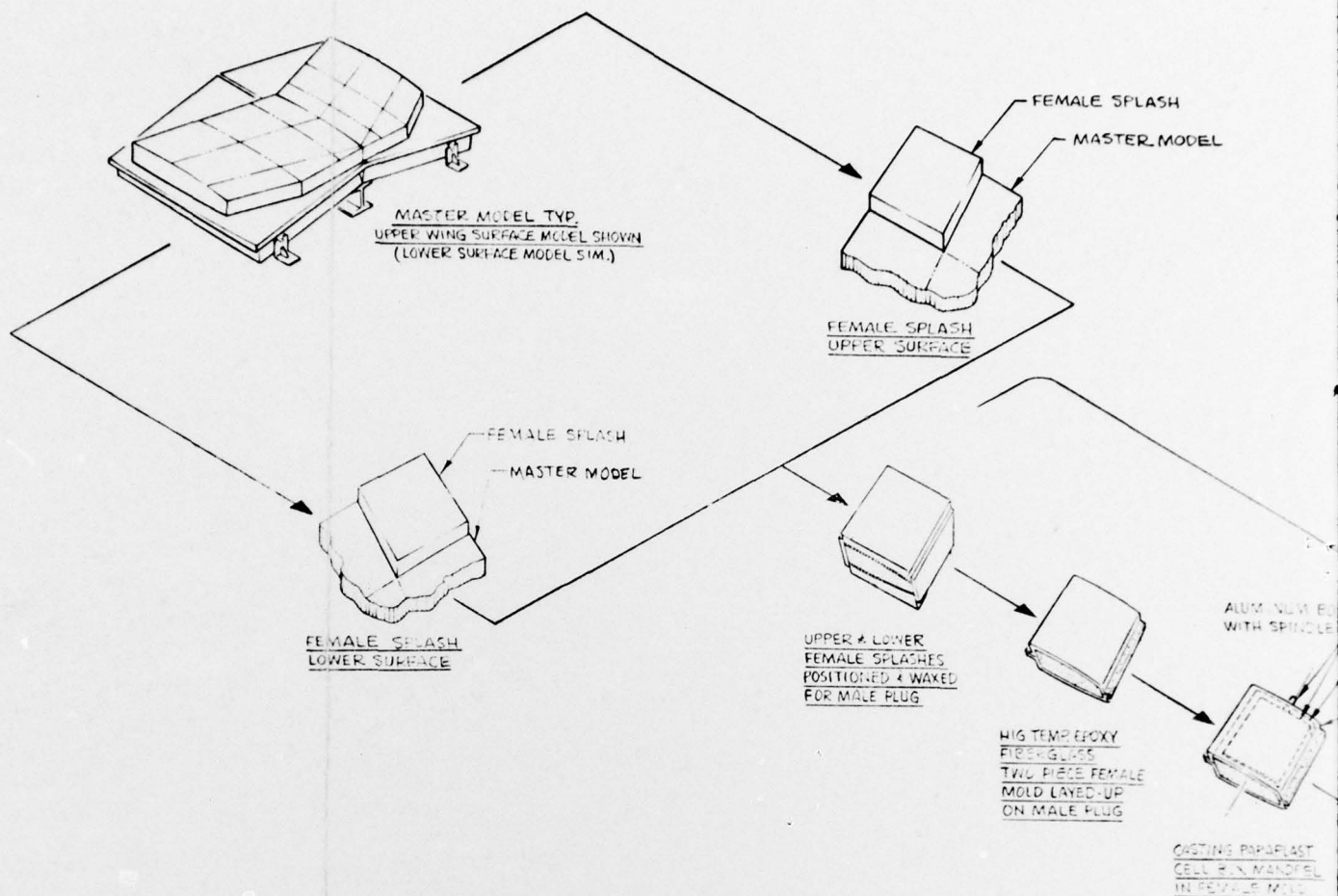
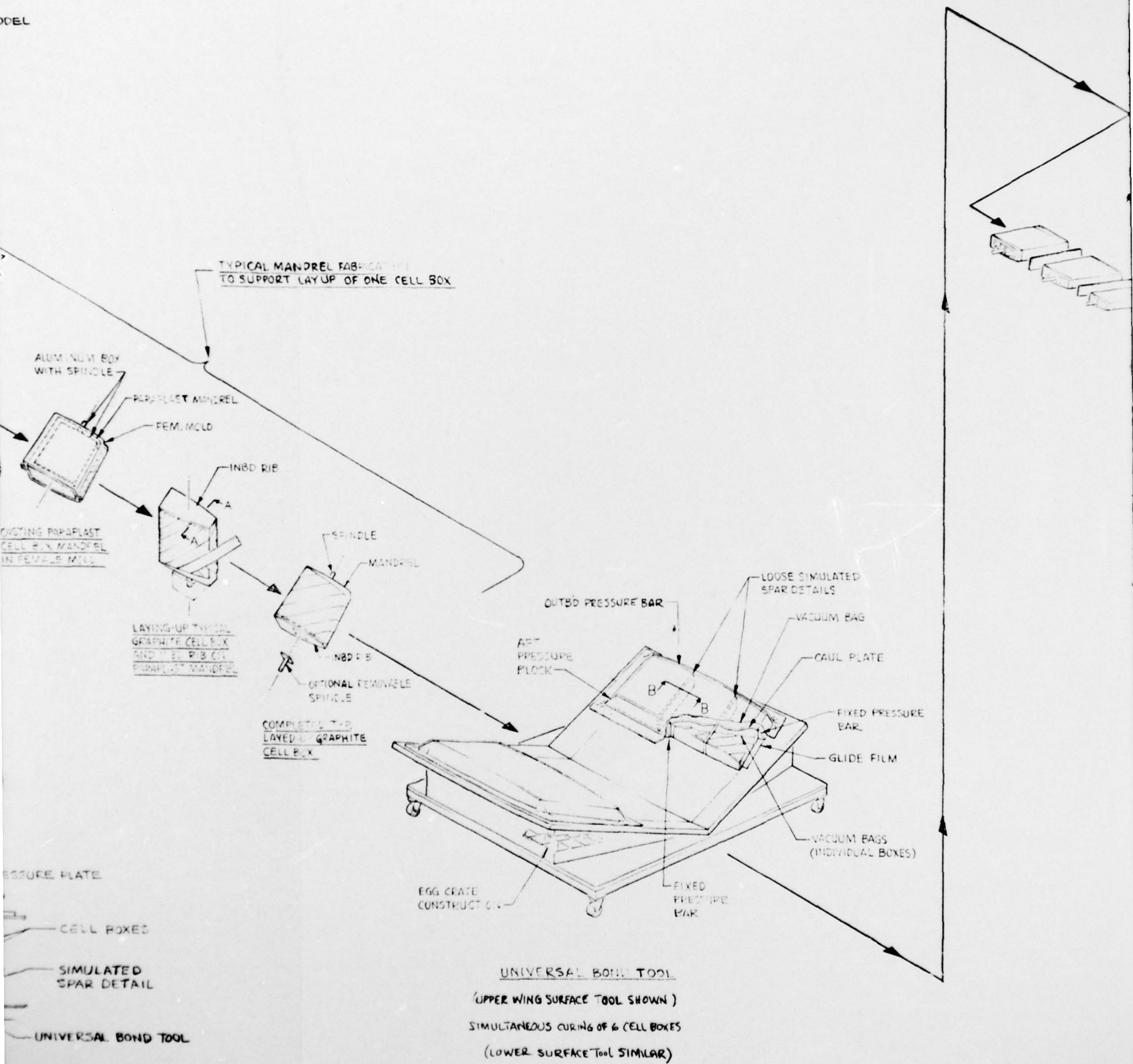


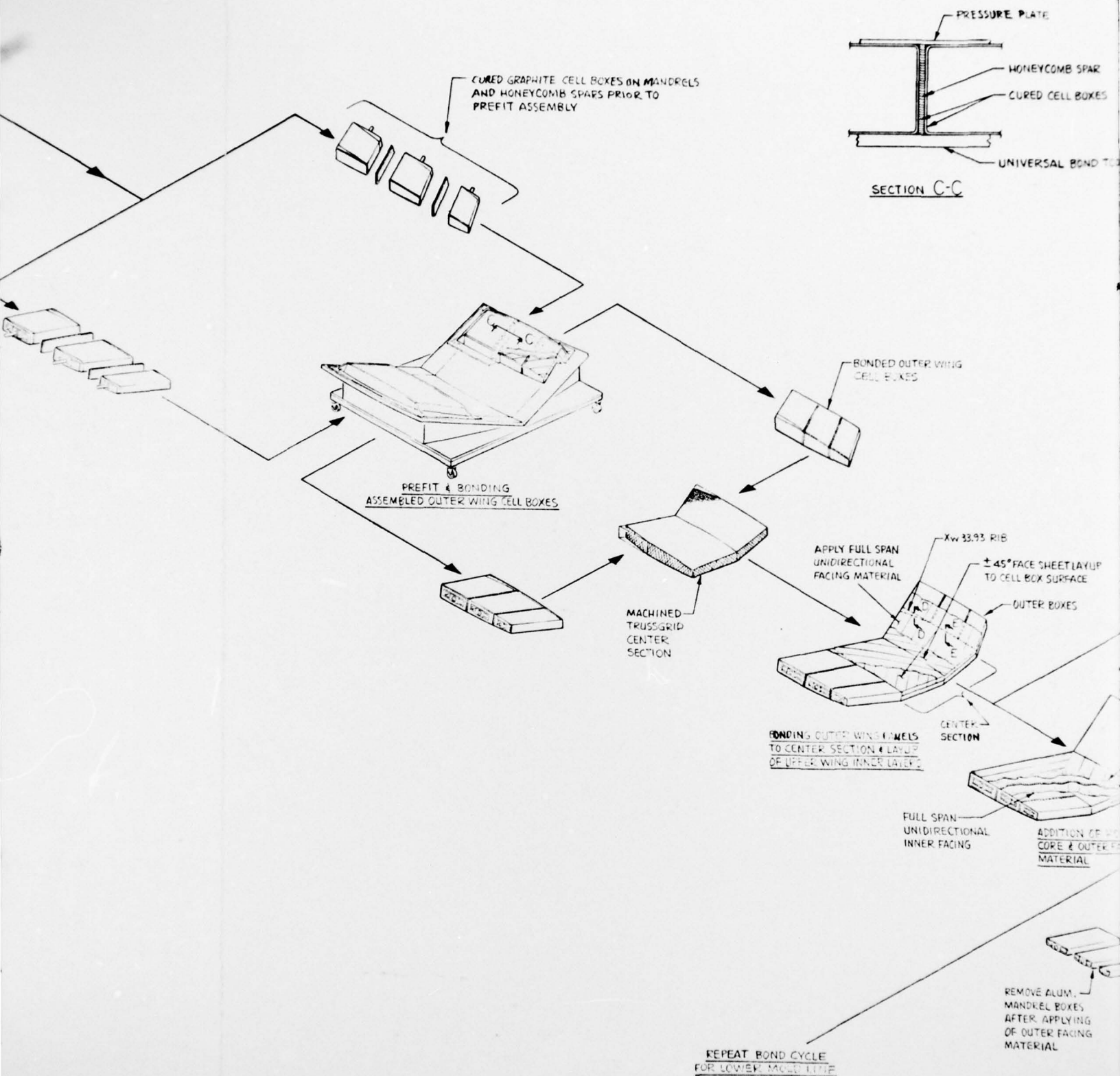
FIGURE B-7  
**WING STRUCTURAL CONCEPT**  
"CONFIGURATION C"

3



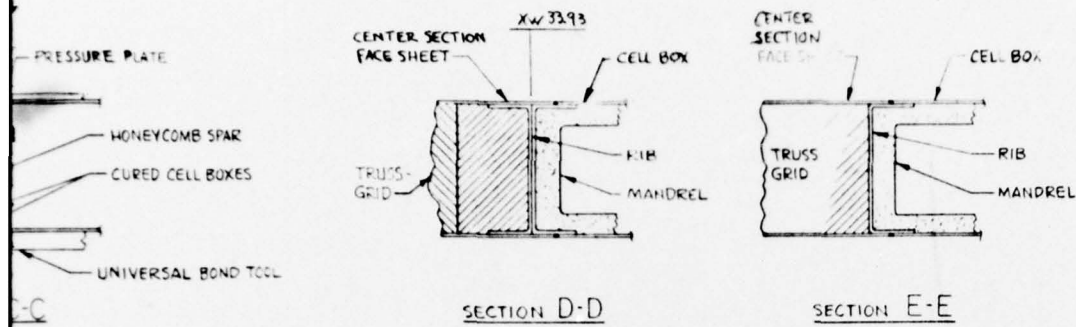






3

NR76H-135  
PG. B-21



BEST AVAILABLE COPY

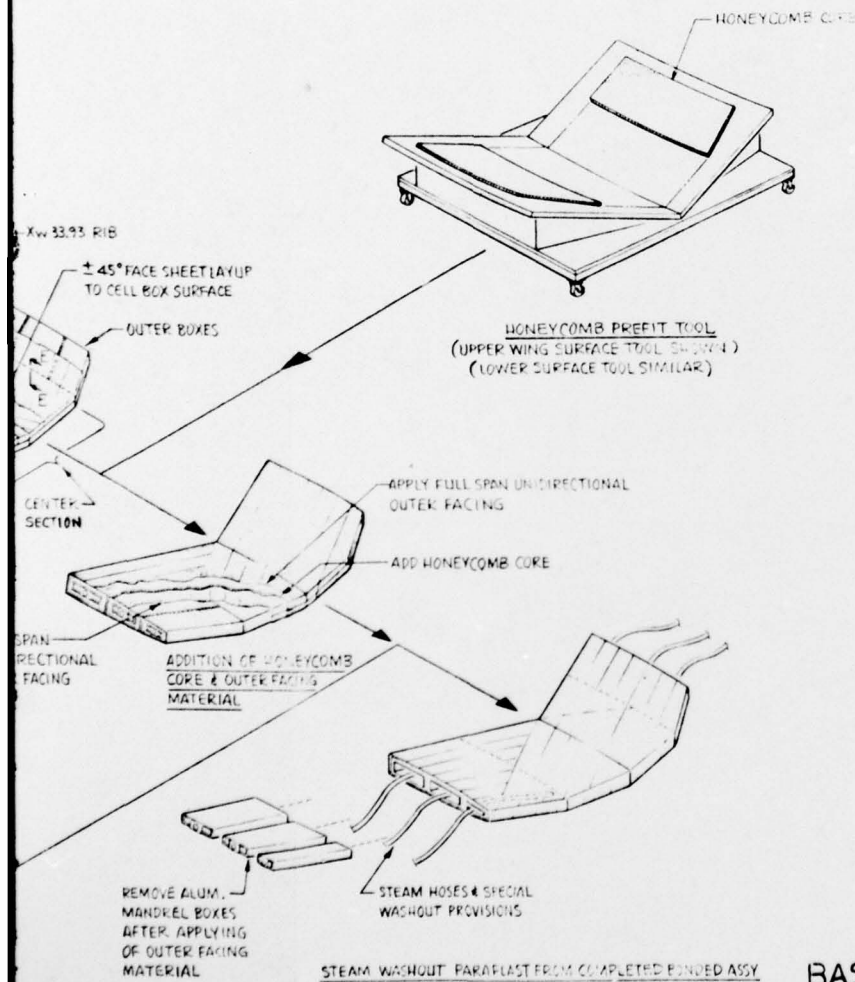


FIGURE B-8  
BASIC PRODUCTION FLOW DIAGRAM  
HSK-1167 "CONFIGURATION C"

BASIC PRODUCTION FLOW DIAGRAM  
GRAPHITE WING STUDY  
CONFIGURATION FULL DETAILED IN CENTER OF C-13

4

# DISTRIBUTION LIST

## Government Activities

	No. of Copies
NAVAIRSYSCOM, AIR-954 (2 for retention), 2 for AIR-530, 1 for AIR-320B, AIR-52032D, AIR-5302, AIR-53021, AIR-530215). . .	9
NAVSEASYSYSCOM, Washington, D. C. 20362 (Attn: Code 035, Mr. C. Pohler). . . . .	1
NAVSEC, Hyattsville, MD 20782 (Attn: Code 6101E03, Mr. W. Graner). . . . .	1
ONR, Washington, D. C. 20362 (Attn: Dr. N. Perrone) . . . . .	1
NAVSHIPPRANDCEN, Bethesda, MD 20034 (Attn: Code 173.2, Mr. W. P. Cauch). . . . .	1
NAVSHIPPRANDCEN, Annapolis, MD 21402 (Attn: Code 2870, Mr. H. Edelstein). . . . .	1
NOL, White Oak, MD 20910 (Attn: Mr. F. R. Barnet) . . . . .	1
NRL, Washington, D. C. 20375 (Attn: Dr. I. Wolock). . . . .	1
NAVPGSCHL, Monterey, CA 95940 (Attn: Prof. R. Ball, Prof M. H. Bank) . . . . .	2
AFOSR, Washington, D. C. 20333 (Attn: Mr. J. Pomerantz) . . . . .	1
AFML, WPAFB, OH 45433 (Attn: LAM (Technical Library)). . . . .	1
(Attn: LT-1/Mr. W. R. Johnston). . . . .	1
(Attn: LTF/Mr. T. Cordell) . . . . .	1
(Attn: FBSC/Mr. L. Kelly). . . . .	1
(Attn: MAC/Mr. G. P. Peterson) . . . . .	1
(Attn: MXA/Mr. F. J. Fechek) . . . . .	1
(Attn: MBC/Mr. T. G. Reinhard, Jr) . . . . .	1
AFFDL, WPAFB, OH 45433 (Attn: FB/Mr. P. A. Parmley) . . . . .	2
(Attn: FBC/Mr. C. Wallace) . . . . .	1
(Attn: FBC/Mr. E. E. Zink) . . . . .	1
USAMATRESAG, Watertown, MA (Attn: Dr. E. Lenoe) . . . . .	1
USARESOFC, Durham, MC 27701 . . . . .	1
USAAVMATLAB, Fort Eustis, VA 23603 (Attn: Mr. R. Beresford) . . . . .	1
PLASTEC, Picatinny Arsenal, Dover, NJ 07801 (Attn: Librarian, Bldg. 176, SARPA-FR-M-D and Mr. H. Peibly). . .	2
NASA (ADM), Washington, D.C. 20546 (Attn: Secretary). . . . .	1
Naval Air Development Center, Warminster, PA 18974 (Attn: Receiving Officer, AVTD (Code 3033) . . . . .	remainder req'd under contract



### Government Activities (Cont.)

Scientific & Technical Information Facility, College Park, MD (Attn: NASA Representative) . . . . .	1
NASA, Langley Research Center, Hampton, VA 23365 (Attn: Mr. J. P. Peterson, Mr. R. Pride, and Dr. M. Card) . . .	3
NASA, Lewis Research Center, Cleveland, OH 44153 (Attn: Tech. Library) . . . . .	1
NASA, George C. Marshall Space Flight Center, Huntsville, AL 35812 (Attn: S & E-ASTN-ES/Mr. E. E. Engler) . . . . .	1
(Attn: S & E-ASTN-M/Mr. R. Schwinghamer) . . . . .	1
(Attn: S & E-ASTM-MNM/Dr. J. M. Stuckey) . . . . .	1
DDC. . . . .	12
FAA, Airframes Branch, FS-120, Washington, D. C. 20553 (Attn: Mr. J. Dougherty) . . . . .	1

### Non-Government Agencies

Avco Aero Structures Division, Nashville, TN 37202 (Attn: Mr. W. Ottenville) . . . . .	1
Avco Space Systems Division, Lowell, MA 01851 (Attn: Dr. M. J. Salkind) . . . . .	1
Bell Aerospace Company, Buffalo, NY 14240 (Attn: Zone I-85, Mr. F. M. Anthony) . . . . .	1
Bell Helicopter Company, Fort Worth, TX 76100 (Attn: Mr. Charles Harvey) . . . . .	1
Bendix Products Aerospace Division, South Bend, IN 46619 (Attn: Mr. R. V. Cervelli) . . . . .	1
Boeing Aerospace Company, P.O. Box 3999, Seattle, WA 98124 (Attn: Code 206, Mr. R. E. Horton) . . . . .	1
Boeing Company, Renton, Washington 98055 (Attn: Dr. R. June) . . . . .	1
Boeing Company, Vertol Division, Phila., PA 19142 (Attn: Mr. R. L. Pinckney, Mr. D. Hoffstedt) . . . . .	2
Boeing Company, Wichita, KS 67210 (Attn: Mr. V. Reneau/MS 16-39) . . . . .	1
Cabot Corporation, Billerica Research Center, Billerica, MA 01821 . . . . .	1
Drexel University, Phila., PA 19104 (Attn: Dr. P. C. Chou) . . . . .	1
E. I. DuPont Company, Wilmington, DE 19898 (Attn: Dr. Carl Zweben) Bldg. 262/Room 316 . . . . .	1
Fairchild Industries, Hagerstown, MD 21740 (Attn: Mr. D. Ruck) . . . . .	1
Ferro Corporation, Huntington Beach, CA 92646 (Attn: Mr. J. L. Bauer) . . . . .	1
Georgia Institute of Technology, Atlanta, GA (Attn: Prof. W. H. Horton) . . . . .	1

# Non-Government Agencies (Cont.)

General Dynamics/Convair, San Diego, CA 92138 (Attn: Mr. D. R. Dunbar, W. G. Scheck) . . . . .	2
General Dynamics, Fort Worth, TX 76101 (Attn: Mr. P. D. Shockey, Dept. 23, Mail Zone P-46). . . . .	1
General Electric Company, Phila., PA 19101 (Attn: Mr. L. McCreight) . . . . .	1
Great Lakes Carbon Corp., N.Y., NY 10017 (Attn: Mr. W. R. Benn, Mgr., Markey Development) . . . . .	1
Grumman Aerospace Corporation, Bethpage, L.I., NY 11714 (Attn: Mr. R. Hadcock, Mr. S. Dastin). . . . .	2
Hercules Powder Company, Inc., Cumberland, MD 21501 (Attn: Mr. D. Hug) . . . . .	1
H. I. Thompson Fiber Glass Company, Gardena, CA 90249 (Attn: Mr. N. Myers) . . . . .	1
ITT Research Institute, Chicago, IL 60616 (Attn: Dr. R. Cornish) . . . . .	1
J. P. Stevens & Co., Inc., N.Y., NY 10036 (Attn: Mr. H. I. Shulock). . . . .	1
Kaman Aircraft Corporation, Bloomfield, CT 06002 (Attn: Tech. Library). . . . .	1
Lehigh University, Bethlehem, PA 18015 (Attn: Dr. G. C. Sih). . . . .	1
Lockheed-California Company, Burbank, CA 91520 (Attn: Mr. E. K. Walker, R. L. Vaughn) . . . . .	2
Lockheed-Georgia Company, Marietta, GA (Attn: Advanced Composites Information Center, Dept. 72-14, Zone 42). . . . .	1
LTV Aerospace Corporation, Dallas, TX 75222 (Attn: Mr. O. E. Dhonau/2-53442, C. R. Foreman). . . . .	2
Martin Company, Baltimore, MD 21203 (Attn: Mr. J. E. Pawken) . . . . .	1
Materials Sciences Corp., Blue Bell, PA 19422 . . . . .	1
McDonnell Douglas Corporation, St. Louis, MO 63166 (Attn: Mr. R. C. Goran, O. B. McBee, C. Stenberg). . . . .	3
McDonnell Douglas Corporation, Long Beach, CA 90801 (Attn: H. C. Schjelderup, G. Lehman) . . . . .	2
Minnesota Mining and Manufacturing Company, St. Paul, MN 55104 (Attn: Mr. W. Davis) . . . . .	1
Northrop Aircraft Corp., Norair Div., Hawthorne, CA 90250 (Attn: Mr. R. D. Hayes, J. V. Noyes, R. C. Isemann). . . . .	3
Rockwell International, Columbus, OH 43216 (Attn: Mr. O. G. Acker, K. Clayton). . . . .	2
Rockwell International, Los Angeles, CA 90053 (Attn: Dr. L. Lackman) . . . . .	1
Rockwell International, Tulsa, OK 74151 (Attn: Mr. E. Sanders, Mr. J. H. Powell) . . . . .	2
Owens Corning Fiberglass, Granville, OH 43023 (Attn: Mr. D. Mettes). . . . .	1

# Non-Government Agencies (Cont.)

Rohr Corporation, Riverside, CA 92503	
(Attn: Dr. F. Riel and Mr. R. Elkin) . . . . .	2
Ryan Aeronautical Company, San Diego, CA 92112	
(Attn: Mr. R. Long). . . . .	1
Sikorsky Aircraft, Stratford, CT 06497	
(Attn: Mr. J. Ray) . . . . .	1
Southwest Research Institute, San Antonio, TX 78206	
(Attn: Mr. G. C. Grimes) . . . . .	1
University of Oklahoma, Norman, OK 93069	
(Attn: Dr. G. M. Nordby) . . . . .	1
Union Carbide Corporation, Cleveland, OH 44101	
(Attn: Dr. H. F. Volk) . . . . .	1
Battelle Columbus Laboratories, Metals and Ceramics Information Center, 505 King Avenue, Columbus, OH 43201. . . . .	1